NIPTERK P-32 SPRAY ICE ISLAND

ABLATION PROTECTION EXPERIMENT

BY

J.P. POPLIN

ERCL.RS.89.24

PROPRIETARY

DECEMBER 1989

SUMMARY

This report documents results of the Nipterk P-32 Spray Ice Island Ablation Protection Experiment. The experiment was carried out by Esso Resources Canada Ltd. as a joint-industry project. The other original participants were Chevron Resources Canada Ltd., Canada Oil and Gas Lands Administration/U.S. Minerals Management Service, and Mobil Research and Development Corporation.

The experiment was undertaken to assess the feasibility of various methods for extending the use of exploration spray ice platforms through breakup and into the summer season. The objective of this research was to develop technology that could contribute toward providing significant increases in available drilling and testing time as well as the feasibility to offset construction and/or drilling problems by demobilizing the rig after landfast ice breakup. Additionally, the technology developed from this study could offer the potential benefit of extending the application of spray ice platforms into deeper waters.

Nipterk Spray Ice Island was constructed during the previous 1988/1989 winter in the southern Canadian Beaufort Sea off the MacKenzie River Delta at Latitude N60°40'46.9" and longitude W135°22'42.5" in a water depth of 6.5 m. The ice island was originally about 320 m in diameter with a 3.5 to 4.5 m freeboard.

Test plots consisting of different configurations and thicknesses of sawdust, various thicknessess of gravel, fabric sheets and wood were constructed atop the spray ice to assess the degree of ablation protection each afforded. All of these materials provided at least some measure of ablation protection. The most effective materials were 15 cm thick sawdust bags, 20 cm thick timbers, and a layer of gravel greater than 0.6 m thick. Each of these materials drastically limited the magnitude of cumulative spray ice surface ablation to amounts less than 20 cm over the duration of the experiment.

Above-freezing air temperatures were prevalent from late-May until the island broke up. This condition along with solar radiation were most responsible for the average of 2.25 m of spray ice ablation documented in the unprotected portion of

the island through July 5. However, even relatively thin layers of materials on the surface provided substantial ablation protection leading to the conclusion that surface ablation can be effectively mitigated and managed with coatings in a cost effective manner.

A portion of the experiment was designed to evaluate the performance of impermeable sheets draped over the edge of the island to protect the edges from mechanical and thermal wave erosion due to wave action and currents. Open water conditions persisted after breakup until the island completely desintegrated two and one-half weeks later. The island appeared to break up predominantly due to lack of freeboard rather than from wave erosion. Still the degree of stabilization afforded by the edge protection system both in regard to edge erosion and surface ablation protection was readily apparent leading to the conclusion that the rate of edge erosion can be significantly decreased by deploying a system of impermeable sheets and nets.

Breakup of the landfast ice occurred by June 24. The island withstood ice forces imposed on it during breakup without undergoing any apparent sliding along the sea floor. A thermal equilibrium condition in the spray ice was reached by June 10, when the temperature throughout the island was very close to 0°C. The island mass decreased rapidly following the advent of landfast ice breakup, due to an instability condition resulting from loss of freeboard and mechanical and thermal wave and current erosion. The final island remnant broke up on July 10, some two and one-half weeks following breakup of the surrounding ice sheet. The water temperature measured the day following complete island disintegration was 12°C.

Studies relating to barge docking and trafficability were not fully addressed as part of the experiment due to the relatively early breakup of the island. However, based on a supplemental study drawing upon operational experiences of spray ice features in western Alaska by a subcontractor, the edge of a spray ice island can be shaped by excavating and wheelwashing with a tugboat to provide a barge docking area.

As a result of this experiment it is concluded that drilling operations on a spray ice platform can be extended to at least June 1 and potentially beyond. It is also concluded that marine demobilization of a drilling rig is feasible. Even with the

relatively early breakup of Nipterk, ice conditions would have enabled sufficient time to complete the rig demobilization effort.

The most promising materials for surface ablation protection are gravel, sawdust, and rig mats in areas where minimal ablation is needed and tarps and extra spray ice (i.e. higher freeboard) where ablation only need be reduced. Similarly the most promising method of edge protection against waves and currents are impermeable sheets.

TABLE OF CONTENTS

LIST OF FIGURES

LIST OF TABLES

INTRODUCTION

PRIOR FIELD EXPERIENCE

The use of grounded spray ice platforms for exploration drilling in shallow waters of the Beaufort Sea has been successfully demonstrated. To date, two spray ice platforms have been constructed in Canada by Esso and two have been built in Alaska, one by Amoco and the other by Chevron (see table 1).

Table 1 Spray Ice Island Summary

Year	1986	1987	1989	1989
Operator	Amoco	Esso	Esso	Chevron
Name	Mars	Angasak L-03	Nipterk P-32	Karluk
Location	U.S. Beaufort Sea	Canadian Beaufort Sea	Canadian Beaufort Sea	U.S. Beaufort Sea
Water Depth	7.6 m	5.6 m	6.5 m	7.6 m

There are three major advantages for using spray ice platforms. First, they are less costly to construct and drill from than other platforms such as steel or concrete structures and dredged sand and/or gravel islands, particularly in instances when borrow materials are not available nearby. Second, they are more attractive from an environmental standpoint than sand islands since manmade ice islands are constructed with the local water supply and break up during the summer season. Third, because of their size and the relative degree of ductility they afford, spray ice islands are capable of protecting the drilling rig from ice forces which are the major design criterion in the Beaufort Sea. These advantages provide strong motivation to advance the technology of spray ice and thereby extend the applicability of spray ice platforms.

To date, the use of spray ice islands has been limited to water depths 7.6 m and shallower. Moreover, the drilling and testing window has been restricted to about 75 days. Extension of spray ice platforms into deeper waters would reduce the length of drilling window even further.

EXPERIMENT OBJECTIVES

Over the past few years, Esso Resources Canada Ltd. has been active in researching methods to extend spray ice technology into deeper waters and to increase the length of the drilling and testing period available with the use of these structures. Useful improvements have been made and opportunities for "breakthrough" advances identified. One such advance would be to demobilize the rig by barge in late June after breakup rather than by floating ice road in late April which is the current method. This approach would enable drilling operations to continue through May and potentially longer, leading to a 50 to 100% increase in the drilling and testing period and/or water depth range. However, before such an approach could be applied, confirmatory research was deemed necessary.

Towards this end, the Nipterk Spray Ice Island Ablation Experiment was undertaken to assess the feasibility of various methods for extending the use of exploration spray ice platforms through breakup and possibly into the summer season. The objective of this research was to develop technology that could contribute toward providing significant additional drilling and testing time as well as the flexibility to offset construction and/or drilling problems by demobilizing the rig after breakup. Additionally, the technology developed from this study could offer the potential benefit of extending the application of spray ice platforms into deeper water.

The overall goal of this project was to develop sufficient knowledge of ablation, erosion rates, and protective methods to allow the marine demobilization option to be included in the plans for future spray ice islands. Specific objectives were to:

1) monitor surface ablation and edge erosion rates until early summer,
2) assess the effectiveness of various methods toward mitigating ablation and erosion,
3) assess surface trafficability and edge stability in relation to docking and offloading,
4) investigate methods of improving surface trafficability and edge stability, and

5) assess how methods of providing edge protection could be developed to extend the operational life of spray ice islands into the open-water season.

These objectives were accomplished by covering sections of the island with various thicknesses and configurations of gravel, sawdust, timbers and white tarps. Spray ice surface ablation was measured for each of these areas during the study period. Protective sheets and netting were also used over a portion of the island in an attempt to reduce wave erosion after breakup of the surrounding ice sheet. Measurements of edge erosion were carried out from late-June until the island broke up in July.

Tasks addressing surface trafficability, edge stability, and docking were not fully addressed as part of the field experiment due to the relatively early breakup of the island. Consequently, a supplemental study drawing upon operational experiences of spray ice features in western Alaska was performed by a subcontractor and the pertinent results included in this report.

BACKGROUND

GEOGRAPHIC LOCATION, OCEANOGRAPHIC AND LANDFAST ICE CONDITIONS

Nipterk P-32 Spray Ice Island was constructed during 1988/89 winter. The well location was off the Mackenzie River Delta, 6 km north-northeast of Pelly Island at latitude N60° 41' 46.9" and longitude W135° 22' 42.5". The location of the island is presented in Figure 1. The dashed lines in Figure 1a denote the 8 and 12 m water depth contours. Average and minimum extents of the landfast ice are depicted by solid lines. As can be seen, the island was well within a relatively stable ice regime. A number of other Beaufort Sea wells drilled from sand islands and/or caissons are also shown. Figure 1b is a map showing a more detailed view of the island location. The camp, construction equipment, and drilling consumables were transported aboard ice strengthened barges deployed in September 1988 behind the Pelly Island Spit. The link to the island was via a 10 km long floating ice road.

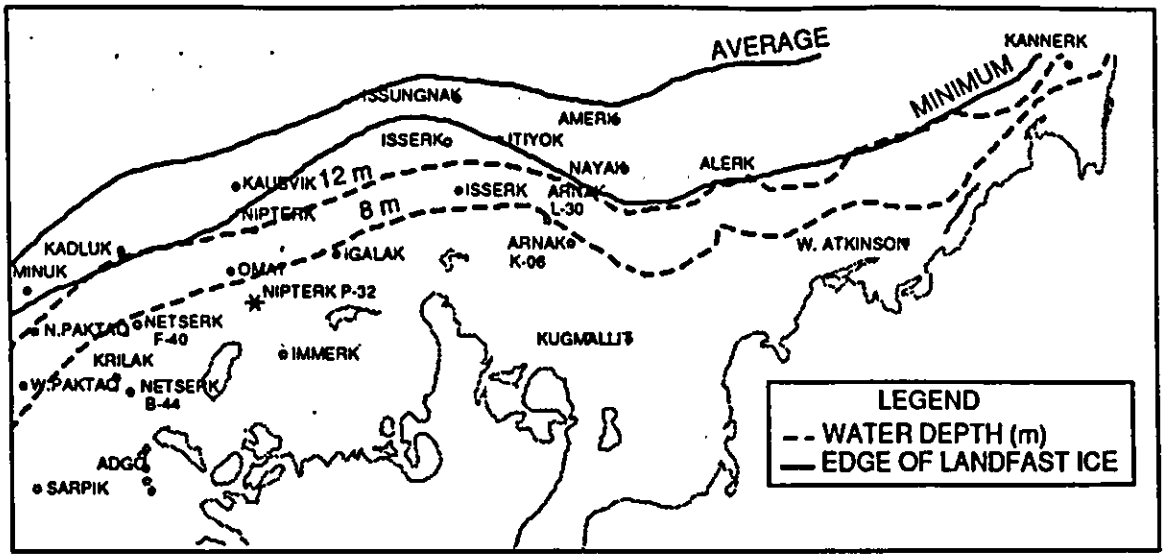

(a)

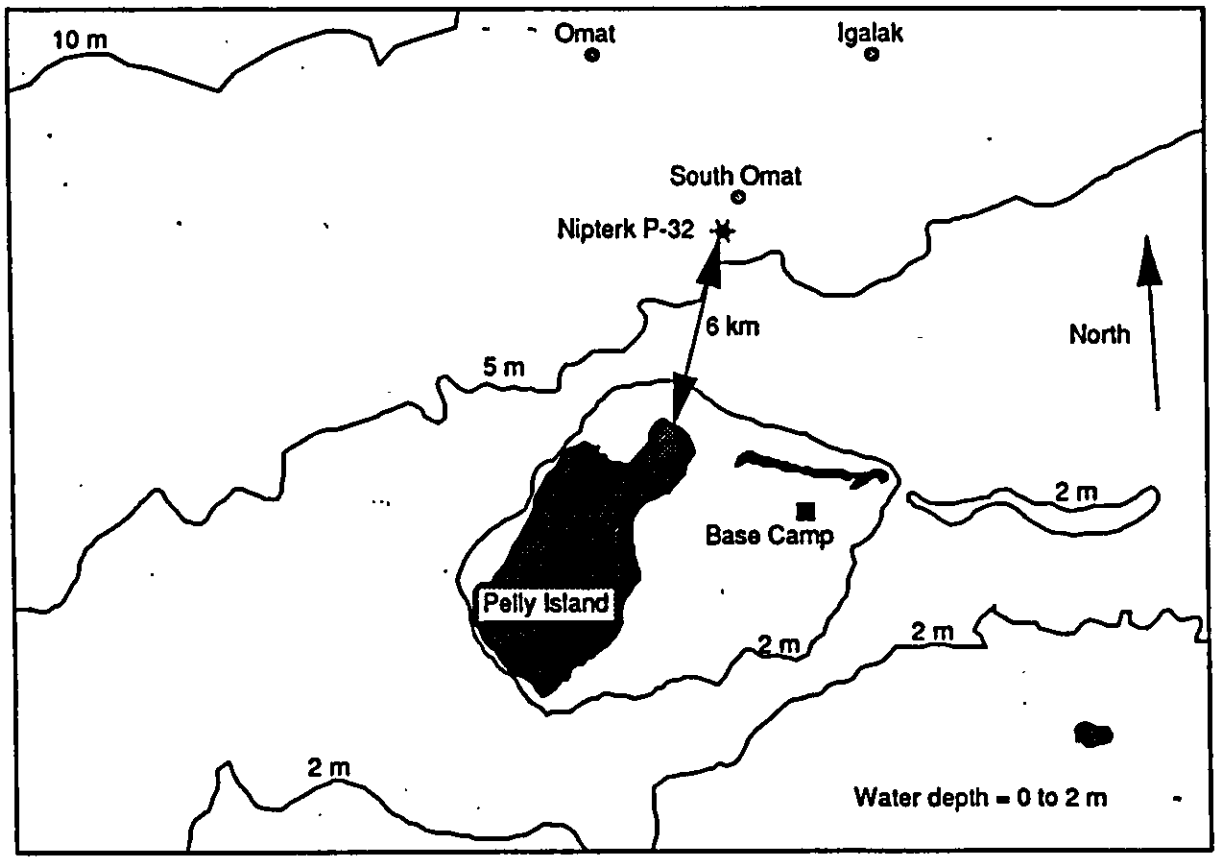

(b)

Figure 1. Nipterk P-32 Location Plan

Bathymetry was measured at the site prior to island construction and found to average 6.5 m with a range of 6.38 to 6.65 m, inclusive. A map showing the of water depth measurements at the side is presented as Figure 2. Also shown are ice thicknesses measured in mid-November. Note that the first-year ice sheet was rubbled and rafted.

Ice and water column salinity and temperature profiles were measured in mid-November, 1988. At the time, fresh water was present to a depth 4 m below the surface. The remainder of the water column consisted of saline (15 ppt) water. Water temperatures ranged from about 0°C in the freshwater layer to about -1°C in the saline layer.

ISLAND CONSTRUCTION OVERVIEW

In response to an early freezeup, full-scale spray ice construction operations commenced November 28, 1989 and were completed 53 days later on January 20, 1989. Island construction involved four identical spray units enclosed in skid-mounted containers. Each unit consisted of a diesel engine, a 12,000 liters per minute capacity suction pump, and a spray monitor that could be programmed to sweep from side to side. Several nozzle configurations were used to optimize spray ice productivity at the different air temperatures and wind speeds experienced during the construction period.

A diagram showing the island design geometry is presented as Figure 3. Several environmental conditions necessitated that the design of Nipterk be different than previously constructed spray ice islands. First, Nipterk was built at a more exposed location. Second, the seabed soils were relatively weak which necessitated that the size of the island be greater. Third, due to its proximity to the Mackenzie River, source water used to construct the island was essentially fresh, resulting in warmer underwater spray ice.

Island construction was performed in three phases. The submerged portion of the island was largely built during the initial phase in layers 1 to 3 m thick. Spray pumps were frequently repositioned to provide total island coverage. The working surface drilling pad (150 m diameter) was built to final grade in Phase II by

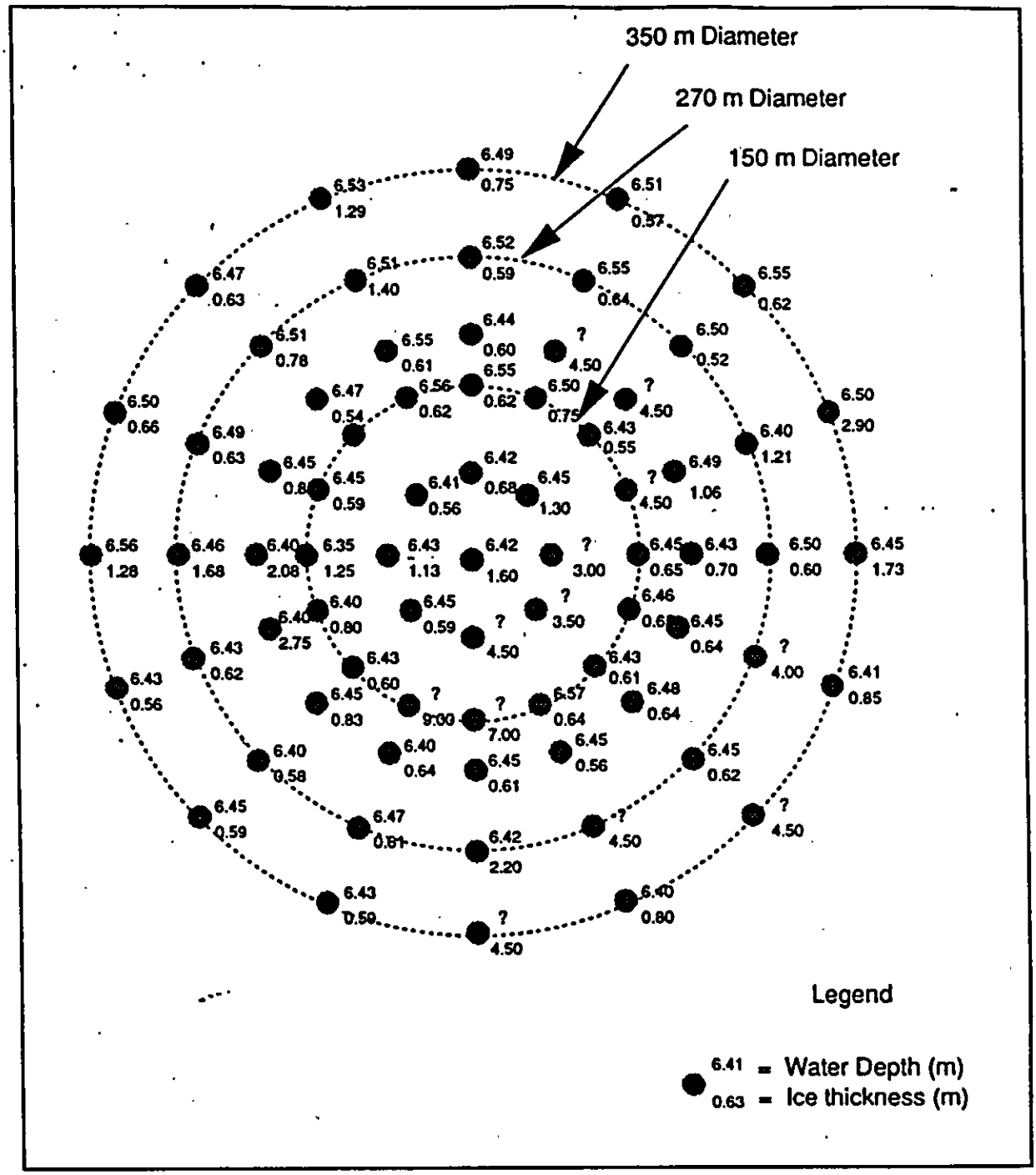

Figure 2. Site Bathymetry and Initial Ice Thicknesses

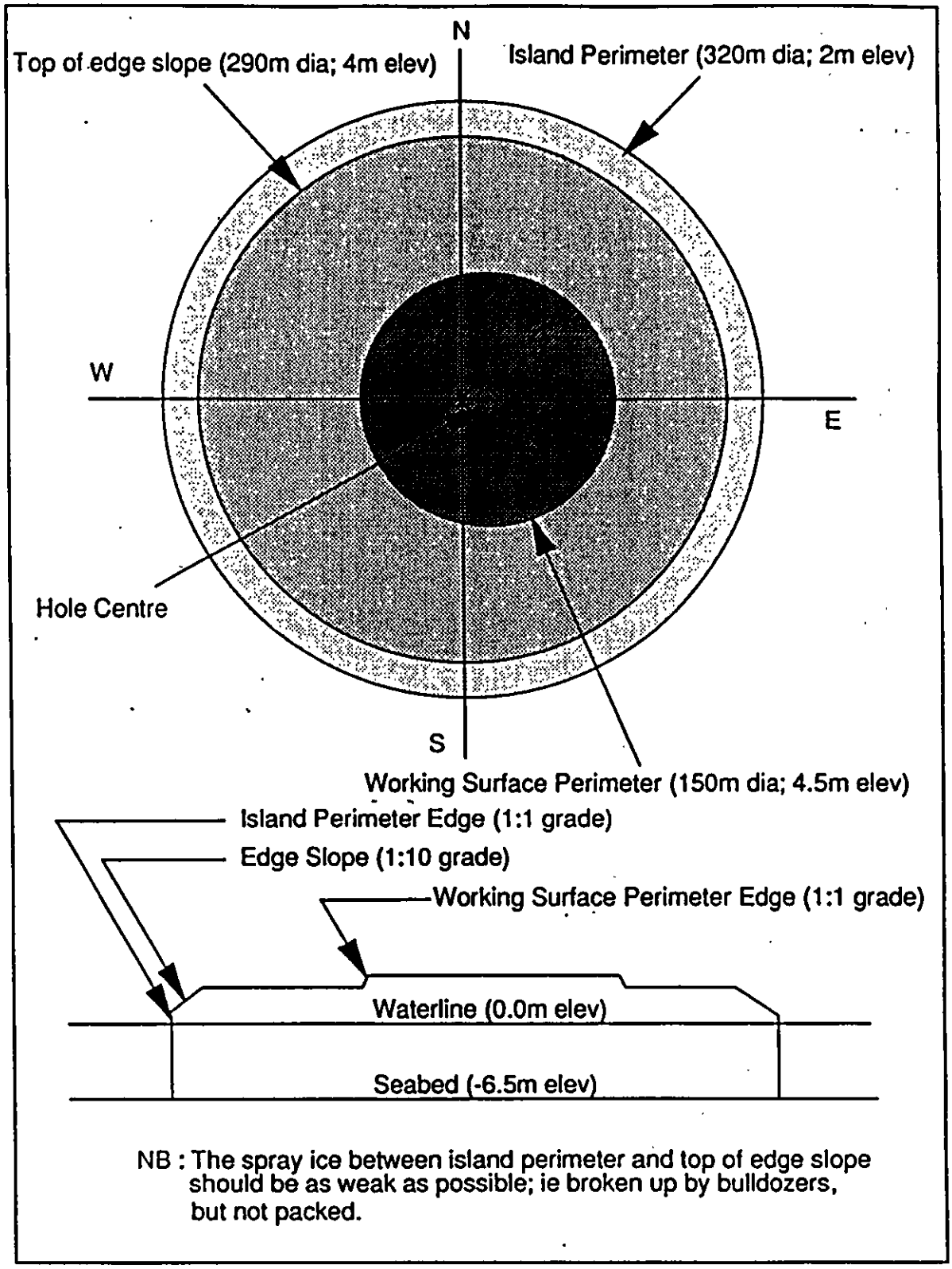

Figure 3. Island Design Geometery

positioning the pumps about 100 m from island center, directing spray toward the center, and using bulldozers (Caterpillars) to both pack and level the spray ice. Due to the roughness of the first-year ice sheet, the island grounded unevenly. This condition resulted in the formation of cracks which were subsequently filled with reworked spray ice. Finally, the remainder of the island was built to grade during the last phase of construction. Oblique aerial and ground-based island photographs are shown in Figure 4.

A spray ice volume of approximately 825,000 m^3 was required to complete the island. The island seabed contact (or grounded) area was estimated from about 125 thermal drill holes, 21 gravity penetrometer tests, and 13 cone penetrometer tests. An as-built contour map of the island is presented in Figure 5. The average freeboard over the 150 m diameter island working surface was 4.15 m. The remainder of the grounded region had an average freeboard of 3.73 m. Freeboard gradually diminished as the island settled. The amount of settlement between the end of construction (January 20) and the time of maximum design ice load (May 1) was estimated to be less than 0.5 m.

EXPERIMENT INSTALLATION

EXPERIMENT SITE SELECTION

Two options were considered during the early planning stages of the experiment. One option investigated was to protect a portion of the Nipterk island. The other option evaluated was to protect the relief well pad, a 125 m diameter spray ice feature built over a five day period in March, about 500 m east of Nipterk P-32.

There were a number of disadvantages identified with using the relief well pad. First, a road to the site was required. Second, bulldozers would have been needed to flatten the island surface since, unlike Nipterk, the relief pad was not leveled after construction. Third, between two and three times more tarp material would have been necessary to protect the relief pad than for a test section on Nipterk. And fourth, ablation measurements on the relief pad would have been unrealistic because the spray ice surface had not been soiled as a result of use.

Figure 4a. Oblique Aerial View of Nipterk on April 21

Figure 4b. Veiw of Island From Ice Level

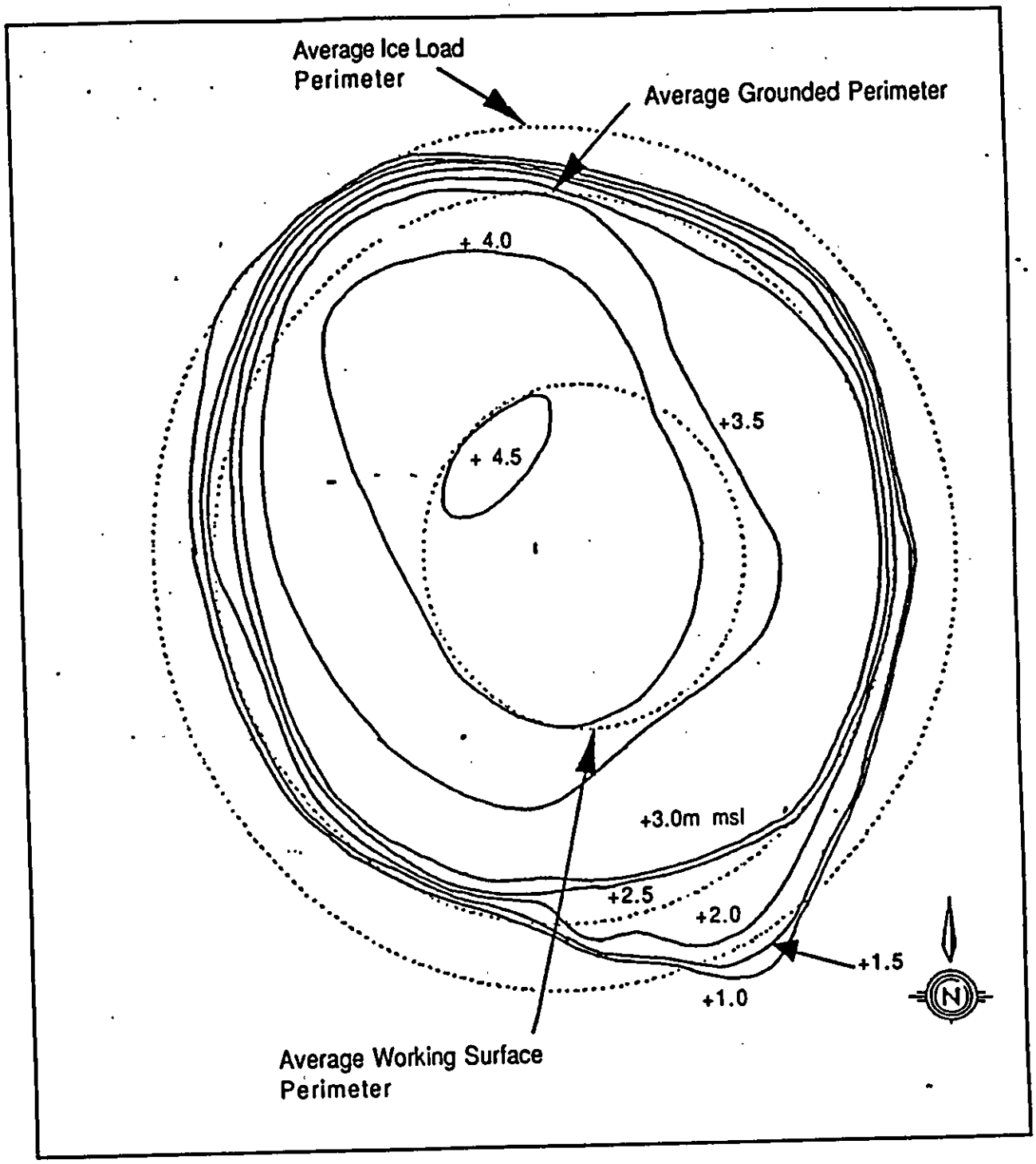

Figure 5. As-Built Contour Map of Island

Utilization of the Nipterk Spray Ice Island offered the following advantages. First, because of the island's size, different edge protection materials could be evaluated. Second, any benefit afforded by the edge protection system could be more easily assessed because most of the island edge was not protected. Third, personnel and equipment necessary for the experiment setup were more readily available and could be drawn upon on an as-needed basis, thus minimizing costs. Finally, instrumentation was already available on Nipterk from the winter monitoring program, enabling measurements of island sliding, settlement, and spray ice temperature to be continued. For these reasons, a decision was made to undertake the experiment on the main island.

INSTALLATION SCHEDULE/LOCATION

A relatively short lead-time existed for planning, procurement of materials and instrumentation, and experiment installation. These time-constraints were imposed by impending ice road closures both north and south of Inuvik as well as demobilization of the drilling rig along with support equipment and personnel. Table 2 is a schedule identifying the major milestones pertaining to the experiment installation.

A proposal describing the study was transmitted to industry and government on March 15. In the meantime, project planning was initiated, equipment suppliers contacted, and competitive bids obtained. Authorization to proceed with the project was received on April 5. Orders were placed immediately thereafter for all of the equipment required. Edge protection sheets were purchased from three suppliers to expedite delivery. Nets were assembled at the Esso Research Lab because they were not available commercially in the time frame required. Approximately 50% of the sandbags were filled in Calgary because gravel availability on the island could not be guaranteed at the time of edge protection system installation. Installation of the island edge protection systems and surface ablation test plots commenced on April 20 and was completed on April 25.

Any side of the island with the possible exception of the north would have been suitable to set up the experiment from a representative environmental condition standpoint. However, the area least affected by drilling operations was the

TABLE 2. EXPERIMENT INSTALLATION SCHEDULE

MARCH 15	-	PROJECT PROPOSAL
MARCH 27	-	DETAILED PLANNING STARTS
	-	TARP SUPPLIERS CONTACTED, COMPETITIVE BIDS OBTAINED
APRIL 5	-	PARTICIPANTS COMMITMENT - PROJECT GO AHEAD
APRIL 6	-	ORDER ROPE FOR NETTING
	-	ORDERS PLACED FOR 3 TARPS (3 SUPPLIERS)
APRIL 10	-	INITIATED NET FABRICATION AND SANDBAG FILLING AT ESSO LAB
APRIL 14	-	TRUCK LOADED AND SENT NORTH WITH ALL NETS, TARPS & SANDBAGS
APRIL 20	-	COMMENCE FIELD INSTALLATION
APRIL 23	-	GRAVEL AND SAWDUST DELIVERED TO ISLAND
APRIL 25	-	INSTALLATION COMPLETE WITH EXCEPTION OF ELECTRONIC INSTRUMENTATION

island's west-southwest side. Everything not needed for the experiment set up was removed from this location prior to April 20. The surface was smoothed and the snowbanks at the island edge leveled to facilitate deployment of the edge protection system.

EDGE EROSION PROTECTION SYSTEM

As illustrated in Figure 6, four edge protection systems were placed along the west-southwest perimeter of the island. They were installed to shield the island edge against thermal and mechanical erosion induced by wave action after break-up of the surrounding ice sheet and to mitigate surface ablation. These consisted of the following:

- •Net - a 50 m by 60 m, 1.5 m mesh size net consisting of 13 mm diameter white nylon rope.
- •Sheet 1 - 35 m by 50 m, 18 oz. per square yard white polyester reinforced vinyl with roped hems and D-rings on edges.
- •Sheet 2 - 35 m by 50 m, 13 oz. per square yard white polyester reinforced vinyl with roped hems and D-rings on edges.
- •Sheet 3 - 50 m by 60 m Rufco SB 12 white reinforced polyethylene tarp (pit liner).

The net was designed to hold back fragments of the island once they calved, thus mitigating at least for a while, the affects of wave erosion against the still intact spray ice. This system offered dual advantages of facilitated installation and potentially significantly lower cost especially if polypropylene rope were used and the net mesh spacing increased.

White 13 mm diameter nylon rope was used to manufacture the 50 by 60 m net. Even though the nylon rope was twice as expensive as polypropylene rope, its use

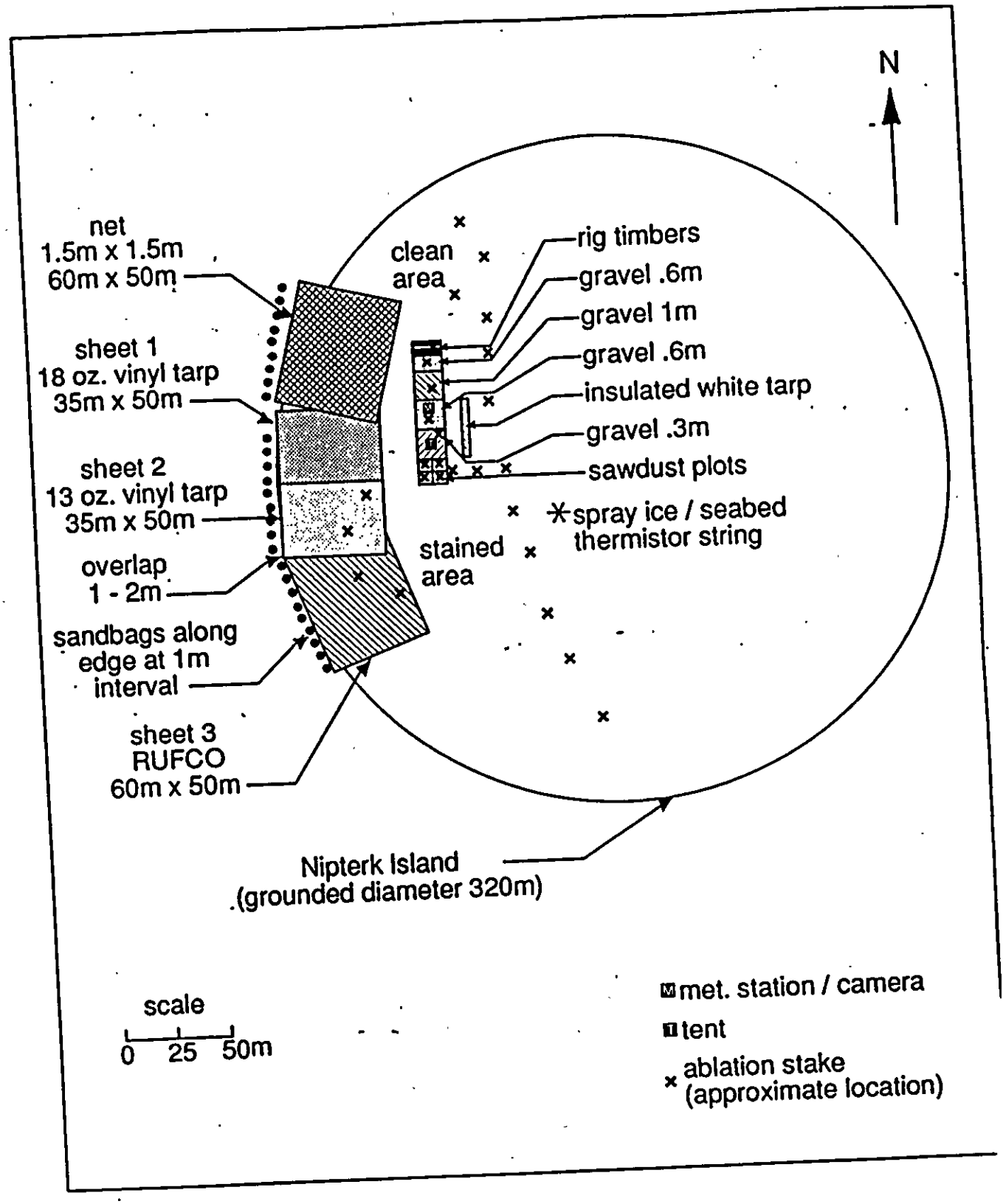

Figure 6. Island Protection System and Ablation Plot Layouts

was justified at the time based on ablation concerns regarding coloured material. No white polypropylene rope was available.

The purpose of the sheets was to isolate the island even further from wave erosion by placing an impervious barrier between the island and the sea. Two different weights of polyester were used to evaluate the abrasion resistance of the material (which was identified as an area of concern). A third type of sheet, the Rufco pit liner, was used to evaluate a less expensive option.

Both the sheets and net edge protection systems were extended just beyond the grounded edge of the island perimeter which was denoted by a crack (see Fig. 7). The net was relatively easy to deploy with five or six men. Contrastingly, because of their weight and stiffness characteristics in the cold, installation of the sheets required the assistance of a front end loader for handling and unrolling as well as an additional three to six men. Sheet installation took place during a period when winds were less than 10 to 15 knots. One factor which greatly facilitated stretching the sheets over the ice was the presence of entrapped air between the two surfaces.

Sheets were overlapped several meters inward of the island and 1 to 2 m outward of the island edge. Nets, consisting of 19 mm polypropylene rope forming 5 m by 5 m mesh were placed atop each protection sheet. 14 kg sandbags were attached loosely to the radial portion of the net, one at each node (see Fig. 8) to help hold the sheet in place. Sandbags were originally placed at about 2.5 m intervals along the island edge.

The inner edge (island center side) of the net was anchored into the spray ice. This was accomplished by attaching 10 m long ropes to the net and 0.5 m by 0.3 m by 0.3 m wooden timbers to the free end of each rope. A front end loader having an auger attachment (Fig. 9) was utilized to drill out 0.3 m diameter, 2-3 m deep holes into which the timbers (anchors) were lowered. Holes containing the deadmen were subsequently refilled with snow and saturated with water to form ice. To further reduce the potential for premature melt out, anchors were either buried beneath ablation plots or covered with 1 to 1.5 m high snow piles. The deadman served as anchors that were designed to melt out before the island broke

Figure 7. Sheet (foreground) and Net. Edge of Grounded Island Perimeter Denoted by Crack.

Figure 8. Close-up of Sand Bag Attachment.

Figure 9. Front End Loader Equipped With Auger Drilling a Hole for the Anchor

up to facilitate recovery of the sheets. Piles of snow were also placed along the south edge of the Rufco sheet and atop edges of the other sheets.

ABLATION TEST PLOTS

Test plots designed to assess spray ice ablation were constructed following deployment of the island edge protection systems. A number of different plots of various sizes and configurations were created at the inner edge of the sheets and net (see Fig. 6). These consisted of the following:

- Sawdust — 1 cm, 1.5 cm, 2 cm, 3 cm and 15 cm thick bags.
- Gravel — Thicknesses of 0.3 m, 0.6 m, and about 1 m. Each plot was approximately 180 m^2.
- Simulated Rig Mats — 20 cm by 20 cm timbers placed side by side to simulate rig mats.
- Insulated Tarp — Reinforced white vinyl having dimensions 30.5 m by 2.4 m.
- Sheets — Rufco and 13 oz. per square yard polyester reinforced vinyl.
- Ice — Unprotected spray ice; both clean and stained.

Approximately 425 m^3 of gravel was hauled to the island from a surplus stockpile located about 30 km to the southwest on Garry Island. Once dumped onto the island surface, the gravel was leveled by a front end loader to the desired thicknesses (0.3, 0.6, and 1 m) over areas of about 12 by 15 m.

A 15 m by 15 m sawdust ablation plot was constructed by hand using four pallet boxes of sawdust available from the drilling program. A number of subplots were created to (see Fig. 10) evaluate the degree of surface ablation protection afforded by different thicknesses of sawdust ranging from 1 to 15 cm. At the time the

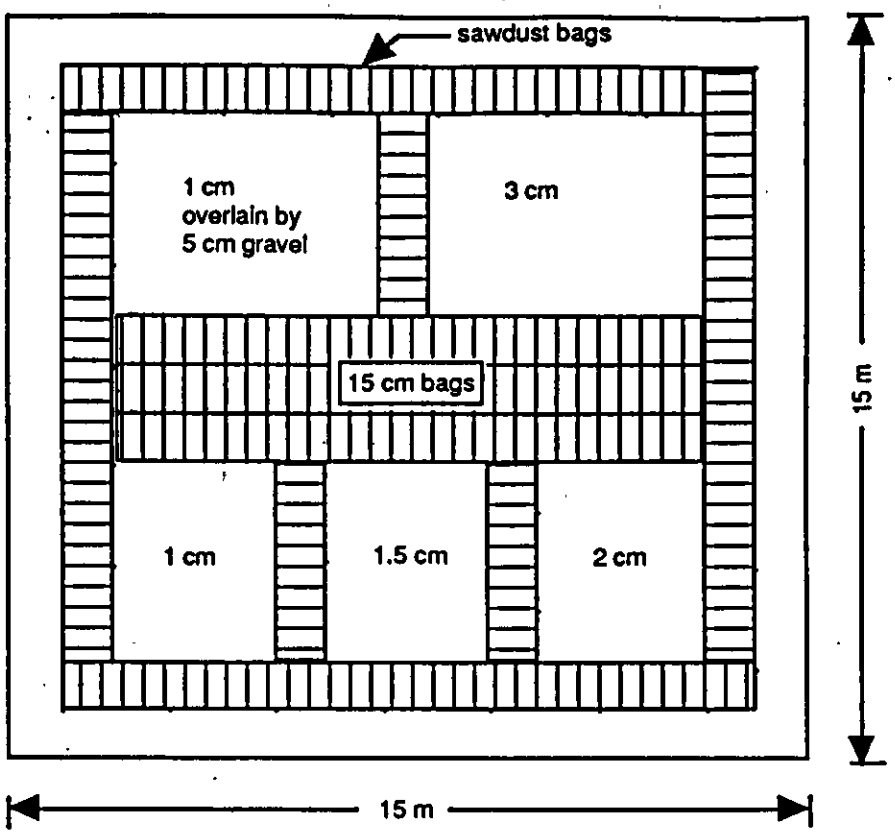

Figure 10. Layout of Sawdust Ablation Test Plots

subplots were being constructed, the extent to which the sawdust would be blown away by wind was not known. To gain an understanding of the insulating qualities of the sawdust even in the event plots were adversely affected by wind, two subplots were constructed in a different manner. In one subplot, the sawdust was retained in bags while in the other, a 1 cm veneer of sawdust was held in place by 5 cm of gravel.

The insulating capabilities of rig mats were simulated in another surface ablation test plot prepared adjacent to the gravel plots. Rig mats were not used due to costs and environmental (recovery) concerns. Rather, the rig cellar which consisted of 20 by 20 cm timbers was dismantled and the timbers placed side by side atop the spray ice. At the conclusion of the project it was planned to dispose of the timbers by burning them on site.

Lastly, the ablation protection afforded by a white insulated tarp having dimensions 30.5 m by 2.4 m was evaluated. This tarp was placed atop the spray ice in front of the gravel ablation plots. The tarp was held in place by sandbags.

Surface Ablation Measurement Stakes

Once the island edge protection system and surface ablation test plots were in place, 35 - 5 cm by 5 cm by 4.9 m long graduated wooden ablation stakes were inserted into the island using a thermal ice drill to create the 5 cm diameter hole required. Attempts were made to install the stakes so that they extended between 0.25 and 0.75 m above the island surface. In some instances, the hole created for the ablation stake was too deep. For these cases, snow and/or gravel was dropped down the hole to shorten it. To ensure that the stakes did not slip into the hole a level survey was performed. Subsequent surveys confirmed that no stake slippage had occurred.

A total of 15 ablation stakes were placed into the unprotected spray ice. Roughly one-half of these were in clean spray ice whereas the remaining stakes were placed in spray ice where the surface had been stained as a result of previous activity on the island. The remaining 20 stakes were placed in ablation plots and beneath the Rufco and 13 oz. per square yard vinyl edge protection sheets.

Additional Instrumentation

Several types of instrumentation were deployed and/or utilized from the winter island stability alert program. A 24 bead thermistor string which measured the spray ice and seabed temperature profile was left in place and read manually. Another 12 bead string previously used to measure spray ice temperature under the rig was placed beneath a number of ablation plots to monitor warming. Ice temperatures measured by this string were collected automatically by a Campbell Scientific 21X Data Logger at a sampling frequency of one hour. Data collected from this thermistor string were used to further assess the insulating characteristics of the materials used in the ablation plots.

An environmental enclosure housed a time-lapse video camera system that was set up, but not turned on due to the cold ambient air temperature prevalent at the time. The purpose of the camera was to document surrounding ice conditions, wave state, and performance of the edge protection sheets following breakup of the surrounding ice sheet. A meteorological station was erected to measure wind speed, wind direction, air temperature, and incoming solar radiation, but was not hooked up to a data logger at this time.

Finally, the five Sondex settlement and slope indicator stations originally installed in January were left in place so that measurements could be continued. Locations of these stations are shown in Figure 11. Initial (baseline) settlement and inclinometer surveys were performed on April 22.

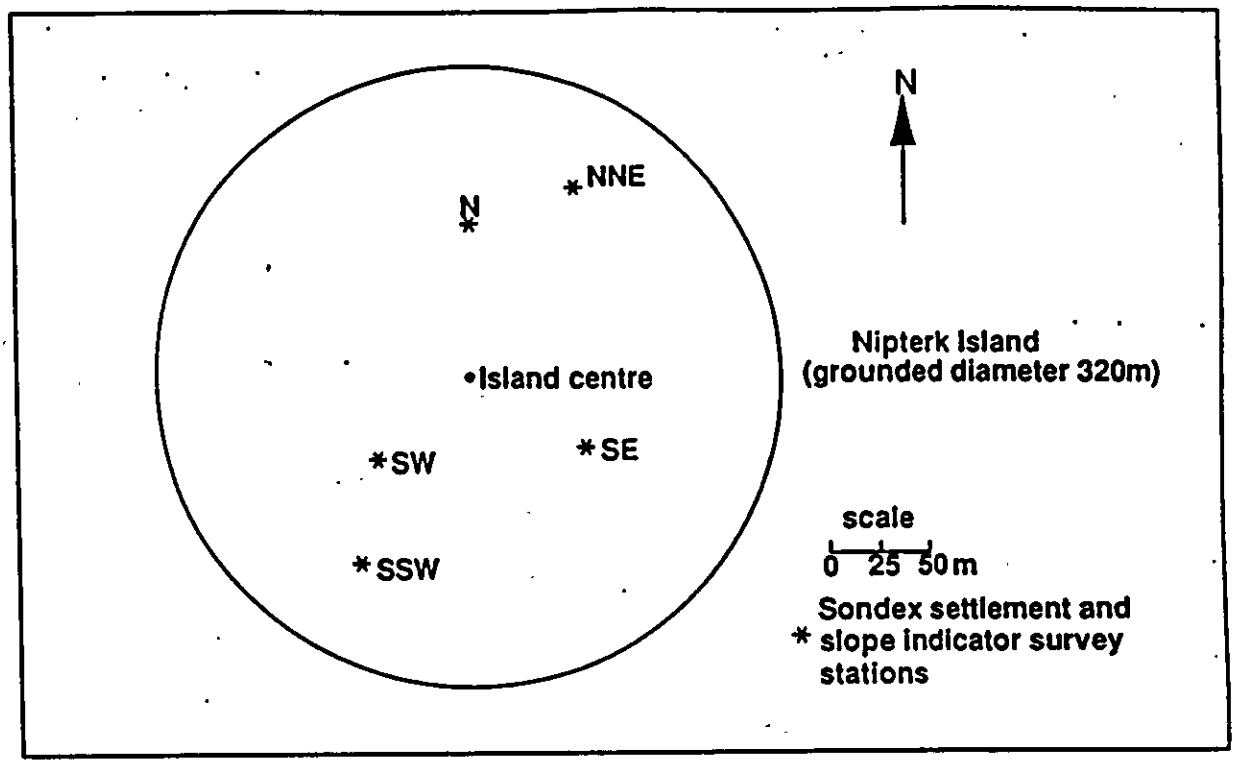

Figure 11. Sondex Settlement and Slope Indicator Survey Stations

MONITORING SURVEYS

Field monitoring surveys were carried out primarily by Esso personnel with occasional assistance provided by participating company's representatives. One survey of limited scope was undertaken for us by our helicopter pilot. The aerial photography survey was performed by Inuvik-based Photo Script Ltd.

A timetable showing the dates of the monitoring surveys as well as those for other experiment milestones is presented as Figure 12. Six comprehensive surveys were undertaken between April 22 and July 5, inclusive. Except for the initial (reference) survey which was undertaken over the course of three days, monitoring surveys typically consisted of an 8-10 hour period on the island during which the following information was collected:

- General documentation of the surrounding ice conditions
- Island settlement (Sondex) and horizontal deformation (inclinometer readings)
- Surface ablation measurements in the unprotected spray ice and ablation test plots
- Performance evaluation/erosion rate observations associated with the island edge protection system
- Spray ice/seabed temperature profile
- Spray ice temperature measurements beneath ablation plots
- Meteorological conditions (wind speed, wind direction, air temperature, and solar radiation)
- General description of the spray ice surface (size, extent, and orientation of cracks, trafficability, degree of deformation)
- Aerial and surface photographs, and
- Condition of the ice road

Shorter duration visits to the island during which general conditions were described and/or the functionality of various instrumentation confirmed are identified in the Figure as brief surveys. Several of these trips were combined with island cleanup and inspection trips to minimize costs.

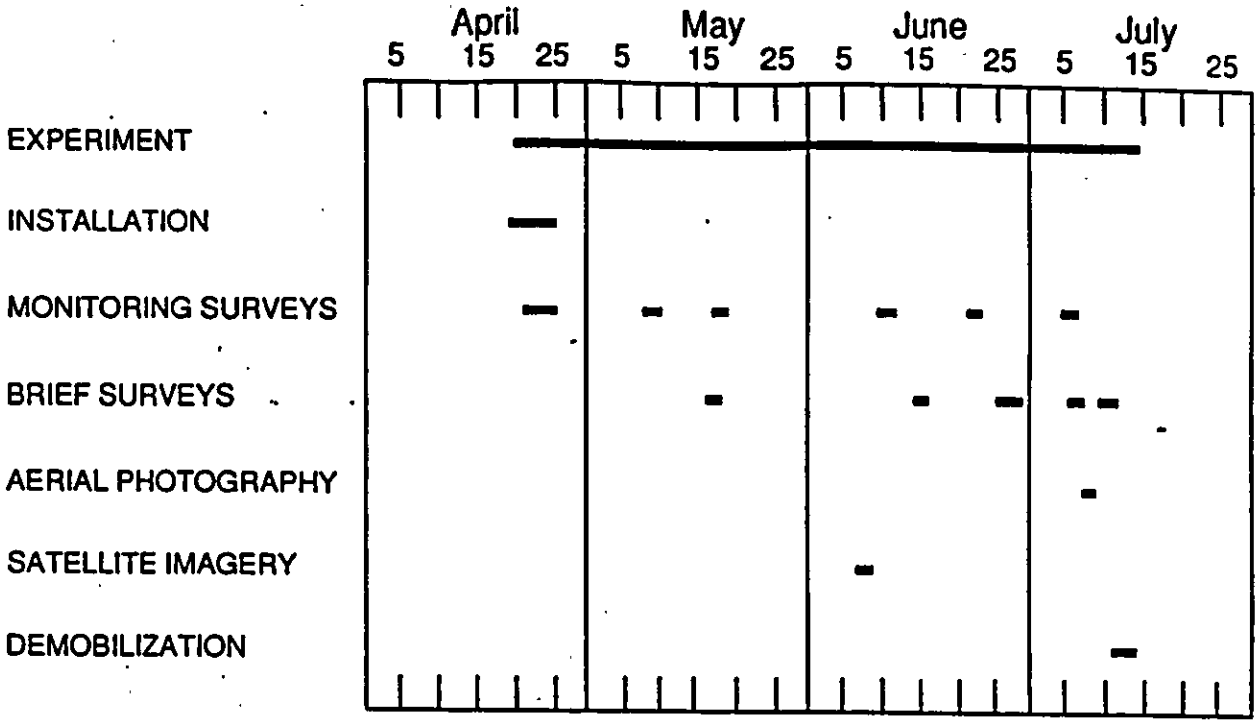

Figure 12. Experiment Timetable

RESULTS

METEOROLOGICAL CONDITIONS

Meteorological data (i.e. wind speed, wind direction, air temperature, and solar radiation) are important because they are used in the analysis of surface ablation and island erosion. During the course of the experiment, meteorological data were gathered from two sources. These were: Tuktoyaktuk, some 140 km to the east of Nitperk and from measurements taken on the island. These data are provided in Appendix A.

Wind speed, wind direction, and maximum and minimum air temperature data were relied upon exclusively when our met station was not yet in operation early in the program and between the period July 5 until island breakup. Tuk wind speed and direction data are recorded at six hour intervals whereas maximum and minimum air temperatures represent a 24 hour period. From June 7 through July 5, wind speed, wind direction, air temperature, and solar radiation were measured on the island at 15 minute intervals. These data were recorded by a Campbell Scientific 21X data logger.

Wind speed and direction were monitored by a RM Young 05103 wind monitor. The wind speed sensor is an injection molded helicoid-shaped propeller. Vane positioning was transmitted to a precision conductive plastic potentiometer located in a sealed chamber just below the wind speed transducer coil. Air temperature was measured by three thermistors and the Data loggers' sensor at hourly intervals. These data were also collected by the data logger. The air temperatures were then averaged.

A LI-COR LI-200SZ pyranometer sensor was used to measure solar radiation. The instrument is suitable for measuring global sun plus sky radiation. Output from the sensor to the logger was in terms of voltage (millivolts). This output was eventually converted to units of kWm^{-2}.

A comparison of Tuk and island wind speed data revealed that they were similar. Island wind directions were also found to compare favorably with those measured in Tuk. Plots of wind speed and direction are provided in Appendix A.

Figure 13 is a plot of average daily air temperature. The data set utilizes air temperatures measured on the island whenever they are available. Prior to landfast ice sheet breakup, air temperatures measured on the island were generally similar to those observed in Tuk. Following breakup, island air temperatures were usually less than those recorded in Tuk due to the influence of the water and in some cases ice near the island. On the other hand, the island did not receive the degree of warming that Tuk was subjected to as a result of land-derived winds due to its distance offshore.

As can be seen from the figure, average daily air temperatures rose above 0°C on May 25 and consistently remained above freezing thereafter. The arrival of above-freezing air temperatures was associated with a warming of the spray ice surface which eventually manifested itself in the onset of surface ablation. Historical daily average temperatures for Tuk are shown in the figure for comparison. From these data, it is apparent that the temperatures observed on the island were typical and that it is reasonable to expect that spray ice surface ablation will commence sometime during the latter part of May when planning future operations.

A plot of solar radiation over time is shown in as Figure A2 in Appendix A. Solar radiation varied for a number of reasons, including cloud extent, cloud thickness, surface albedo, and solar zenith angle.

ICE TEMPERATURE

Spray ice/seabed temperatures were measured by an 11 m long thermistor string deployed adjacent to the southwest Sondex/Slope Indicator survey station (75 m from island center). The thermistor string was installed in January as part of the winter island performance monitoring program undertaken in support of exploration drilling. The configuration of the string is illustrated in Figure 14. As can be seen the string was made up of 24 thermistors whose spacings varied.

The lowermost portion of the string consisted of a plastic cone tip which was driven 1 m into the soft seabed. For this portion of the string, 11 thermistors were

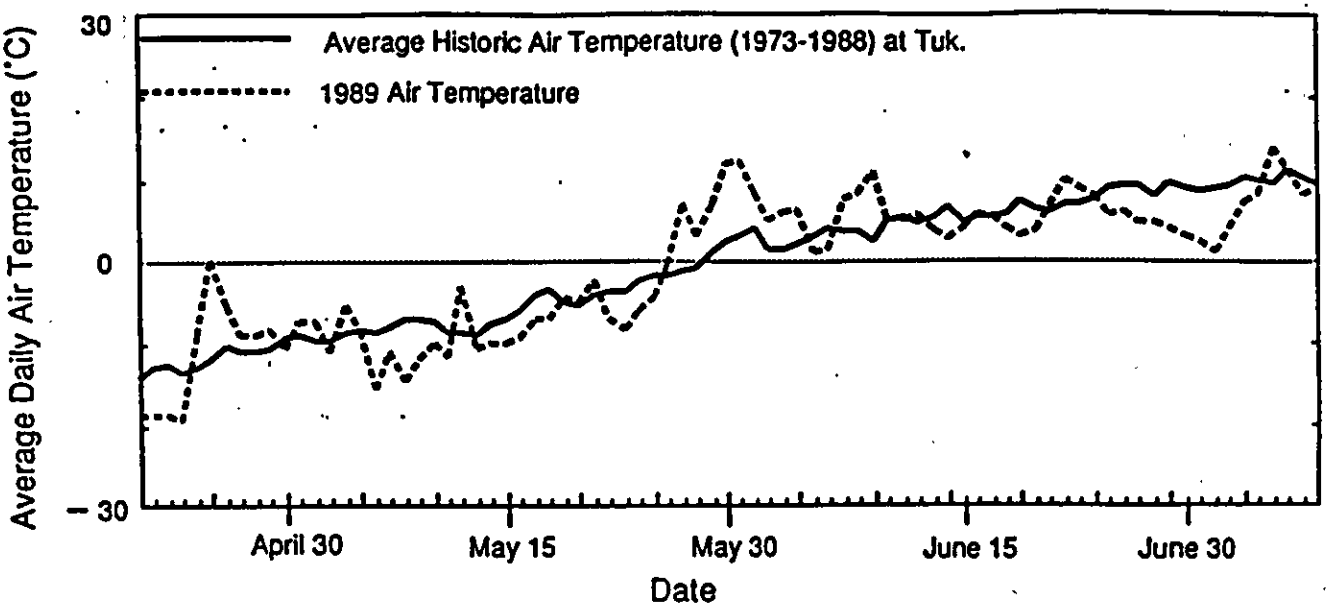

Figure 13. Comparison of 1989 and Historical Air Temperatures. 1989 Temperatures are Based on Island Measurements Supplemented with Data from Tuktoyaktuk

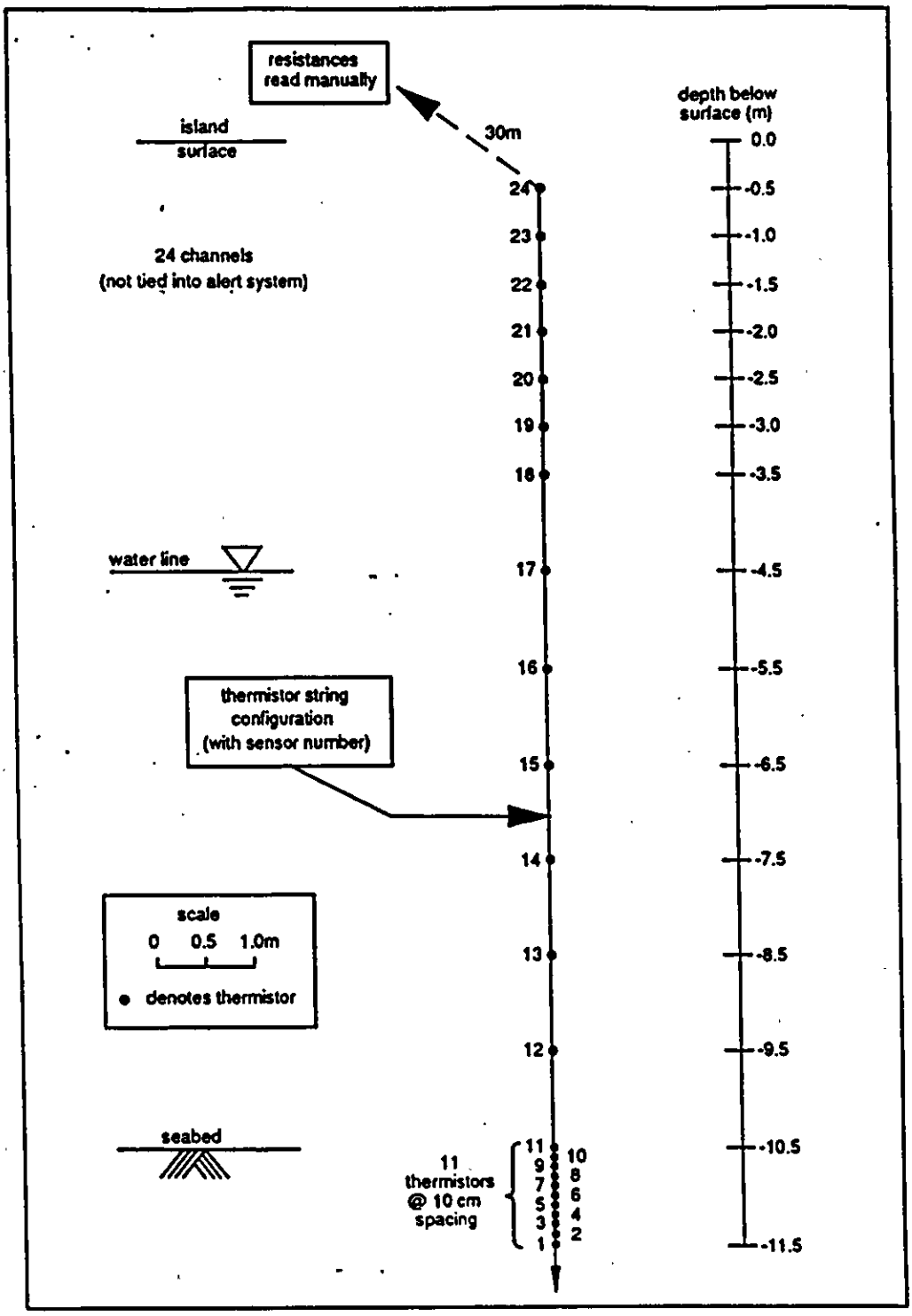

Figure 14. Configuration of Spray Ice / Seabed Thermistor String

spaced at 10 cm intervals. Contrastingly, temperature of the submerged spray ice was measured at 1 m intervals whereas in most of the freeboard, the thermistor spacing was 0.5 m.

Yellow Springs Instrument Company (YSI) Model 44007 thermistors were used. These thermistors, sensitive to temperatures over the range -80° (3684KΩ) to 150°C (92.70KΩ) had an interchangeability of ±0.2°C.

Thermistor resistance readings were taken on April 22, May 9, May 18, June 10, and June 22 (Appendix B). Temperature profiles (for all but June 22) are shown in Figure 15. The abscissa represents ice temperature in degrees Celsius and the ordinate represents the depth in meters measured from the ice surface at the time of thermistor string installation. The ice surface locations at the time of subsequent measurements are also plotted.

Three thermal regions can be distinguished from the profiles: the above-water ice, submerged ice, and seabed. Up until June 10, the lowest ice temperatures were associated with the above-water ice. Over the period April 22 to June 10, the ice in this zone increased from a minimum of about -13°C (at a depth 0.5 m below the surface) to near 0°C on June 10 in response to warmer air temperatures and the ablated ice surface. The average temperature rise for this period was 0.28°C day^{-1}.

The submerged ice temperature remained reasonably constant with time. At the water table to a depth of nearly 4 m below it, the ice temperature was about 0°C. Below this level to the seabed, the ice temperature decreased to about -1°C probably due to the presence of brine. Seabed temperatures tended to remain constant over time. Near the surface of the seabed, the temperature was about -1°C increasing to -0.5°C, 1 m below the seabed.

WATER TEMPERATURE

The water column temperature profile was measured in mid-November, 1988 whereas the surface water temperature was measured on July 11, 1989, one day after island breakup. At the time of the November survey, water temperatures

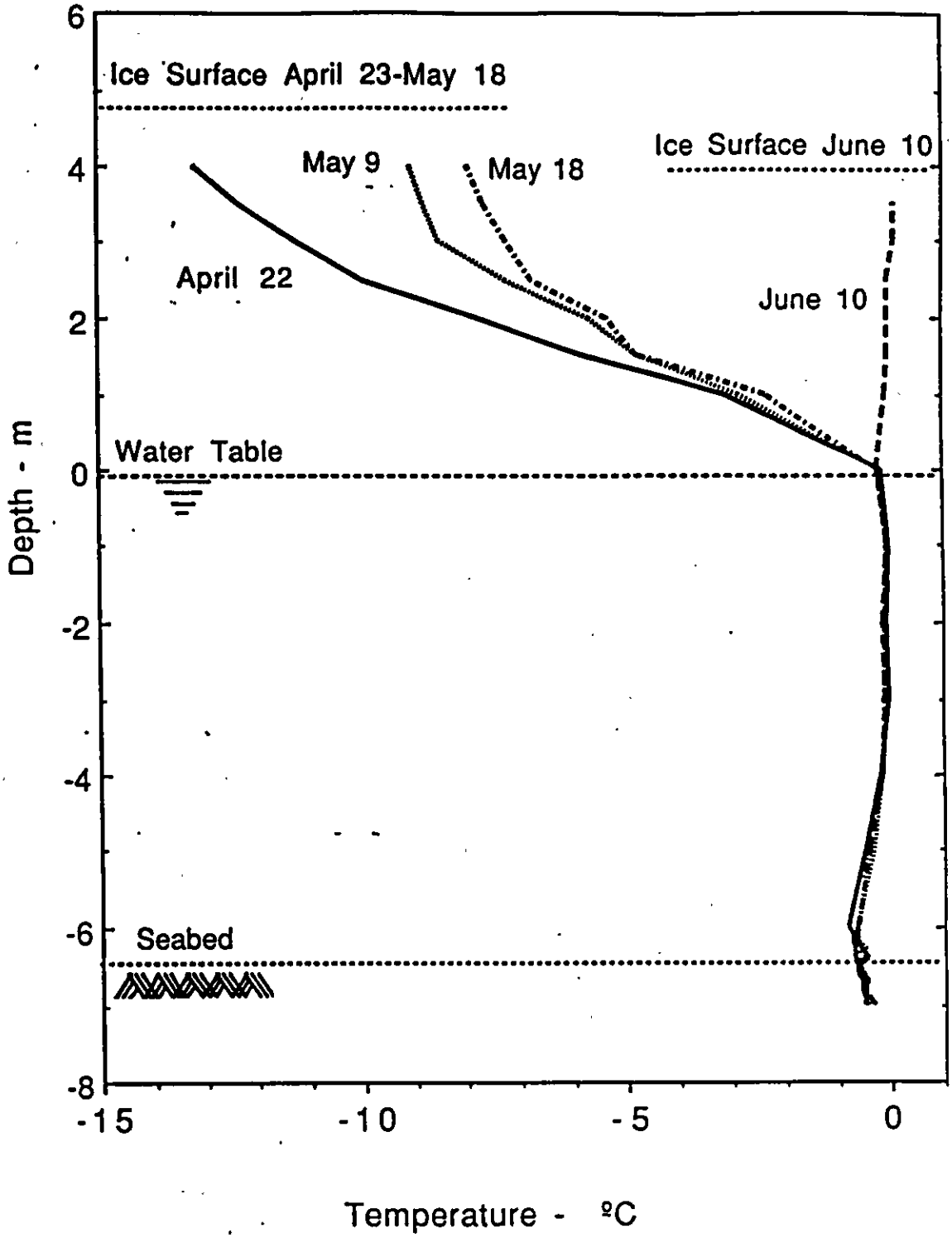

Figure 15. Spray Ice/Seabed Temperature Profiles

ranged from about 0°C in the freshwater layer (surface to a depth of 4 m below the surface) to about -1°C in the underlying saline (15 ppt) layer. For comparison, the water temperature at a depth of 0.3 m was 12°C on July 11 which is attributed to Mackenzie River outflow. It is anticipated that much of the water column was at or near this temperature due to the degree of mixing associated with the Mackenzie outflow. The effects of the relatively high water temperature on the island are discussed under the section: Island Erosion.

SURFACE ABLATION

Net ablation experienced by a spray ice island during the melt season can be characterized by solving an energy balance equation such as the following:

$$F_r + F_l + F_s + F_e + F_w + F_c + F_i = F_a \qquad (1)$$

Where:
- F_r = net solar radiative flux
- F_l = net long wave radiative flux
- F_s = sensible heat flux
- F_e = evaporative heat flux
- F_w = heat flux from wave action
- F_c = heat flux from forced convection
- F_i = conductive heat flux, and
- F_a = heat absorbed by melting ice

This equation was adapted for spray ice islands by Connolly [1], based on a solution to the energy balance equation developed by Maykut and Untersteiner [2] for natural growth of sea ice in the central Arctic and adding terms used by El-Tahan et al. [3] in modeling iceberg detection. The evaporative heat flux term represents heat either released or absorbed as a result of water evaporating, ice sublimating, or to condensation. According to Connolly [1], this term can be essentially ignored during the melt season since these processes are much slower than others associated with ablation processes. Forced convection and wave action are processes described in the section entitled: Island Erosion.

Figure 16 is a diagram showing the energy transfer parameters. Processes responsible for energy transfer in only one direction are denoted by an arrow pointing in that direction whereas processes responsible for incoming and outgoing energy are denoted by arrows in both directions. Note that outgoing fluxes are negative.

Albedo is defined as the ratio of reflected to incident shortwave radiation. Spray ice albedo decreases after construction and as the melt season progresses due to the accumulation of dust and debris on the surface, largely from the drilling operation. However, the addition of foreign materials on the island surface does not necessarily increase the melt rate since an insulating layer can be formed that actually protects the surface. Consequently, materials, debris, etc. on the island surface will act to reduce the melt rate below its naturally occurring value if sufficient material is present as demonstrated in the surface ablation studies.

Loss of island freeboard was monitored with ablation stakes. Stakes were placed at locations in the "clean" and "soiled" unprotected spray ice, in ablation test plots, as well as in two of three edge protection sheets. Ablation stakes were confined to the west half of the island so that they would not be destroyed during the ensuing island cleanups.

Stakes were graduated at 10 cm intervals starting from the top. The visible stake length from the top of the stake to the spray ice surface was measured during each site survey. Initial baseline measurements were recorded on April 23 and subsequent surveys were undertaken on May 9, June 10, June 22, and July 5. (Measurements were not taken during the May 18 survey due to extensive drifting snow which had accumulated over the western half of the island, obscuring many of the stakes). The differences between initial and subsequent measurements yielded the magnitude of ice surface ablation at a particular location.

Unprotected Spray Ice

Average cumulative surface ablation of the unprotected spray ice (in centimeters) as a function of time is plotted in Figure 17. Individual ablation stake

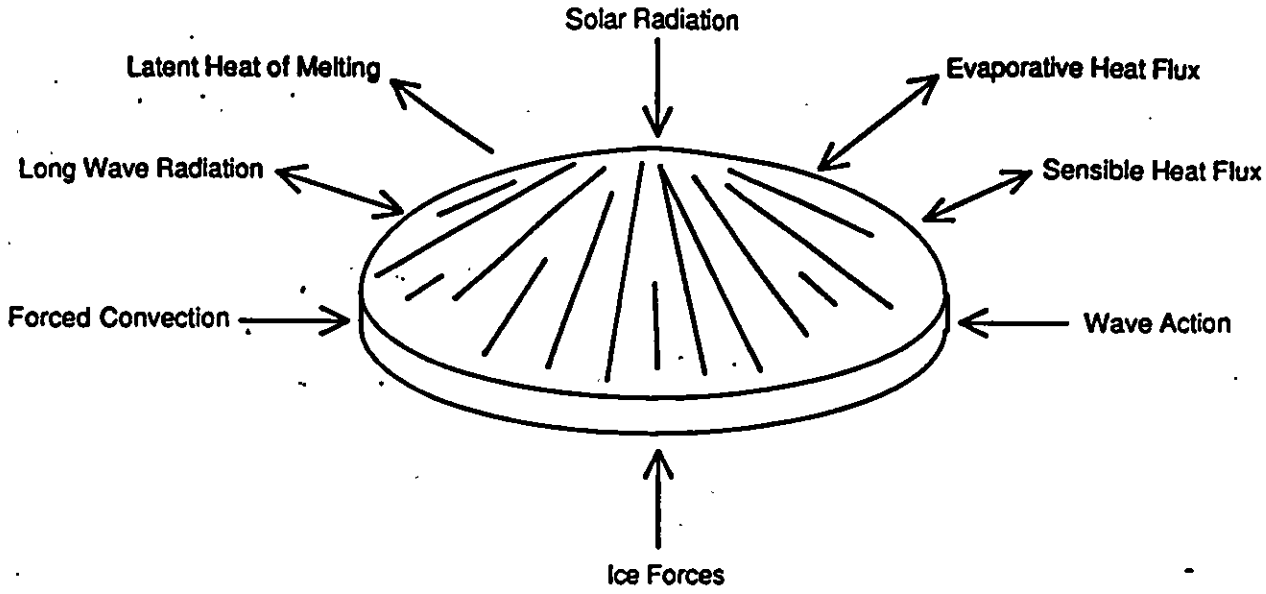

Figure 16. Energy Transfer Parameters. From Connolly [1].

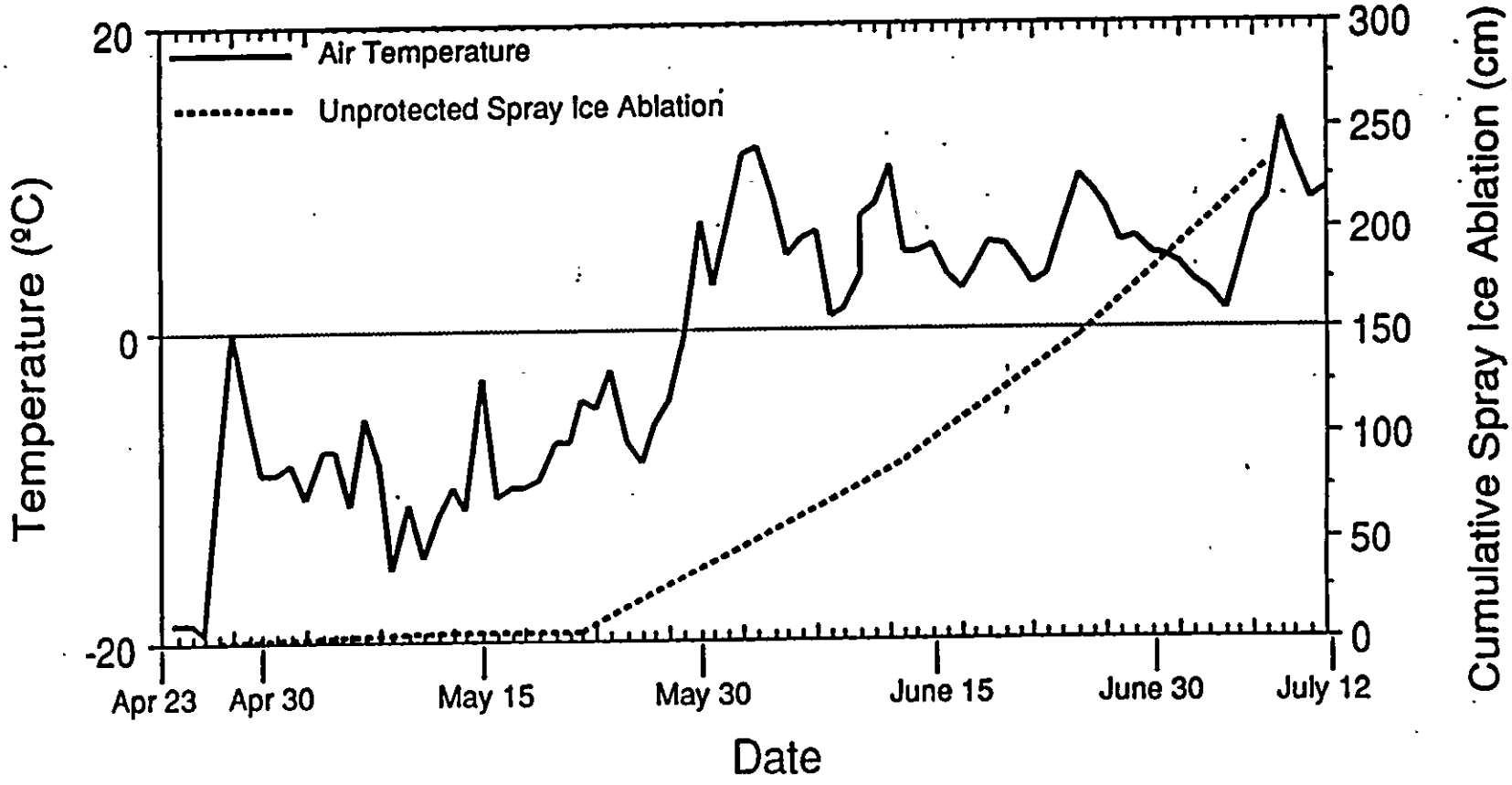

Figure 17. Cumulative Ablation of Unprotected Spray Ice

measurements are provided in Appendix C. Ablation was computed from measurements at 15 unprotected spray ice survey stake locations. Also shown are the average daily temperatures for the study period.

Up until air temperatures consistently exceeded 0°C (the last week of May) the most significant spray ice ablation was observed in areas where the surface had been soiled such as in vicinity of the rig and heavily trafficked areas. This was due to the absorption of solar radiation by debris-laden spray ice which hastened ablation.

Similar observations have been reported in published literature. Warren and Wiscombe in Colbeck [4] noted that small highly absorbent particles are capable of reducing snow albedo from 5 to 15% even in quantities as low as 1 part per million. According to Colbeck [4], there appears to be a consensus among investigators that the persistence of the effect of albedo reduction decreases with time, but that the rate appears to vary significantly depending on several factors such as the size of material used and the surface over which it is spread. Snow (spray ice) surfaces would be expected to retain the effect longer, especially for smaller particles.

Ashwell and Hannell [5] noted that ablation was weather-dependent from a standpoint of conditions being overcast with winds or calm and sunny. This distinction according to Colbeck [4] correlates well from the mechanisms involved. That is, either mostly convective heating in the former case or radiative heating in the latter. Rhodes et al. [6] reported that when solar input is restricted, the optimum thickness of the dark layer required to enhance melting is only about 1 mm depending on the nature of the controlling parameters including the type of material. The optimum thickness of the dark layer to enhance ablation was reported to range from 3 to 24 mm by a number of other investigators cited in Colbeck [4]. The optimum thickness to enhance melt was influenced by weather conditions and the type of material used. Finer materials appear to insulate better than coarser materials as they can be more finely dispersed. According to Colbeck [4], the optimum thickness of the dark layer required to promote melting increases absorption much more than it increases thermal insulation. Once a sufficient thickness is obtained, the insulative effects become more important

than increased solar absorption resulting in a melt rate that decreases below its natural value.

One means of reducing the amount of surface meltback in heavily soiled areas that was demonstrated to be extremely effective on Nipterk when air temperatures periodically exceeded 0°C was to cover the spray ice with a thin layer of clean snow. This operation was performed routinely in the vicinity of the drilling rig in early April during a warm spell when air temperatures exceeded 0°C, skies were sunny, and winds calm. Covering the spray ice with a clean layer of snow to slow melting even worked well in highly trafficked areas though the snow required grooming at periodic intervals. The benefit of using fresh snow to eliminate the effect of dark materials has been previously reported in public literature (see Colbeck [4]).

Addition of the snow layer was accomplished by a loader with a bucket. Snow was first dumped over a large area and smeared to a 3 to 5 cm thickness.

By early June, the debris-layer which had earlier promoted melting had reached sufficient thickness that it proved to be an effective insulator, thereby mitigating spray ice ablation. Areas overlain with as little as 0.5 cm of soiled material were observed to have reduced surface meltback by up to 1 m on June 10 as evidenced by a number of hummocks (see Fig. 18). A set of annotated slides showing examples of ablation and erosion is provided in Appendix D.

Cumulative average ablation prior to May 18 was only 3 cm which represents an ablation rate of 0.84 $cmwk^{-1}$ for the period April 23 to May 18. Significant ablation occurred sometime after May 18 (probably commencing the last week of May based on air temperature data) as the average ablation rate for the period May 18 to June 10 was 25.3 $cmwk^{-1}$. Ablation intensity increased to an average of 35.0 $cmwk^{-1}$ during the interval June 10 to July 22. The most severe ablation was documented for the period June 22 through July 5 when the average ablation rate was 45.2 $cmwk^{-1}$. This surface meltback rate increase may have been partly attributed to rain which was observed to have fallen over a prolonged period in late-June.

Figure 18. Hummocks, June 10

Colbeck [4] reported that the dominant energy fluxes are at the upper surface for glacial firn and deep snow covers. This is also the case for the ice island during the winter. These fluxes are dominated by radiation as well as sensible and latent heat fluxes. On the other hand, Colbeck suggested that for shallow snow covers, ground heating needs to be considered and input from rain can be important. It is apparent that this is the case for the spray ice island as temperatures approach and then rise above freezing. The ground heating though would be dominated by the temperature of the surrounding water, which would result in enhanced ablation at the perimeter of the island.

The average cumulative ablation of the unprotected spray ice was 2.3 m. The maximum cumulative ablation at one location was 2.8 m in an area where the island surface was soiled. Although the highest magnitude of ablation was identified at one ablation stake in this area, the average cumulative ablation measured at a number of locations in this dirt-contaminated region was essentially the same as that measured for the "clean" spray ice. The least amount of ablation of the unprotected spray ice, 1.8 m, was measured near the base of the sawdust test plots.

With the onset of warmer air temperatures and ablation, changes were noted in spray ice surface characteristics. Through the early part of the experiment when below freezing air temperatures predominated, the spray ice surface was hard and crusty. Because of its permeability, the spray ice surface allowed melt water to drain vertically. Due to the effects of warming, the uppermost island surface softened to the extent that it could be dislodged with a boot into particles typically less than 0.5 in diameter.

Over time, surface cracks which at the time of island construction had been filled with reworked spray ice were visible. Most of the major cracks were located near the edge or outside the working surface. Once surface ablation became so extensive that less than 1 m freeboard remained, new cracks developed as parts of the island became buoyant.

Ablation Test Plot Measurements

As previously mentioned, in addition to documenting ablation of the unprotected spray ice, ablation was measured in the test sections of a variety of materials to assess their effectiveness with regard to mitigating surface meltback. These materials included sheets, tarps, timbers, and various thicknesses of sawdust and gravel. Ablation stake measurements from each of these test plots are provided in Appendix C.

Sheets and Insulated Tarp

The effectiveness of the sheets and insulated tarp in protecting the spray ice is demonstrated in Figure 19 which compares cumulative spray ice ablation with time. Surface ablation of the unprotected spray ice is also shown. Both the 13 oz. nylon sheet and the Rufco sheet had the effect of cutting the ablation rate by about one-half that measured for unprotected spray ice. The insulated tarp further enhanced protection of the spray ice. Over the course of the measurement period, the average cumulative ablation was only 0.5 m, compared to 0.85 m for the Rufco sheet and 1.25 m for the vinyl sheet. The ablation reduction benefits afforded by the sheets are attributed to a combination of the increased albedo and the insulating effects provided by the entrapped air layer between the surface of the ice and the sheet.

Because ablation data were collected at only two locations in areas covered by each sheet, it is not possible to establish with certainty whether the Rufco sheet actually provided insulating qualities superior to those of the 13 oz. vinyl sheet. Although the two spray ice ablation stakes beneath the Rufco sheet revealed less overall surface meltback than was observed under the vinyl sheet, there was a greater variability between locations. Up to a 30 cm difference was found between the Rufco ablation stakes compared to a total ablation difference of 10 cm exhibited by measurement locations beneath the two vinyl sheets. On the other hand, the superiority of the insulated tarp at mitigating ablation was supported by nearly identical measurements at three locations. Moreover, the ablation rate associated with the insulated tarp remained more uniform with time than the sheets. And finally, the average ablation rate associated with the insulated tarp (1.5 $cmday^{-1}$)

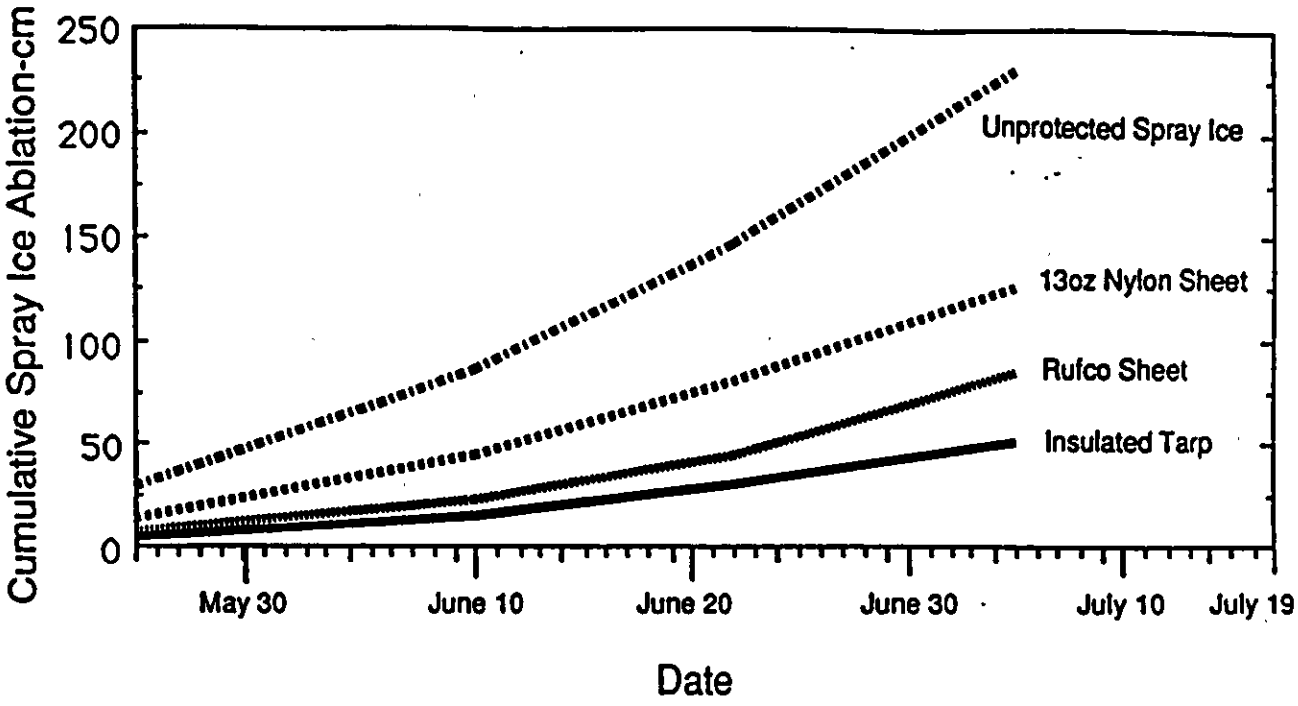

Figure 19. Sheet/Tarp Ablation Mitigation Comparisons

during the latter stages of the measurement period was less than half that (3.1 to 3.5 cmday^{-1}) measured by the sheets.

By June 10, all of the snow which had accumulated on the sheets had melted. This snow melt and subsequent rainfall accumulated in depressions which grew in size throughout the program (see Figure 20) because the meltwater thawed the underlying spray ice. No attempt was made to drain the water as it served to further hold the sheets in place. As the melt season progressed, the degree of spray ice degradation became so extensive that pools developed. The largest was roughly 15m in diameter, 4m deep, and contained two meters of water. Thus it is evident from an operational and an island stability context that draining the water at some point in time is desirable.

Sawdust Plots

Six subplots were constructed as part of the 15 m by 15 m sawdust ablation plot system to quantify the effectiveness of sawdust as an insulating material. Under operational conditions, wood chips rather than sawdust would likely be the form of wood product used. However, sawdust was utilized in this study because it was available on-site at minimal cost to the project.

Subplots consisting of 1, 1.5, 2 and 3 cm thick layers of sawdust were constructed. The remaining two subplots consisted of 15 cm thick sawdust bags and 1 cm of sawdust blanketed by approximately 5 cm of gravel to insure that the sawdust remained in place. The latter configuration was investigated because a more durable surface would be required to support even limited island operations. Sawdust bags were placed around each subplot and ablation stakes positioned in the center of each subplot to isolate as much as possible, the impact of ablation at one subplot from that of a neighboring plot. Sawdust bags were also placed along the outside edge of the ablation plot to retard spray ice meltback in this region with the onset of summer. A photograph of the test plot taken on July 5 is presented as Figure 21.

A comparison of cumulative spray ice ablation beneath the sawdust ablation plots with time is presented as Figure 22. One can see from the plot that the magnitude

Figure 20. Puddles/Ponds on Sheets

Figure 21. Sawdust Ablation Plot - July 5

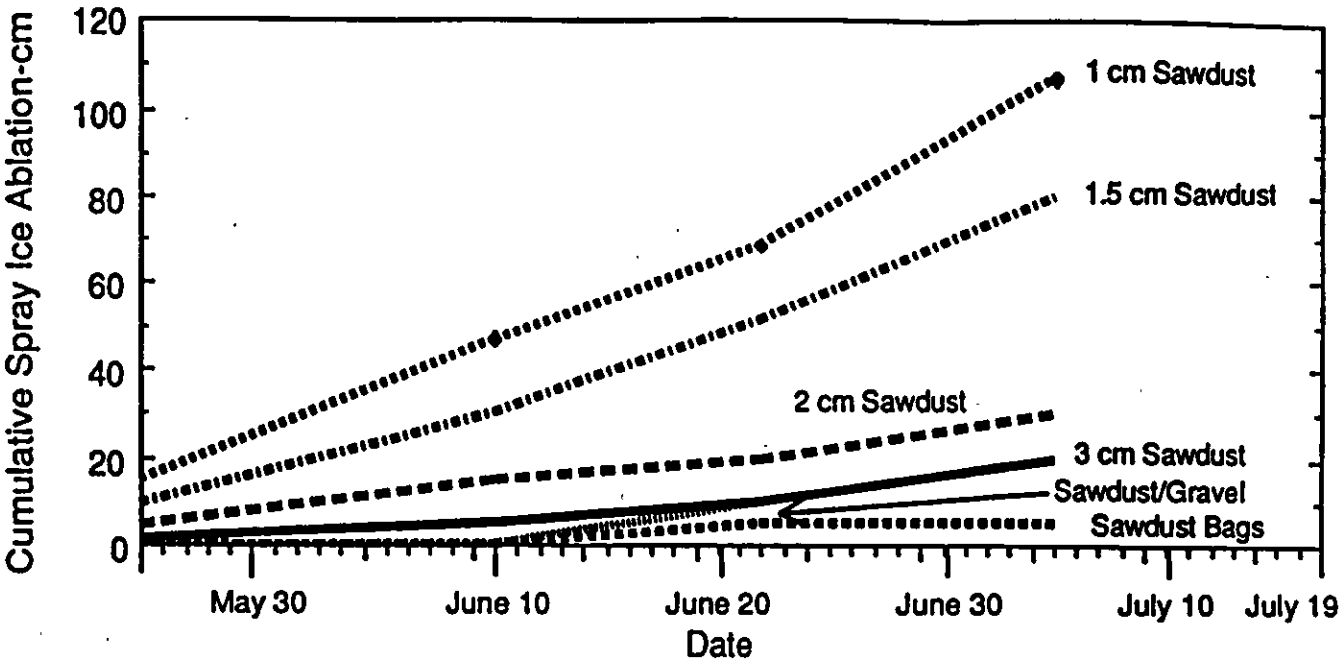

Figure 22. Sawdust Ablation Test Plot Comparisons

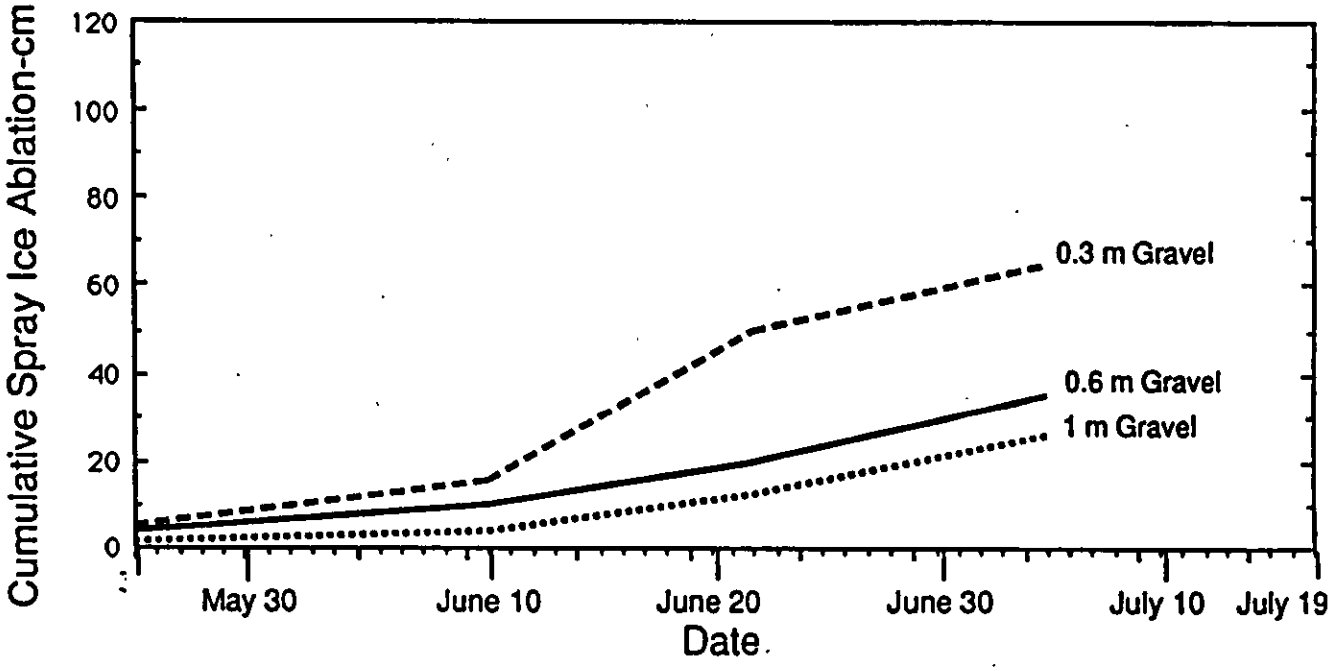

Figure 23. Gravel Ablation Test Plot Comparisons

of ablation decreased with increasing thickness of sawdust. A 1 cm veneer of sawdust was sufficient to reduce the ablation by over 50% from an average of 2.25 m for unprotected spray ice to only 1.07 m on July 5. Doubling the thickness of the sawdust cover had a dramatic impact on reducing the magnitude of ablation. Over the same evaluation period, the magnitude of ablation associated with 2 cm of sawdust was only 30 cm. Increases in the thickness of sawdust resulted in nominal reductions in the amount of spray ice ablation measured. A 3 cm thick blanket of sawdust limited cumulative ablation to 20 cm on July 5, the same amount as for a 1 cm thick layer of sawdust overlain by 5 cm of gravel. Finally, the most effective subplot examined was 15 cm thick sawdust bags. As with the sawdust/gravel subplot, virtually no ablation was apparent until the June 22 survey. Total spray ice ablation measured beneath the sawdust bags was only 5 cm over the entire measurement program.

During the period June 22 to July 5, the rate of ablation increased substantially particularly in subplots having a thin layer of sawdust. This increase in ablation rate was also observed at other surface ablation measurement locations in permeable and impermeable plots. A factor which accelerated melting of the spray ice is rain.

Gravel Plots

Spray ice ablation was measured beneath three thicknesses of gravel, each test plot covering a 15 m by 12 m area. Gravel was studied not only to investigate its insulating qualities with regard to ablation protection, but also as a base material to operate on during the rig marine demobilization. The use of gravel as a surface coating to enable heavy equipment to operate was demonstrated by Polar Alpine during a construction project and is described in the section detailing extended operations on spray ice.

Figure 23 is a comparison of cumulative spray ice ablation over time for each of the gravel test plots. The baseline from which subsequent ablation is compared was adjusted to be on May 9 rather than April 23 due to spray ice creep which occurred following placement of the gravel. Evidence for creep (as opposed to ablation) accounting for the change in stake stick-up observed above ground was

that almost no ablation of the unprotected spray ice was documented for this period.

Cumulative spray ice ablation associated with the 0.3 m thick gravel cover totaled 65 cm. This magnitude of ablation was similar to that recorded for an equivalent 1.5 to 2 cm thickness of sawdust and somewhat less than that associated with the Rufco sheet (85 cm) but more than was experienced by the insulated tarp (50 cm). Doubling the thickness of the gravel cover had the effect of cutting spray ice ablation nearly in half. The 1 m thick gravel cover was only marginally better than the 0.6 m thick cover. Identification of the optimum thickness of gravel required for maximum insulating qualities is significant as it reduces the amount of material required and thereby lowers cost. The ablation protection provided by the thicker gravel plots was superior to any tarp and comparable to a 2-3 cm blanket of sawdust and a thin veneer of sawdust held in place by gravel.

Ablation rates varied for each of the gravel test plots throughout the monitoring period. The highest average ablation rate (2.92 $cmday^{-1}$) was associated with the 0.3 m gravel plot for the period June 10-22. This rate was 3.5 to over 4 times those observed for the other two gravel ablation plots. Average ablation rates before and after this time period were substantially lower. Contrastingly, average ablation rates associated with the 0.2 and 1 m thick gravel plots increased over time. The average ablation rates documented for the two thicknesses of gravel were similar during the periods June 10-22 and June 22-July 5. The average ablation rates measured at all three plots near the end of the study were also similar (1.04 $cmday^{-1}$ to 1.15 $cmday^{-1}$).

Ablation has also been predicted using an in-house finite difference thermal model developed by Dr. J. Nixon of ERCL. This model is quite rigorous and yet sufficiently versatile to accommodate a non-linear surface temperature-time relationship. In brief, this model has been used to predict the start date of ablation beneath the gravel pads and the depth of spray ice thaw beneath the gravel pads. The following assumptions and material properties were found to yield a very good fit of the observed data.

- ice content of gravel is 5% (by weight)
- bulk density of gravel is 1.8 Mg/m^3

- unfrozen thermal conductivity of gravel is 2.1 w/mC
- frozen thermal conductivity of gravel is 2.0 w/mC
- "n" factor for gravel is 1.5
- zero snow cover
- specific heat of soil grains is 0.2 cals/gmC
- bulk density of spray ice is 0.65 Mg/m^3
- temperature of spray ice at sea level is fixed at 0°C
- initial temperature profile varies linearly from -8.5°C at gravel surface to 0°C at sea level
- Computations start on Julian Day 116 (April 26)

The above gravel properties are very reasonable for the gravel used at Nipterk. A comparison of the observed and predicted thaw is presented in Table 3.

Gravel Thickness	Date of Onset of Spray	Depth of Spray Ice Thaw on July 5	
		Observed	Predicted
0.3 m	June 2	0.65 m	0.56 m
0.6 m	June 11	0.23 m	0.28 m
1.0 m	June 20	0.15 m	0.12 m

Table 3 Comparison of Observed and Predicted Thaw Beneath Gravel Pads

Inspection of Table 3 reveals that the 0°C isotherm quickly penetrates the gravel layer. The mean daily air temperature rose above 0°C on May 25 (Figure 17) and the time to melt the gravel was 7, 16, and 25 days for the 0.3, 0.6 and 1.0 m pads respectively. Therefore the time to thaw out the gravel is approximately proportional to the latent heat (or ice content) of the gravel. This suggests that a 0.5 m gravel pad of ice content % is just as effective at preventing spray ice thaw as a 1 m gravel pad of 5% ice content. Therefore in the future, perhaps more emphasis should be placed on increasing the ice content rather than the thickness of the gravel pad. This could be achieved by flooding the gravel after placement.

In light of the reasonable agreement in Table 3 and the reasonable assumption used in the model, it is concluded that Dr. J. Nixon's thermal model can be reliably used to predict spray ice thaw beneath gravel pads.

Simulated Rig Mat Plot

One test plot was constructed out of 20 cm by 20 cm by 4 m long timbers removed from the rig cellar. Rig mats were not left on the island because of the high cost of removal. Therefore rig timbers were used. The rig timbers could be burned on-site as part of the island cleanup. Therefore, to minimize costs, the cellar was dismantled and the timbers used to build the simulated rig mat ablation plot. Under an operating scenario rig mats could be placed beneath relatively heavy rig loads awaiting marine demobilization and along the access road to the barge to reduce the potential for spray ice degradation associated with the rig demobilization operation.

Following the June 22 site survey, the simulated rig mat test plot was accidently burned during the general island cleanup. Even so, extremely encouraging data were collected until that time. Total cumulative spray ice ablation measured beneath the timbers through June 22 was only 8 cm, a mere 3 cm greater than that measured beneath the sawdust bags.

Under operational conditions, rig mats may be a far better alternative than sawdust bags for several reasons. First, rig mats would likely already be on site since they are used in the drilling operation. Thus additional materials would not have to be purchased and transported to the island. Second, rig mats could be placed along the barge accessway once the rig component they formally supported is transported aboard the barge. This scenario would reduce the likelihood of trafficability problems. Third, rig mats could be easily picked up during the marine demobilization, thus avoiding potential environmental concerns associated with the use of either sawdust or wood chips. And fourth, rig mats can be reused whereas sawdust and/or woodchips must be considered expendable.

Ablation Test Plot Comparisons

Figure 23b is a plot comparing the ablation protection performance of some of the most beneficial insulating materials identified from each of the categories evaluated. As can be seen, wood products (i.e. 15 cm thick blanket of sawdust and 20 cm thick timbers) provided the highest degree of protection.

Spray Ice Temperatures Beneath Ablation Plots

Spray ice temperatures were measured beneath most of the sawdust ablation subplots and all of the gravel ablation plots for a one month period beginning in early June. These data are useful in further evaluating the insulating qualities of the overlying materials.

Average daily temperature time series plots were prepared for each of the ablation plots and subplots for which these data are available. Obscured by averaging the data at one day intervals is the diurnal warming and cooling which was apparent in all of the data. However, the effectiveness of various materials with regard to mitigating ablation is readily apparent.

Figure 24 is a time series plot of surface spray ice temperature measurements collected beneath the gravel ablation plots. Also included in the Figure are averaged daily air temperatures recorded on the island during the same period. One can see from the Figure that a 1 m thickness of gravel offered the best degree of insulation, limiting the average temperature to about 0.3°C throughout most of the measurement period. Minimal fluctuation from day to day is documented, except in early July where a slight warming trend is observed. Similarly, average spray ice temperature data from the 0.6 m thick gravel ablation plot show the same trend. However, the average daily temperature is typically warmer by 0.1 to 0.2°C. Spray ice ablation measured at these two sites was nevertheless similar.

Contrastingly, spray ice temperatures associated with the 0.3 m thick gravel ablation plot were significantly higher than the thicker gravel plots, generally by amounts ranging from 0.5 to 1°C. Moreover, ice temperatures appeared to be

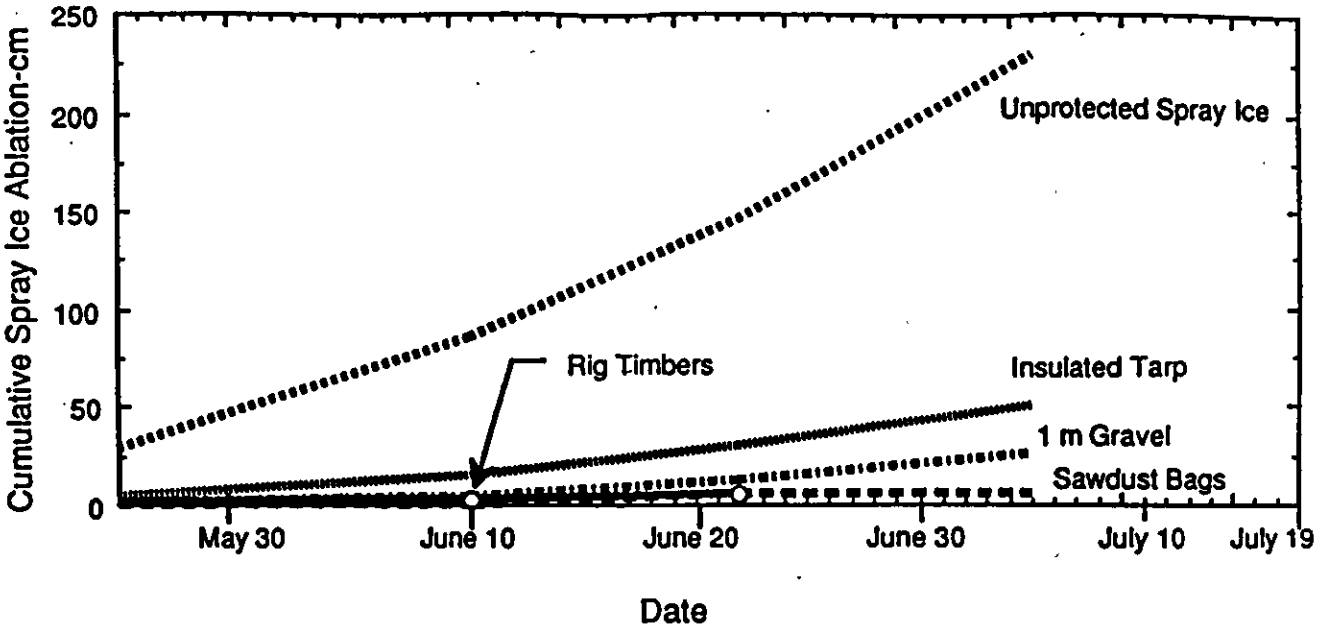

Figure 23b. Selected Ablation Test Plot Data Comparisons

influenced to a greater degree by air temperatures. This warming was responsible for the greater degree of spray ice ablation observed.

Comparisons of spray ice temperatures measured beneath the sawdust ablation subplots are indicated by the temperature - time series plots shown in Figure 25 . Again, both the spray ice and air temperatures were averaged on a daily basis. Like the gravel ablation plots, there was a strong correlation between spray ice temperature and ablation, i.e. the thicker the sawdust layer, the lower the spray ice temperature, and the less ablation observed. One anomaly was noted in the spray ice temperature data beneath the sawdust bags at the end of June. Neither air temperatures, solar radiation, nor wind speed data can adequately account for the rise in spray ice temperature observed beneath the sawdust bags. On the other hand, spray ice temperature increases documented in July for each of the sawdust subplots appeared to be attributable to warm air temperatures.

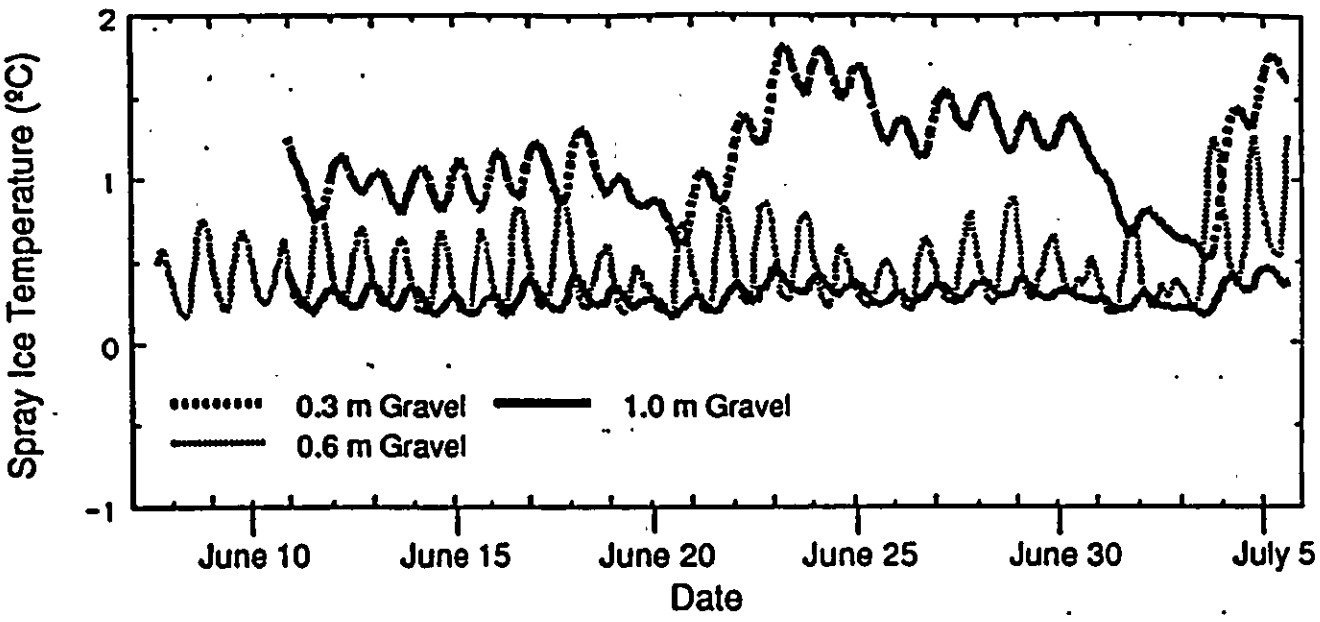

Figure 24. Spray Ice Temperatures Beneath Gravel Plots

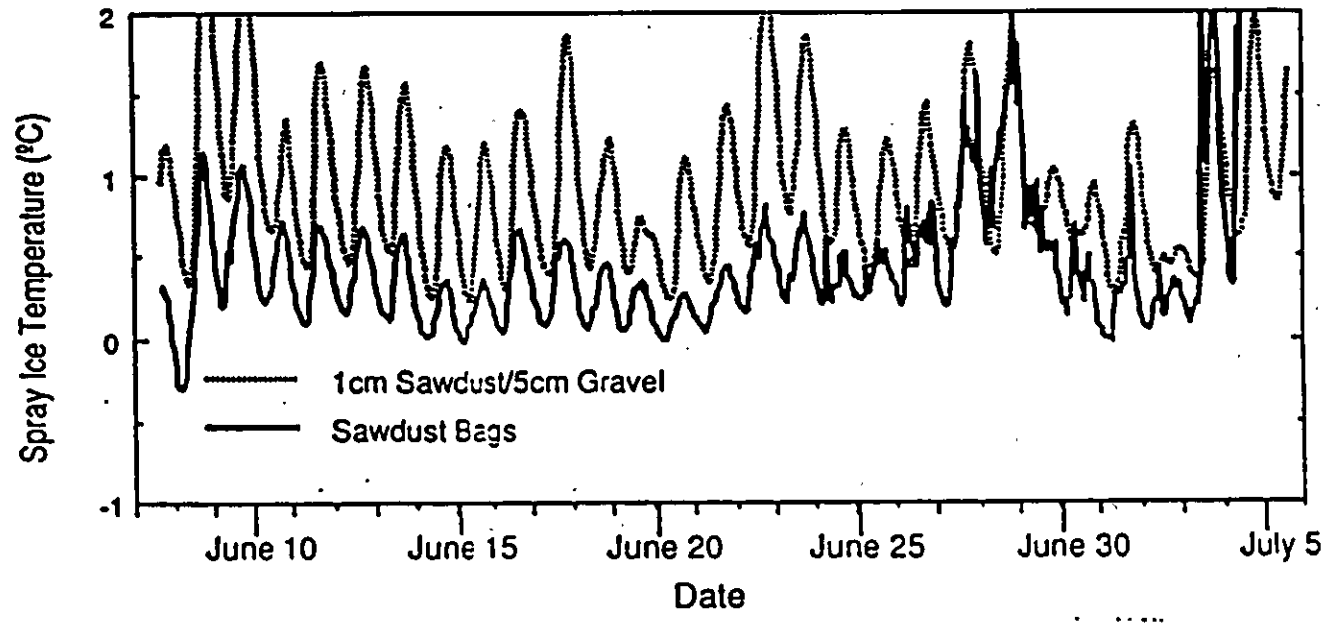

Figure 25. Spray Ice Temperatures Beneath Selected Ablation Plots

Additional Spray Ice Ablation Observations

Significant spray ice ablation was documented during the first month of the experiment at locations where the island surface had been soiled. This is attributed to the albedo reduction and absorption of solar radiation by the dark materials.

Ablation of the clean spray ice commenced in earnest with the onset of above-freezing air temperatures in late-May. During this period, the ablation rate of soiled areas was drastically diminished, due to the fact that the layer of dark materials had reached sufficient thickness such that it now served to insulate the spray ice surface. This resulted in the formation of a number of mounds and hummocks which grew higher with time as the relatively cleaner surrounding spray ice ablated at a comparatively more rapid rate.

The thickness of the insulating layer necessary to retard ablation varied depending on the material (i.e. sawdust, sand, cement, pit liner, etc.). However, except for foam insulation it was seldom over 1 to 2 cm thick. One portion of the island not part of our ablation experiment, but from which data could be collected nonetheless was the air drilling discharge area on the northeast side. A photograph of this area is shown as Figure 26. The thickness of the drilling mud, insulating the spray ice ranged from 10 to 20 cm. Because of the insulating quality afforded by the mud, island freeboard was maintained in this area.

The central portion of the island where the drilling rig had operated was another area that experienced relatively limited spray ice ablation due to the presence of debris (especially before the late-June cleanup). Cumulative ablation in this area was estimated to be less than 0.5 m where the spray ice had been covered. Hummocks 2.5 to 3.5 m high were observed to be covered with 1 to 2 cm of sawdust and/or cement.

Sand also proved to be effective in slowing the rate of spray ice ablation. Evidence to support this claim was collected at the inclinometer stations and at several isolated sites where hummocks had been created as a result of a thin (2 cm) layer of sand covering the spray ice. Sand was originally packed around the inclinometer casing at the time of installation in January. As spray ice meltback

Figure 26. Air Drill Discharge Area

progressed, inclinometer stickup increased, exposing a greater quantity of sand. This sand was eventually spread atop the spray ice surface in the vicinity of the inclinometer casing. During subsequent visits, the spray ice beneath the sand had not ablated appreciably whereas that beyond the cover of the sand had to the point where a mound developed. Over time, it was impossible to reach the top of the casing from the unprotected spray ice due to differential ablation. Therefore, the sand and spray ice protected by the sand which surrounded the casing had to be removed. At the time it was found to be hard and competent and could only be dislodged by chipping with a sharp object.

ABLATION SUMMARY AND IMPLICATIONS

Based on an assessment of the ablation data collected over the course of the experiment, it appears that protecting the spray ice island from excessive ablation is feasible from both a technical and an economic standpoint. The following comments and observations pertaining to spray ice ablation are provided toward the development of a scenario that would enable drilling to continue until June and the drill rig to be demobilized by barge after breakup of the landfast ice sheet.

- Island design should take into account that between 2.5 m and 4 m of freeboard will be ablated from the unprotected spray ice (depending upon the timing of rig marine demobilization). The design freeboard of a spray ice island should be at least several meters higher than the expected ablation to ensure that the island does not break up due to loss of freeboard before the demobilization operation is completed.

- A 3 cm thick layer of sawdust or wood chips placed on the working surface in the vicinity of the rig prior to deployment of rig mats and mobilization of the rig would be beneficial to guard against undue warming of the spray ice associated with higher air temperatures prevalent in April and May which could result in unacceptable settlement or differential settlement rates.

- Rig mats or sawdust/wood chips placed atop the spray ice in the vicinity of warm rig buildings and radiators will mitigate undue warming of the spray ice.

- One potentially cost effective manner of reducing spray ice ablation (environmental regulations permitting) is to save and stockpile used drilling mud for subsequent spreading atop the ice surface later in the season.

- Floor temperatures of rig buildings should be closely monitored and kept as cool as possible, especially with the onset of warmer air temperatures later in the drilling season. Undue warming may be at least partially prevented by opening access doors and vents and redirecting radiator airflow.

- A thin cover of clean snow smeared over soiled spray ice surfaces during short periods of near or above freezing temperatures and/or intense solar radiation and calm winds is an effective means of mitigating ablation.

- It may be advisable to ascertain the extent and density of hidden cracks in that portion of the island eventually underlying the stacked rig to minimize the potential for operational problems associated with the marine demobilization.

- A thin (3 cm) veneer of sawdust/wood chips should be spread over the spray ice near the stacked rig to minimize surface ablation. Rig components should be placed atop rig mats whenever possible.

- Ablation protection materials may need to be placed as much as 15-20 m beyond rig components to avoid the formation of a scarp too close to the stacked rig. A gentle slope could be created by gradually reducing the thickness of ablation protection materials with distance from rig components.

- To minimize costs, application of ablation protection materials could be limited to the vicinity of the stacked rig and along routes allowing access to the edge of the island. The remainder of the island could be considered sacrificial and thereby left unprotected.

- It may be worthwhile to consider constructing primary and secondary access routes from the stacked rig to the barge docking location. This

scenario could potentially minimize barge standby time in the event of persistent adverse weather conditions during the planned demobilization. Access routes should be constructed wide enough to allow vehicles and equipment to pass side by side. Spray ice along the access routes could temporarily be protected with sawdust or woodchips until the barge docking point is identified. Then, the spray ice could be covered with gravel and rig mats to reduce disturbance to the spray ice. Rig mats should first be placed near the barge, gradually working toward island center to minimize the risk and consequences of encountering a crack near the edge of the island.

- Cracks could be spanned by rig mats used in conjunction with timbers.

- Ablation of the protected and unprotected spray ice should be monitored until the rig has been demobilized to the barges. Routine maintenance of ablation protection materials will probably be required.

- Stacking the drilling rig on or near the edge of the working surface rather than the edge of the island minimizes the consequences imposed by a prolonged intense storm severely eroding the island.

- The access route from the staging area to the loading dock may need to be continually groomed so that the underlying spray ice is not overly degraded.

ISLAND EROSION

A portion of the experiment was designed to evaluate the performance of the edge protection system to protect the island edges from thermal and mechanical erosion due to wave action and currents. (An evaluation of the edge protection system with regard to protecting the island surface from ablation was presented in the section entitled: Surface Ablation). A knowledge of spray ice erosion rates is an essential part of a marine demobilization in that the island needs to be protected long enough into the open water season to allow for the demobilization operation to be completed.

Island erosional processes, rates, and patterns were monitored from the time of island breakup (on June 23 or 24) through final island breakup on July 10. Two forms of wave erosion were evident - thermal and mechanical.

The affects of thermal wave erosion were probably most readily observed on the relief pad and on portions of the island outside of the experiment setup area having a relatively high freeboard. These regions appeared to be breaking up predominantly as a result of thermal wave erosion which is similar to that observed for previously constructed spray ice features Jahns, et al. [7]. In this mode, wave action produces high local water velocities which cause a high effective heat transfer rate between the near-surface water and the ice edge. Wave induced heat transfer tends to undercut the island edges creating notches. As the notches grow inward at the waterline, ice overhangs and underwater terraces are created. Eventually the overhangs collapse due to gravity forces and the terraces either break upward because of buoyancy or possibly disintegrate in place depending on the cohesion at the seabed [8].

Nipterk appeared to break up predominantly due to a lack of freeboard rather than from wave erosion. Except for the experiment setup area and other regions in which the spray ice was protected, ablation reduced the freeboard to between 0.5 and 1 m on July 5. A network of newly formed cracks, the largest of which could readily be seen from the air (see Figure 27) were probably due to an instability condition created by the lack of freeboard as a part of the island became buoyant. Small sections of the island tended to periodically lift up off the bottom. These eventually drifted away from the island as a result of mechanical wave action and currents. The wholesale breakup of the island on July 10 is further evidence that it broke up mainly due to a lack of freeboard. Once dislodged from the seabed, fragments were carried away by currents.

Composites of oblique and vertical aerial photographs of the island taken on June 22, July 5, and July 8 are shown in Figure 28. These photographs graphically illustrate the succession of island breakup. On June 22, the island diameter is 320 m (area = 80,500 m^2) as complete landfast ice breakup had not yet occurred.

Open water conditions persisted on July 5 and the edge protection system was draped over the edge as per design. Based on an assessment of ice and weather

conditions, barges could have been mobilized to the island from Tuktoyaktuk for the rig demobilization by this time.

An analysis of an aerial photograph to determine island area was performed by VTA Photogrammetric Consults. Island area was estimated to 58,000 m^2 at this time. An error of up to ± 10% was introduced in the calculation because the photograph was taken at an oblique rather than vertical orientation. The effectiveness of the island edge protection system at mitigating edge erosion is clearly visible from the photo. A 25 m protrusion was created due to the presence of the system. An outline showing the original island diameter is shown in Figure 29 so that the location and extent of erosion can be identified. As can be seen from the Figure, erosion was most intense on the south half of the island.

During the July 5 site survey, 20 cm by 20 cm by 3 m long wooden timbers were placed at the southwest, southeast, north and north-northeast slope indicator stations in such a manner that they would serve as ground reference points in aerial photographs. Ground reference points were required to accurately determine island area. Distances between the storage tent and southwest and north stations were also measured. The hole center cellar was another known reference point which could be used. The distances between the hole center and slope indicator stations had been measured in January.

Vertical aerial photographs of the island were taken the morning of July 8 on our behalf by Inuvik based Photo Script Ltd. using a Twin Otter aircraft chartered from Aklak Air Ltd. The aircraft had a stereo camera mounting hatch on the underside of its fuselage which facilitated the collection of vertical photographs.

The negative of one color image was analyzed by VTA to determine its area. Using the control points which we provided, a scale factor was computed such that a conversion from the instrument units to true ground units was performed. A perimeter was digitized from which the polygon area was calculated. Three

FIGURE 27

FIGURE 28

FIGURE 29

areas were computed: 1) the main ice island excluding the four fragments which appear to have already calved, 2) the area covered by the four fragments, and 3) the area covered by the edge protection system. Figure 30 shows the digitized island perimeter used to calculate the area.

Prior to the initiation of erosion, the original island area was about 80,500 m^2. According to calculations performed by VTA, the island area was between 28,600 - 29,400 m^2 (the latter value including apparently calved fragments) on July 8. Thus, about 36% of the original island area was still intact.

The actual area covered by the sheets and net was initially about 8,000 m^2. This amount takes into account overlap and extension of the system beyond the grounded portion of the island which was estimated at 1,500 m^2. VTA calculated that 790 m^2 or 10% of the sheet protection system was still covering the island surface on July 8.

At the time, the net protection system was no longer in place due to insufficient anchoring. This factor in conjunction with minimal freeboard induced by ablation were responsible for that portion of the island protected by the net calving as soon as it did. Omitting the original island area covered by the net resulted in an island area of 5,600 m^2 originally protected by the sheets. Utilizing this value, it can be calculated that 14% of the area originally covered by the sheets was still in place.

The degree of stabilization afforded by the edge protection system is readily apparent from Figure 31 which is a diagram comparing the original and remnant (July 8) island areas. The next least amount of radial erosion documented at a different location was more than twice that observed at the sheets. Also evident from the Figure is that erosion was most pronounced on the south and east sides of the island which is attributed to the warm outflow from the MacKenzie River.

It is not possible to determine with any degree of certainty whether one type of sheet was more effective in retarding erosion than another. Collectively through, the sheets appeared to be significantly better at slowing erosion than the net

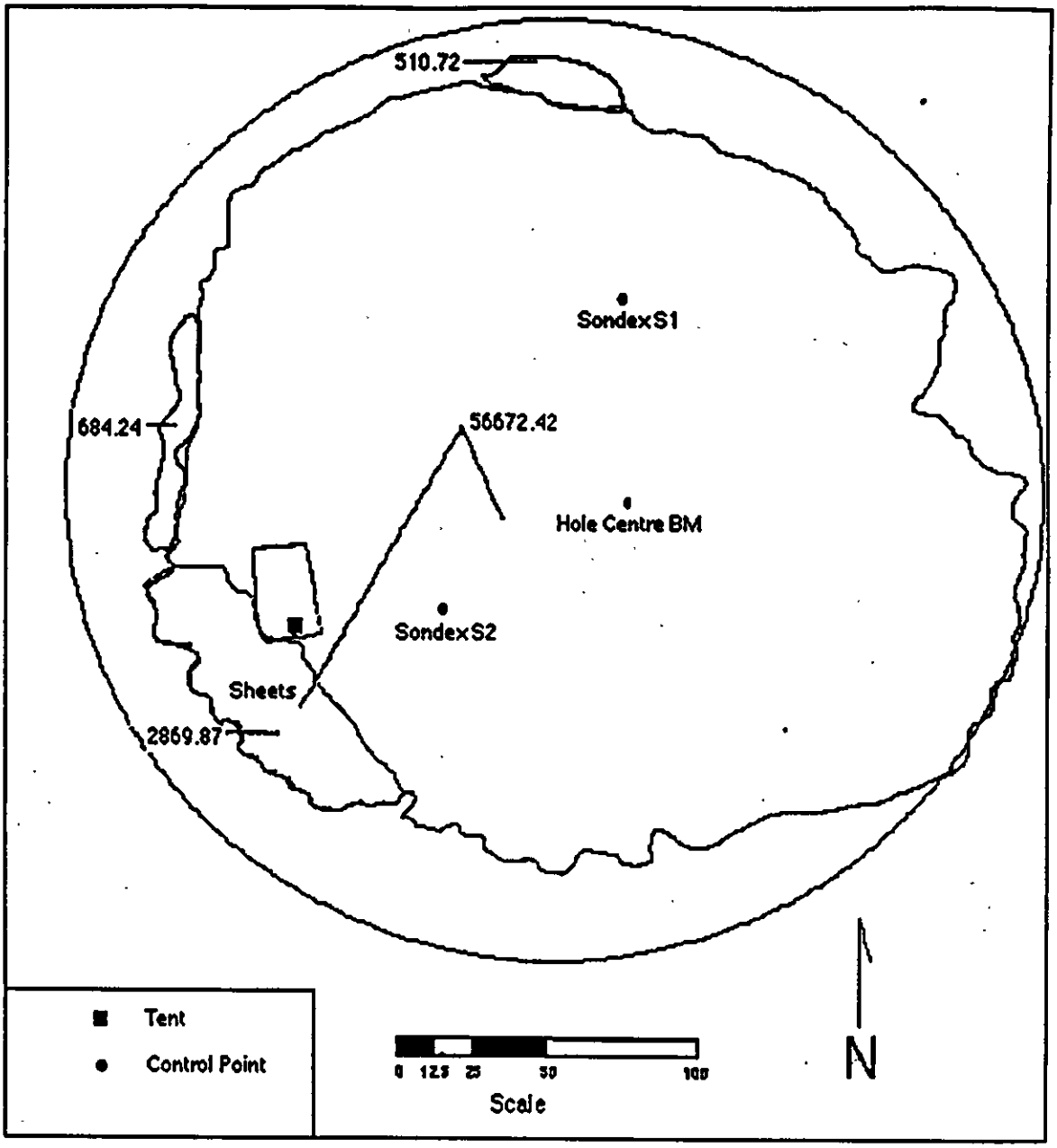

Figure 30. Digitized Island Perimeter

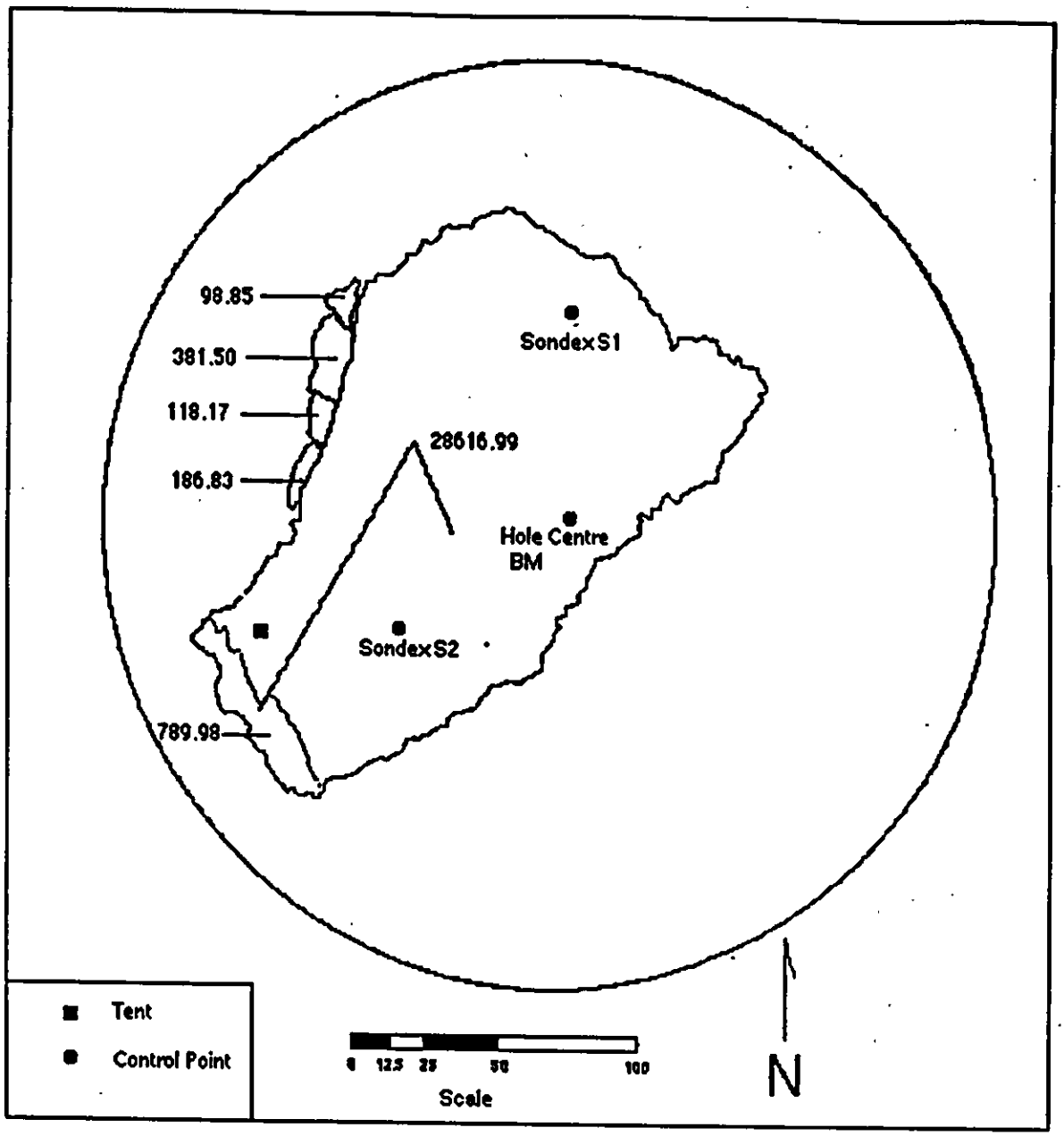

Figure 31. Comparison of Original and Remnant Island Areas

system. However, at least a portion of the success attributed to the sheets in this instance was due to spray ice ablation protection provided by them.

As of July 5, there was only minor tearing of the sheets due to abrasion with the spray ice. The degree of abrasion resistance was an area of concern identified during the planning stages of the experiment. However, with time this concern was alleviated. None of the sheets appeared to have been more susceptible to the effects of abrasion than the others. This is an important finding because the Rufco sheet costs only half the amount of the vinyl sheets. Moreover, the Rufco sheet is also easier to install resulting in greater cost savings.

Unlike the sheets, the nylon reinforced sandbags at the edge of the island experienced a high degree of abrasion due to being in contact with the spray ice. A number of bags were deteriorated to the extent that their gravel contents spilled out onto the ice. Still others became dislodged from the nets holding down the sheet. In light of these short comings other materials should be considered for sandbag fabrication.

Another problem connected with sandbags pertains to the degree of sheet anchoring capability they provided. Westerly component winds in excess of 20 knots tended to push the sheets back on to the island. Only after additional sandbags were placed at 1 m intervals along the island edge were the sheets held securely in place. The weight associated with the placement of additional sandbags would have made it even more difficult to retrieve the sheets from the island prior to complete island disintegration had this option been required.

Contrastingly, the number and spacing of sandbags used to retain the net protection system was adequate. Because of ablation which resulted in most of the anchors being exposed and the spray ice to disintegrate due to lack of freeboard, it is not possible to accurately assess whether the net edge erosion system by itself would have been sufficient to mitigate erosion long enough to enable the rig to be demobilized by barge. Consequently, the edge protection system designed for future island should rely predominantly on sheets. Nets could be placed on both sides of the sheets to further mitigate erosion. One way to decrease the overall cost of the net is to use polypropylene rope and increase the mesh spacing. In light of the data collected from this program, neither of these modifications are

anticipated to have a significant adverse effect on the performance of the net protection system.

EROSION RATES

Previous Information

To date, few data are available regarding the erosion rate of unprotected spray ice. One if not the earliest account of erosion rate data was collected during the Exxon Ice Island Experiment. The maximum degree of radial erosion measured during the experiment was 7.9 $mday^{-1}$ in August whereas average radial erosion was less than 3 m day [9]. However, due to differing construction techniques, much of the island was built out of ice that was significantly more dense and thus less porous than typical spray ice islands. Therefore, the aforementioned erosion rates may be considered low.

Additional insight into spray ice erosion rates is provided in Jahns et al. [7]. The information presented is based on data acquired from a large spray ice barrier surrounding Global Marine's Concrete Island Drilling System (CIDS) at the Exxon Antares Drillsite in 14.9 water depth in the Alaskan Beaufort Sea. Jahns et al. [7] reported that following breakup, thermal erosion associated with wave action was more detrimental to the barrier than spray ice ablation. Wave undercutting was observed to be particularly severe during storms and resulted in calving of large pieces of spray ice from above and below water. Breakup of the landfast ice sheet occurred on July 3. From an analysis of time-lapse camera data collected during the open water season, the rate of barrier retreat was as high as 30 $mday^{-1}$. Nearly 50% of the barrier was reported to be still intact when the structure was towed out on August 17. Portions of the barrier were still in place in early September.

Numerical Simulation

Background

Connolly [1] developed a numerical model to calculate the amount of spray ice that would be lost by a spray ice island due to surface melting and erosion from waves and currents during the open water season for a site in the landfast ice region of the Alaskan Beaufort Sea. The simulation was refined and rerun as part of this study.

Overview

In order to explain the physics behind the ablation and erosion processes on the spray ice island, an effort has been made to model these processes. The model was developed from earlier work done by Connolly [1] in which a hypothetical ice island was used to determine the survivability of a spray ice island through a summer melt season in the Alaskan Beaufort Sea. For that study, climatological data were parameterized in order to determine the average energy balance of a spray ice island. For the current study, the models were modified to use data collected by Esso directly on the ice island. A more detailed account of this work undertaken by Analytic Applications, Inc. is provided as Appendix E.

By incorporating the data collected into physically meaningful models, the deterioration processes of the island can be observed independently and the capability of predicting the behavior of future islands can be enhanced.

The modeling effort was broken into two parts; the ablation of the top surface of the island, and the erosion of the perimeter. The ablation of the top surface involves the energy transfer between the ice and the atmosphere. In this case the standard energy balance equation was used. This equation is given as:

$$F_s + F_l + L + S = \gamma \rho D + C \qquad (2)$$

where F_s is the net short wave radiation, F_l is the net long wave radiation, L is the latent heat flux, S is the sensible heat flux, γ is the latent heat of fusion, ρ is

the spray ice density, D is the depth to which the ice has melted, and C is the heat conducted through the ice. All these quantities are averaged over the surface of the island.

The erosion of the perimeter of the island begins when the natural ice breaks up, leaving the spray ice exposed to the action of the waves and currents. Although the currents erode over the entire vertical cross section of the perimeter and the wave action is only at the waterline, the wave action term dominates because of greater amount of heat transferred. White et al. [10] use a Reynolds analogy to compute heat transfer to an iceberg as a function of wave friction:

$$F_w = 0.000219\left(\frac{R}{H}\right)^{0.2}\left(\frac{H}{P}\right)\rho\chi(T_w - 273) \qquad (3)$$

where F_w is the heat flux due to wave action, R is the roughness length of the ice, H is the average wave height, P is the average wave period, and T_w is the water surface temperature.

Equations (2) and (3) were used in separate models and run independently. For the ablation model, data were taken from the island data set from June 7, 1989 to July 5, 1989. From the measured ablation data and spray ice temperature data June 7 corresponds roughly to the onset of significant ablation. Data from the instruments were not collected after July 5 and the island broke up July 10. The ablation model was first run to simulate unprotected spray ice. In this case the albedo is high, reflecting much of the incoming solar radiation. The island is assumed to be isothermal at 0° C, so that any addition of heat at the surface is converted into melting ice.

The sensible and latent heat flux terms were calculated from the measured temperature gradients and energy transfer coefficients. The coefficients are dependent mainly on wind speed, stability, and roughness length. Because the differences between the sensible and latent heat flux coefficients are within measurement error, they were taken to be equal for this study. A number of different coefficients were tried in the model to determine the model sensitivity. Figure 2 shows some of these results compared with the data measured on the

island. From this figure it appears that 0.0014 provides the best fit to the measured data.

The flat parts in the ablation curves correspond to the night time periods when net heat flux is away from the island. Since there is no heat entering the island surface, no ice is melted. Instead, some of the liquid water present in the surface can then be refrozen which requires subsequent energy absorption to melt again. This accounts for the hard crust on the island surface in the mornings.

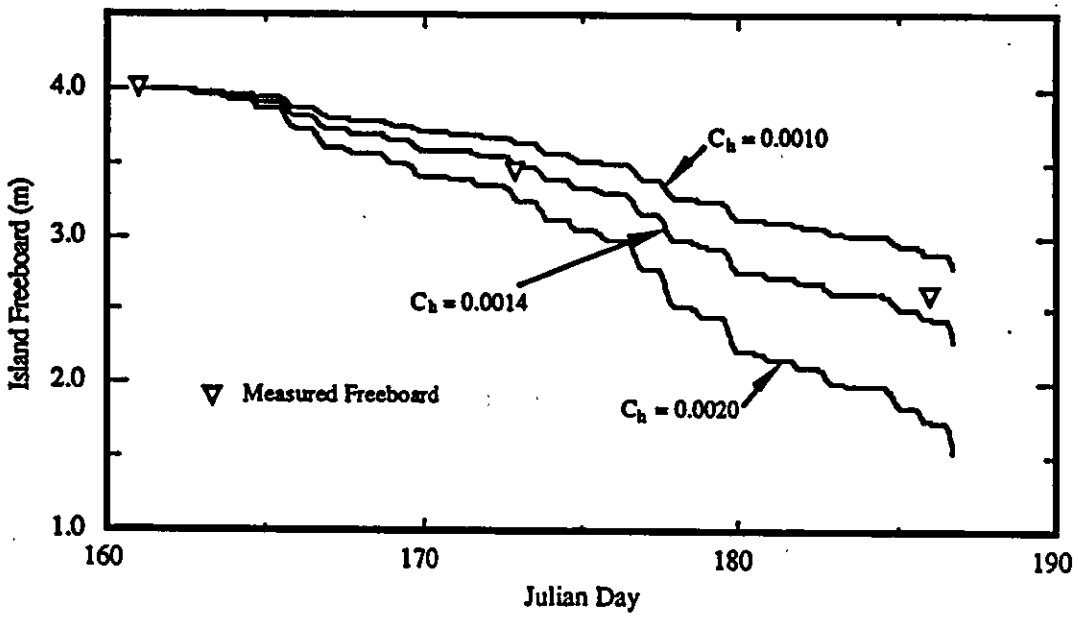

Figure 32. Ablation of the top surface of the ice island compared with measured data.

The model was changed in order to simulate the presence of various ablation protection materials. These materials consisted of gravel pads of various thickness, sawdust layers, and fabric sheets. A protective material spread over the ice serves to insulate the ice from solar and longwave radiation, and sensible and latent heat flux. The approach taken here was to calculate the energy transfer between the material and the atmosphere and then to calculate the heat conducted through the material to the ice. The resultant heat transferred through the protection material was used to melt the ice.

The results from the gravel test are shown in Figure 3. The data presented in this figure were compared only for the last day that data were collected, July 5. Although the results compare favorably, some discrepancies arise due to the fact that the gravel was modeled as a material of homogeneous thermal conductivity. This may not be the case due to an inhomogeneous distribution of ice or water in the gravel, which would lead to changes in the thermal conductivity of the material. These thermal conductivity inhomogeneities could also change with time since water is added with rainfall, percolates out the bottom, refreezes or thaws.

The wave erosion has been distributed evenly around the perimeter of the island so that the island retains the shape of a disc. In reality the erosional forces are directional and the island quickly becomes asymmetrical depending on the predominant directions of the forces. However, one of the most important factors in island survivability is sliding friction between the ice and the seabed. Since the sliding friction is a function of area of contact, the

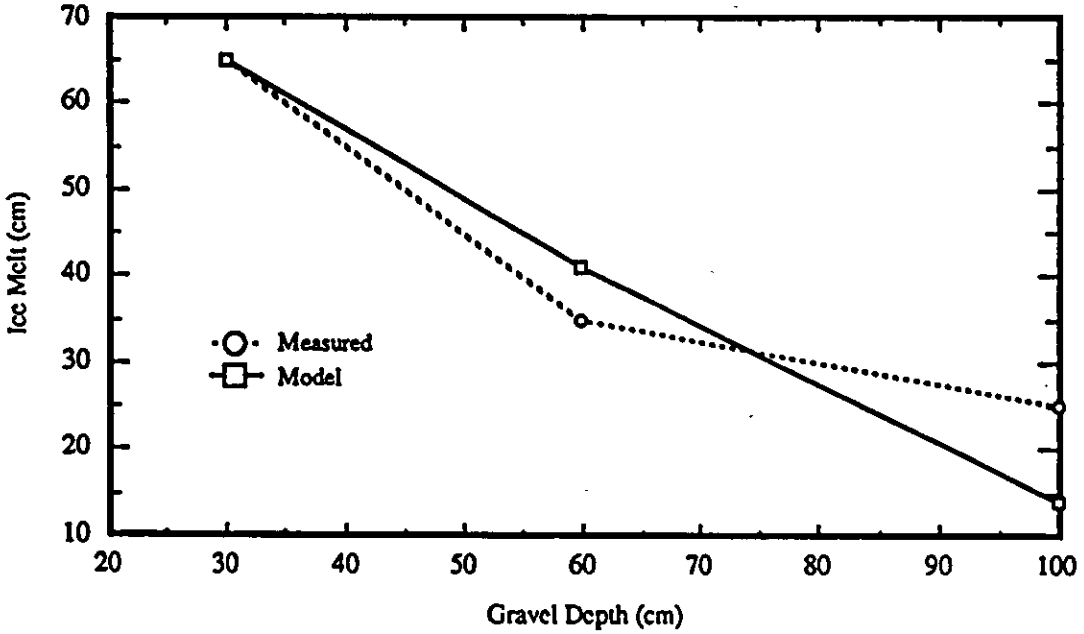

Figure 33. Comparison between measured and modeled ice meltback under gravel pads of various thicknesses.

shape of the island is not as critical of a term.

Wave height, period, and water temperature are important factors in the erosion model. Since data were sparse concerning these terms, a variety of different wave heights and periods were input into the model to determine the sensitivity of the model. The results are shown in Figure 3. Waves of 0.25m, 0.5m, and 1.0m were input along with periods of 3 and 4 seconds. The model was run from the first day of open water, June 23, until July 5.

As can be expected, the higher wave heights and shorter periods cause the greatest amount of erosion. The closest fit to the data is achieved with an average wave height of 0.5m and a period of 4 seconds.

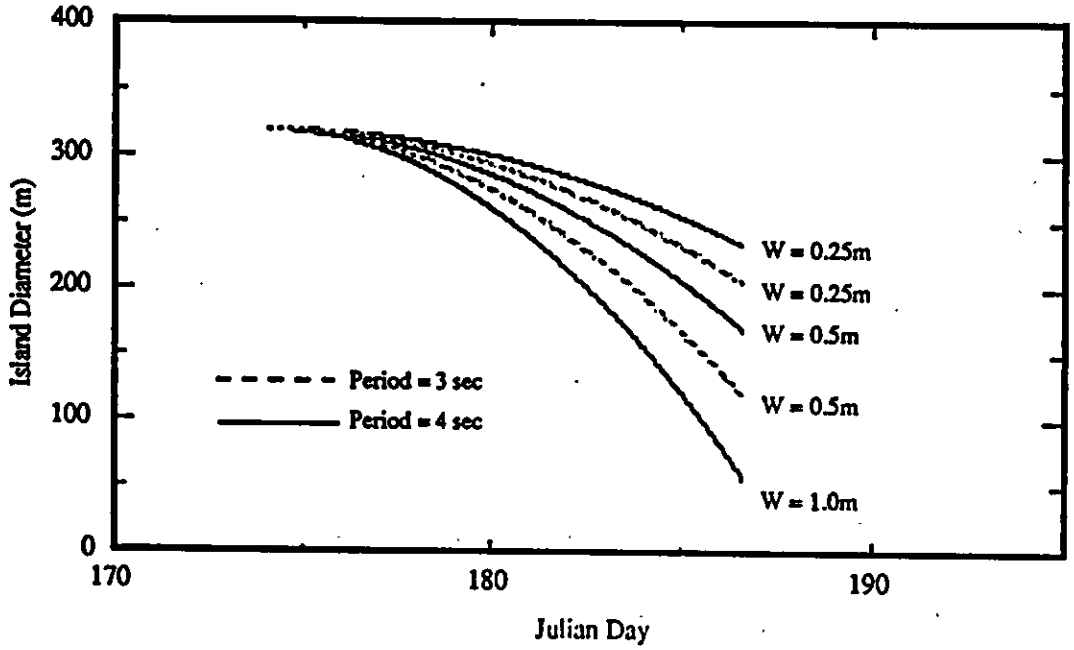

Figure 34. Results of the use of different wave parameters in the perimeter erosion model.

The use of various island edge protection materials has shown definite value in protecting the perimeter of the island from erosion. Although a number of different protective materials were used, it was difficult to determine from the aerial photos if any showed better results than the others. Another comparison problem arose due to the fact that the protective sheets were only used on a portion of the island. Since the perimeter erosion was asymmetric it was difficult to determine what erosion would be for an unprotected edge with the same exposure. Nevertheless, the island radius was observed to decrease from 160m to

135m where the edge protection was used. The edge protection is seen as a baffle between the waves and the ice, in effect damping out the amplitude of the waves. From the model a diameter of 260m corresponds to an average wave height of 0.2m if the period remains at 4 seconds. Thus, the edge protection effectively attenuates the waves by 40% of their original height.

The results of the modeling effort have provided some new information on the behavior of a spray ice island during the melt season. The results of the ablation and erosion protection experiments have also added valuable information along the lines of protecting an island and extending its operating period. Of equal importance are results of the sensitivity studies which have shown the response of the model to differing environmental conditions.

ISLAND BREAKUP

Breakup of the landfast ice sheet occurred sometime between June 23-24. The island withstood the lateral ice forces imposed by the ice sheet breakup. As indicated in the section entitled "Monitoring Surveys", the last complete site survey was carried out on July 5. At the time, the island was surrounded by open water which extended several kilometers in all directions. Only isolated, relatively small first-year ice floes were observed to drift past the island during the 12 hour site survey.

Most of the grounded portion of the spray ice relief pad located about 500 m to the east was also intact. Because of its higher freeboard, the relief pad appeared to be diminishing in size predominantly as a result of calving induced by wave thermal and mechanical erosion along the edges. This form of behavior is similar to that observed for other spray ice features [7]. The wave action produces high local water velocities causing a high effective heat transfer rate between the near-surface water and the ice edge. The wave-induced heat transfer undercuts the island edge creating notches which grow inward at the waterline. Eventually, these overhangs become sufficiently large that they break off as a result of gravity. The underwater terraces which tend to adhere to the seafloor [8] are eventually brought to the surface by buoyancy or are melted in place.

As of July 5, approximately 28% (by area) of the grounded portion of Nipterk (320 m) had calved. Due to cumulative ablation, island freeboard was typically reduced to between 0.5 to 1 m except in areas where the spray ice surface had been protected. The island appeared to be disintegrating in a different manner than that observed at the relief pad. At Nipterk, calving appeared to occur due to an instability condition created as a result of insufficient freeboard. Small portions of the island periodically lifted off the bottom and were eventually carried away by winds and current.

After break out of the first-year ice sheet, the protection sheets were draped over the island edge as per design. The south edge of the Rufco sheet was almost entirely in contact with open water on July 5.

Island breakup was anticipated in the near future due to the instability created by the lack of freeboard. Several new cracks had already developed where portions of the island became buoyant. However, even though the island was deteriorating at an accelerated pace, there was no evidence of significant horizontal sliding along the seabed at any of the slope indicator survey stations which may have been indicative of a precursor to eventual catastrophic breakup.

The performance of the sheets on mitigating edge erosion had, to date, only been evaluated for a brief period. Therefore, in order to continue collecting data for as long a period as possible, a decision was made not to terminate the experiment. Most of the nonessential equipment was removed from the island by helicopter on July 5.

To monitor the progression of island deterioration more closely, another site survey was scheduled for July 10. Based on the condition of the island at that time, the option existed to immediately demobilize the edge protection system onto a barge as Arctic Transportation Ltd. (ATL) would be undertaking salvage operations of equipment which had broken through the ice at the base of the island earlier in the year. Alternatively, another option available was to demobilize following completion of the salvage operation. The timing for retrieval of ablation and edge erosion monitoring instrumentation would also be assessed at the time. It was felt that this approach would enable a maximum data collection effort and still afford the opportunity for a quickly instituted complete

demobilization in the event of imminent island breakup. Selection of this option also enabled us to go ahead with plans to dock a barge alongside the island since this operation would be required in demobilizing a drilling rig during the open water season.

The island was next visited on July 6 for a brief period by an Esso representative during a final cleanup site inspection. Small-scale calving was reported as was a newly formed crack in the vicinity of the gravel ablation plots. An aerial photography survey was undertaken on the morning of July 8 to determine the island area, effectiveness of the edge erosion sheets, and the general state of the island. By this time, only about 35% of the island (by area) remained.

Nipterk was next visited by Esso personnel on July 10. However, the remaining portion of the island had broken up into a number of small fragments in only a matter of a few hours according to ATL personnel. The date of complete island breakup was about 2.5 weeks after breakup of the surrounding ice sheet. Most of the fragments subsequently drifted westward under the influence of light easterly winds and currents.

From an ensuing aerial reconnaissance survey, it was determined that the island remnants were still located within 500 m of their original calving site. Several fragments appeared to have drifted only a short distance and temporarily grounded. Unfortunately, even after a thorough search, the island fragments containing the ablation plots and geotechnical instrumentation could not be spotted. These fragments probably rolled onto their side due to an instability condition created by the ablation protection materials (mainly gravel). ATL personnel confirmed that several island fragments rolled shortly after calving.

DEMOBILIZATION OF THE EDGE PROTECTION SYSTEM

After island break-up the edge protection system had to be recovered due to the potential environmental and navigation hazards it imposed. On the afternoon of July 10, two of the three edge protection sheets were visible just to the west of the former island site. Both the Rufco and 18 oz. per square yard nylon sheet had entrapped air beneath them so that a portion of each was raised out of the water.

The netting from all four protection systems was also easily identified by their wooden 20 cm by 20 cm anchors which were now afloat. At the time of our survey, the location of the 13 oz. vinyl tarp could not be identified, though it was speculated that the sheet was still being held in place by the netting. Arrangements were made with ATL to recover the edge protection system as soon as the salvage operation was completed.

Another helicopter aerial reconnaissance survey was instituted the following day. The wind direction had reversed from that the previous day and was now west-northwesterly. No island fragments were visible; the nearest ice being 10 km away. The sheets could no longer be seen in the heavily silted water, but the netting was known to still be on-site as evidenced by the floating anchors.

The entire edge protection system was successfully retrieved over a 12-hour period on July 12. To perform this operation, divers first determined the exact positions of the sheets. Then, the crane barge was moved into position so that sheets could be reached. A clam bucket was used to lift the sheets onto the barge. After successfully completing the recovery operation, the barge was towed back to Tuktoyaktuk and the edge protection system disposed of.

ISLAND SETTLEMENT

The spray ice foundation beneath rig structures must not only provide an adequate bearing capacity for all dead and live loads, but also exhibit acceptable settlement. Since spray ice is viscoelastic, the allowable bearing pressure will be controlled by consideration of settlement rather than bearing capacity. Surface subsidence caused by time-dependent deformation of the spray ice mass, is one of the critical aspects of a spray ice drilling platform. The anticipated total and differential settlements are of particular interest for rig foundations. Predicted subsidence characteristics could potentially impact both planning of the drilling operation (by allowing time for initial settlement prior to rig up) or the type of rig and foundation mat used including special means for rig leveling.

During their operating period, drilling rigs are capable of withstanding a certain magnitude of creep settlement without a disruption in drilling activities. Surface

settlement rates will likely increase as the spray ice temperature increases above -5°C.

Towards this end, measurements of surface settlement were performed at as many as five locations during the experiment. The survey locations shown in Figure 11 were the same as those at which inclinometer surveys were undertaken.

The Sondex settlement system utilized was installed in January as part of the winter island monitoring program. System components consisted of a Sondex probe, an electrical cable graduated in meters, a readout unit, and the flexible casing. A measurement stand was located above the casing to facilitate depth measurement. Over time, spray ice ablation progressed to the extent that the base of the stand melted out and the stand could no longer be utilized.

Sensing rings were originally mounted to the outside of the Sondex casing at approximately 0.5 m intervals. The precise location of the sensing points was determined by means of electrical induction. The sensor's meter peaked when the probe's internal coil was aligned with the sensing point. Probe depth was measured by picking off the depth indicated on the cable corresponding to a graduated measurement tape on the reader stand (or affixed to the inclinometer casing). Since the sensing rings move (or settle) with the surrounding ice, the change in elevation of each ring with time can be directly related to settlement.

Sondex settlement surveys were performed at varying frequencies and locations during the experiment due to a number of reasons including time constraints, restricted access to the station or to the bottom of the casing, and in the case of the June 10 survey, a lack of alternative means available to perform the measurements due to loss of the reader stands. Settlement data are available throughout the experiment period for stations located near the edge of the island working surface.

Figure 35 is a representative settlement profile measured at the southwest edge of the island working surface. Settlement profiles for the other survey locations are presented along with the raw settlement data in Appendix F. The seabed is at a depth of about 10.5 to 11 m whereas the submerged spray ice is represented by the

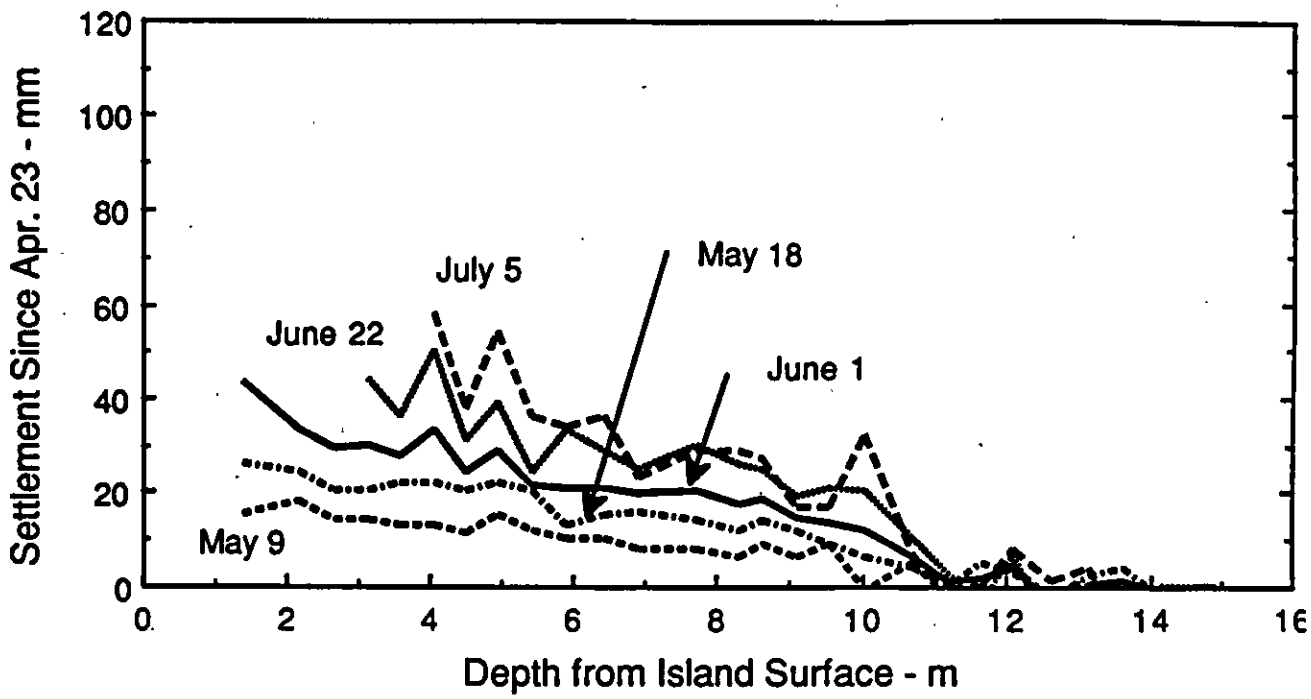

Figure 35. Spray Ice Settlement at Southwest Survey Statior

level 4.5 m below the surface to the seabed. As a result of spray ice ablation the uppermost 2 m of Sondex casing was cut off on June 22 due to the height of stick up. An additional meter of casing was removed on July 5. Consequently, settlement data for the upper 3-4 m of the island were not collected after the June 22 survey.

An extrapolation of the settlement data on June 1 was performed for each of the three drilling pad settlement monitoring stations. The extrapolation may be a bit conservative in that it does not take into account the below freezing air temperatures prevalent throughout most of May. Based on the interpolation, maximum settlements ranged from 37 cm to 45 mm. Neither the magnitude nor rate of settlement documented would have posed any operational problems for a drilling rig. In fact, from a standpoint of total surface settlement, the drilling rig could have operated through to at least July 5. Maximum differential settlement across the working surface was estimated to be less than 1 cm on June 1. Like total surface settlement, the maximum differential settlement estimated for June 1 is not expected to impose any restrictions on operating a drilling rig until this time. It appears from the profiles, that differential settlement would not have created any drilling restrictions until after at least June 22. By July 5, only the southeast station appears to be settling at an accelerated rate. However, this apparent trend may actually be at least partially due to bending of the casing.

Surface settlement measured near the southwest edge of the island was only measured on May 9 and 18. The inclinometer casing had buckled at the seabed prior to the June 10 survey to the extent that the sensor could not be completely lowered down to the bottom. The maximum total surface settlement of 1 cm documented on May 18 was only one-half to one-third that measured on the drilling pad. In apparent contrast, total settlement observed at the north-northeast edge of the island on May 18 appeared to be significantly greater. It appears that most of the apparent settlement may have been due to localized failure. If this 50 to 60 mm offset is removed from the data, the total surface settlement observed is similar to that measured on the drilling pad.

ISLAND HORIZONTAL MOVEMENT

Nipterk was constructed at a site having relatively weak soils. In fact, the soil strength rather than the spray ice strength had the greatest impact on island design. The drilling rig can only withstand a certain magnitude of island lateral deformation before operations are affected. Therefore, monitoring of lateral deformation is required throughout the drilling program as a means to assess island stability.

Five manually read inclinometers (slope indicators) were installed in January as part of the winter island stability monitoring program. Three of the five were at the periphery of the drilling pad whereas the other two were near the edge of the island (see Figure 11). Inclinometer casings were installed inside Sondex casings which in turn were anchored at different depths below the seabed. These stations were left intact at the conclusion of the drilling program so that measurements could be continued.

Casing consisted of 7 cm outside diameter self-aligning 3.05 m (10 ft) long ABS plastic pipes. The inner surface of the casing was inscribed with four equispaced longitudinal grooves milled to control inclinometer orientation in a preselected direction (north-south or east-west). Casings were originally installed such that they projected about 0.3 m above the island surface. Propylene glycol was poured into the casing to prevent it from filling with water and eventually freezing.

A standard metric Digitilt Inclinometer probe manufactured by Slope Indicator Company (SINCO) was utilized. It consisted of a watertight aluminum cylinder that contained two servo-accelerometers mounted with the sensitive axes 90° apart which measure the angle of inclination of the longitudinal axis of the sensor in two orthogonal planes. The sensor was supported laterally in the casing by means of two sets of wheels which are guided by the casing grooves.

The inclinometer was supported by a heavy duty electrical cable graduated in one-half meter increments. To perform a survey, the probe was first lowered to the bottom of the casing and allowed to equilibrate. Then, the inclinometer was raised to the surface at 0.5 m increments and readings were collected in both the

A and B (orthogonal) directions. After completion of the first survey, the probe was rotated 180° and a second survey was performed for greater accuracy.

Inclinometer data were collected using the SINCO Recorder Printer Processor (RPP) system. The RPP collected, stored, processed and displayed the digitilt data in terms of deflection vs. depth profiles.

Slope indicator surveys were undertaken during each complete site survey except at the south-southwest survey station where the casing deformed to the point that surveys could not be performed after May 18. An initial (reference) slope indicator survey was carried out on April 22 and data from subsequent surveys were compared relatively.

Inclinometer data and plots containing lateral deformation profiles for each of the stations in the north-south and east-west directions are provided in Appendix G. Representative profiles from north-south and east-west direction for the survey station at the southwest edge of the drilling pad are shown in Figures 33 and 34 Deflections are given in millimeters and depths are shown in meters with regard to mean sea level which is denoted by a depth of 0 m. Positive depths correspond to the freeboard. Negative depths to as low as -6 to -6.5 m are associated with submerged spray ice whereas the seabed is below this depth. Relative changes in the surface of the island are also apparent from the profiles.

As can be seen from the Figure 36, 36, and Appendix H, total deflections measured at the stations near the edge of the drilling pad (i.e. southwest, southeast, and north) were typically small (maximum 13 mm in any one direction). Also note that most of the movement resulted from sliding along the seabed.

Up until June 10 or June 22, depending upon the location, the island moved predominantly to the north. Then in late-June and early July the island movement direction reversed. Movements were greater in the north-south direction than in the east-west direction.

Due to the presence of cracks, both the magnitude and direction of horizontal displacements often varied from measurement location to measurement location.

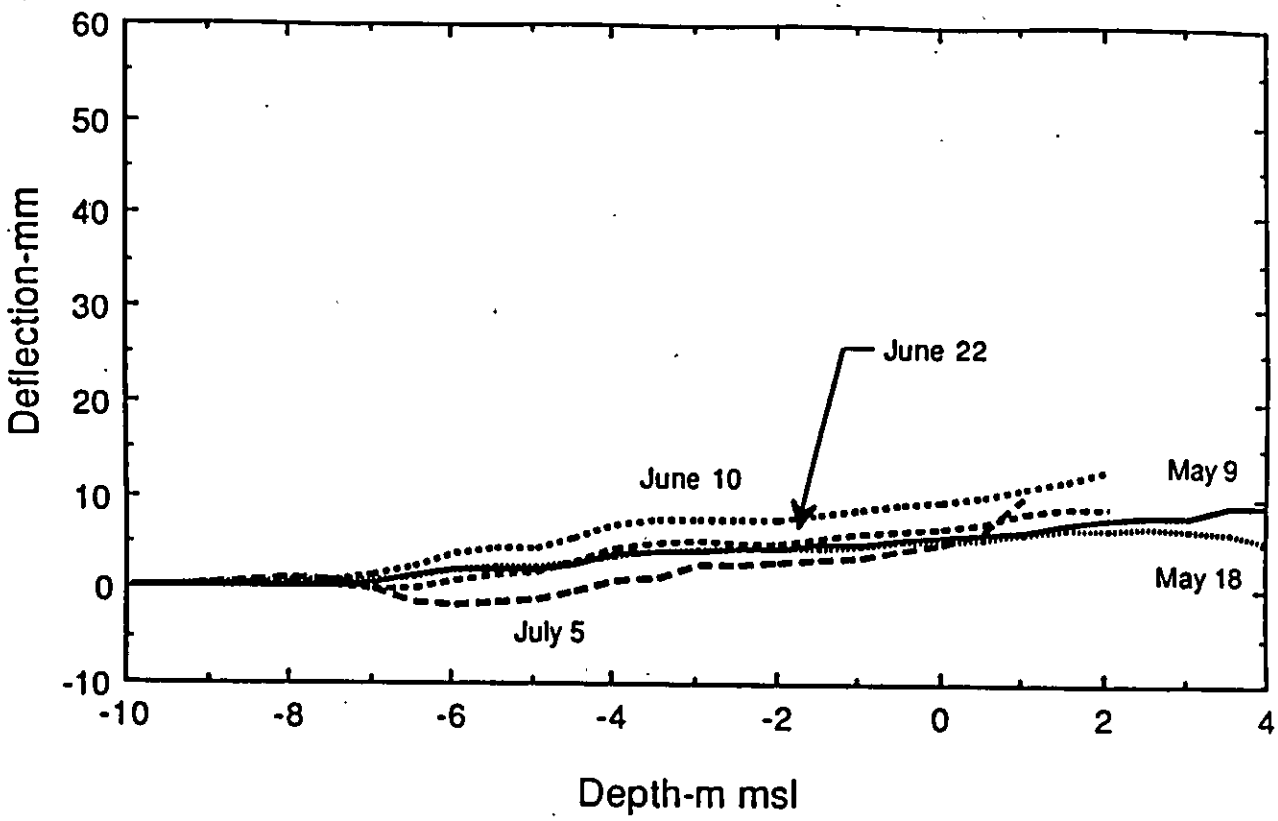

Figure 36. Southwest Slope Indicator Station Deformation Profiles (North-South Direction)

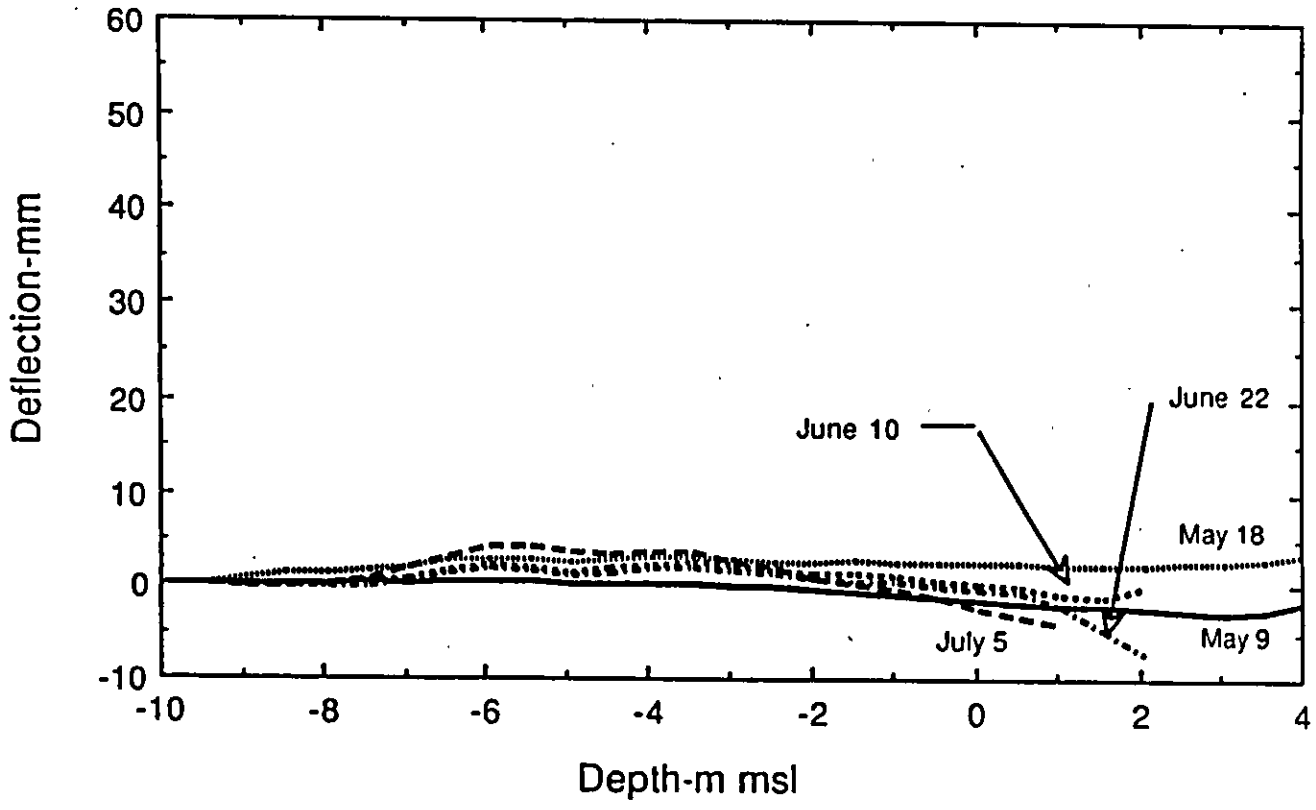

Figure 37. Southwest Slope Indicator Station Deformation Profiles (East-West Direction)

Horizontal movements were, however, typically much less in magnitude and more similar in direction on the working surface than near the island edge.

Deformation profiles from inclinometer stations near the island periphery are shown in Figures in Appendix H. The magnitude of deformation was significantly greater at these sites than on the working surface. Most of the deformation at the south-southwest survey station occurred along the seabed. Over 6 cm of movement along the seabed was measured on May 18. Cumulative casing buckling became so great shortly after this time that the slope indicator probe could no longer be lowered to a level below the seabed.

Unlike any of the other survey sites, deformation at the north-northeast site appeared to be over a larger plane of failure in the saturated spray ice above the seabed at least in the north-south direction. The total magnitude of deflection was 5.8 cm on July 5. By this time, the island had eroded to within 15 m of the station and several new cracks were apparent between the station and island center. The dominant movement direction was to the north throughout the measurement period. As with the other sites, deflections measured in the east-west direction were substantially smaller than those measured in the north-south direction. Most of the movement (albeit small), was observed along the seabed. Movement directions changed from westerly to easterly over time.

EXTENDED OPERATIONS ON SPRAY ICE

OVERVIEW

This section addresses operations on spray ice in conditions and operating regimes that have not been generally considered for normal Arctic operations. The information presented was gained by Polar Alpine over two seasons of constructing spray ice structures in sub-arctic and marginally arctic conditions. A more detailed account of these operations is provided in Polar Alpine's report - see Appendix H.

Two spray ice structures constructed by Polar Alpine were built at Nome, Alaska during the 1987/88 and 1988/89 winter seasons. The primary function of the spray

ice barriers at Nome was to protect a gold dredge and tugboat that could not be moored in the inner harbor at Nome. As a result, the two vessels wintered over alongside the causeway that forms the Port of Nome. The Nome jetty is 600 m long and projects southward into Norton Sound. Vessels moored alongside the jetty are subjected to the force of ice movements as a result of movements of the active Norton Sound ice pack. For vessels required to winter alongside the Nome Jetty some type of protection against ice forces is mandatory. In addition to protection, the spray ice barrier at Nome also acted as a work platform from which heavy equipment could operate to repair and service the vessels through the winter. The spray ice barrier at Nome proved successful during the first season it was employed. A spray ice barrier was again constructed during the 1988-1989 winter season.

Special construction techniques were employed to construct the barrier at the relatively high ambient temperatures experienced at Nome. The construction also extended our knowledge of how to operate on relatively warm spray ice surfaces, how to operate heavy equipment close to the edge of spray ice and how to remove spray ice quickly and efficiently when required.

A spray ice structure was also built at the Red Dog Port Site 26 km south of Kivaline, Alaska, during the 1988-1989 winter. The purpose of the spray ice structure at the Red Dog Site was to provide a jetty over which heavy equipment could be moved to construct a gravel-filled sheet pile sea cell. In addition to constructing a jetty for the movement of equipment, a barrier was also constructed to protect the structure while it was being built.

The spray ice jetty and barrier at the Red Dog Site provided information regarding the extent to which operations can be safely carried out on spray ice. Polar Alpine's report includes an overview of the operations carried out at both Nome and the Red Dog Port Site. Their review considers: over-ice operations on spray ice with heavy equipment, a stress analysis of the loads imposed on spray ice, surface preparation and ablation protection of spray ice to increase its durability, and the removal and excavation of spray ice.

In terms of over-ice operations, the various types of equipment operated over the spray ice at the two construction sites is considered. In general the main concern

in their report centers on our experience at moving heavy equipment over narrow spray ice structures at high ambient air temperatures. Often, the temperatures at both the Nome site and the Red Dog site were above freezing for extended periods of time. Also, since the spray ice structures were used for platforms for off-ice construction, it was necessary to operate the equipment close to the edge of the spray ice. To accommodate these operations extensive use was made of crane mats to lower the ground pressure of the equipment. Crane mats (rig mats) were used to effectively facilitate operations of high ground-pressure equipment on spray ice in proximity with the edge of the spray ice structures.

Stresses imposed on narrow spray ice structures by heavy equipment operations were also considered. The primary objective of the analysis was to look at loads that are causing failures in spray ice structures. To carry out this work, information available on the state of stress at failure in spray ice was discussed. This information is used as the criteria for failure in a four-material finite element stress analysis. Several different types of spray ice loads are considered. In the first instance, a narrow spray ice structure is considered subjected only to body loadings. The primary objective of this analysis is to show that the magnitude of stresses due to gravitational forces are small and generally uniform, even over narrow structures.

The second type of load considered is the magnitude of the pressure required to induce an incipient failure in the spray ice and the pattern of failure within the spray ice. In this case a centrally located load was spread over a width of 6 m on a spray ice structure 16 m wide. This model reproduced typical situations encountered at the Nome and Red Dog Port Site. It was found that subsurface failure was induced when the ground pressure exceeded 276 kPa.

In the third case the situation was investigated where the load was moved to the vertical edge of the spray ice structure. Using the same load distribution considered in case two Polar Alpine found that the upper edge of the spray ice failed when the ground pressure rose above 145 kPa. The analysis was consistent with observations of equipment that were made on spray ice while operating in the field.

Of considerable interest was how to harden the surface of spray ice in the absence of low temperatures. Spray ice surfaces are typically hardened by spraying water on the surface and letting it soak in and freeze. At both Nome and the Red Dog Site the temperatures were too high to utilize this technique. To operate around this limitation Polar Alpine found that coating the surface with a layer of gravel served to harden it sufficiently to operate heavy equipment over it continuously. They also found that a layer of material such as gravel spread over the surface tended to act as an insulating layer, slowing the rate at which surface melting occurred.

The final topic in Polar Alpine's report deals with methods for removing and excavating spray ice. In terms of excavating spray ice, Polar Alpine found that ordinary excavation techniques could be used to remove both above-and-below water spray-ice. Typically a backhoe and dragline can be used to excavate spray ice at rates as fast if not faster as when similar equipment is used on gravel. For constructing docking facilities for barges and vessels, standard excavation techniques are applicable to spray ice. For completely removing spray ice structures, wheelwashing with tugboats or ice breakers proved extremely effective. In one instance, 150,000 m^3 of spray ice were removed in a period of eight to ten hours.

The Polar Alpine report sums up a great deal of experience concerning extended operations on spray ice. As a means of further extending spray ice operations they offer suggestions for further work that could be carried out to improve our understanding of the limits to which operations on spray ice can be carried.

CONCLUSIONS

General

As a result of this study, the feasibility of protecting the edges and surface of a spray ice island against ablation to extend drilling operations through the breakup period and to demobilize drilling equipment from the island immediately after landfast ice breakup was demonstrated. The island provided a stable platform from which drilling operations could have continued until early July.

More specific conclusions are detailed below under the headings of Surface Ablation, Edge Erosion, Island Stability, and Equipment Demobilization.

Surface Ablation

1. Ablation of clean spray ice commenced when the mean daily air temperature rose above 0°C, which in this experiment occurred on May 25. The average cumulative ablation of clean spray ice was 2.25 m by July 5.

2. Ablation of heavily soiled spray ice commenced in early April due to the low albedo of the dirty spray ice, increased solar radiation, and a period of near 0°C air temperatures. As the spray ice ablated, dirt concentrated as a thin surficial veneer. When this layer reached a critical thickness it served to insulate the underlying spray ice and therefore mitigate further ablation. The critical thickness of this layer was not measured but it is estimated to be about 0.5 to 2 cm. The maximum measured ablation coincided with soiled spray ice and was found to be 2.8 m by July 5.

3 Spray ice ablation was effectively controlled with surface coatings. The following minimum thicknesses were required to effectively prevent ablation up until July 5:

- 0.6 m of gravel
- 0.15 m of sawdust
- 0.2 m of wood (i.e. rig matting)

Smaller thicknesses of the above materials were effective in reducing ablation. For example, areas covered with 1 cm of sawdust ablated only 0.8 m up until July 5.

4. Fabric sheets also mitigated ablation. Areas covered with uninsulated tarps experienced about 1.0 m of ablation by July 5 whereas cumulative ablation was one-half this amount beneath an insulated tarp.

5. Ablation also played a major role in edge erosion in that large portions of the island became buoyant and floated away when the freeboard was reduced (by ablation) to about 0.75 m.

Edge Erosion

1. Edge erosion resulted from *in situ* melting and calving after breakup of the landfast ice sheet. *In situ* melting was due to warm currents, air temperatures, and solar radiation. Calving occurred when either warm currents or waves undercut the island edge or the spray ice became buoyant due to loss of freeboard through surface ablation. Accelerated edge erosion was observed on the south side of the island following the arrival of warm water outflow from the Mackenzie River on June 23.

2. Impermeable sheets effectively reduced edge erosion to about 25 m by July 8. Several types of fabric sheets were evaluated, but no one sheet appeard to be superior to the others in regard to erosion and ablation protection. The Rufco sheet was considered best overall however, by virtue of its lower cost and ease of installation.

Island Stability

1. Horizontal island movements within the working surface area were less than 15 mm up until the working surface disintgrated after July 5.

2. The average island surface settlement over the period April 23 to June 1 was about 45 mm. The maximum differential settlement across the working surface over the same period was estimated to be less than 10 mm.

Equipment Demobilization

1. A barge docking area can be created by shaping the spray ice at the island edge with a backhoe or a crane positioned near the island edge.

2. If necessary, wheelwash from a tugboat can be used to remove potentially unstable areas at the edge of the island.

3. A crane barge can be used to offload rig equipment from the island immediately prior to and immediately after landfast ice breakup.

4. Adequate surface trafficability can be assured by placing about 0.6 m of gravel on the island surface.

RECOMMENDATIONS

A logical follow-up to this investigation would be to perform a detailed design study for a drilling rig marine demobilization operation from a spray ice platform. Such an analysis should include an assessment of risks and costs.

Because a rig demobilization from a spray ice island has not yet been attempted, the initial effort would likely be undertaken in a conservative and not necessarily cost effective manner in order to guarantee its success as soon after landfast ice breakup as feasible. Some of the perceived risks presently associated with this operation could be minimized or better defined by performing another experiment on a future ice island demobilized prior to breakup utilizing the design and methodology identified in the design study.

ACKNOWLEDGEMENTS

REFERENCES

1. Connolly, S.T., 1986: Artificial Ice Islands for Deep Water and Production Structures, In Proceedings Fourth International Conference on Cold Regions Engineering, Anchorage, Alaska, ASCE, pp. 58-68.

2. Maykut, G.A. and Untersteiner, N., 1976, Some Results from a Time-Dependent Thermo-Dynamic Model of Sea Ice, Journal of Geophysical Research, Vol. 76, No. 6.

3. El-Tahan, M., Venkatech, S., and El-Tahan, H., 1984: Validation and Quantitative Assessment of the Deterioration Mechanisms of Arctic Icebergs, in the Proceedings-ASME Offshore Mechanics/Arctic Engineering Symposium, New Orleans, LA., Feb. 1984, ASME, NY.

4. Colbeck, S.C., 1988: Snowmelt Increase Through Albedo Reduction, U.S. Army Corps. of Engineers Cold Regions Research and Engineering Laboratory Special Report 88-26, December, 11 p.

5. Ashwell, I.Y. and Hannell, F.G., 1966: Experiments on a Snow-Patch in the Mountains of Sweden, Journal of Glaciology, Vol. 6, No. 43, pp. 135-144.

6. Rhodes, J.J., Armstrong, R.L., and Waren, S.G., 1987: Mode of Formation of "Ablation Hollows" Controlled by Dirt Content of Snow, Journal of Glaciology, Vol. 33, No. 114, pp. 135-139.

7. Jahns, H.O., Petrie, D.H., and Lockett, A.V., 1986: CIDS Spray Ice Barrier, 18th Annual Offshore Technology Conference, Houston, Texas, pp. 575-584.

8. St. Lawrence, W., 1989: Extended Operations on Spray Ice, Proprietary Report Prepared by Polar Alpine, Inc., 31 p.

9. Prodanovic, A., 1981: Ice Island Experiment - Summer Monitoring Report, Exxon Production Research Company Production Operations Report EPR. 43 PS.81 prepared for AOGA 49, 89 p.

10. White, F.M., Spalding, M.L., and Gominho, L., 1980: Theoretical Estimates of the Various Mechanisms Involved in Iceberg Deterioration in the Open Environment, U.S. Coast Guard Report No. CG-0-62-80.

APPENDIX A

METEOROLOGICAL MEASUREMENTS

Meteorological data were gathered from the island during the period June 7 to July 5. Tuktoyaktuk data were used to supplement the island measurements during the first half of the study before the weather station was deployed and after the July 5 site survey through island breakup. Island-based data were utilized in the analysis whenever possible as these data are indicative of conditions on the island.

		Meteorological Data					
	Wind			Temperature			Solar
Date	Date Fraction	Direction (degrees)	Speed	maximum	straight	minimum	Radiation
	(Julian Day)	(N=0,360 S=180)	(knots)	(ºC)	(ºC)	(ºC)	(kW/m2)
20-Apr	110.75	247	4	-14		-24	
21-Apr	111.00		0	-15		-23	
	111.25	90	12				
	111.50	67	10				
	111.75	22	2				
22-Apr	112.00	0	6	-15		-23	
	112.25	270	6				
	112.50		0				
	112.75						
23-Apr	113.00	67	14	-16		-23	
	113.25	67	10				
	113.50	90	8				
	113.75	90	8				
24-Apr	114.00	90	12	-1		-17	
	114.25	67	12				
	114.50	90	2				
	114.75	157	5				
25-Apr	115.00		0	7		-7	
	115.25		0				
	115.50	112	2				
	115.75	112	7				
26-Apr	116.00		0	-3		-8	
	116.25	292	10				
	116.50	0	6				
	116.75	270	12				
27-Apr	117.00	270	2	-7		-11	
	117.25	292	8				
	117.50	292	10				

			Meteorological Data					
		Wind		Temperature			Solar	
Date	Date Fraction	Direction (degrees)	Speed	maximum	straight	minimum	Radiation	
	(Julian Day)	(N=0,360 S=180)	(knots)	(ºC)	(ºC)	(ºC)	(kW/m2)	
	117.75	292	8					
28-Apr	118.00	292	20	-5		-13		
	118.25	292	18					
	118.50	339	10					
	118.75	135	8					
29-Apr	119.00	135	14	-5		-12		
	119.25	45	10					
	119.50	22	12					
	119.75	22	10					
30-Apr	120.00	339	12	-7		-14		
	120.25		0					
	120.50	225	4					
	120.75	270	8					
1-May	121.00	270	18	-3		-12		
	121.25	270	10					
	121.50	270	4					
	121.75	247	14					
2-May	122.00	247	10	-5		-10		
	122.25	339	5					
	122.50	292	6					
	122.75	270	6					
3-May	123.00	292	14	-8		-14		
	123.25	292	10					
	123.50	315	10					
	123.75	339	5					
4-May	124.00	180	8	2		-13		
	124.25	135	10					
	124.50	135	6					

		Meteorological Data					
	Wind			Temperature			Solar
Date	Date Fraction (Julian Day)	Direction (degrees) (N=0,360 S=180)	Speed (knots)	maximum (°C)	straight (°C)	minimum (°C)	Radiation (kW/m2)
	124.75	157	7				
5-May	125.00		0	-3		-14	
	125.25	45	8				
	125.50	0	15				
	125.75	315	13				
6-May	126.00	292	8	-12		-19	
	126.25	0	4				
	126.50	67	8				
	126.75	67	14				
7-May	127.00	67	14	-7		-15	
	127.25	67	2				
	127.50	67	8				
	127.75	67	10				
8-May	128.00	67	6	-10		-19	
	128.25	45	8				
	128.50	67	10				
	128.75	45	10				
9-May	129.00	292	12	-10		-14	
	129.25						
	129.50						
	129.75	22	10				
10-May	130.00	45	10	-8		-12	
	130.25	45	8				
	130.50	67	15				
	130.75	67	22				
11-May	131.00			-3		-20	
	131.25	67	6				
	131.50	45	6				

				Meteorological Data						
			Wind			Temperature				Solar
Date		Date Fraction	Direction (degrees)	Speed		maximum	straight	minimum		Radiation
		(Julian Day)	(N=0,360 S=180)	(knots)		(ºC)	(ºC)	(ºC)		(kW/m2)
		131.75	90	4						
12-May		132.00		0		4		-10		
		132.25	67	9						
		132.50	67	20						
		132.75	67	14						
13-May		133.00	0	10		-7		-14		
		133.25	315	10						
		133.50	315	10						
		133.75	339	8						
14-May		134.00	315	5		-8		-12		
		134.25	67	5						
		134.50	90	10						
		134.75	90	10						
15-May		135.00	90	16		-5		-15		
		135.25	90	18						
		135.50	90	14						
		135.75	90	15						
16-May		136.00	67	12		-8		-11		
		136.25	45	12						
		136.50	0	10						
		136.75	315	12						
17-May		137.00	339	10		-5		-9		
		137.25	339	10						
		137.50	339	8						
		137.75	270	5						
18-May		138.00	112	6		-3		-11		
		138.25	90	5						
		138.50	90	10						

			Meteorological Data				
	Wind			Temperature			Solar
Date	Date Fraction	Direction (degrees)	Speed	maximum	straight	minimum	Radiation
	(Julian Day)	(N=0,360 S=180)	(knots)	(ºC)	(ºC)	(ºC)	(kW/m2)
	138.75	45	5				
19-May	139.00			-3		-6	
	139.25	339	3				
	139.50	22	6				
	139.75	0	2				
20-May	140.00	315	5	-1		-9	
	140.25	45	4				
	140.50	90	4				
	140.75	90	4				
21-May	141.00	90	3	2		-7	
	141.25	90	6				
	141.50	90	2				
	141.75	67	4				
22-May	142.00	67	2	-7		-7	
	142.25	67	6				
	142.50	45	15				
	142.75	67	12				
23-May	143.00	67	15	-3		-14	
	143.25	67	12				
	143.50						
	143.75	90	14				
24-May	144.00	90	15	-1		-11	
	144.25	90	18				
	144.50	90	8				
	144.75	90	14				
25-May	145.00	67	10	1		-10	
	145.25	67	15				
	145.50	90	5				

			Meteorological Data				
		Wind		Temperature			Solar
Date	Date Fraction	Direction (degrees)	Speed	maximum	straight	minimum	Radiation
	(Julian Day)	(N=0,360 S=180)	(knots)	(ºC)	(ºC)	(ºC)	(kW/m2)
	145.75	90	8				
26-May	146.00	90	8	6		-7	
	146.25	90	10				
	146.50	90	2				
	146.75	112	5				
27-May	147.00	90	8	12		2	
	147.25	112	5				
	147.50		0				
	147.75	157	6				
28-May	148.00	135	6	9		-3	
	148.25	157	2				
	148.50	0	4				
	148.75	339	4				
29-May	149.00	45	2	13		1	
	149.25	90	5				
	149.50	90	4				
	149.75	90	10				
30-May	150.00	90	10	19		4	
	150.25	90	10				
	150.50	90	10				
	150.75	90	10				
31-May	151.00		1	19		5	
	151.25	90	10				
	151.50	112	8				
	151.75	90	10				
1-Jun	152.00			14		3	
	152.25	45	6				
	152.50	270	8				

				Meteorological Data						
			Wind			Temperature				Solar
Date		Date Fraction	Direction (degrees)	Speed		maximum	straight	minimum		Radiation
		(Julian Day)	(N=0,360 S=180)	(knots)		(ºC)	(ºC)	(ºC)		(kW/m2)
		152.75	270	4						
2-Jun		153.00	339	4		9		1		
		153.25	270	5						
		153.50	270	8						
		153.75	270	8						
3-Jun		154.00	292	10		11		1		
		154.25	270	5						
		154.50	90	4						
		154.75	112	4						
4-Jun		155.00	90	15		13		0		
		155.25	90	4						
		155.50	90	6						
		155.75		0						
5-Jun		156.00	270	10		3		-1		
		156.25	292	20						
		156.50	339	12						
		156.75	292	10						
6-Jun		157.00				3		0		
		157.25	339	6						
		157.50	0	6						
		157.75	0	8						
7-Jun		158.00				9		-2		
		158.25	45	5						
		158.50	45	4						
		158.67					7.11			0.684
		158.71					7.61			0.649
		158.75	90	5			8.21			0.591
		158.79					8.53			0.516

			Meteorological Data					
		Wind		Temperature			Solar	
Date	Date Fraction	Direction (degrees)	Speed	maximum	straight	minimum	Radiation	
	(Julian Day)	(N=0,360 S=180)	(knots)	(ºC)	(ºC)	(ºC)	(kW/m2)	
	158.83				8.49		0.431	
	158.88				8.1		0.342	
	158.92				7.34		0.255	
	158.96				6.44		0.173	
8-Jun	159.00			19	5.43	2	0.111	
	159.04				3.98		0.068	
	159.08				2.91		0.040	
	159.13				2.1		0.039	
	159.17				1.8		0.053	
	159.21				1.68		0.048	
	159.25	90	12		1.84		0.135	
	159.29				2.35		0.195	
	159.33				2.99		0.273	
	159.38				3.81		0.353	
	159.42				4.95		0.444	
	159.46				6.37		0.517	
	159.50	90	2		7.99		0.592	
	159.54				9.52		0.637	
	159.58				10.89		0.666	
	159.63				12.08		0.677	
	159.67				13.12		0.666	
	159.71				14.47		0.628	
	159.75	135	2		15.35		0.570	
	159.79				15.9		0.496	
	159.83				15.79		0.416	
	159.88				15.47		0.328	
	159.92				14.69		0.241	
	159.96				13.69		0.162	

		Meteorological Data					
	Wind		Temperature			Solar
Date	Date Fraction (Julian Day)	Direction (degrees) (N=0,360 S=180)	Speed (knots)	maximum (ºC)	straight (ºC)	minimum (ºC)	Radiation (kW/m2)
9-Jun	160.00			21	12.95	8	0.101
	160.04				11.2		0.041
	160.08				9.24		0.028
	160.13				8.01		0.040
	160.17				6.92		0.050
	160.21				6		0.042
	160.25	112	6		5.65		0.127
	160.29				5.81		0.183
	160.33				6.24		0.255
	160.38				6.85		0.352
	160.42				7.43		0.414
	160.46				8.4		0.519
	160.50	157	10		9.34		0.577
	160.54				10.35		0.559
	160.58				11.34		0.619
	160.63				12.34		0.669
	160.67				13.44		0.659
	160.71				14.29		0.634
	160.75	157	6		15		0.566
	160.79				15.51		0.443
	160.83				15.26		0.405
	160.88				14.63		0.168
	160.92				13.76		0.227
	160.96				12.45		0.098
10-Jun	161.00	180	12	18	9.35	2	0.056
	161.04				7.34		0.021
	161.08				5.83		0.010
	161.13				4.84		0.013

		Meteorological Data				
	Wind		Temperature			Solar
Date	Date Fraction	Direction (degrees)	Speed	maximum	straight	minimum	Radiation
	(Julian Day)	(N=0,360 S=180)	(knots)	(ºC)	(ºC)	(ºC)	(kW/m2)
	161.17				3.98		0.044
	161.21				3.57		0.031
	161.25	157	8		3.08		0.045
	161.29				2.81		0.073
	161.33				2.74		0.092
	161.38				2.8		0.132
	161.42				2.93		0.080
	161.46				2.81		0.167
	161.50	270	4		3.19		0.155
	161.54				3.73		0.249
	161.58				4.32		0.270
	161.63				4.98		0.277
	161.16						
	161.17						
	161.75	270	10		9.13		0.433
	161.79				9.3		0.304
	161.83				8.66		0.183
	161.88				7.3		0.090
	161.92				5.98		0.066
	161.96				4.88		0.040
11-Jun	162.00	315	8	11	3.99	0	0.021
	162.04				3.36		0.016
	162.08				2.82		0.014
	162.13				2.4		0.018
	162.17				2.09		0.014
	162.21				1.82		0.021
	162.25	0	6		1.63		0.049
	162.29				1.56		0.038

					Meteorological Data							
			Wind			Temperature				Solar		
Date		Date Fraction	Direction (degrees)	Speed		maximum	straight	minimum		Radiation		
		(Julian Day)	(N=0,360 S=180)	(knots)		(ºC)	(ºC)	(ºC)		(kW/m2)		
		162.33					1.47			0.056		
		162.38					1.58			0.133		
		162.42					2.11			0.216		
		162.46					2.92			0.289		
		162.50	339	4			3.91			0.357		
		162.54					5.34			0.449		
		162.58					6.82			0.468		
		162.63					7.7			0.403		
		162.67					8.15			0.645		
		162.71					8.63			0.608		
		162.75	0	5			8.86			0.534		
		162.79					8.76			0.544		
		162.83					9.03			0.407		
		162.88					9.2			0.319		
		162.92					8.8			0.207		
		162.96					8.49			0.138		
12-Jun		163.00	339	5		11	8.04	1		0.094		
		163.04					7.34			0.076		
		163.08					6.73			0.041		
		163.13					6.15			0.036		
		163.17					5.14			0.049		
		163.21					4.25			0.041		
		163.25	135	8			3.55			0.060		
		163.29					3.05			0.102		
		163.33					2.85			0.172		
		163.38					2.94			0.225		
		163.42					3.31			0.319		
		163.46					3.91			0.414		

				Meteorological Data						
			Wind			Temperature				Solar
Date		Date Fraction	Direction (degrees)	Speed		maximum	straight	minimum		Radiation
		(Julian Day)	(N=0,360 S=180)	(knots)		(ºC)	(ºC)	(ºC)		(kW/m2)
		163.50	202	5			4.7			0.454
		163.54					5.06			0.381
		163.58					5.68			0.493
		163.63					6.81			0.567
		163.67					7.66			0.449
		163.71					7.99			0.458
		163.75	270	12			8.31			0.346
		163.79					8.05			0.267
		163.83					7.06			0.192
		163.88					6.15			0.151
		163.92					5.35			0.079
		163.96					4.59			0.048
13-Jun		164.00	270	4		3	3.88	0		0.035
		164.04					3.26			0.016
		164.08					2.7			0.013
		164.13					2.29			0.011
		164.17					1.96			0.019
		164.21					-0.02			0.040
		164.25					1.76			0.027
		164.29	315	4			1.66			0.052
		164.33					1.63			0.063
		164.38					1.67			0.109
		164.42					1.8			0.125
		164.46					2.07			0.200
		164.50					2.56			0.239
		164.54	315	10			3.68			0.464
		164.58					4.74			0.468
		164.63					5.31			0.404

					Meteorological Data							
			Wind				Temperature				Solar	
Date		Date Fraction	Direction (degrees)		Speed		maximum	straight	minimum		Radiation	
		(Julian Day)	(N=0,360 S=180)		(knots)		(ºC)	(ºC)	(ºC)		(kW/m2)	
		164.67						5.84			0.404	
		164.71						6.42			0.415	
		164.75						6.62			0.364	
		164.79	315		10			6.74			0.343	
		164.83						6.2			0.252	
		164.88						5.22			0.166	
		164.92						4.34			0.104	
		164.96						3.47			0.089	
14-Jun		165.00					7	3.04	-2		0.145	
		165.04	315		10			3.05			0.063	
		165.08						2.14			0.028	
		165.13						1.28			0.016	
		165.17						0.65			0.027	
		165.21						-0.44			0.038	
		165.25	45		6			-0.53			0.108	
		165.29						-0.46			0.118	
		165.33						-0.49			0.191	
		165.38						-0.16			0.214	
		165.42						0.25			0.319	
		165.46						0.98			0.539	
		165.50	45		12			2.11			0.579	
		165.54						3.13			0.610	
		165.58						4.09			0.665	
		165.63						4.86			0.613	
		165.67						5.64			0.662	
		165.71						6.22			0.577	
		165.75	45		15			6.39			0.576	
		165.79						6.92			0.437	

			Meteorological Data					
		Wind		Temperature				Solar
Date	Date Fraction	Direction (degrees)	Speed	maximum	straight	minimum		Radiation
	(Julian Day)	(N=0,360 S=180)	(knots)	(ºC)	(ºC)	(ºC)		(kW/m2)
	165.83				6.49			0.404
	165.88				6.67			0.357
	165.92				6.43			0.255
	165.96				5.64			0.195
15-Jun	166.00	45	8	8	4.75	-2		0.130
	166.04				3.52			0.083
	166.08				2.53			0.055
	166.13				1.67			0.051
	166.17				1.03			0.063
	166.21				0.65			0.046
	166.25	45	10		0.56			0.140
	166.29				0.7			0.199
	166.33				1			0.270
	166.38				1.36			0.351
	166.42				1.86			0.436
	166.46				2.58			0.533
	166.50	45	10		3.46			0.594
	166.54				4.39			0.645
	166.58				5.17			0.680
	166.63				5.8			0.694
	166.67				6.47			0.687
	166.71				7.09			0.657
	166.75	45	10		7.57			0.604
	166.79				7.8			0.533
	166.83				7.74			0.450
	166.88				7.47			0.365
	166.92				7.03			0.277
	166.96				7.1			0.187

		Meteorological Data					
	Wind		Temperature				Solar
Date	Date Fraction	Direction (degrees)	Speed	maximum	straight	minimum	Radiation
	(Julian Day)	(N=0,360 S=180)	(knots)	(ºC)	(ºC)	(ºC)	(kW/m2)
16-Jun	167.00	67	16	17	6.61	2	0.122
	167.04				5.29		0.078
	167.08				3.94		0.052
	167.13				2.98		0.046
	167.17				2.31		0.060
	167.21				1.93		0.045
	167.25	90	12		1.85		0.135
	167.29				2.14		0.190
	167.33				2.6		0.258
	167.38				3.27		0.331
	167.42				4.23		0.412
	167.46				5.47		0.502
	167.50	135	5		7.01		0.575
	167.54				8.44		0.720
	167.58				9.01		0.679
	167.63				9.02		0.565
	167.67				9.48		0.680
	167.71				10.45		0.593
	167.75	180	6		10.7		0.583
	167.79				10.34		0.298
	167.83				8.66		0.171
	167.88				7.08		0.127
	167.92				5.9		0.102
	167.96				4.81		0.021
17-Jun	168.00	270	14	15	3.71	1	0.017
	168.04				2.91		0.020
	168.08				2.3		0.008
	168.13				1.83		0.007

		Meteorological Data				
	Wind		Temperature			Solar
Date	Date Fraction (Julian Day)	Direction (degrees) (N=0,360 S=180)	Speed (knots)	maximum (ºC)	straight (ºC)	minimum (ºC)	Radiation (kW/m2)
	168.17				1.46		0.012
	168.21				1.2		0.026
	168.25	292	10		1.03		0.049
	168.29				0.96		0.078
	168.33				1.02		0.120
	168.38				1.31		0.162
	168.42				1.68		0.195
	168.46				2.17		0.239
	168.50	315	5		2.76		0.325
	168.54				4.04		0.454
	168.58				5.69		0.613
	168.63				6.97		0.681
	168.67				8.26		0.675
	168.71				9.62		0.643
	168.75	247	8		10.94		0.593
	168.79				12.13		0.529
	168.83				13.01		0.444
	168.88				13.92		0.326
	168.92				13.57		0.186
	168.96				10.54		0.033
18-Jun	169.00	270	8	15	8.34	0	0.019
	169.04				6.52		0.009
	169.08				5		0.006
	169.13				3.83		0.013
	169.17				2.94		0.045
	169.21				2.29		0.029
	169.25	225	6		1.72		0.044
	169.29				1.3		0.066

				Meteorological Data				
		Wind		Temperature				Solar
Date	Date Fraction	Direction (degrees)	Speed	maximum	straight	minimum		Radiation
	(Julian Day)	(N=0,360 S=180)	(knots)	(ºC)	(ºC)	(ºC)		(kW/m2)
	169.33				1.11			0.113
	169.38				1.07			0.250
	169.42				1.33			0.337
	169.46				1.85			0.405
	169.50	0	25		2.26			0.344
	169.54				2.61			0.391
	169.58				3.09			0.338
	169.63				3.47			0.403
	169.67				4.33			0.461
	169.71				5.02			0.400
	169.75	339	16		5.57			0.421
	169.79				7.04			0.522
	169.83				8.14			0.273
	169.88				7.77			0.184
	169.92				7.1			0.133
	169.96				6.4			0.124
19-Jun	170.00			12	5.04	-1		0.038
	170.04				3.74			0.022
	170.08				2.56			0.016
	170.13				1.38			0.018
	170.17				0.75			0.028
	170.21				0.69			0.038
	170.25	135	4		0.96			0.098
	170.29				1.49			0.121
	170.33				1.98			0.133
	170.38				2.52			0.208
	170.42				3.27			0.207
	170.46				3.99			0.274

		Meteorological Data					
	Wind		Temperature			Solar
Date	Date Fraction	Direction (degrees)	Speed	maximum	straight	minimum	Radiation
	(Julian Day)	(N=0,360 S=180)	(knots)	(ºC)	(ºC)	(ºC)	(kW/m2)
	170.50	180	10		4.76		0.309
	170.54				5.13		0.188
	170.58				4.78		0.095
	170.63				4.61		0.164
	170.67				4.51		0.102
	170.71				3.88		0.075
	170.75	180	18		3.42		0.222
	170.79				3.46		0.243
	170.83				3.19		0.181
	170.88				2.78		0.093
	170.92				2.11		0.088
	170.96				1.6		0.062
20-Jun	171.00			7	1.11	-1	0.033
	171.04				0.55		0.014
	171.08				0.08		0.014
	171.13				-0.44		0.031
	171.17				-0.81		0.032
	171.21				-1.07		0.050
	171.25	315	20		-0.85		0.132
	171.29				-0.42		0.160
	171.33				0.18		0.254
	171.38				0.72		0.339
	171.42				1.29		0.428
	171.46				2.02		0.523
	171.50	45	5		2.93		0.584
	171.54				3.92		0.636
	171.58				4.74		0.670
	171.63				5.3		0.684

		Meteorological Data				
	Wind		Temperature			Solar
Date	Date Fraction (Julian Day)	Direction (degrees) (N=0,360 S=180)	Speed (knots)	maximum (ºC)	straight (ºC)	minimum (ºC)	Radiation (kW/m2)
	171.67				5.83		0.677
	171.71				6.97		0.650
	171.75	90	2		8.29		0.599
	171.79				9.3		0.531
	171.83				9.86		0.447
	171.88				9.83		0.363
	171.92				9.5		0.273
	171.96				8.81		0.184
21-Jun	172.00	90	6	17	7.78	2	0.121
	172.04				6.22		0.076
	172.08				4.87		0.049
	172.13				3.81		0.042
	172.17				3.13		0.044
	172.21				2.76		0.034
	172.25	90	15		2.72		0.112
	172.29				2.75		0.157
	172.33				3.02		0.239
	172.38				3.56		0.338
	172.42				4.34		0.424
	172.46				5.15		0.500
	172.50	180	4		6.03		0.560
	172.54				6.95		0.612
	172.58				7.77		0.651
	172.63				8.55		0.678
	172.67				9.45		0.663
	172.71				10.21		0.642
	172.75	135	10		10.77		0.552
	172.79				11.27		0.467

			Meteorological Data					
		Wind		Temperature			Solar	
Date	Date Fraction	Direction (degrees)	Speed	maximum	straight	minimum	Radiation	
	(Julian Day)	(N=0,360 S=180)	(knots)	(ºC)	(ºC)	(ºC)	(kW/m2)	
	172.83				11.16		0.397	
	172.88				10.79		0.353	
	172.92				10.24		0.229	
	172.96				9.27		0.159	
22-Jun	173.00			23	8.34	7	0.118	
	173.04				7.19		0.072	
	173.08				6.22		0.040	
	173.13				5.42		0.041	
	173.17				4.98		0.054	
	173.21				4.72		0.036	
	173.25	90	8		4.69		0.117	
	173.29				4.8		0.152	
	173.33				5.1		0.254	
	173.38				5.56		0.252	
	173.42				6.14		0.384	
	173.46				7.22		0.487	
	173.50	135	10		8.66		0.566	
	173.54				9.51		0.602	
	173.58				10.3		0.618	
	173.63				10.62		0.573	
	173.67				14.65		0.643	
	173.71				19.91		0.612	
	173.75	157	10		16.67		0.564	
	173.79				15.88		0.499	
	173.83				16.06		0.315	
	173.88				16.02		0.293	
	173.92				15.23		0.078	
	173.96				12.98		0.031	

			Meteorological Data				
	Wind		Temperature			Solar	
Date	Date Fraction (Julian Day)	Direction (degrees) (N=0,360 S=180)	Speed (knots)	maximum (ºC)	straight (ºC)	minimum (ºC)	Radiation (kW/m2)
23-Jun	174.00	157	10	21	11.21	9	0.034
	174.04				10		0.017
	174.08				9.01		0.017
	174.13				7.8		0.023
	174.17				7.15		0.023
	174.21				6.49		0.033
	174.25	157	4		6.3		0.094
	174.29				5.96		0.098
	174.33				5.75		0.146
	174.38				6.24		0.300
	174.42				6.49		0.246
	174.46				6.39		0.354
	174.50	135	10		6.68		0.410
	174.54				6.97		0.450
	174.58				7.86		0.616
	174.63				8.8		0.470
	174.67				9.54		0.526
	174.71				10.38		0.499
	174.75	247	8		11.55		0.468
	174.79				12.97		0.516
	174.83				14.06		0.368
	174.88				14.29		0.360
	174.92				13.98		0.099
	174.96				13.09		0.200
24-Jun	175.00	339	6	26	12.74	9	0.118
	175.04				11.36		0.075
	175.08				9.79		0.049
	175.13				8.39		0.028

			Meteorological Data				
		Wind		Temperature			Solar
Date	Date Fraction	Direction (degrees)	Speed	maximum	straight	minimum	Radiation
	(Julian Day)	(N=0,360 S=180)	(knots)	(ºC)	(ºC)	(ºC)	(kW/m2)
	175.17				7.25		0.050
	175.21				6.65		0.035
	175.25	22	4		6.24		0.104
	175.29				6.04		0.165
	175.33				6.04		0.140
	175.38				5.93		0.120
	175.42				5.76		0.242
	175.46				6.43		0.418
	175.50	90	8		7.21		0.521
	175.54				7.94		0.506
	175.58				8.57		0.548
	175.63				8.8		0.511
	175.67				8.76		0.427
	175.71				8.93		0.604
	175.75	112	5		9.11		0.272
	175.79				8.34		0.323
	175.83				8.4		0.362
	175.88				8.5		0.228
	175.92				7.74		0.108
	175.96				6.94		0.095
25-Jun	176.00	90	18	13	6.11	5	0.035
	176.04				5.29		0.026
	176.08				4.64		0.019
	176.13				4.07		0.019
	176.17				3.64		0.037
	176.21				3.42		0.049
	176.25	67	16		3.28		0.063
	176.29				3.1		0.097

					Meteorological Data								
			Wind				Temperature					Solar	
Date		Date Fraction	Direction (degrees)	Speed		maximum	straight	minimum				Radiation	
		(Julian Day)	(N=0,360 S=180)	(knots)		(ºC)	(ºC)	(ºC)				(kW/m2)	
		176.33					3.1					0.147	
		176.38					3.24					0.282	
		176.42					3.67					0.246	
		176.46					3.93					0.433	
		176.50	45	16			4.54					0.558	
		176.54					5.24					0.596	
		176.58					5.78					0.474	
		176.63					6.23					0.650	
		176.67					6.97					0.638	
		176.71					7.73					0.586	
		176.75	22	16			8.42					0.540	
		176.79					8.98					0.488	
		176.83					9.27					0.432	
		176.88					9.38					0.350	
		176.92					9.26					0.241	
		176.96					8.57					0.197	
26-Jun		177.00				17	8.06	3				0.144	
		177.04					7.15					0.083	
		177.08					6.05					0.059	
		177.13					4.98					0.046	
		177.17					4.11					0.050	
		177.21	22	20			3.51					0.039	
		177.25					3.16					0.111	
		177.29					3.06					0.158	
		177.33					3.11					0.222	
		177.38					3.35					0.297	
		177.42					3.62					0.379	
		177.46					3.98					0.468	

				Meteorological Data						
			Wind			Temperature				Solar
Date		Date Fraction	Direction (degrees)	Speed		maximum	straight	minimum		Radiation
		(Julian Day)	(N=0,360 S=180)	(knots)		(ºC)	(ºC)	(ºC)		(kW/m2)
		177.50	22	16			4.41			0.542
		177.54					5			0.594
		177.58					5.79			0.634
		177.63					6.77			0.655
		177.67					8.1			0.655
		177.71					9.58			0.632
		177.75	22	11			9.17			0.503
		177.79					8.87			0.503
		177.83					8.53			0.428
		177.88					8.22			0.342
		177.92					7.93			0.257
		177.96					7.48			0.174
27-Jun		178.00	45	12		20	6.85	9		0.109
		178.04					6.01			0.069
		178.08					5.37			0.030
		178.13					4.61			0.014
		178.17					4.02			0.017
		178.21					3.62			0.021
		178.25	45	8			3.3			0.033
		178.29					3.05			0.099
		178.33					3.25			0.221
		178.38					3.67			0.305
		178.42					3.98			0.378
		178.46					4.52			0.412
		178.50	90	4			4.83			0.408
		178.54					4.91			0.367
		178.58					5.09			0.520
		178.63					5.35			0.436

		Meteorological Data				
	Wind		Temperature			Solar
Date	Date Fraction	Direction (degrees)	Speed	maximum	straight	minimum	Radiation
	(Julian Day)	(N=0,360 S=180)	(knots)	(ºC)	(ºC)	(ºC)	(kW/m2)
	178.67				6.03		0.452
	178.71				6.3		0.447
	178.75	339	6		6.08		0.170
	178.79				5.56		0.204
	178.83				5.37		0.188
	178.88				5.08		0.151
	178.92				4.95		0.242
	178.96				5.47		0.190
28-Jun	179.00			10	5.42	5	0.107
	179.04				4.74		0.064
	179.08				4.18		0.027
	179.13				3.59		0.025
	179.17				3.25		0.035
	179.21				3.11		0.039
	179.25	339	10		3.14		0.106
	179.29				3.14		0.113
	179.33				2.98		0.136
	179.38				3.01		0.248
	179.42				3.29		0.322
	179.46				3.34		0.439
	179.50	315	12		3.47		0.545
	179.54				3.59		0.591
	179.58				3.74		0.629
	179.63				4.08		0.679
	179.67				4.8		0.664
	179.71				5.61		0.621
	179.75	315	8		6.6		0.571
	179.79				7.48		0.508

		Meteorological Data				
	Wind		Temperature			Solar
Date	Date Fraction	Direction (degrees)	Speed	maximum	straight	minimum	Radiation
	(Julian Day)	(N=0,360 S=180)	(knots)	(°C)	(°C)	(°C)	(kW/m2)
	179.83				8.03		0.433
	179.88				7.98		0.266
	179.92				7		0.108
	179.96				6.03		0.103
29-Jun	180.00			13	5.58	6	0.074
	180.04				4.88		0.037
	180.08				4.21		0.023
	180.13				3.64		0.029
	180.17				3.24		0.032
	180.21				3.07		0.045
	180.25	0	6		2.95		0.074
	180.29				2.96		0.095
	180.33				3.09		0.104
	180.38				3.19		0.164
	180.42				3.34		0.162
	180.46				3.51		0.291
	180.50	45	4		3.8		0.065
	180.54				3.58		0.153
	180.58				3.86		0.407
	180.63				4.59		0.329
	180.67				4.88		0.253
	180.71				5.03		0.239
	180.75	45	8		5.17		0.309
	180.79				5.59		0.275
	180.83				5.74		0.211
	180.88				5.5		0.120
	180.92				5.08		0.126
	180.96				4.91		0.094

		Meteorological Data				
	Wind		Temperature			Solar
Date	Date Fraction	Direction (degrees)	Speed	maximum	straight	minimum	Radiation
	(Julian Day)	(N=0,360 S=180)	(knots)	(ºC)	(ºC)	(ºC)	(kW/m2)
30-Jun	181.00			12	4.55	2	0.045
	181.04				3.99		0.021
	181.08				3.58		0.007
	181.13				3.26		0.007
	181.17				2.96		0.013
	181.21	90	5		2.75		0.021
	181.25				2.7		0.039
	181.29				2.85		0.040
	181.33				3.06		0.066
	181.38				3.35		0.137
	181.42				3.44		0.061
	181.46				3.03		0.052
	181.50	315	3		2.7		0.167
	181.54				2.64		0.260
	181.58				2.68		0.225
	181.63				2.62		0.306
	181.67				2.92		0.431
	181.71				3.31		0.408
	181.75	315	18		3.29		0.323
	181.79				3.18		0.223
	181.83				2.99		0.234
	181.88				2.94		0.150
	181.92				2.82		0.163
	181.96				2.77		0.121
1-Jul	182.00	0	20	5	2.47	1	0.080
	182.04				2.06		0.071
	182.08				1.71		0.036
	182.13				1.3		0.045

				Meteorological Data						
			Wind			Temperature				Solar
Date		Date Fraction	Direction (degrees)	Speed		maximum	straight	minimum		Radiation
		(Julian Day)	(N=0,360 S=180)	(knots)		(ºC)	(ºC)	(ºC)		(kW/m2)
		182.17					1.15			0.051
		182.21					1.1			0.041
		182.25	339	12			1.1			0.108
		182.29					1.13			0.151
		182.33					1.17			0.185
		182.38					1.15			0.266
		182.42					1.33			0.301
		182.46					1.65			0.339
		182.50	0	10			1.91			0.285
		182.54					2.15			0.362
		182.58					2.49			0.451
		182.63					2.92			0.556
		182.67					3.51			0.490
		182.71					3.9			0.495
		182.75	0	10			4.41			0.534
		182.79					4.93			0.419
		182.83					5.16			0.263
		182.88					4.61			0.144
		182.92					3.91			0.080
		182.96					3.18			0.043
2-Jul		183.00	339	12		5	2.52	2		0.034
		183.04					2.02			0.018
		183.08					1.59			0.012
		183.13					1.21			0.013
		183.17					0.94			0.019
		183.21					0.73			0.036
		183.25	315	8			0.64			0.049
		183.29					0.7			0.080

			Meteorological Data					
		Wind			Temperature			Solar
Date	Date Fraction	Direction (degrees)	Speed	maximum	straight	minimum		Radiation
	(Julian Day)	(N=0,360 S=180)	(knots)	(ºC)	(ºC)	(ºC)		(kW/m2)
	183.33				0.81			0.082
	183.38				0.92			0.094
	183.42				1.04			0.139
	183.46				1.24			0.127
	183.50	292	10		1.25			0.103
	183.54				1.1			0.099
	183.58				0.99			0.097
	183.63				0.93			0.109
	183.67				0.99			0.110
	183.71				1.12			0.114
	183.75	339	10		1.3			0.150
	183.79				1.52			0.115
	183.83				1.56			0.085
	183.88				1.53			0.093
	183.92				1.51			0.064
	183.96				1.44			0.051
3-Jul	184.00	292	22	15	1.33	0		0.036
	184.04				1.2			0.011
	184.08				1.04			0.006
	184.13				0.88			0.004
	184.17				0.75			0.010
	184.21				0.66			0.022
	184.25	0	12		0.62			0.032
	184.29				0.68			0.060
	184.33				0.85			0.062
	184.38				1			0.108
	184.42				1.32			0.150
	184.46				1.96			0.329

			Meteorological Data					
		Wind		Temperature				Solar
Date	Date Fraction	Direction (degrees)	Speed	maximum	straight	minimum		Radiation
	(Julian Day)	(N=0,360 S=180)	(knots)	(ºC)	(ºC)	(ºC)		(kW/m2)
	184.50	0	3		2.94			0.504
	184.54				3.98			0.581
	184.58				4.67			0.615
	184.63				5.3			0.640
	184.67				6.15			0.654
	184.71				6.97			0.562
	184.75	202	7		7.6			0.477
	184.79				8.34			0.511
	184.83				9.01			0.445
	184.88				9.65			0.362
	184.92				9.95			0.270
	184.96				9.9			0.184
4-Jul	185.00	180	12	19	9.53	9		0.100
	185.04				8.48			0.042
	185.08				7.37			0.024
	185.13				6.41			0.016
	185.17				5.6			0.019
	185.21				5.19			0.044
	185.25	157	8		5.42			0.086
	185.29				5.43			0.032
	185.33				5.42			0.067
	185.38				5.65			0.049
	185.42				5.72			0.062
	185.46				6.14			0.284
	185.50	157	7		7.01			0.381
	185.54				7.45			0.493
	185.58				7.61			0.433
	185.63				8.27			0.654

		Meteorological Data				
	Wind		Temperature			Solar
Date	Date Fraction	Direction (degrees)	Speed	maximum	straight	minimum	Radiation
	(Julian Day)	(N=0,360 S=180)	(knots)	(ºC)	(ºC)	(ºC)	(kW/m2)
	185.67				8.97		0.636
	185.71				9.35		0.619
	185.75	270	4		9.39		0.497
	185.79				8.96		0.198
	185.83				8.18		0.306
	185.88				8.01		0.212
	185.92				7.85		0.294
	185.96				8.09		0.144
5-Jul	186.00	315	6	22	7.99	10	0.065
	186.04				7.46		0.013
	186.08				6.94		0.006
	186.13				6.68		0.014
	186.17				6.54		0.023
	186.21				6.41		0.024
	186.25	339	10		6.29		0.046
	186.29				6.21		0.124
	186.33				6.45		0.178
	186.38				6.82		0.287
	186.42				7.41		0.324
	186.46				8.02		0.460
	186.50	270	18		8.67		0.552
	186.54				9.2		0.566
	186.58				9.64		0.617
	186.63				9.93		0.643
	186.67				11.91		0.635
	186.75	270	12				
6-Jul	187.00	225	15	18		9	
	187.25	339	15				

		Meteorological Data					
		Wind		Temperature			Solar
Date	Date Fraction	Direction (degrees)	Speed	maximum	straight	minimum	Radiation
	(Julian Day)	(N=0,360 S=180)	(knots)	(ºC)	(ºC)	(ºC)	(kW/m2)
	187.50	339	4				
	187.75	270	5				
7-Jul	188.00	0	8	17		5	
	188.25	112	6				
	188.50	180	6				
	188.75	0	10				
8-Jul	189.00			16		1	
	189.25	339	10				
	189.50	67	4				
	189.75	180	4				
9-Jul	190.00	22	4	12		6	
	190.25	0	8				
	190.50	339	6				
	190.75	315	4				
10-Jul	191.00			26		9	
	191.25	0	5				
	191.50	157	2				
	191.75	135	10				
	*All data for days110-158 and 187-191 was						
	obtained at Tucktoyaktuk, while solar radiation						
	and straight temperature data for days 158-						
	186 was obtained on the island.						

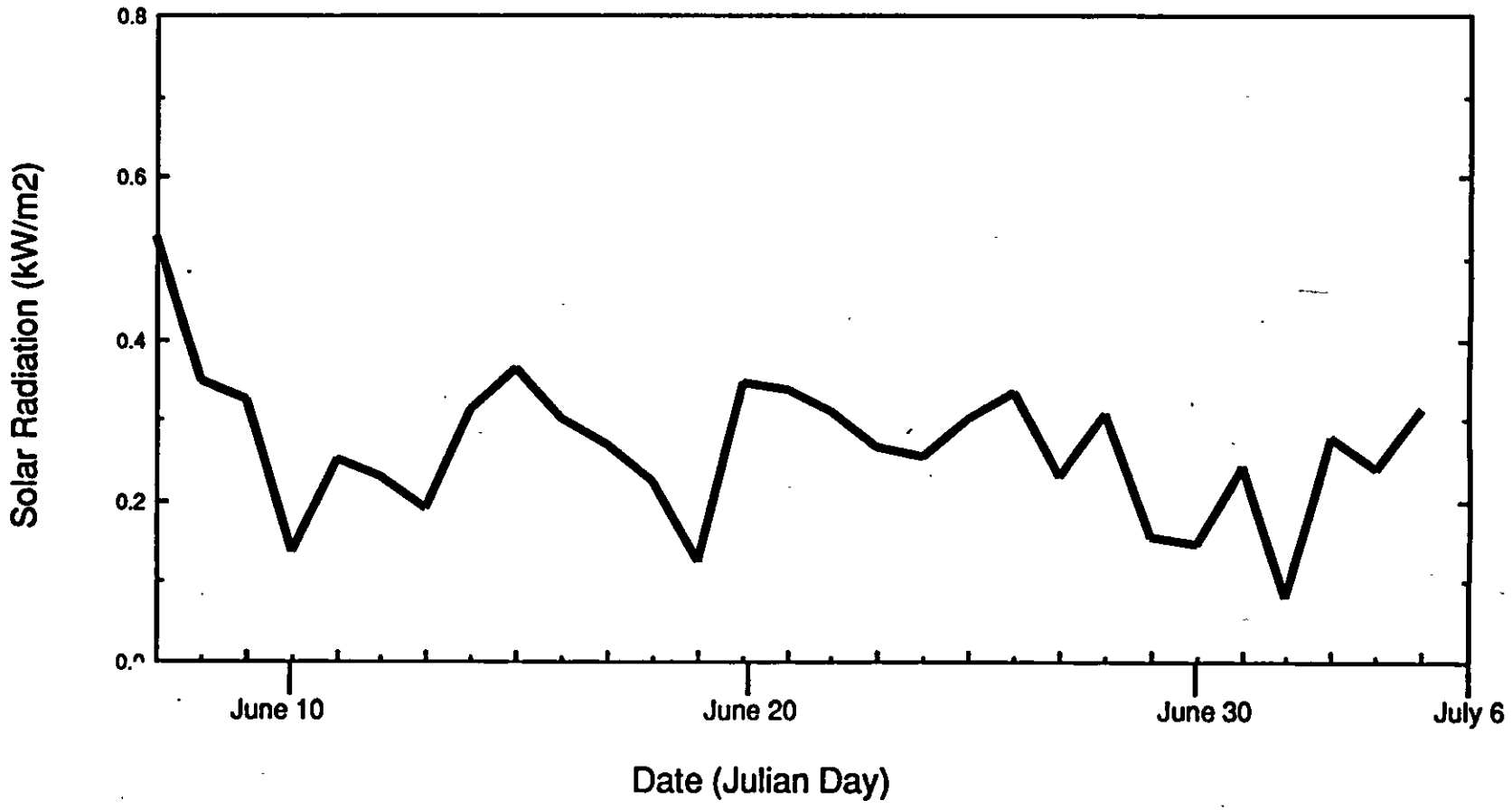

Daily Averaged Solar Radiation

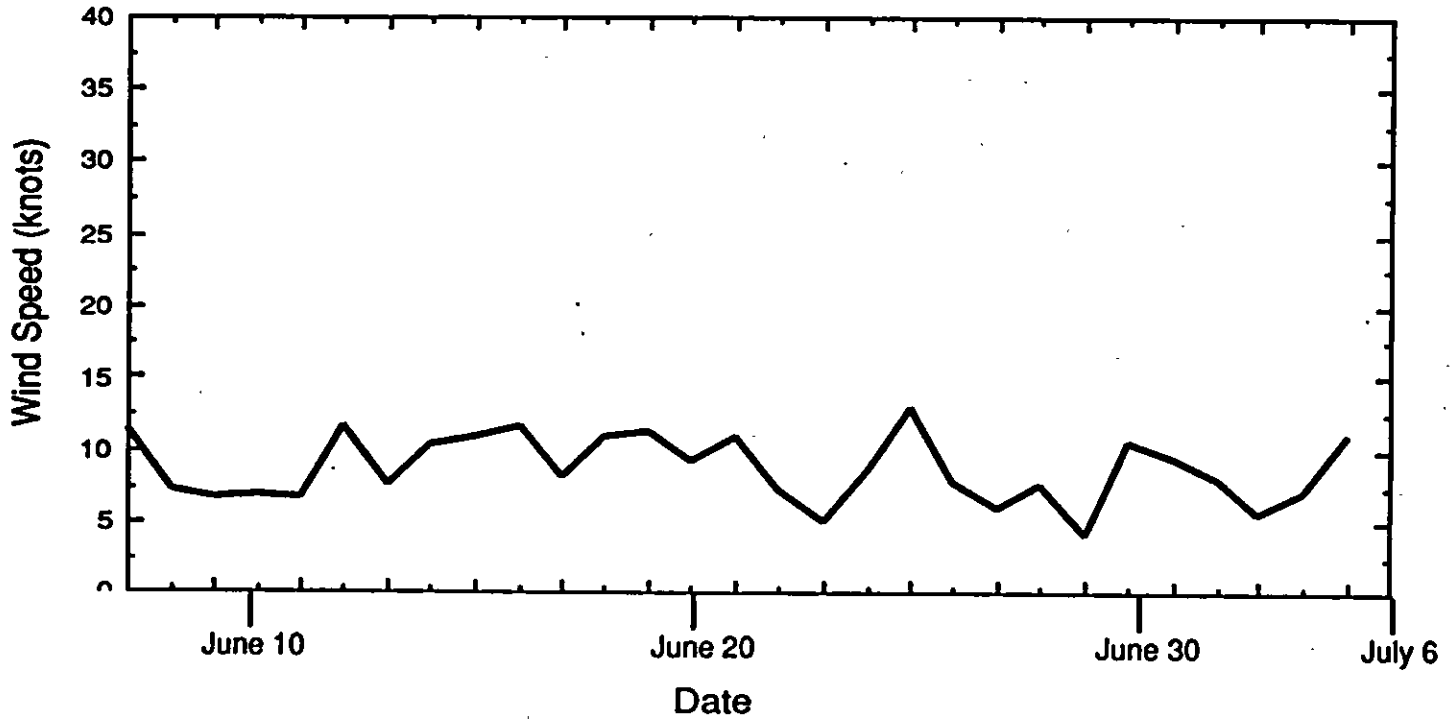

Wind Speed (on Island)

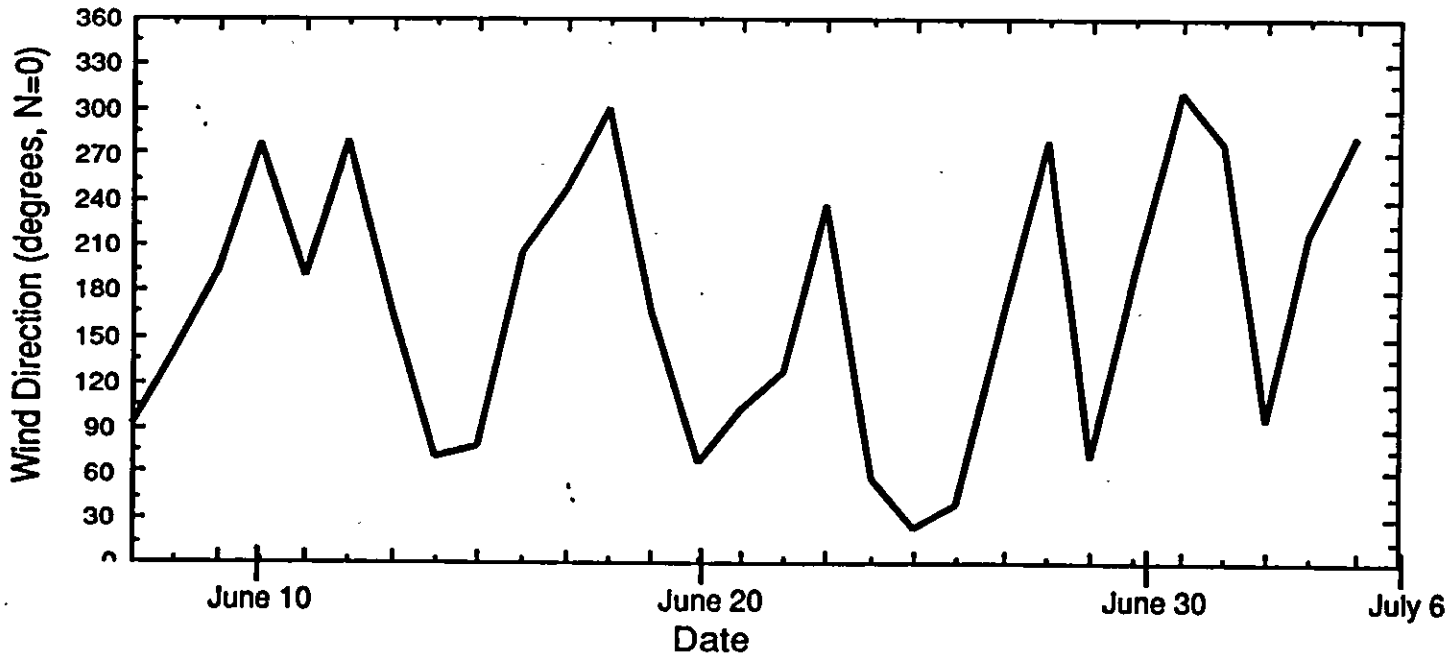

Wind Direction (on island)

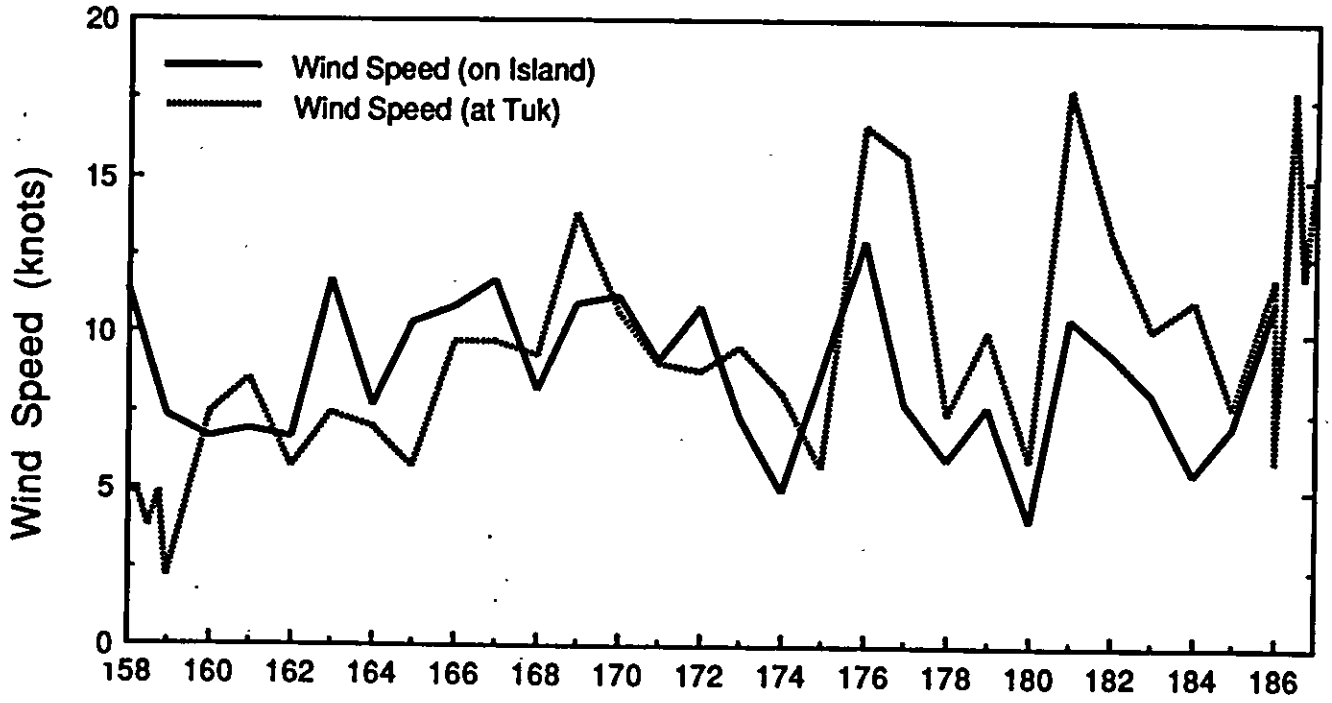

Wind Speed Comparison

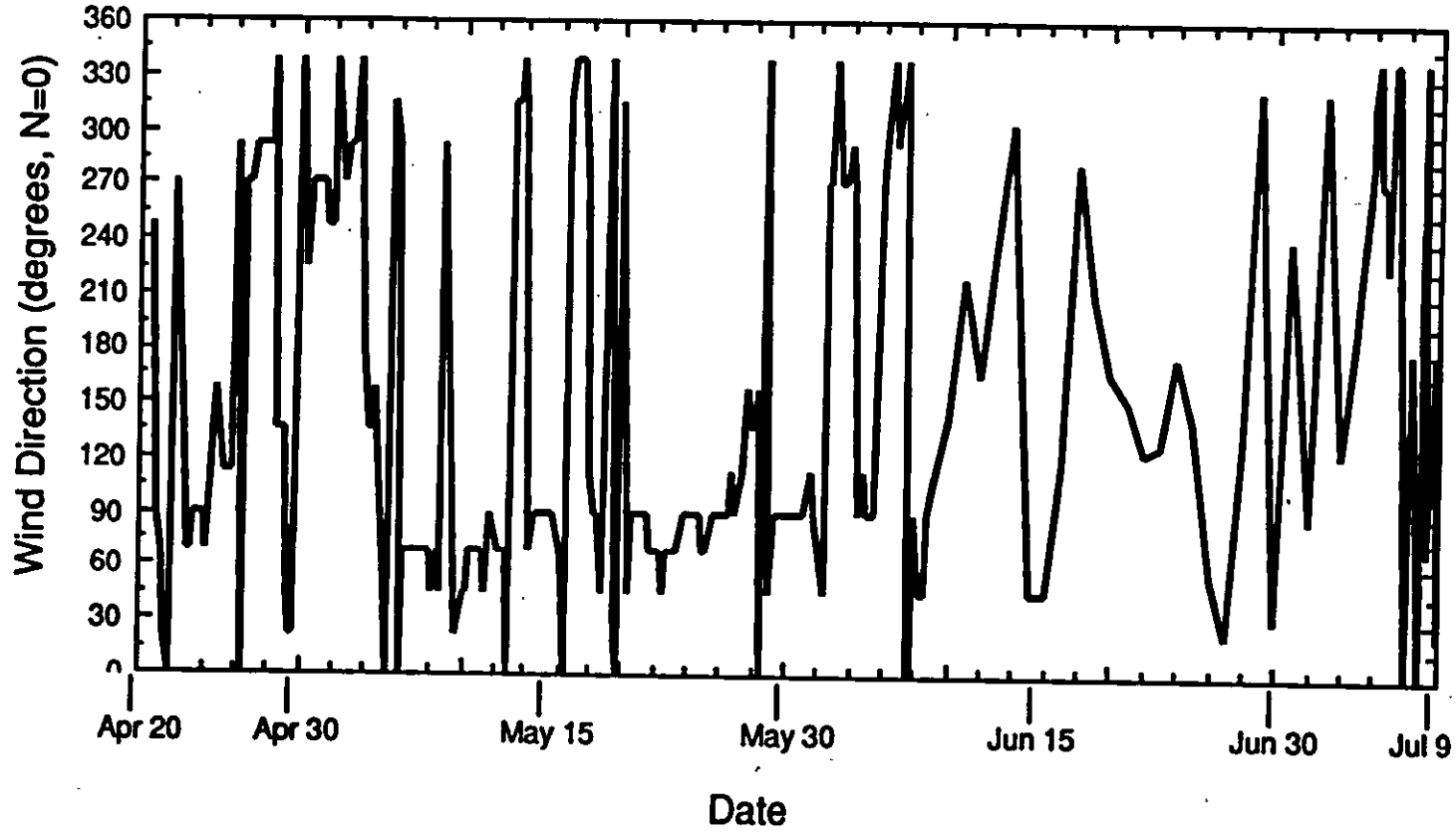

Wind Direction (at Tuk)

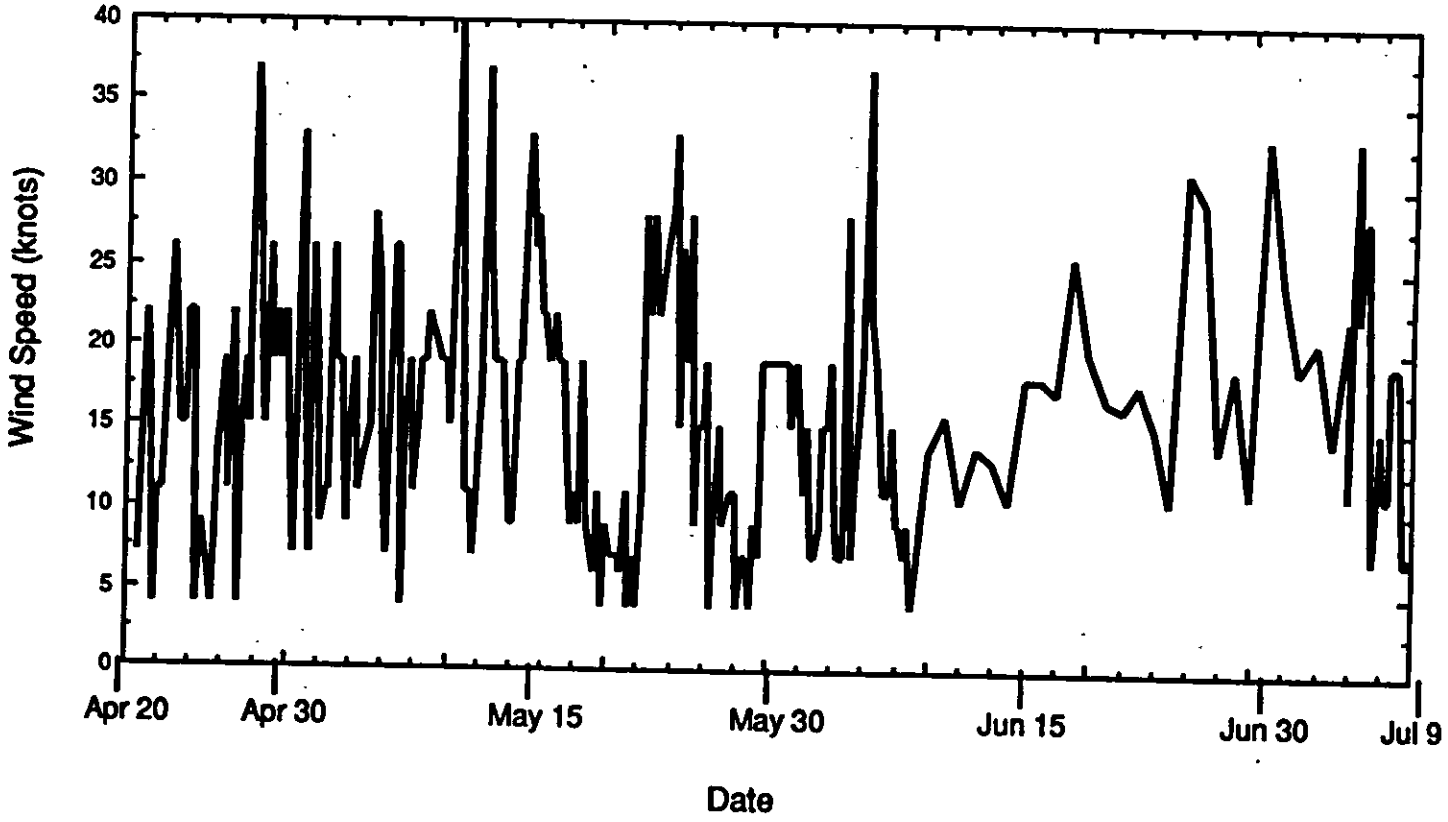

Wind Speed (at Tuk.)

APPENDIX B

ICE TEMPERATURE MEASUREMENTS

Spray ice/seabed temperatures were measured by an 11 m long thermistor string deployed adjacent to the southwest Sondex/Slope Indicator survey station (75 m from island center). The string was made up of 24 thermistors whose spacings varied. Thermistor readings were performed on April 22, May 9, May 18, June 10, and June 22 and the corresponding temperatures are presented in this Appendix. Thermistor resistance readings were taken manually. The resistances in Kohms were then translated into Degrees Celsius using information provided by the thermistor manufacturer.

				Data from Thermistor String									
Thermistor Conversion Table			Spray Ice/Seabed Temperature										
			4/23/89	5/9/89		5/18/89		6/10/89		6/22/89	
Temp.	Resistance	Therm.	Temp.	Resistance	Temp.	Resistance	Temp.	Resistance	Temp.	Resistance	Temp.
(C)	(kohm)	Number	(C)	(kohm)	(C)	(kohm)	(C)	(kohm)	(C)	(kohm)	(C)
-21	51.47	1	-0.510	16.70	-0.43	16.777	-0.52	16.59	-0.30	16.74	-0.48
-20	48.56	2	-0.517	16.75	-0.49	16.756	-0.50			16.75	-0.49
-19	45.83	3	-0.563	16.77	-0.51			16.78	-0.52	16.75	-0.49
-18	43.27	4	-0.555	16.76	-0.50	16.792	-0.54	16.73	-0.47	16.75	-0.49
-17	40.86	5	-0.641	16.78	-0.52			16.82	-0.57	16.75	-0.49
-16	38.61	6	-0.659	16.87	-0.63	16.872	-0.63	16.87	-0.63	16.81	-0.56
-15	36.49	7	-0.701	16.79	-0.53			16.73	-0.47	16.84	-0.59
-14	34.50	8	-0.689	16.74	-0.48			16.81	-0.56	16.83	-0.58
-13	32.63	9	-0.732	16.87	-0.63	16.908	-0.67	16.88	-0.64	16.83	-0.58
-12	30.88	10	-0.765	16.88	-0.64			16.89	-0.65	16.86	-0.62
-11	29.23	11	-0.812	16.89	-0.65			16.89	-0.65	16.9	-0.66
-10	27.67	12	-0.506	16.60	-0.31	16.724	-0.46	16.68	-0.41	16.66	-0.38
-9	26.21	13	-0.185	16.47	-0.16	16.472	-0.17	16.45	-0.14	16.47	-0.16
-8	24.83	14	-0.028	16.40	-0.08			16.42	-0.10	16.42	-0.10
-7	23.54	15	-0.064	16.43	-0.12	16.429	-0.12	16.47	-0.16	16.41	-0.09
-6	22.32	16	-0.019	16.39	-0.07	16.393	-0.07	16.38	-0.06	16.36	-0.03
-5	21.17	17	-0.156	16.50	-0.20	16.538	-0.24	16.52	-0.22	16.46	-0.15
-4	20.08	18	-3.067	18.90	-2.83	18.4	-2.31	16.37	-0.05	16.35	-0.02
-3	19.06	19	-5.766	20.90	-4.75	20.9	-4.75	16.36	-0.03	16.36	-0.03
-2	18.10	20	-7.753	21.90	-5.63	21.53	-5.31	15.81	0.64	16.33	0.00
-1	17.19	21	-9.942	23.80	-7.20	23.2	-6.72	16.36	-0.03	16.45	-0.14
0	16.33	22	-11.194	25.50	-8.49	23.82	-7.22	16.21	0.15	16.39	-0.07
1	15.52	23	-12.315	25.90	-8.78	24.39	-7.66	16.21	0.15		
2	14.75	24	-13.172	26.30	-9.06	24.74	-7.93	15.25	1.35		

			Spray Ice Temperatures Beneath Ablation Plots (Hourly)								
							Temperature (ºC)				
Date	Date Fraction		Average Air Temp.	1.5 cm	2 cm	3 cm	Sawdust	Gravel/	0.3m	0.6 m	1.0 m
	(Julian Day)		(ºC)	Sawdust	Sawdust	Sawdust	Bags	Sawdust	Gravel	Gravel	Gravel
7-Jun	158.67		10.30	1.182	2.394	2.766	0.307	0.944		0.478	
	158.71		9.58	1.066	1.916	2.413	0.305	1.066		0.544	
	158.75		9.59	1.089	1.656	1.984	0.293	1.146		0.567	
	158.79		9.42	1.075	1.449	1.528	0.268	1.188		0.564	
	158.83		8.78	1.007	1.120	0.973	0.222	1.188		0.541	
	158.88		6.44	0.916	0.825	0.712	0.154	1.154		0.507	
	158.92		4.38	0.734	0.598	0.405	0.074	1.098		0.484	
	158.96		3.27	0.567	0.498	0.157	-0.003	1.021		0.441	
8-Jun	159.00		1.54	0.467	0.467	0.045	-0.069	0.944		0.398	
	159.04		0.45	0.096	0.438	-0.007	-0.178	0.859		0.358	
	159.08		-0.44	-0.024	0.375	-0.036	-0.276	0.762		0.318	
	159.13		-0.66	-0.022	0.332	-0.056	-0.319	0.685		0.275	
	159.17		-0.17	-0.008	0.357	-0.031	-0.305	0.585		0.232	
	159.21		0.28	-0.005	0.360	-0.028	-0.314	0.485		0.200	
	159.25		1.64	0.040	0.360	-0.017	-0.291	0.417		0.177	
	159.29		4.37	0.246	0.588	0.029	-0.222	0.360		0.177	
	159.33		6.33	0.517	1.324	0.118	-0.111	0.334		0.163	
	159.38		8.47	0.810	2.374	0.377	0.035	0.332		0.161	
	159.42		11.02	1.273	3.230	1.012	0.044	0.386		0.158	
	159.46		12.87	1.199	3.596	1.857	0.153	0.483		0.187	
	159.50		14.55	1.794	3.950	2.823	0.296	0.626		0.262	
	159.54		15.43	2.320	4.034	3.673	0.439	0.825		0.348	
	159.58		16.17	2.472	3.780	4.129	0.593	1.069		0.456	
	159.63		17.01	2.703	3.931	4.438	0.746	1.336		0.553	
	159.67		17.32	2.956	3.609	4.498	0.911	1.602		0.628	
	159.71		18.68	3.085	3.389	4.402	1.076	1.867		0.690	
	159.75		17.59	2.910	2.899	4.013	1.150	2.088		0.730	
	159.79		17.47	2.874	2.648	3.436	1.135	2.254		0.750	

			Spray Ice Temperatures Beneath Ablation Plots (Hourly)								
							Temperature (ºC)				
Date	Date Fraction		Average Air Temp.	1.5 cm	2 cm	3 cm	Sawdust	Gravel/	0.3m	0.6 m	1.0 m
	(Julian Day)		(ºC)	Sawdust	Sawdust	Sawdust	Bags	Sawdust	Gravel	Gravel	Gravel
	159.83		15.35	2.690	2.172	2.645	1.053	2.375		0.748	
	159.88		12.95	2.386	1.743	1.980	0.940	2.420		0.736	
	159.92		11.30	2.096	1.396	1.475	0.830	2.378		0.694	
	159.96		8.67	1.749	1.229	1.150	0.696	2.279		0.640	
9-Jun	160.00		7.88	1.786	1.152	0.994	0.608	2.136		0.574	
	160.04		6.49	1.180	1.022	0.761	0.511	1.961		0.500	
	160.08		4.29	0.232	0.596	0.403	0.437	1.797		0.460	
	160.13		3.71	0.115	0.456	0.274	0.343	1.613		0.399	
	160.17		3.90	0.174	0.482	0.254	0.265	1.446		0.356	
	160.21		3.17	-0.003	0.396	0.134	0.202	1.282		0.305	
	160.25		5.28	0.421	0.398	0.102	0.193	1.137		0.273	
	160.29		7.93	1.094	1.140	0.253	0.242	0.992		0.230	
	160.33		9.17	1.503	2.487	0.606	0.344	0.890		0.207	
	160.38		11.82	1.941	3.206	1.273	0.535	0.853		0.193	
	160.42		12.34	1.950	3.338	1.961	0.453	0.873		0.202	
	160.46		14.64	1.834	3.741	2.794	0.598	0.950		0.222	
	160.50		15.00	2.091	3.760	3.422	0.641	1.061		0.300	
	160.54		14.69	2.280	3.690	4.061	0.684	1.217		0.388	
	160.58		15.73	2.477	3.537	4.201	0.792	1.393		0.474	
	160.63		16.16	2.768	3.714	4.468	0.869	1.560		0.528	
	160.67		19.86	3.392	3.809	4.551	1.022	1.746		0.591	
	160.71		18.24	3.333	3.446	4.233	1.053	1.913		0.634	
	160.75		18.27	3.766	3.045	3.867	1.070	2.076		0.685	
	160.79		16.92	3.537	2.727	3.031	1.034	2.186		0.682	
	160.83		14.21	2.986	2.130	2.445	0.943	2.231		0.671	
	160.88		13.09	3.031	2.039	2.051	0.943	2.231		0.648	
	160.92		11.43	2.527	1.692	1.794	0.889	2.189		0.628	
	160.96		10.44	3.386	1.458	1.424	0.812	2.090		0.574	

		Spray Ice Temperatures Beneath Ablation Plots (Hourly)								
						Temperature (ºC)				
Date	Date Fraction	Average Air Temp.	1.5 cm	2 cm	3 cm	Sawdust	Gravel/	0.3m	0.6 m	1.0 m
	(Julian Day)	(ºC)	Sawdust	Sawdust	Sawdust	Bags	Sawdust	Gravel	Gravel	Gravel
10-Jun	161.00	4.36	0.854	0.730	0.843	0.628	1.964		0.548	
	161.04	4.07	0.684	0.650	0.479	0.524	1.817		0.502	
	161.08	3.07	0.476	0.578	0.316	0.430	1.622		0.430	
	161.13	3.17	0.492	0.651	0.264	0.356	1.446		0.378	
	161.17	2.06	0.290	0.540	0.233	0.278	1.267		0.335	
	161.21	3.09	0.589	0.657	0.224	0.270	1.111		0.304	
	161.25	2.61	0.568	0.648	0.249	0.238	0.978		0.272	
	161.29	2.51	0.639	0.696	0.275	0.206	0.867		0.252	
	161.33	3.42	0.833	0.855	0.355	0.229	0.787		0.241	
	161.38	3.96	0.992	0.958	0.457	0.241	0.719		0.241	
	161.42	4.50	1.503	1.253	0.628	0.298	0.674		0.252	
	161.46	3.07	0.890	1.003	0.674	0.263	0.662		0.263	
	161.50	5.33	1.752	1.344	0.799	0.320	0.662		0.275	
	161.54	5.61	1.775	1.435	0.981	0.366	0.662		0.298	
	161.58	6.34	2.270	1.726	1.239	0.477	0.682		0.329	
	161.63	7.81	2.606	1.893	1.463	0.543	0.748		0.372	
	161.67	7.28	2.298	1.789	1.539	0.586	0.836		0.438	
	161.71									
	161.75	10.58	3.519	2.108	2.018	0.703	0.998		0.498	
	161.79	10.32	2.968	1.964	2.235	0.729	1.115		0.559	
	161.83	8.32	1.986	1.692	1.862	0.661	1.262		0.615	
	161.88	4.78	1.106	1.197	1.412	0.595	1.333		0.629	
	161.92	3.20	0.782	0.851	0.941	0.544	1.338		0.601	
	161.96	1.81	0.572	0.697	0.640	0.469	1.253		0.526	
11-Jun	162.00	1.31	0.301	0.563	0.427	0.392	1.131	1.256	0.449	0.427
	162.04	1.45	0.272	0.546	0.261	0.318	1.001	1.194	0.363	0.386
	162.08	1.41	0.261	0.523	0.192	0.272	0.876	1.171	0.329	0.375
	162.13	1.09	0.104	0.423	0.104	0.206	0.765	1.140	0.286	0.343

		Spray Ice Temperatures Beneath Ablation Plots (Hourly)								
						Temperature (ºC)				
Date	Date Fraction (Julian Day)	Average Air Temp. (ºC)	1.5 cm Sawdust	2 cm Sawdust	3 cm Sawdust	Sawdust Bags	Gravel/ Sawdust	0.3m Gravel	0.6 m Gravel	1.0 m Gravel
	162.17	1.35	0.243	0.483	0.061	0.163	0.665	1.108	0.255	0.323
	162.21	1.09	0.175	0.483	0.072	0.141	0.585	1.085	0.243	0.312
	162.25	1.28	0.257	0.519	0.086	0.109	0.519	1.054	0.223	0.292
	162.29	1.58	0.451	0.622	0.155	0.098	0.474	1.031	0.223	0.280
	162.33	1.13	0.292	0.599	0.212	0.075	0.440	1.009	0.223	0.257
	162.38	2.29	0.736	0.781	0.292	0.098	0.440	0.986	0.223	0.246
	162.42	4.31	1.315	1.122	0.519	0.120	0.428	0.952	0.246	0.234
	162.46	5.93	2.309	1.732	1.085	0.232	0.460	0.915	0.278	0.220
	162.50	8.66	3.007	2.216	1.616	0.320	0.537	0.878	0.343	0.195
	162.54	15.88	4.301	2.857	2.484	0.432	0.671	0.841	0.420	0.192
	162.58	14.44	3.945	3.404	2.919	0.540	0.859	0.813	0.518	0.176
	162.63	14.82	4.938	3.699	3.350	0.703	1.112	0.782	0.635	0.179
	162.67	11.58	2.368	2.808	3.045	0.657	1.395	0.771	0.748	0.202
	162.71	14.75	2.263	2.331	3.087	0.689	1.596	0.757	0.791	0.222
	162.75	14.17	2.249	1.944	2.430	0.675	1.684	0.754	0.823	0.243
	162.79	12.57	2.023	1.639	1.921	0.641	1.695	0.766	0.834	0.265
	162.83	13.06	2.215	1.673	1.537	0.618	1.639	0.788	0.788	0.277
	162.88	12.13	2.215	1.491	1.163	0.561	1.537	0.811	0.720	0.288
	162.92	9.98	2.193	1.356	0.959	0.504	1.424	0.857	0.675	0.300
	162.96	8.51	2.249	1.220	0.788	0.447	1.322	0.913	0.607	0.322
12-Jun	163.00	5.43	2.102	1.197	0.766	0.402	1.208	0.970	0.538	0.322
	163.04	4.61	1.653	1.234	0.905	0.348	1.075	1.007	0.461	0.325
	163.08	3.77	1.157	1.134	0.828	0.316	0.976	1.044	0.407	0.328
	163.13	4.68	1.692	0.910	1.194	0.296	0.876	1.069	0.353	0.319
	163.17	1.51	0.413	0.560	0.583	0.230	0.788	1.106	0.321	0.310
	163.21	1.01	0.335	0.563	0.301	0.199	0.700	1.120	0.278	0.313
	163.25	1.28	0.406	0.600	0.235	0.178	0.623	1.134	0.258	0.304
	163.29	1.32	0.363	0.625	0.192	0.158	0.546	1.137	0.238	0.295

		Spray Ice Temperatures Beneath Ablation Plots (Hourly)								
						Temperature (ºC)				
Date	Date Fraction	Average Air Temp.	1.5 cm	2 cm	3 cm	Sawdust	Gravel/	0.3m	0.6 m	1.0 m
	(Julian Day)	(ºC)	Sawdust	Sawdust	Sawdust	Bags	Sawdust	Gravel	Gravel	Gravel
	163.33	1.86	0.514	0.696	0.275	0.149	0.491	1.140	0.241	0.286
	163.38	3.01	0.878	0.969	0.457	0.172	0.457	1.128	0.252	0.263
	163.42	4.44	1.253	1.174	0.685	0.218	0.457	1.105	0.275	0.252
	163.46	6.21	1.729	1.525	1.128	0.286	0.480	1.083	0.309	0.229
	163.50	8.66	2.338	1.817	1.590	0.352	0.557	1.046	0.386	0.227
	163.54	7.06	1.746	1.554	1.848	0.384	0.680	1.021	0.463	0.213
	163.58	8.14	2.173	1.743	1.755	0.472	0.825	1.006	0.529	0.221
	163.63	12.20	3.345	2.216	2.148	0.560	0.947	0.970	0.560	0.219
	163.67	12.64	3.454	2.156	2.574	0.603	1.080	0.944	0.615	0.216
	163.71	10.96	3.214	2.131	2.583	0.635	1.259	0.919	0.669	0.225
	163.75	11.04	3.279	2.060	2.354	0.689	1.438	0.916	0.700	0.245
	163.79	9.71	2.896	1.936	2.117	0.678	1.562	0.905	0.700	0.257
	163.83	6.79	1.970	1.506	1.845	0.643	1.653	0.927	0.689	0.291
	163.88	5.15	1.545	1.058	1.398	0.592	1.658	0.944	0.637	0.319
	163.92	3.88	1.151	0.913	1.083	0.526	1.605	0.958	0.572	0.333
	163.96	2.98	0.722	0.836	0.791	0.472	1.506	0.972	0.518	0.347
13-Jun	164.00	2.27	0.520	0.680	0.577	0.406	1.395	0.998	0.452	0.361
	164.04	1.83	0.398	0.614	0.409	0.341	1.250	1.012	0.398	0.352
	164.08	1.37	0.252	0.514	0.275	0.275	1.117	1.026	0.355	0.355
	164.13	1.32	0.255	0.505	0.175	0.232	0.983	1.029	0.312	0.346
	164.17	1.14	0.220	0.483	0.129	0.198	0.870	1.040	0.278	0.334
	164.21	1.46	0.314	0.519	0.120	0.166	0.759	1.031	0.257	0.314
	164.25	1.64	0.371	0.565	0.155	0.143	0.667	1.031	0.246	0.303
	164.29	2.16	0.576	0.702	0.246	0.143	0.611	1.020	0.234	0.292
	164.33	2.48	0.667	0.747	0.303	0.143	0.565	1.009	0.246	0.280
	164.38	2.84	1.031	0.906	0.405	0.120	0.542	0.986	0.246	0.257
	164.42	3.57	1.111	0.952	0.554	0.120	0.531	0.963	0.257	0.246
	164.46	5.44	1.792	1.236	0.838	0.189	0.531	0.929	0.280	0.234

		Spray Ice Temperatures Beneath Ablation Plots (Hourly)								
						Temperature (ºC)				
Date	Date Fraction (Julian Day)	Average Air Temp. (ºC)	1.5 cm Sawdust	2 cm Sawdust	3 cm Sawdust	Sawdust Bags	Gravel/ Sawdust	0.3m Gravel	0.6 m Gravel	1.0 m Gravel
	164.50	9.18	3.021	1.857	1.415	0.300	0.574	0.915	0.312	0.220
	164.54	12.13	3.692	2.383	2.123	0.409	0.671	0.876	0.386	0.204
	164.58	9.47	2.899	2.097	2.414	0.463	0.827	0.850	0.486	0.201
	164.63	10.98	3.111	2.173	2.354	0.540	1.029	0.836	0.563	0.210
	164.67	12.66	3.187	2.283	2.227	0.583	1.208	0.822	0.595	0.219
	164.71	11.16	2.619	2.156	2.088	0.603	1.341	0.808	0.615	0.228
	164.75	11.26	2.890	2.168	2.009	0.637	1.455	0.797	0.626	0.250
	164.79	9.19	2.043	1.783	1.783	0.603	1.523	0.808	0.626	0.273
	164.83	6.69	1.367	1.276	1.299	0.526	1.559	0.822	0.606	0.299
	164.88	4.07	0.734	0.995	0.950	0.483	1.539	0.859	0.563	0.324
	164.92	2.66	0.327	0.748	0.645	0.406	1.474	0.884	0.509	0.338
	164.96	2.61	0.400	0.605	0.412	0.343	1.344	0.912	0.434	0.343
14-Jun	165.00	1.43	0.696	0.594	0.275	0.252	1.196	0.935	0.377	0.332
	165.04	-0.01	-0.067	0.412	0.047	0.218	1.049	0.969	0.332	0.343
	165.08	-0.82	-0.234	0.360	-0.017	0.155	0.895	1.009	0.280	0.337
	165.13	-0.93	-0.311	0.351	-0.037	0.112	0.761	1.034	0.248	0.328
	165.17	-2.61	-0.584	0.320	-0.069	0.057	0.627	1.060	0.205	0.320
	165.21	-2.47	-0.788	0.311	-0.066	0.025	0.516	1.062	0.197	0.299
	165.25	-1.18	-0.616	0.356	-0.066	0.025	0.425	1.074	0.197	0.288
	165.29	-0.22	-0.295	0.425	-0.009	0.014	0.356	1.074	0.185	0.265
	165.33	-0.24	-0.593	0.402	-0.055	0.002	0.311	1.062	0.197	0.254
	165.38	1.56	-0.146	0.459	0.014	0.014	0.277	1.040	0.185	0.231
	165.42	2.71	0.002	0.493	0.025	0.014	0.254	1.017	0.174	0.208
	165.46	4.33	0.354	0.627	0.114	0.046	0.263	0.980	0.183	0.205
	165.50	8.47	1.080	1.011	0.488	0.112	0.294	0.943	0.237	0.180
	165.54	9.64	1.494	1.471	1.403	0.152	0.380	0.915	0.346	0.175
	165.58	10.75	2.046	1.888	2.114	0.206	0.514	0.878	0.469	0.172
	165.63	12.05	2.360	2.304	2.338	0.272	0.682	0.841	0.568	0.170

		Spray Ice Temperatures Beneath Ablation Plots (Hourly)								
						Temperature (ºC)				
Date	Date Fraction (Julian Day)	Average Air Temp. (ºC)	1.5 cm Sawdust	2 cm Sawdust	3 cm Sawdust	Sawdust Bags	Gravel/ Sawdust	0.3m Gravel	0.6 m Gravel	1.0 m Gravel
	165.67	12.00	2.368	2.074	2.165	0.315	0.850	0.827	0.634	0.178
	165.71	11.09	2.193	1.888	1.865	0.344	0.992	0.822	0.663	0.196
	165.75	9.73	1.820	1.525	1.412	0.333	1.106	0.811	0.674	0.207
	165.79	13.05	2.552	1.704	1.126	0.353	1.171	0.819	0.649	0.228
	165.83	6.81	1.364	1.228	0.910	0.307	1.182	0.842	0.615	0.228
	165.88	10.08	2.224	1.319	0.785	0.307	1.171	0.876	0.581	0.250
	165.92	7.21	1.840	0.921	0.569	0.228	1.114	0.899	0.524	0.250
	165.96	4.83	1.185	0.572	0.276	0.162	1.038	0.947	0.469	0.264
15-Jun	166.00	1.20	0.745	0.552	0.130	0.119	0.938	0.984	0.404	0.267
	166.04	-0.01	-0.095	0.463	0.042	0.076	0.827	1.032	0.349	0.281
	166.08	-0.82	-0.319	0.400	-0.010	0.047	0.708	1.060	0.286	0.286
	166.13	-1.69	-0.534	0.289	-0.053	0.026	0.585	1.085	0.232	0.278
	166.17	-2.02	-0.830	0.314	-0.051	0.006	0.485	1.111	0.200	0.269
	166.21	-2.01	-1.080	0.271	-0.048	-0.014	0.397	1.114	0.191	0.260
	166.25	-1.24	-0.641	0.251	-0.057	-0.034	0.331	1.105	0.183	0.240
	166.29	0.38	-0.091	0.479	-0.012	-0.023	0.285	1.094	0.183	0.217
	166.33	2.06	0.636	0.625	0.054	0.020	0.271	1.080	0.180	0.214
	166.38	3.17	1.011	0.738	0.169	0.077	0.248	1.045	0.169	0.191
	166.42	4.82	1.409	0.966	0.397	0.089	0.237	1.011	0.169	0.180
	166.46	7.82	1.542	1.667	0.724	0.109	0.269	0.975	0.166	0.177
	166.50	9.11	1.834	2.276	1.176	0.141	0.346	0.938	0.163	0.163
	166.54	10.84	2.239	2.352	1.729	0.172	0.469	0.901	0.263	0.172
	166.58	11.77	2.448	2.142	2.335	0.224	0.623	0.873	0.418	0.178
	166.63	12.03	2.467	2.207	2.558	0.267	0.791	0.847	0.540	0.187
	166.67	12.37	2.724	2.193	2.487	0.321	0.947	0.822	0.629	0.207
	166.71	12.43	2.698	1.998	2.168	0.353	1.069	0.819	0.672	0.216
	166.75	11.78	2.481	1.656	1.769	0.362	1.157	0.817	0.692	0.225
	166.79	11.74	2.594	1.395	1.395	0.339	1.202	0.828	0.669	0.236

			Spray Ice Temperatures Beneath Ablation Plots (Hourly)							
						Temperature (ºC)				
Date	Date Fraction	Average Air Temp.	1.5 cm	2 cm	3 cm	Sawdust	Gravel/	0.3m	0.6 m	1.0 m
	(Julian Day)	(ºC)	Sawdust	Sawdust	Sawdust	Bags	Sawdust	Gravel	Gravel	Gravel
	166.83	11.50	2.616	1.293	1.021	0.316	1.202	0.862	0.646	0.248
	166.88	9.79	2.402	1.134	0.726	0.293	1.168	0.896	0.612	0.259
	166.92	7.12	1.972	0.976	0.441	0.259	1.100	0.941	0.567	0.282
	166.96	5.21	1.341	0.808	0.216	0.205	1.001	0.990	0.501	0.273
16-Jun	167.00	1.90	0.907	0.635	0.031	0.179	0.896	1.032	0.441	0.293
	167.04	0.78	0.102	0.524	-0.023	0.148	0.797	1.080	0.387	0.296
	167.08	0.16	-0.029	0.506	-0.018	0.119	0.711	1.120	0.335	0.301
	167.13	-0.25	-0.070	0.352	-0.047	0.090	0.603	1.137	0.272	0.295
	167.17	-0.54	-0.136	0.412	-0.056	0.058	0.526	1.162	0.229	0.286
	167.21	-0.15	-0.145	0.357	-0.053	0.038	0.437	1.165	0.186	0.278
	167.25	0.86	0.246	0.349	-0.051	0.029	0.371	1.156	0.177	0.257
	167.29	3.02	0.963	0.713	0.029	0.029	0.314	1.134	0.166	0.234
	167.33	4.83	1.811	1.188	0.141	0.106	0.300	1.120	0.175	0.232
	167.38	7.26	2.773	2.332	0.391	0.198	0.300	1.085	0.163	0.209
	167.42	9.41	3.368	2.917	0.912	0.263	0.355	1.060	0.161	0.195
	167.46	12.08	3.531	3.340	1.758	0.349	0.463	1.021	0.224	0.190
	167.50	14.62	4.182	3.528	2.648	0.404	0.620	0.972	0.358	0.176
	167.54	18.12	5.603	3.654	3.519	0.521	0.817	0.941	0.498	0.191
	167.58	15.21	4.076	2.791	3.648	0.629	1.050	0.925	0.652	0.208
	167.63	13.37	2.836	2.125	2.971	0.641	1.242	0.913	0.777	0.231
	167.67	11.33	2.509	1.627	2.159	0.641	1.356	0.902	0.834	0.254
	167.71	12.63	2.653	1.523	2.551	0.672	1.387	0.888	0.808	0.263
	167.75	10.65	2.334	1.169	2.774	0.601	1.373	0.897	0.817	0.283
	167.79	9.88	2.150	1.053	2.116	0.565	1.370	0.928	0.803	0.303
	167.83	5.44	1.191	0.863	1.475	0.522	1.361	0.976	0.772	0.340
	167.88	3.84	0.868	0.754	1.061	0.493	1.322	1.038	0.720	0.368
	167.92	3.12	0.669	0.657	0.805	0.430	1.225	1.078	0.635	0.384
	167.96	2.44	0.572	0.617	0.629	0.378	1.106	1.117	0.549	0.378

		Spray Ice Temperatures Beneath Ablation Plots (Hourly)								
						Temperature (ºC)				
Date	Date Fraction (Julian Day)	Average Air Temp. (ºC)	1.5 cm Sawdust	2 cm Sawdust	3 cm Sawdust	Sawdust Bags	Gravel/ Sawdust	0.3m Gravel	0.6 m Gravel	1.0 m Gravel
17-Jun	168.00	1.22	0.224	0.475	0.384	0.304	0.998	1.145	0.475	0.384
	168.04	0.97	0.204	0.466	0.227	0.249	0.887	1.182	0.409	0.375
	168.08	0.69	0.138	0.446	0.149	0.206	0.787	1.196	0.343	0.366
	168.13	0.59	0.095	0.426	0.084	0.163	0.688	1.210	0.300	0.357
	168.17	0.54	0.075	0.428	0.052	0.120	0.611	1.213	0.269	0.337
	168.21	0.53	0.075	0.428	0.040	0.098	0.542	1.213	0.246	0.326
	168.25	0.73	0.169	0.465	0.054	0.089	0.488	1.193	0.226	0.306
	168.29	0.93	0.260	0.511	0.100	0.077	0.442	1.182	0.226	0.294
	168.33	1.70	0.477	0.613	0.180	0.077	0.408	1.159	0.226	0.271
	168.38	2.82	0.807	0.784	0.328	0.100	0.397	1.136	0.237	0.260
	168.42	4.16	1.273	1.102	0.533	0.134	0.397	1.102	0.248	0.237
	168.46	4.91	1.451	1.225	0.679	0.177	0.417	1.077	0.303	0.234
	168.50	6.49	1.834	1.426	0.904	0.232	0.460	1.040	0.346	0.220
	168.54	11.03	3.891	2.389	1.505	0.357	0.505	1.006	0.391	0.209
	168.58	15.48	5.211	3.103	2.538	0.497	0.600	0.964	0.475	0.201
	168.63	16.07	3.987	2.950	3.119	0.469	0.765	0.936	0.606	0.196
	168.67	17.81	4.184	2.887	3.406	0.521	0.998	0.907	0.726	0.202
	168.71	18.17	4.507	2.817	3.042	0.552	1.245	0.871	0.803	0.188
	168.75	17.95	4.782	2.641	2.574	0.593	1.477	0.865	0.843	0.206
	168.79	20.12	4.967	2.613	2.229	0.610	1.653	0.848	0.860	0.223
	168.83	18.33	5.928	2.663	1.884	0.593	1.783	0.866	0.854	0.241
	168.88	18.73	5.677	2.897	1.769	0.579	1.848	0.886	0.818	0.261
	168.92	14.50	4.489	2.463	1.492	0.540	1.853	0.937	0.767	0.279
	168.96	4.03	1.180	0.886	1.090	0.454	1.791	1.010	0.738	0.329
18-Jun	169.00	4.15	1.361	0.953	0.806	0.454	1.690	1.089	0.670	0.374
	169.04	2.26	0.825	0.814	0.768	0.405	1.494	1.143	0.564	0.393
	169.08	1.07	0.330	0.546	0.490	0.307	1.319	1.205	0.478	0.410
	169.13	0.60	0.176	0.461	0.256	0.244	1.143	1.245	0.392	0.415

		Spray Ice Temperatures Beneath Ablation Plots (Hourly)								
						Temperature (°C)				
Date	Date Fraction	Average Air Temp.	1.5 cm	2 cm	3 cm	Sawdust	Gravel/	0.3m	0.6 m	1.0 m
	(Julian Day)	(°C)	Sawdust	Sawdust	Sawdust	Bags	Sawdust	Gravel	Gravel	Gravel
	169.17	0.25	0.056	0.409	0.090	0.170	0.989	1.273	0.318	0.398
	169.21	0.57	0.092	0.423	0.035	0.127	0.844	1.287	0.275	0.389
	169.25	0.13	0.049	0.403	0.015	0.084	0.710	1.301	0.243	0.380
	169.29	0.25	0.052	0.405	0.006	0.063	0.611	1.304	0.223	0.360
	169.33	0.82	0.155	0.440	0.029	0.063	0.531	1.304	0.212	0.337
	169.38	1.13	0.260	0.465	0.043	0.054	0.465	1.284	0.203	0.317
	169.42	4.60	1.307	0.693	0.191	0.077	0.431	1.261	0.203	0.283
	169.46	6.35	1.511	0.761	0.545	0.134	0.420	1.227	0.226	0.260
	169.50	5.30	1.451	0.827	1.031	0.189	0.451	1.190	0.280	0.246
	169.54	5.32	1.233	0.801	1.188	0.175	0.540	1.165	0.346	0.243
	169.58	5.97	1.426	0.904	1.233	0.209	0.619	1.120	0.380	0.232
	169.63	5.39	1.321	0.878	1.298	0.252	0.708	1.083	0.423	0.229
	169.67	9.07	2.487	1.276	1.389	0.320	0.776	1.037	0.446	0.229
	169.71	9.07	2.594	1.327	1.610	0.372	0.861	1.009	0.486	0.235
	169.75	9.20	2.738	1.494	1.653	0.427	0.938	0.984	0.529	0.233
	169.79	12.26	2.874	1.619	1.596	0.438	1.018	0.950	0.552	0.233
	169.83	12.13	3.079	1.905	1.610	0.464	1.078	0.907	0.555	0.225
	169.88	8.07	2.037	1.483	1.392	0.450	1.154	0.905	0.587	0.245
	169.92	6.38	1.531	1.270	1.066	0.430	1.202	0.919	0.601	0.271
	169.96	3.31	0.828	1.168	0.714	0.384	1.225	0.930	0.578	0.305
19-Jun	170.00	2.13	0.307	0.706	0.216	0.307	1.182	0.944	0.524	0.319
	170.04	1.09	0.007	0.372	-0.027	0.247	1.111	0.952	0.452	0.327
	170.08	-0.16	-0.070	0.363	-0.116	0.192	1.012	0.978	0.386	0.341
	170.13	-2.09	-0.236	0.323	-0.099	0.106	0.892	0.995	0.334	0.346
	170.17	-1.89	-0.220	0.328	-0.094	0.066	0.773	1.000	0.260	0.340
	170.21	0.09	0.020	0.397	-0.014	0.054	0.647	1.011	0.214	0.328
	170.25	1.19	0.146	0.431	0.020	0.043	0.533	1.000	0.191	0.317
	170.29	3.00	0.499	0.545	0.066	0.054	0.442	0.989	0.180	0.283

		Spray Ice Temperatures Beneath Ablation Plots (Hourly)								
						Temperature (ºC)				
Date	Date Fraction	Average Air Temp.	1.5 cm	2 cm	3 cm	Sawdust	Gravel/	0.3m	0.6 m	1.0 m
	(Julian Day)	(ºC)	Sawdust	Sawdust	Sawdust	Bags	Sawdust	Gravel	Gravel	Gravel
	170.33	3.79	0.804	0.702	0.109	0.075	0.405	0.986	0.177	0.269
	170.38	4.45	0.929	0.940	0.177	0.086	0.394	0.963	0.200	0.246
	170.42	6.70	2.095	1.675	0.437	0.163	0.403	0.938	0.232	0.232
	170.46	7.08	2.465	1.944	0.878	0.195	0.434	0.912	0.275	0.218
	170.50	8.00	2.677	2.157	1.182	0.238	0.489	0.887	0.329	0.204
	170.54	8.20	2.719	1.961	1.633	0.315	0.566	0.861	0.384	0.201
	170.58	4.93	1.483	1.335	1.267	0.301	0.654	0.859	0.461	0.221
	170.63	5.38	1.452	1.282	0.952	0.304	0.714	0.850	0.463	0.224
	170.67	5.53	1.814	1.304	0.952	0.349	0.736	0.839	0.441	0.235
	170.71	2.65	0.861	0.873	1.213	0.338	0.725	0.839	0.441	0.258
	170.75	2.24	0.682	0.705	0.750	0.284	0.705	0.841	0.409	0.261
	170.79	5.46	1.639	1.083	0.787	0.320	0.662	0.833	0.355	0.263
	170.83	3.32	1.083	0.810	1.015	0.241	0.628	0.833	0.343	0.263
	170.88	2.95	0.924	0.787	0.844	0.229	0.639	0.844	0.355	0.263
	170.92	0.96	0.209	0.414	0.642	0.163	0.642	0.858	0.346	0.266
	170.96	0.97	0.234	0.462	0.326	0.120	0.622	0.861	0.314	0.269
20-Jun	171.00	0.19	0.109	0.417	0.177	0.086	0.599	0.861	0.292	0.269
	171.04	-0.44	0.009	0.385	0.066	0.066	0.545	0.864	0.260	0.271
	171.08	-0.92	-0.046	0.365	0.000	0.057	0.502	0.866	0.228	0.263
	171.13	-2.44	-0.194	0.320	-0.046	0.023	0.456	0.866	0.205	0.263
	171.17	-2.54	-0.203	0.334	-0.043	0.014	0.391	0.858	0.197	0.254
	171.21	-2.32	-0.201	0.325	-0.029	-0.018	0.336	0.838	0.188	0.233
	171.25	-0.47	0.028	0.405	0.005	-0.006	0.302	0.826	0.188	0.233
	171.29	1.21	0.233	0.439	0.028	-0.018	0.268	0.792	0.176	0.211
	171.33	2.90	0.903	0.596	0.082	0.037	0.254	0.778	0.185	0.197
	171.38	4.25	1.400	0.889	0.228	0.103	0.251	0.753	0.171	0.183
	171.42	5.05	1.695	1.457	0.502	0.103	0.251	0.718	0.171	0.160
	171.46	7.69	1.692	1.647	0.955	0.123	0.294	0.693	0.169	0.157

		Spray Ice Temperatures Beneath Ablation Plots (Hourly)								
						Temperature (ºC)				
Date	Date Fraction	Average Air Temp.	1.5 cm	2 cm	3 cm	Sawdust	Gravel/	0.3m	0.6 m	1.0 m
	(Julian Day)	(ºC)	Sawdust	Sawdust	Sawdust	Bags	Sawdust	Gravel	Gravel	Gravel
	171.50	9.45	1.610	1.939	1.633	0.143	0.394	0.656	0.234	0.155
	171.54	11.05	2.329	2.080	2.284	0.184	0.514	0.639	0.377	0.161
	171.58	11.92	2.428	1.840	2.733	0.215	0.659	0.614	0.512	0.170
	171.63	11.67	2.335	1.927	2.888	0.247	0.816	0.600	0.623	0.178
	171.67	12.14	2.354	1.834	2.795	0.267	0.961	0.597	0.688	0.199
	171.71	11.60	2.103	1.661	2.476	0.276	1.060	0.606	0.731	0.207
	171.75	11.49	1.950	1.565	2.142	0.271	1.100	0.601	0.714	0.214
	171.79	10.75	1.540	1.347	1.551	0.245	1.098	0.621	0.689	0.222
	171.83	10.14	1.353	1.296	0.990	0.217	1.069	0.661	0.650	0.229
	171.88	8.26	0.999	1.112	0.488	0.192	1.021	0.715	0.601	0.249
	171.92	6.49	0.831	1.058	0.138	0.160	0.945	0.763	0.536	0.251
	171.96	5.05	0.695	1.035	0.058	0.149	0.865	0.831	0.468	0.274
21-Jun	172.00	2.10	0.516	0.959	0.003	0.129	0.788	0.879	0.413	0.277
	172.04	1.42	0.225	0.805	-0.003	0.111	0.703	0.930	0.362	0.282
	172.08	0.67	0.036	0.606	-0.021	0.093	0.629	0.981	0.310	0.287
	172.13	0.31	0.030	0.304	-0.027	0.076	0.554	1.009	0.270	0.281
	172.17	0.46	0.067	0.466	-0.013	0.067	0.489	1.035	0.227	0.272
	172.21	0.81	0.104	0.491	0.001	0.047	0.434	1.037	0.206	0.263
	172.25	1.99	0.631	0.528	0.026	0.038	0.380	1.040	0.186	0.243
	172.29	2.71	1.210	1.063	0.095	0.049	0.346	1.029	0.186	0.232
	172.33	4.87	2.126	1.718	0.332	0.104	0.343	1.026	0.195	0.229
	172.38	6.46	2.973	2.171	0.799	0.161	0.343	1.003	0.195	0.206
	172.42	8.69	3.760	2.597	1.568	0.204	0.375	0.978	0.215	0.204
	172.46	11.09	3.949	2.798	2.188	0.213	0.452	0.952	0.270	0.190
	172.50	12.82	3.686	2.953	2.637	0.244	0.552	0.916	0.381	0.187
	172.54	14.02	4.697	3.175	3.074	0.276	0.674	0.890	0.504	0.185
	172.58	15.06	4.525	2.868	3.691	0.307	0.831	0.865	0.603	0.193
	172.63	16.17	4.428	2.997	3.380	0.359	0.996	0.859	0.700	0.211

		Spray Ice Temperatures Beneath Ablation Plots (Hourly)								
						Temperature (ºC)				
Date	Date Fraction (Julian Day)	Average Air Temp. (ºC)	1.5 cm Sawdust	2 cm Sawdust	3 cm Sawdust	Sawdust Bags	Gravel/ Sawdust	0.3m Gravel	0.6 m Gravel	1.0 m Gravel
	172.67	17.01	4.233	2.870	3.422	0.402	1.140	0.857	0.766	0.220
	172.71	16.44	3.656	2.788	3.284	0.411	1.262	0.854	0.808	0.229
	172.75	16.51	3.112	2.661	2.943	0.420	1.350	0.863	0.828	0.249
	172.79	16.56	2.759	2.624	2.365	0.440	1.393	0.894	0.814	0.269
	172.83	14.59	2.441	2.497	1.752	0.426	1.424	0.937	0.800	0.289
	172.88	12.43	1.969	2.263	1.302	0.383	1.381	0.985	0.746	0.303
	172.92	11.00	1.766	2.207	0.985	0.360	1.325	1.041	0.678	0.315
	172.96	8.01	1.305	1.859	0.715	0.328	1.237	1.112	0.624	0.340
22-Jun	173.00	4.98	1.069	1.692	0.502	0.297	1.149	1.183	0.559	0.354
	173.04	3.80	0.700	1.494	0.336	0.257	1.030	1.222	0.484	0.348
	173.08	3.11	0.464	1.225	0.328	0.236	0.941	1.282	0.419	0.362
	173.13	2.60	0.481	0.731	0.310	0.196	0.833	1.321	0.356	0.356
	173.17	2.82	0.529	0.893	0.347	0.176	0.756	1.358	0.313	0.335
	173.21	3.29	0.654	0.995	0.381	0.164	0.677	1.369	0.278	0.335
	173.25	4.15	1.279	0.802	0.404	0.164	0.620	1.381	0.267	0.324
	173.29	5.62	1.950	1.316	0.475	0.156	0.566	1.372	0.247	0.304
	173.33	7.45	2.817	2.139	0.745	0.233	0.552	1.369	0.256	0.290
	173.38	10.35	3.731	2.795	1.211	0.335	0.552	1.358	0.244	0.278
	173.42	10.04	4.032	2.758	1.650	0.390	0.606	1.333	0.253	0.276
	173.46	13.56	4.325	2.972	2.159	0.424	0.674	1.310	0.299	0.253
	173.50	18.86	5.265	3.643	2.797	0.589	0.805	1.270	0.396	0.248
	173.54	17.23	5.653	2.419	3.095	0.595	0.993	1.254	0.527	0.265
	173.58	18.07	4.872	2.980	3.419	0.479	1.217	1.239	0.638	0.263
	173.63	18.76	4.753	3.143	3.706	0.542	1.449	1.223	0.724	0.292
	173.67	20.39	4.629	3.199	3.987	0.656	1.664	1.234	0.803	0.326
	173.71	23.25	4.577	3.306	3.868	0.711	1.887	1.232	0.836	0.348
	173.75	25.37	4.909	5.089	3.034	0.814	2.011	1.210	0.825	0.327
	173.79	24.54	3.846	4.442	2.473	0.722	2.101	1.243	0.858	0.336

		Spray Ice Temperatures Beneath Ablation Plots (Hourly)								
		Average				Temperature (ºC)				
Date	Date Fraction	Air Temp.	1.5 cm	2 cm	3 cm	Sawdust	Gravel/	0.3m	0.6 m	1.0 m
	(Julian Day)	(ºC)	Sawdust	Sawdust	Sawdust	Bags	Sawdust	Gravel	Gravel	Gravel
	173.83	21.58	3.039	3.917	2.082	0.657	2.161	1.280	0.850	0.362
	173.88	16.77	2.428	3.138	1.537	0.609	2.135	1.334	0.836	0.382
	173.92	13.85	2.304	3.250	1.334	0.598	2.045	1.390	0.790	0.393
	173.96	5.59	1.169	1.407	1.068	0.569	1.949	1.475	0.750	0.433
23-Jun	174.00	5.73	1.019	1.166	0.770	0.509	1.834	1.562	0.690	0.463
	174.04	5.26	0.607	1.016	0.562	0.448	1.673	1.627	0.585	0.460
	174.08	5.54	1.109	1.211	0.542	0.428	1.517	1.675	0.508	0.462
	174.13	2.37	0.206	0.661	0.331	0.331	1.353	1.726	0.445	0.456
	174.17	3.61	0.496	0.871	0.222	0.291	1.211	1.755	0.382	0.450
	174.21	3.12	0.567	0.839	0.225	0.248	1.066	1.780	0.328	0.430
	174.25	5.00	1.375	0.956	0.319	0.239	0.956	1.794	0.296	0.421
	174.29	4.17	1.330	1.262	0.421	0.205	0.865	1.794	0.285	0.410
	174.33	4.83	1.163	1.695	0.560	0.230	0.799	1.786	0.276	0.390
	174.38	11.60	3.536	2.035	0.947	0.390	0.765	1.775	0.276	0.367
	174.42	9.38	3.387	2.054	1.511	0.364	0.762	1.749	0.273	0.353
	174.46	7.94	2.348	1.772	1.477	0.342	0.842	1.726	0.319	0.342
	174.50	12.48	3.556	1.817	1.658	0.410	0.921	1.692	0.376	0.342
	174.54	9.85	2.899	1.791	1.757	0.430	0.998	1.667	0.441	0.339
	174.58	15.93	5.412	2.504	2.153	0.555	1.078	1.633	0.510	0.328
	174.63	21.68	6.694	3.414	3.110	0.666	1.200	1.596	0.575	0.314
	174.67	15.39	4.414	2.678	2.768	0.607	1.401	1.571	0.698	0.322
	174.71	16.01	4.362	2.672	2.627	0.692	1.588	1.554	0.760	0.317
	174.75	20.51	5.417	3.503	2.590	0.769	1.709	1.540	0.769	0.326
	174.79	17.83	4.116	3.193	2.235	0.707	1.794	1.534	0.786	0.321
	174.83	16.93	3.693	3.806	1.901	0.622	1.845	1.517	0.781	0.315
	174.88	12.92	2.778	3.420	1.322	0.563	1.842	1.537	0.756	0.324
	174.92	15.12	2.643	3.532	0.994	0.529	1.797	1.571	0.722	0.347
	174.96	7.94	1.786	2.451	0.699	0.495	1.707	1.627	0.688	0.381

		Spray Ice Temperatures Beneath Ablation Plots (Hourly)								
						Temperature (°C)				
Date	Date Fraction (Julian Day)	Average Air Temp. (°C)	1.5 cm Sawdust	2 cm Sawdust	3 cm Sawdust	Sawdust Bags	Gravel/ Sawdust	0.3m Gravel	0.6 m Gravel	1.0 m Gravel
24-Jun	175.00	6.86	1.913	3.367	0.588	0.418	1.585	1.664	0.599	0.384
	175.04	4.27	0.829	2.874	0.284	0.341	1.452	1.690	0.523	0.398
	175.08	2.62	0.073	1.876	0.061	0.278	1.322	1.740	0.460	0.414
	175.13	1.83	0.032	0.590	-0.025	0.226	1.169	1.757	0.397	0.431
	175.17	2.24	0.402	0.607	-0.008	0.208	1.015	1.774	0.334	0.425
	175.21	2.91	0.601	0.885	0.065	0.214	0.873	1.780	0.282	0.407
	175.25	2.80	1.896	0.615	0.216	0.239	0.751	1.772	0.250	0.398
	175.29	4.16	2.913	1.012	0.410	0.592	0.660	1.772	0.250	0.387
	175.33	6.94	5.122	1.557	0.785	0.512	0.603	1.749	0.239	0.364
	175.38	5.92	1.873	1.681	0.921	0.239	0.581	1.726	0.228	0.353
	175.42	6.00	2.758	1.435	0.879	0.207	0.572	1.695	0.230	0.344
	175.46	15.01	7.800	2.137	1.219	0.321	0.595	1.661	0.253	0.333
	175.50	11.25	5.415	2.755	1.930	0.307	0.615	1.613	0.296	0.307
	175.54	16.33	6.720	2.470	2.492	0.316	0.703	1.588	0.396	0.305
	175.58	15.30	5.634	2.342	2.647	0.314	0.837	1.551	0.484	0.291
	175.63	14.65	5.517	2.181	2.419	0.334	0.993	1.525	0.561	0.300
	175.67	15.68	5.108	2.562	2.032	0.513	1.137	1.511	0.604	0.308
	175.71	16.43	5.123	2.644	1.650	0.504	1.231	1.491	0.584	0.322
	175.75	15.48	3.994	2.788	1.500	0.524	1.274	1.489	0.547	0.320
	175.79	8.27	3.521	2.077	1.137	0.377	1.274	1.511	0.547	0.343
	175.83	12.09	3.208	2.464	0.947	0.356	1.242	1.537	0.493	0.356
	175.88	10.01	2.949	2.486	0.811	0.322	1.140	1.548	0.447	0.345
	175.92	5.52	2.328	1.808	0.675	0.311	1.050	1.582	0.425	0.356
	175.96	4.05	1.800	1.449	0.496	0.279	0.973	1.619	0.405	0.370
25-Jun	176.00	3.08	1.576	1.304	0.396	0.248	0.885	1.644	0.362	0.373
	176.04	2.32	1.353	1.069	0.319	0.262	0.785	1.670	0.342	0.376
	176.08	2.09	1.290	1.018	0.256	0.267	0.700	1.675	0.301	0.370
	176.13	1.73	1.066	0.907	0.224	0.224	0.623	1.678	0.281	0.361

		Spray Ice Temperatures Beneath Ablation Plots (Hourly)								
						Temperature (°C)				
Date	Date Fraction	Average Air Temp.	1.5 cm	2 cm	3 cm	Sawdust	Gravel/	0.3m	0.6 m	1.0 m
	(Julian Day)	(°C)	Sawdust	Sawdust	Sawdust	Bags	Sawdust	Gravel	Gravel	Gravel
	176.17	1.68	0.986	0.827	0.178	0.247	0.566	1.678	0.258	0.349
	176.21	2.12	1.091	1.012	0.170	0.261	0.523	1.670	0.249	0.341
	176.25	2.91	2.586	1.114	0.238	0.443	0.477	1.647	0.238	0.318
	176.29	2.75	1.786	1.105	0.252	0.275	0.446	1.616	0.229	0.309
	176.33	4.11	2.634	1.367	0.343	0.275	0.434	1.582	0.229	0.286
	176.38	4.83	4.068	1.412	0.480	0.298	0.423	1.548	0.241	0.275
	176.42	7.20	6.298	2.043	0.841	0.409	0.443	1.511	0.249	0.272
	176.46	7.06	4.696	2.134	0.921	0.375	0.489	1.466	0.272	0.261
	176.50	12.78	5.260	2.021	1.307	0.443	0.557	1.420	0.306	0.249
	176.54	14.76	8.740	2.176	1.712	0.589	0.645	1.384	0.349	0.235
	176.58	14.59	7.000	2.275	1.777	0.552	0.768	1.347	0.392	0.233
	176.63	12.56	4.742	2.385	1.537	0.435	0.913	1.310	0.435	0.242
	176.67	16.09	5.325	3.014	1.511	0.512	1.024	1.285	0.467	0.239
	176.71	16.07	4.679	3.293	1.429	0.521	1.112	1.259	0.487	0.248
	176.75	15.26	4.338	3.583	1.245	0.541	1.177	1.234	0.507	0.245
	176.79	14.66	3.535	3.727	0.925	0.482	1.220	1.231	0.516	0.254
	176.83	13.86	2.960	3.839	0.811	0.402	1.208	1.231	0.504	0.254
	176.88	12.42	2.382	3.847	0.650	0.388	1.183	1.239	0.490	0.274
	176.92	10.22	1.839	3.678	0.490	0.343	1.126	1.262	0.456	0.274
	176.96	5.77	1.251	2.811	0.365	0.343	1.058	1.285	0.433	0.286
26-Jun	177.00	5.77	2.136	3.163	0.311	0.311	0.970	1.310	0.402	0.300
	177.04	3.33	0.893	2.884	0.291	0.257	0.882	1.324	0.348	0.302
	177.08	2.15	0.567	1.938	0.134	0.225	0.805	1.350	0.328	0.316
	177.13	1.38	0.264	0.811	0.071	0.196	0.720	1.355	0.299	0.310
	177.17	0.92	0.039	0.620	-0.007	0.221	0.654	1.369	0.267	0.313
	177.21	1.01	0.076	0.861	-0.050	0.270	0.577	1.372	0.247	0.304
	177.25	1.82	3.388	0.512	0.021	0.625	0.512	1.364	0.227	0.295
	177.29	3.72	6.324	1.094	0.229	0.799	0.457	1.344	0.206	0.275

		Spray Ice Temperatures Beneath Ablation Plots (Hourly)								
						Temperature (ºC)				
Date	Date Fraction	Average Air Temp.	1.5 cm	2 cm	3 cm	Sawdust	Gravel/	0.3m	0.6 m	1.0 m
	(Julian Day)	(ºC)	Sawdust	Sawdust	Sawdust	Bags	Sawdust	Gravel	Gravel	Gravel
	177.33	6.21	8.420	1.582	0.594	0.628	0.423	1.332	0.206	0.263
	177.38	9.74	11.620	1.763	1.140	0.594	0.423	1.298	0.195	0.263
	177.42	11.42	11.700	1.806	1.704	0.546	0.477	1.273	0.204	0.261
	177.46	13.75	10.980	1.806	2.077	0.512	0.568	1.250	0.227	0.249
	177.50	13.13	6.599	2.199	2.436	0.429	0.691	1.225	0.304	0.258
	177.54	15.85	9.590	2.572	2.696	0.486	0.816	1.191	0.384	0.247
	177.58	19.01	10.030	2.738	2.795	0.620	0.972	1.165	0.472	0.256
	177.63	19.59	8.190	3.266	2.859	0.651	1.117	1.151	0.538	0.264
	177.67	20.22	6.573	3.586	2.741	0.726	1.259	1.134	0.589	0.282
	177.71	19.20	5.608	3.817	2.475	0.618	1.356	1.129	0.618	0.277
	177.75	15.47	4.756	3.743	2.006	0.567	1.407	1.146	0.624	0.294
	177.79	19.98	4.208	4.748	1.591	0.763	1.443	1.171	0.627	0.308
	177.83	12.83	2.644	5.033	1.299	0.550	1.344	1.197	0.618	0.311
	177.88	11.37	2.294	5.326	0.891	0.652	1.231	1.254	0.595	0.334
	177.92	10.44	1.924	5.588	0.632	0.837	1.188	1.290	0.552	0.336
	177.96	6.94	1.698	4.822	0.461	0.768	1.075	1.347	0.507	0.348
27-Jun	178.00	3.93	1.327	4.184	0.350	0.384	0.976	1.395	0.464	0.350
	178.04	3.02	0.956	3.353	0.250	0.330	0.910	1.443	0.410	0.353
	178.08	2.71	1.049	2.521	0.207	0.276	0.822	1.480	0.367	0.356
	178.13	2.14	0.813	1.143	0.176	0.221	0.745	1.506	0.313	0.347
	178.17	2.45	1.066	1.089	0.213	0.190	0.657	1.520	0.281	0.349
	178.21	3.00	1.262	1.148	0.261	0.192	0.614	1.522	0.272	0.341
	178.25	3.09	1.330	1.216	0.306	0.192	0.580	1.522	0.261	0.329
	178.29	2.71	1.355	1.219	0.320	0.206	0.537	1.514	0.252	0.320
	178.33	4.74	5.545	1.673	0.582	0.434	0.514	1.503	0.252	0.309
	178.38	10.47	11.520	2.182	1.230	0.605	0.503	1.469	0.241	0.286
	178.42	11.87	10.240	2.394	1.806	0.546	0.534	1.443	0.238	0.284
	178.46	16.93	12.990	2.609	2.496	0.648	0.614	1.409	0.261	0.261

		Spray Ice Temperatures Beneath Ablation Plots (Hourly)								
						Temperature (ºC)				
Date	Date Fraction	Average Air Temp.	1.5 cm	2 cm	3 cm	Sawdust	Gravel/	0.3m	0.6 m	1.0 m
	(Julian Day)	(ºC)	Sawdust	Sawdust	Sawdust	Bags	Sawdust	Gravel	Gravel	Gravel
	178.50	16.01	8.550	2.651	3.046	0.827	0.759	1.384	0.361	0.258
	178.54	15.18	9.460	2.809	2.888	0.793	0.975	1.350	0.475	0.258
	178.58	15.89	10.410	3.483	2.682	1.097	1.188	1.335	0.563	0.267
	178.63	15.80	9.230	3.799	2.592	1.324	1.347	1.324	0.609	0.278
	178.67	22.35	9.170	4.813	2.716	1.471	1.483	1.301	0.654	0.278
	178.71	16.78	7.190	4.303	2.645	1.276	1.627	1.299	0.708	0.287
	178.75	14.20	6.355	4.246	2.159	1.287	1.752	1.310	0.765	0.299
	178.79	6.54	3.728	2.961	1.378	1.072	1.808	1.344	0.788	0.321
	178.83	8.70	4.385	3.664	1.131	1.143	1.766	1.369	0.722	0.335
	178.88	6.21	4.024	3.675	1.029	1.177	1.664	1.392	0.654	0.358
	178.92	5.98	3.178	3.054	0.893	1.018	1.539	1.426	0.586	0.370
	178.96	9.43	3.258	5.659	0.802	1.619	1.392	1.449	0.529	0.370
28-Jun	179.00	5.26	2.072	4.926	0.631	1.438	1.267	1.460	0.483	0.358
	179.04	2.82	1.029	3.133	0.370	0.984	1.154	1.483	0.461	0.370
	179.08	2.62	0.986	2.425	0.235	0.748	1.043	1.497	0.406	0.372
	179.13	1.81	0.466	1.386	0.147	0.557	0.932	1.500	0.352	0.375
	179.17	1.72	0.466	1.454	0.101	0.659	0.830	1.511	0.318	0.375
	179.21	1.62	0.537	1.491	0.081	0.719	0.730	1.491	0.275	0.366
	179.25	2.23	2.578	1.423	0.127	0.981	0.639	1.480	0.252	0.355
	179.29	3.04	4.316	1.695	0.275	1.049	0.571	1.457	0.241	0.343
	179.33	3.37	3.052	1.854	0.400	0.662	0.526	1.435	0.241	0.332
	179.38	5.05	3.684	2.273	0.548	0.765	0.503	1.412	0.241	0.320
	179.42	7.87	8.810	2.148	0.946	1.049	0.514	1.378	0.263	0.309
	179.46	10.11	8.750	2.533	1.446	1.140	0.548	1.355	0.309	0.298
	179.50	10.78	6.223	2.352	2.137	1.117	0.651	1.310	0.377	0.286
	179.54	14.49	10.060	2.383	2.394	1.284	0.796	1.284	0.477	0.284
	179.58	14.77	9.100	3.004	2.564	1.284	0.978	1.262	0.580	0.284
	179.63	15.76	8.230	3.467	2.654	1.330	1.171	1.228	0.671	0.284

		Spray Ice Temperatures Beneath Ablation Plots (Hourly)								
						Temperature (°C)				
Date	Date Fraction	Average Air Temp.	1.5 cm	2 cm	3 cm	Sawdust	Gravel/	0.3m	0.6 m	1.0 m
	(Julian Day)	(°C)	Sawdust	Sawdust	Sawdust	Bags	Sawdust	Gravel	Gravel	Gravel
	179.67	17.72	7.510	4.369	2.756	1.386	1.352	1.194	0.728	0.284
	179.71	19.33	6.961	5.392	2.719	1.440	1.520	1.179	0.782	0.281
	179.75	19.84	6.016	6.581	2.577	1.503	1.673	1.174	0.833	0.299
	179.79	20.56	5.471	7.570	2.168	1.568	1.783	1.160	0.853	0.296
	179.83	19.04	4.792	8.850	1.814	1.724	1.859	1.168	0.862	0.293
	179.88	15.65	3.640	7.730	1.222	2.117	1.868	1.188	0.871	0.314
	179.92	8.34	3.516	5.093	0.848	1.777	1.834	1.222	0.837	0.336
	179.96	5.46	2.586	2.868	0.660	1.409	1.749	1.262	0.751	0.364
29-Jun	180.00	5.35	2.159	3.356	0.560	1.808	1.616	1.287	0.651	0.378
	180.04	3.15	1.040	2.592	0.404	1.426	1.471	1.313	0.552	0.381
	180.08	2.57	0.395	2.108	0.201	1.395	1.316	1.338	0.475	0.384
	180.13	2.40	0.361	1.282	0.099	1.100	1.179	1.361	0.406	0.395
	180.17	2.06	0.021	0.887	0.033	0.648	1.035	1.375	0.341	0.398
	180.21	3.75	1.208	1.140	0.081	0.742	0.901	1.378	0.298	0.377
	180.25	3.61	2.080	1.843	0.263	0.730	0.810	1.367	0.275	0.366
	180.29	4.15	3.289	2.058	0.423	0.833	0.742	1.355	0.275	0.355
	180.33	6.52	3.684	2.465	0.628	0.935	0.685	1.344	0.275	0.343
	180.38	6.80	3.741	2.725	0.821	0.844	0.662	1.321	0.286	0.332
	180.42	8.19	4.496	2.951	0.969	0.742	0.662	1.298	0.309	0.309
	180.46	7.58	4.214	2.996	1.105	0.628	0.674	1.276	0.343	0.298
	180.50	13.36	8.100	4.000	1.537	0.969	0.685	1.253	0.366	0.286
	180.54	4.90	2.518	2.428	1.228	0.512	0.728	1.239	0.420	0.295
	180.58	7.73	4.876	3.286	1.137	0.796	0.750	1.228	0.432	0.295
	180.63	13.17	8.270	4.820	1.885	0.659	0.750	1.194	0.432	0.272
	180.67	11.47	6.679	4.828	2.142	0.520	0.793	1.191	0.532	0.270
	180.71	11.89	6.814	4.704	1.973	0.532	0.873	1.179	0.589	0.270
	180.75	10.74	5.772	4.667	1.789	0.597	0.938	1.177	0.620	0.278
	180.79	14.16	6.325	4.791	1.766	0.552	0.972	1.177	0.609	0.278

		Spray Ice Temperatures Beneath Ablation Plots (Hourly)								
		Average				Temperature (ºC)				
Date	Date Fraction	Air Temp.	1.5 cm	2 cm	3 cm	Sawdust	Gravel/	0.3m	0.6 m	1.0 m
	(Julian Day)	(ºC)	Sawdust	Sawdust	Sawdust	Bags	Sawdust	Gravel	Gravel	Gravel
	180.83	11.66	5.467	5.016	1.709	0.563	0.995	1.177	0.609	0.278
	180.88	9.88	4.156	4.506	1.446	0.504	1.026	1.208	0.640	0.287
	180.92	6.15	3.145	3.280	1.075	0.586	1.040	1.222	0.620	0.301
	180.96	7.72	2.829	3.009	0.916	0.404	1.018	1.256	0.575	0.313
30-Jun	181.00	6.28	2.696	2.775	0.793	0.361	0.975	1.270	0.520	0.304
	181.04	3.56	1.247	1.780	0.623	0.213	0.930	1.304	0.486	0.315
	181.08	3.69	1.250	1.284	0.443	0.192	0.876	1.330	0.443	0.329
	181.13	3.72	1.264	1.219	0.377	0.241	0.810	1.344	0.389	0.320
	181.17	2.96	0.958	1.105	0.343	0.138	0.753	1.367	0.355	0.320
	181.21	3.43	1.230	1.083	0.320	0.229	0.696	1.378	0.332	0.320
	181.25	3.89	1.551	1.244	0.346	0.232	0.642	1.369	0.300	0.312
	181.29	5.23	2.716	1.777	0.494	0.232	0.597	1.358	0.289	0.300
	181.33	5.45	2.985	2.080	0.639	0.526	0.594	1.355	0.309	0.298
	181.38	5.97	3.639	2.612	0.787	0.708	0.582	1.332	0.320	0.286
	181.42	6.51	4.699	3.357	0.935	0.674	0.594	1.310	0.343	0.275
	181.46	3.00	1.763	1.775	0.787	0.355	0.628	1.298	0.389	0.275
	181.50	2.19	1.616	1.525	0.526	0.298	0.651	1.287	0.389	0.286
	181.54	4.29	2.999	1.981	0.562	0.391	0.631	1.256	0.357	0.278
	181.58	4.96	3.800	2.185	0.790	0.369	0.619	1.233	0.346	0.266
	181.63	3.35	2.570	1.653	0.858	0.209	0.631	1.210	0.369	0.266
	181.67	6.80	4.161	2.038	1.006	0.391	0.665	1.188	0.380	0.266
	181.71	9.04	4.880	2.894	1.469	0.514	0.719	1.162	0.423	0.252
	181.75	6.09	3.278	2.171	1.344	0.343	0.810	1.140	0.491	0.252
	181.79	6.29	3.154	2.420	1.094	0.343	0.901	1.117	0.514	0.252
	181.83	5.33	2.759	2.114	0.890	0.298	0.935	1.105	0.503	0.252
	181.88	5.21	2.702	2.499	0.753	0.252	0.946	1.094	0.469	0.252
	181.92	3.55	1.559	1.854	0.594	0.149	0.912	1.083	0.457	0.263
	181.96	2.66	0.779	2.321	0.369	0.106	0.870	1.051	0.426	0.255

		Spray Ice Temperatures Beneath Ablation Plots (Hourly)								
						Temperature (ºC)				
Date	Date Fraction (Julian Day)	Average Air Temp. (ºC)	1.5 cm Sawdust	2 cm Sawdust	3 cm Sawdust	Sawdust Bags	Gravel/ Sawdust	0.3m Gravel	0.6 m Gravel	1.0 m Gravel
1-Jul	182.00	0.86	0.243	1.721	0.152	0.072	0.801	1.040	0.380	0.255
	182.04	0.26	0.004	1.040	0.038	0.061	0.733	1.040	0.334	0.266
	182.08	-0.39	-0.074	0.736	-0.005	0.018	0.645	1.031	0.280	0.257
	182.13	-0.76	-0.131	0.349	-0.017	0.006	0.554	1.020	0.234	0.269
	182.17	-0.89	-0.220	0.363	-0.026	-0.003	0.454	1.000	0.191	0.260
	182.21	-0.79	-0.266	0.374	-0.014	-0.014	0.385	0.989	0.180	0.248
	182.25	-0.47	0.602	0.351	-0.014	0.009	0.317	0.966	0.180	0.237
	182.29	0.27	2.236	0.431	0.020	-0.026	0.283	0.943	0.169	0.237
	182.33	2.23	4.991	0.511	0.123	0.123	0.260	0.909	0.169	0.226
	182.38	3.21	5.544	0.511	0.226	0.214	0.260	0.886	0.169	0.214
	182.42	4.88	6.607	0.579	0.465	0.283	0.294	0.852	0.169	0.214
	182.46	5.04	4.958	0.693	0.773	0.260	0.351	0.818	0.169	0.203
	182.50	5.62	4.886	0.918	1.020	0.303	0.451	0.793	0.246	0.200
	182.54	5.32	3.995	1.304	1.043	0.257	0.554	0.759	0.337	0.200
	182.58	6.78	4.774	2.154	1.179	0.326	0.645	0.724	0.394	0.189
	182.63	10.83	5.594	1.970	1.471	0.312	0.744	0.710	0.460	0.198
	182.67	11.57	6.257	2.973	2.035	0.457	0.855	0.696	0.537	0.206
	182.71	9.49	5.229	3.086	1.729	0.491	1.015	0.674	0.639	0.206
	182.75	10.49	4.256	3.219	1.590	0.534	1.159	0.659	0.694	0.204
	182.79	11.86	3.452	4.422	1.282	1.043	1.259	0.668	0.714	0.213
	182.83	12.62	2.956	4.884	1.123	0.861	1.304	0.657	0.714	0.213
	182.88	5.81	2.843	2.527	0.770	0.372	1.304	0.668	0.714	0.235
	182.92	3.60	1.973	1.610	0.611	0.281	1.282	0.702	0.680	0.258
	182.96	1.93	1.023	0.955	0.443	0.204	1.205	0.728	0.614	0.272
2-Jul	183.00	0.99	0.400	0.560	0.252	0.149	1.094	0.753	0.537	0.286
	183.04	0.77	0.129	0.426	0.106	0.118	0.983	0.767	0.449	0.289
	183.08	0.46	0.040	0.405	0.040	0.075	0.861	0.781	0.371	0.292
	183.13	-0.02	-0.005	0.394	-0.005	0.063	0.759	0.793	0.326	0.303

		Spray Ice Temperatures Beneath Ablation Plots (Hourly)								
		Average				Temperature (ºC)				
Date	Date Fraction	Air Temp.	1.5 cm	2 cm	3 cm	Sawdust	Gravel/	0.3m	0.6 m	1.0 m
	(Julian Day)	(ºC)	Sawdust	Sawdust	Sawdust	Bags	Sawdust	Gravel	Gravel	Gravel
	183.17	0.12	0.043	0.408	-0.003	0.054	0.659	0.795	0.283	0.294
	183.21	0.12	0.100	0.431	-0.003	0.054	0.579	0.807	0.248	0.283
	183.25	0.71	0.205	0.456	0.011	0.068	0.502	0.798	0.217	0.274
	183.29	1.95	0.593	0.570	0.034	0.148	0.445	0.798	0.205	0.263
	183.33	2.64	1.332	0.787	0.080	0.194	0.411	0.775	0.205	0.251
	183.38	3.29	2.250	1.185	0.240	0.228	0.399	0.764	0.228	0.240
	183.42	3.48	2.180	1.375	0.397	0.248	0.420	0.761	0.271	0.237
	183.46	5.01	3.423	1.794	0.568	0.408	0.431	0.738	0.294	0.226
	183.50	2.95	2.417	1.636	0.659	0.283	0.465	0.727	0.328	0.226
	183.54	0.71	0.920	0.704	0.442	0.134	0.499	0.716	0.351	0.214
	183.58	0.58	0.909	0.590	0.294	0.134	0.499	0.704	0.328	0.226
	183.63	1.09	1.193	0.682	0.283	0.169	0.477	0.704	0.283	0.226
	183.67	2.35	1.919	0.989	0.374	0.237	0.454	0.693	0.271	0.226
	183.71	2.63	2.361	1.522	0.522	0.271	0.442	0.682	0.283	0.214
	183.75	3.43	2.508	1.772	0.613	0.317	0.454	0.670	0.317	0.214
	183.79	4.21	3.231	2.032	0.659	0.363	0.465	0.659	0.351	0.203
	183.83	3.26	2.349	1.624	0.602	0.340	0.488	0.647	0.374	0.191
	183.88	2.57	1.758	1.236	0.531	0.303	0.531	0.645	0.394	0.212
	183.92	2.64	1.942	1.386	0.477	0.351	0.533	0.636	0.363	0.203
	183.96	2.26	1.534	1.239	0.454	0.306	0.533	0.625	0.351	0.203
3-Jul	184.00	1.68	1.068	1.102	0.408	0.248	0.533	0.636	0.340	0.203
	184.04	1.59	1.011	0.977	0.328	0.237	0.522	0.636	0.317	0.214
	184.08	0.97	0.442	0.693	0.226	0.157	0.511	0.636	0.306	0.214
	184.13	0.81	0.271	0.579	0.146	0.123	0.477	0.636	0.283	0.214
	184.17	0.70	0.180	0.499	0.089	0.112	0.454	0.636	0.260	0.214
	184.21	0.75	0.251	0.491	0.057	0.080	0.411	0.616	0.228	0.205
	184.25	1.14	0.650	0.605	0.080	0.148	0.388	0.616	0.217	0.205
	184.29	1.97	1.151	0.855	0.160	0.194	0.365	0.605	0.217	0.194

		Spray Ice Temperatures Beneath Ablation Plots (Hourly)								
						Temperature (ºC)				
Date	Date Fraction	Average Air Temp.	1.5 cm	2 cm	3 cm	Sawdust	Gravel/	0.3m	0.6 m	1.0 m
	(Julian Day)	(ºC)	Sawdust	Sawdust	Sawdust	Bags	Sawdust	Gravel	Gravel	Gravel
	184.33	2.68	1.582	1.241	0.285	0.228	0.354	0.593	0.228	0.194
	184.38	2.06	1.273	1.488	0.442	0.203	0.374	0.590	0.260	0.191
	184.42	4.39	2.576	1.987	0.568	0.408	0.385	0.579	0.294	0.180
	184.46	7.02	5.398	2.802	0.784	0.829	0.408	0.556	0.328	0.169
	184.50	12.43	8.910	2.968	1.395	2.719	0.462	0.542	0.394	0.155
	184.54	16.13	12.260	2.762	2.389	1.981	0.574	0.517	0.528	0.152
	184.58	16.99	10.040	2.869	3.151	1.125	0.819	0.512	0.728	0.158
	184.63	18.88	7.940	3.148	3.622	1.055	1.100	0.509	0.907	0.167
	184.67	21.35	7.100	4.092	3.551	1.109	1.358	0.518	1.052	0.176
	184.71	20.78	5.734	4.618	3.266	1.831	1.514	0.526	1.185	0.196
	184.75	19.71	5.539	5.280	2.744	2.122	1.602	0.558	1.251	0.216
	184.79	18.18	4.882	5.896	2.244	2.074	1.644	0.612	1.248	0.236
	184.83	20.20	4.822	7.680	1.924	2.309	1.619	0.678	1.211	0.257
	184.88	18.52	4.402	8.660	1.480	1.616	1.559	0.754	1.152	0.277
	184.92	17.18	3.836	8.760	1.137	1.228	1.477	0.854	1.092	0.297
	184.96	12.56	3.340	8.090	0.922	0.956	1.387	0.945	0.990	0.308
4-Jul	185.00	9.01	2.607	7.220	0.831	0.888	1.274	1.035	0.877	0.331
	185.04	7.08	2.133	5.345	0.740	0.752	1.160	1.137	0.763	0.365
	185.08	4.99	1.856	2.850	0.609	0.473	1.041	1.211	0.643	0.382
	185.13	4.12	1.610	1.361	0.521	0.384	0.930	1.282	0.544	0.396
	185.17	4.01	1.534	1.035	0.444	0.330	0.831	1.341	0.467	0.410
	185.21	3.74	1.265	1.004	0.401	0.321	0.754	1.389	0.413	0.413
	185.25	5.90	5.208	1.347	0.472	0.597	0.665	1.404	0.358	0.392
	185.29	7.20	5.118	2.298	0.859	0.938	0.609	1.415	0.347	0.381
	185.33	8.88	3.912	2.411	0.961	1.040	0.620	1.426	0.381	0.370
	185.38	9.76	5.636	3.258	1.211	1.902	0.631	1.415	0.392	0.358
	185.42	8.56	4.449	3.232	1.287	1.491	0.663	1.423	0.458	0.356
	185.46	10.56	6.479	3.796	1.423	2.216	0.697	1.412	0.481	0.344

		Spray Ice Temperatures Beneath Ablation Plots (Hourly)								
						Temperature (ºC)				
Date	Date Fraction	Average Air Temp.	1.5 cm	2 cm	3 cm	Sawdust	Gravel/	0.3m	0.6 m	1.0 m
	(Julian Day)	(ºC)	Sawdust	Sawdust	Sawdust	Bags	Sawdust	Gravel	Gravel	Gravel
	185.50	18.50	11.860	4.630	2.023	4.911	0.742	1.378	0.526	0.321
	185.54	14.56	10.830	5.054	2.710	3.815	0.831	1.353	0.649	0.307
	185.58	15.11	9.820	3.834	2.989	3.248	1.021	1.350	0.828	0.316
	185.63	22.10	12.350	3.947	3.710	3.834	1.225	1.327	0.930	0.316
	185.67	22.02	9.810	4.530	3.910	4.045	1.494	1.324	1.075	0.314
	185.71	19.61	8.240	5.134	3.614	5.112	1.752	1.322	1.186	0.322
	185.75	17.30	6.371	5.131	2.878	4.973	1.930	1.353	1.262	0.354
	185.79	13.60	5.503	5.097	2.201	3.870	1.975	1.375	1.239	0.377
	185.83	9.71	4.763	3.355	1.548	2.554	1.967	1.424	1.163	0.413
	185.88	10.73	5.228	3.775	1.404	2.692	1.845	1.472	1.030	0.427
	185.92	8.62	4.282	3.921	1.279	2.726	1.698	1.528	0.927	0.439
	185.96	11.25	4.777	5.126	1.211	3.313	1.540	1.585	0.825	0.450
5-Jul	186.00	9.03	4.484	5.048	1.075	3.177	1.381	1.619	0.780	0.450
	186.04	8.76	4.665	4.484	1.143	3.099	1.268	1.664	0.734	0.450
	186.08	7.55	4.364	4.578	1.214	3.079	1.168	1.701	0.692	0.453
	186.13	7.31	4.341	4.758	1.112	2.458	1.078	1.724	0.635	0.453
	186.17	7.87	4.559	5.280	1.296	2.755	0.990	1.738	0.592	0.444
	186.21	8.06	4.311	5.235	1.319	2.732	0.933	1.749	0.569	0.433
	186.25	8.11	4.671	5.111	1.364	2.698	0.887	1.749	0.558	0.421
	186.29	8.22	4.731	4.844	1.378	2.848	0.856	1.729	0.538	0.413
	186.33	11.06	11.700	4.570	1.557	3.928	0.842	1.738	0.546	0.398
	186.38	13.40	13.160	5.145	1.873	4.581	0.842	1.715	0.535	0.387
	186.42	16.47	17.860	5.956	2.507	6.092	0.865	1.681	0.535	0.364
	186.46	18.00	17.460	6.077	2.729	7.090	0.964	1.667	0.612	0.362
	186.50	19.60	13.420	6.434	3.076	11.610	1.098	1.641	0.780	0.348
	186.54	20.66	15.000	6.702	3.062	6.894	1.276	1.627	0.970	0.345
	186.58	23.54	15.350	6.619	3.014	6.326	1.466	1.613	1.149	0.365
	186.63	21.35	12.230	5.525	3.881	6.393	1.636	1.613	1.274	0.377

		Spray Ice Temperatures Beneath Ablation Plots (Hourly)									
		Average					Temperature (ºC)				
Date	Date Fraction	Air Temp.	1.5 cm	2 cm	3 cm	Sawdust	Gravel/	0.3m	0.6 m	1.0 m	
	(Julian Day)	(ºC)	Sawdust	Sawdust	Sawdust	Bags	Sawdust	Gravel	Gravel	Gravel	
	186.67	22.33	10.910	4.801	3.788	5.116	1.837	1.622	1.361	0.397	

APPENDIX C

ABLATION MEASUREMENTS

A total of 35 - 5 cm by 5 cm by 4.9 m long graduated wooden stakes were inserted into the island to measure spray ice ablation. Fifteen ablation stakes were placed into the unprotected spray ice. Roughly one-half of these were in clean spray ice whereas the remaining stakes were placed in spray ice where the surface had been stained as a result of previous activity on the island. The remaining 20 stakes were placed in ablation plots and beneath the Rufco and 13 oz. per square yard vinyl edge protection sheets.

Stakes were graduated at 10 cm intervals starting from the top. The visible stake length from the top of the stake to the spray ice surface was measured during each site survey. Initial baseline measurements were recorded on April 23 and subsequent surveys were undertaken on May 9, June 10, June 22, and July 5. (Measurements were not taken during the May 18 survey due to extensive drifting snow which had accumulated over the western half of the island, obscuring many of the stakes). This differences between initial and subsequent measurements yielded the magnitude of ice surface ablation at a particular location.

	Spray Ice Ablation Level					
Material		Measure of Ice Level (cm)				
	Baseline	May 9.	May 18.	June 10.	June 22.	July 5.
Sawdust Bags 1	90	90	90	90	95	95
Sawdust Bags 2	80	80	80	80	85	85
1m Gravel 1	55	75	75	75	85	100
1m Gravel 2	10	14	14	21	28	40
0.6m Gravel	5	10	10	20	30	45
0.3m Gravel	35	50	50	65	100	115
Unprotected Spray Ice 1	50	52	52	130	185	230
Unprotected Spray Ice 2	50	53	53	140	200	290
Unprotected Spray Ice 3	40	44	44	140	200	285
Unprotected Spray Ice 4	40	46	46	150	215	
Unprotected Spray Ice 5	40	43	43	122	175	265
Unprotected Spray Ice 6	45	49	49	145	205	285
Unprotected Spray Ice 7	35	39	39	110	170	270
Unprotected Spray Ice 8	43	47	47	115	175	260
Unprotected Spray Ice 9	70	75	75	135	190	270
Unprotected Spray Ice 10	20	23	23	110	185	300
Unprotected Spray Ice 11	55	55	55	130	190	290
Unprotected Spray Ice 12	20	22	22	120	180	270
Unprotected Spray Ice 13	55	56	56	130	180	280
Unprotected Spray Ice 14	72	75	75	160	215	290
Unprotected Spray Ice 15	70	71	71	160	230	300
1cm Sawdust	3	4	4	50	72	110
1.5cm Sawdust	50	50	50	80	102	130
2cm Sawdust	50	50	50	65	70	80
3cm Sawdust	50	50	50	55	60	70
1cm Sawdust/5cm Gravel	50	50	50	50	60	70
Rufco Sheet 1	50	50	50	80	110	150
Rufco Sheet 2	50	50	50	65	80	120
13oz Nylon 1	50	50	50	90	125	170
13oz Nylon 2	50	50	50	100	135	180
Rig Timbers	72	72	72	75	80	
Insulated Tarp 1	195	195	195	210	225	
Insulated Tarp 2	40	40	40	50	70	90
Insulated Tarp 3	178	180	180	200	210	

		Cumulative Ablation to Date (cm)				
Material	April 23	May 9.	May 18.	June 10.	June 22.	July 5.
Sawdust Bags 1	0	0	0	0	5	5
Sawdust Bags 2	0	0	0	0	5	5
Sawdust Bags Average	0	0	0	0	5	5
1m Gravel 1	0	20	20	20	30	45
1m Gravel 2	0	4	4	11	18	30
1m Gravel Average	0	12	12	15.5	24	37.5
0.6m Gravel	0	5	5	15	25	40
0.3m Gravel	0	15	25	30	65	80
Unprotected Spray Ice 1	0	2	2	80	135	180
Unprotected Spray Ice 2	0	3	3	90	150	240
Unprotected Spray Ice 3	0	4	4	100	160	245
Unprotected Spray Ice 4	0	6	6	110	175	
Unprotected Spray Ice 5	0	3	3	82	135	225
Unprotected Spray Ice 6	0	4	4	100	160	240
Unprotected Spray Ice 7	0	4	4	75	135	235
Unprotected Spray Ice 8	0	4	4	72	132	217
Unprotected Spray Ice 9	0	5	5	65	120	200
Unprotected Spray Ice 10	0	3	3	90	165	280
Unprotected Spray Ice 11	0	0	0	75	135	235
Unprotected Spray Ice 12	0	2	2	100	160	250
Unprotected Spray Ice 13	0	1	1	75	125	225
Unprotected Spray Ice 14	0	3	3	88	143	218
Unprotected Spray Ice 15	0	1	1	90	160	230
Unprotected Spray Ice Average	0	3	3	86.13	146	230
1cm Sawdust	0	1	1	47	69	107
1.5cm Sawdust	0	0	0	30	52	80
2cm Sawdust	0	0	0	15	20	30
3cm Sawdust	0	0	0	5	10	20
1cm Sawdust/5cm Gravel	0	0	0	0	10	20
Rufco Sheet 1	0	0	0	30	60	100
Rufco Sheet 2	0	0	0	15	30	70
Rufco Sheet Average	0	0	0	22.5	45	85

		Cumulative Ablation to Date				
			(cm)			
Material	April 23	May 9.	May 18.	June 10.	June 22.	July 5.
13oz Nylon Sheet 1	0	0	0	40	75	120
13oz Nylon Sheet 2	0	0	0	50	85	130
13oz Nylon Sheet Average	0	0	0	45	80	125
Rig Timbers	0	0	0	3	5	
Insulated Tarp 1	0	0	0	15	30	
Insulated Tarp 2	0	0	0	10	30	50
Insulated Tarp 3	0	2	2	22	32	
Insulated Tarp Average	0	0.67	0.67	15.67	30.67	50

	Spray Ice Ablation Rates				
		Rate of Spray Ice Ablation (cm/day)			
Material	April 23-May 9.	May 9-May 18.	May 18-June 10.	June 10-June 22.	June 22-July 5.
Sawdust 1	0	0	0	0.42	0
Sawdust 2	0	0	0	0.42	0
Sawdust Bags Average	0	0	0	0.42	0
1m Gravel 1	1.25	0	0	0.42	1.15
1m Gravel 2	0.25	0	0.30	0.58	0.92
1m Gravel Average	0.75	0	0.15	0.71	1.04
0.6m Gravel	0.31	0	0.44	0.83	1.15
0.3m Gravel	0.94	0	0.65	2.92	1.15
Unprotected Spray Ice 1	0.13	0	3.39	4.58	3.46
Unprotected Spray Ice 2	0.19	0	3.78	5.00	6.92
Unprotected Spray Ice 3	0.25	0	4.17	5.00	6.54
Unprotected Spray Ice 4	0.38	0	4.52	5.42	
Unprotected Spray Ice 5	0.19	0	3.44	4.42	6.92
Unprotected Spray Ice 6	0.25	0	4.17	5.00	6.15
Unprotected Spray Ice 7	0.25	0	3.09	5.00	3.23
Unprotected Spray Ice 8	0.25	0	2.96	5.00	6.54
Unprotected Spray Ice 9	0.31	0	2.61	4.58	6.15
Unprotected Spray Ice 10	0.19	0	3.78	6.25	8.85
Unprotected Spray Ice 11	0	0	3.26	5.00	7.69
Unprotected Spray Ice 12	0.13	0	4.26	5.00	6.92
Unprotected Spray Ice 13	0.06	0	3.22	4.17	7.69
Unprotected Spray Ice 14	0.19	0	3.70	4.58	5.77
Unprotected Spray Ice 15	0.06	0	3.87	5.83	5.39
Unprotected Spray Ice Average	0.19	0	3.62	4.99	6.30
1cm Sawdust	0.06	0	2.00	1.83	2.92
1.5cm Sawdust	0	0	1.30	1.83	2.15
2cm Sawdust	0	0	0.65	0.42	0.77
3cm Sawdust	0	0	0.22	0.42	0.77
1cm Sawdust/5cm Gravel	0	0	0	0.83	0.77
Rufco Sheet 1	0	0	1.30	2.50	3.08
Rufco Sheet 2	0	0	0.65	1.25	3.08

	Spray Ice Ablation Rates				
		Rate of Spray Ice Ablation (cm/day)			
Material	April 23-May 9.	May 9-May 18.	May 18-June 10.	June 10-June 22.	June 22-July 5.
Rufco Sheet Average	0	0	0.98	1.88	3.08
13oz Nylon Sheet 1	0	0	1.74	2.92	3.46
13oz Nylon Sheet 2	0	0	2.17	2.92	3.46
13oz Nylon Sheet Average	0	0	1.96	2.92	3.46
Rig Timbers	0	0	0.13	0.42	
Insulated Tarp 1	0	0	0.65	1.25	
Insulated Tarp 2	0	0	0.44	1.67	1.54
Insulated Tarp 3	0.13	0	0.87	0.83	
Insulated Tarp Average	0.04	0	0.65	1.25	1.54

Cumulative Ablation

Cumulative Ablation (averaged from samples available)						
Material	Cumulative Ablation to Date (cm)					
	Apr. 23.	May 9.	May 18.	Jun. 10.	Jun. 22.	Jul. 5.
Sawdust Bags	0	0	0	0	5	5
1m Gravel	0	0	0	3.5	12	25.5
0.6m Gravel	0	0	0	10	20	35
0.3m Gravel	0	0	0	15	50	65
Unprotected Spray Ice	0	3	3	86.13	146	230
1cm Sawdust	0	1	1	47	69	107
1.5cm Sawdust	0	0	0	30	52	80
2cm Sawdust	0	0	0	15	20	30
3cm Sawdust	0	0	0	5	10	20
1cm Sawdust/5cm Gravel	0	0	0	0	10	20
Rufco Sheet	0	0	0	22.5	45	85
13oz Nylon Sheet	0	0	0	45	80	125
Rig Timbers	0	0	0	3	5	
Insulated Tarp	0	0.667	0.667	15.67	30.67	50

Ablation Measures

	Material	Baseline	Measure of Ice Level (cm) May 9.	May 18.	June 10.	June 22.	July 5.
	Sawdust Bags 1	90	90	90	90	95	95
	Sawdust Bags 2	80	80	80	80	85	85
*	1m Gravel 1	75	75	75	75	85	100
*	1m Gravel 2	14	14	14	21	28	40
*	0.6m Gravel	10	10	10	20	30	45
*	0.3m Gravel	50	50	50	65	100	115
	Unprotected Spray Ice 1	50	52	52	130	185	230
	Unprotected Spray Ice 2	50	53	53	140	200	290
	Unprotected Spray Ice 3	40	44	44	140	200	285
	Unprotected Spray Ice 4	40	46	46	150	215	
	Unprotected Spray Ice 5	40	43	43	122	175	265
	Unprotected Spray Ice 6	45	49	49	145	205	285
	Unprotected Spray Ice 7	35	39	39	110	170	270
	Unprotected Spray Ice 8	43	47	47	115	175	260
	Unprotected Spray Ice 9	70	75	75	135	190	270
	Unprotected Spray Ice 10	20	23	23	110	185	300
	Unprotected Spray Ice 11	55	55	55	130	190	290
	Unprotected Spray Ice 12	20	22	22	120	180	270
	Unprotected Spray Ice 13	55	56	56	130	180	280
	Unprotected Spray Ice 14	72	75	75	160	215	290
	Unprotected Spray Ice 15	70	71	71	160	230	300
	1cm Sawdust	3	4	4	50	72	110
	1.5cm Sawdust	50	50	50	80	102	130
	2cm Sawdust	50	50	50	65	70	80
	3cm Sawdust	50	50	50	55	60	70
	1cm Sawdust/5cm Gravel	50	50	50	50	60	70
	Rufco Sheet 1	50	50	50	80	110	150
	Rufco Sheet 2	50	50	50	65	80	120
	13oz Nylon 1	50	50	50	90	125	170
	13oz Nylon 2	50	50	50	100	135	180
	Rig Timbers	72	72	72	75	80	
	Insulated Tarp 1	195	195	195	210	225	
	Insulated Tarp 2	40	40	40	50	70	90
	Insulated Tarp 3	178	180	180	200	210	

* baseline is adjusted to be May 9 reading as opposed to April 23 due to misleading spray ice creep that took place during this period.

Cumulative Ablation (adj)

			Adjusted Cumulative Ablation			
	Material	Cumulative Ablation to Date (cm)				
		April 23	May 9.	May 18.	June 10.	June 22.	July 5.
	Sawdust Bags 1	0	0	0	0	5	5
	Sawdust Bags 2	0	0	0	0	5	5
	Sawdust Bags Average	0	0	0	0	5	5
*	1m Gravel 1	0	0	0	0	10	25
*	1m Gravel 2	0	0	0	7	14	26
*	1m Gravel Average	0	0	0	3.5	12	25.5
*	0.6m Gravel	0	0	0	10	20	35
*	0.3m Gravel	0	0	0	15	50	65
	Unprotected Spray Ice 1	0	2	2	80	135	180
	Unprotected Spray Ice 2	0	3	3	90	150	240
	Unprotected Spray Ice 3	0	4	4	100	160	245
	Unprotected Spray Ice 4	0	6	6	110	175	
	Unprotected Spray Ice 5	0	3	3	82	135	225
	Unprotected Spray Ice 6	0	4	4	100	160	240
	Unprotected Spray Ice 7	0	4	4	75	135	235
	Unprotected Spray Ice 8	0	4	4	72	132	217
	Unprotected Spray Ice 9	0	5	5	65	120	200
	Unprotected Spray Ice 10	0	3	3	90	165	280
	Unprotected Spray Ice 11	0	0	0	75	135	235
	Unprotected Spray Ice 12	0	2	2	100	160	250
	Unprotected Spray Ice 13	0	1	1	75	125	225
	Unprotected Spray Ice 14	0	3	3	88	143	218
	Unprotected Spray Ice 15	0	1	1	90	160	230
	Unprotected Spray Ice Average	0	3	3	86.133	146	230
	1cm Sawdust	0	1	1	47	69	107
	1.5cm Sawdust	0	0	0	30	52	80
	2cm Sawdust	0	0	0	15	20	30
	3cm Sawdust	0	0	0	5	10	20
	1cm Sawdust/5cm Gravel	0	0	0	0	10	20
	Rufco Sheet 1	0	0	0	30	60	100
	Rufco Sheet 2	0	0	0	15	30	70
	Rufco Sheet Average	0	0	0	22.5	45	85

Cumulative Ablation (adj)

			Adjusted Cumulative Ablation			
Material		Cumulative Ablation to Date (cm)				
	April 23	May 9.	May 18.	June 10.	June 22.	July 5.
13oz Nylon Sheet 1	0	0	0	40	75	120
13oz Nylon Sheet 2	0	0	0	50	85	130
13oz Nylon Sheet Average	0	0	0	45	80	125
Rig Timbers	0	0	0	3	5	
Insulated Tarp 1	0	0	0	15	30	
Insulated Tarp 2	0	0	0	10	30	50
Insulated Tarp 3	0	2	2	22	32	
Insulated Tarp Average	0	0.6667	0.6667	15.667	30.667	50

APPENDIX D

ANNOTATED SLIDE SET

The following is a description of slides taken during the experiment.

APRIL

Slide 1 Oblique aerial view of Nipterk P-32 Spray ice island on April 21, 1989 looking east. The island was constructed over a 53 day period from November 1988 to January 1989 in a water depth of 6.5 m. Ground island diameter was 320 m. Summer ablation experiment set up area is in the right foreground. Installation of net and one sheet was completed by this time. Spray ice relief pad constructed in March can be seen in the distance.

Slide 2 Sandbag attachment technique. Edge protection sheets were held in place with coarse mesh net which was placed atop the sheets. 14 kg. sandbags were tied to radial ropes of net about 30 cm island-center side of node. Sandbag spacing was 5 m on the inner portion of the sheets and 1 m along the island edge.

Slide 3 View looking west-southwest of sawdust ablation and 0.3 m thick gravel test plots (foreground) and edge protection sheets (background) shortly after installation on April 25. Snow was piled on edges of sheets to minimize wind disturbances.

Slide 4 Front end loader with 0.5 m diameter auger attachment used to drill 2-3 m holes into which sheet deadmen anchors were placed on island-center side of sheets.

Slide 5 Oblique aerial view of experiment set-up area (south-southwest) perimeter of island on April 25. Edge erosion protection system consisted of (from left to right) net, 18 oz. and 13 oz. per square yard nylon sheets, and Rufco sheet. Ablation test plots from left to tight

consisted of simulate rig mat, various thicknesses of gravel (in front of 18 oz. nylon sheet), and sawdust (in front of 13 oz. nylon sheet). An insulated tarp was placed on the island-center side of the gravel plots. The blue tent housed a data logger and equipment whereas a meteorological station and time-lapse camera were placed on top of the pallet box. Ablation stakes placed in the spray ice in front of the sheets and in ablation plots can also be seen.

MAY 18

Slide 6 Experiment set-up area looking north. A mid-May snow storm caused extensive snow drifts atop the sheets and ablation plots. Winter air temperatures persisted until the last week in May.

JUNE 10

Slide 7 Nipterk as viewed from the West. Experiment set-up area is in the foreground, mud discharge area in the background. Spray ice relief pad visible in upper right hand corner. Spray ice ablation now apparent. Up until this point, heavily soiled areas exhibited the greatest amount of ablation. By this time, thickness of debris reached sufficient thickness that small (1 m) mounds or hummocks developed due to more rapid ablation of surrounding relatively cleaner spray ice. Ice sheet developing melt ponds. Ice road to Pelly Island barges still appeared to be possible.

Slide 8 Oblique aerial close-up of simulated rig mat, gravel, and insulated tarp ablation test plots looking south. Cumulative spray ice ablation was about 1 m.

Slide 9 Ponds which formed atop edge protection sheets. These formed when snow melt and rainfall originally deposited on sheets accumulated in small depressions which deepened due to thawing of underlying spray ice. The largest ponds by this date were 4 m in diameter and 0.5 m deep. Ponds were not drained because of additional sheet stabilization they provided.

Slide 10 Island edge view of Rufco sheet. Abrupt shelf formed due to ablation of unprotected spray ice. Edge of sheet being lifted by wind which tended to push it back onto the island. This condition was remedied by adding additional sandbags along island edge and exposed areas.

Slide 11 Rufco sheet looking north. Ablation protection afforded by the sheet is clearly visible. Differential ablation between sheet and unprotected spray ice was in excess of 0.5 m by this point.

Slide 12 Unprotected spray ice surface. Surface was still crusty and ablated relatively uniformly except in heavily soiled areas. Insulated tarp, sawdust, and gravel test plots can be seen in the distance. Island is now isothermal.

Slide 13 Simulated rig mat plot. Ablation of the unprotected spray ice at the edge of plot created shelf and disturbance of a portion of the plot. However, center of plot where ablation stake was placed was not affected.

Slide 14 Differential spray ice ablation. Due to ablation protection provided by accumulation of a debris layer which eventually served to insulate and reduce the effects of solar radiation. Mounds or hummocks, seen here were protected with about 1 cm of sawdust. They were about 1 m high at this time.

Slide 15 Edge view close-up of Rufco sheet. Minor amount of wind induced push back of sheet onto the island (black portion of sheet) can be seen.

Slide 16 View of sawdust ablation test plot. Only small amounts of spray ice ablation was observed beneath the plot by this time and ablation was restricted to thinnest layers of sawdust. Amount of ablation not related to ablation stake stick-up as stakes were originally placed with varying amounts of stick-up.

JUNE 22

Slide 17 View of Nipterk and relief pad. From the south along the ice road. Lead opened parallel to ice road from Pelly Island which jointed with a second east-west trending lead which opened south of the island. The two leads joined along with another and continued northward past the west side of the island.

Slide 18 Relief pad (foreground) and Nipterk from the east. Deteriorated state of ice sheet is evident.

Slide 19 Experiment set-up area as viewed from the west. Westerly winds pushed back edge of Rufco tarp a small amount back up onto island. Sheet was later stretched out over island edge.

Slide 20 By 2330 hours on June 22, lead south of island had opened another 50 m and small amounts of rideup and pileup were actively taking place, Complete break up of landfast ice in the area had occurred by June 24 when the island was next visited.

Slide 21 Thawing of spray ice due to trapped water atop sheets accelerated with time. This view also shows small amount of rideup which occurred at island edge.

Slide 22 Sawdust ablation protection plot. Degree of ablation protection provided by plot was approaching 2 m by this time. Contents of several sawdust bags were placed over edges of plot to stabilize slopes and prevent disturbance of ablation measurements at the survey stakes.

Slide 23 Degree of differential ablation near island center. Hummocks protected by veneer of sawdust and other materials ere in excess of 2 m in some locations.

Slide 24 Unprotected spray ice ablation where measure with ablation stakes. Meltwater drained vertically so no drainage paths apparent. Surface could be dislodged by kicking with a boot, but still firm several centimeters below. Cumulative ablation varied among locations.

Slide 25 Sawdust ablation plots. Person standing in plot containing 21 cm veneer of sawdust. Sawdust only 3 cm thick nearly negated spray ice ablation.

Slide 26 Views of sawdust ablation plots. Sawdust bags (foreground) protected best - 1 cm sawdust overlain with 5 cm of gravel (middle-left) provided same degree of protection as 3 cm later of sawdust (middle-left)

Slide 27 Ablation in vicinity of simulated rig mat plot. Only 8 cm of cumulative spray ice ablation was measured beneath the plot on June 22. Timbers used to construct the plot were accidently buried as part of the island clean-up which took place a few days later.

JULY 5

Slide 28 Oblique aerial view of Nipterk about two weeks after landfast ice breakup. Roughly 28% of the island by area had calved to date. Several large cracks in the island can be seen. These were present since construction. Smaller cracks, however, formed as portions of the island became unstable due to lack of freeboard. The benefit of the edge protection system is denoted by a 25 m toe which was created.

APPENDIX E

ABLATION AND EROSION NUMERICAL SIMULATION

REPORT PREPARED BY S.L. CONNOLLY DOCUMENTING ANALYTICAL APPLICATION'S ABLATION AND EROSION NUMERICAL SIMULATION.

DRAFT REPORT TO:
ESSO RESOURCES RESEARCH LABORATORY

SPRAY ICE ISLAND ABLATION MODELING

December, 1989

Submitted by:
Analytic Applications, Inc.
1705 14th St.
Suite 126
Boulder, CO 80302

INTRODUCTION

As spray ice islands become an accepted structure for arctic exploratory drilling, the possibilities for expanding their operational capabilities should be explored. Some of these possibilities include the use of a single spray ice island for multi-year drilling operations, open water demobilization of the drilling rig, and even as an early production platform. Ice, although inexpensive and readily available in the arctic, is a very unstable construction material when compared to conventional materials and undergoes considerable deterioration during the arctic summer season. The degree to which this deterioration takes place and the ability to protect the island from ablation and erosional forces is the subject of this study.

For this particular part of the study, the interaction between the island and the surrounding environment has been quantified in a computer model which is designed to simulate the deterioration of the island due to oceanic and atmospheric forces. In addition to modeling the ice island as unprotected ice, various protection materials were modeled and the results were compared with measurements taken in the field. The sensitivity of these models was also examined from the stand point of accuracy needed, and the effects of different environmental forces on the island.

THE MODEL

The modeling effort was broken into two parts; the ablation of the top surface of the island, and the erosion of the perimeter. Since these two parts operate independent of one another they will be modeled independently.

Ablation

The ablation of the top surface involves the energy transfer between the ice and the atmosphere. In this case the standard energy balance equation was used. This equation is given as:

$$F_s + F_l + L + S = \gamma_i \rho D + G \qquad (1)$$

where F_s is the net short wave radiation, F_l is the net long wave radiation, L is the latent heat flux, S is the sensible heat flux, γ_i is the latent heat of fusion, ρ is the spray ice density, D is the depth to which the ice has melted, and G is the heat conducted through the ice. All these quantities are averaged over the surface of the island. The convention used here is for the terms on the left side of (1) to positive into the island surface and heat conduction to be positive away from the surface.

Incoming short wave radiation is solar radiation whereas outgoing short wave is solar radiation reflected from the surface. Incoming short wave radiation has been measured hourly on the island with a pyranometer. The albedo of the spray ice, the ratio of outgoing radiation to incoming radiation, was taken as 0.9, approximately the same as that for snow. Hence the actual amount of absorbed radiation is relatively small.

Incoming long wave radiation originates mainly from water vapor in the air. Since no direct measurement of long wave radiation was taken, it will be estimated using an empirical relation developed by Idso and Jackson (1969):

$$F_l^i = \varepsilon \sigma T_a^4 \left[1 - 0.261 \exp\left(-7.77 \times 10^{-4} (T_a - 273)^2\right)\right] \qquad (2)$$

where ε is the surface emissivity, σ is the Stefan-Boltzman constant, and T_a is the near-surface air temperature in degrees Kelvin. The surface emissivity for spray ice is taken to be 0.97, the same as that for snow.

Long wave radiation emitted from the surface is given by the equation:

$$F_l^o = -\varepsilon \sigma T_s^4 \qquad (3)$$

where T_s is the temperature of the surface in Kelvin. Since the surface is first considered to be ice at the melting point this number will remain constant at 305 W m^{-2}.

Sensible heat flux is the energy transferred by the turbulent action of the wind. Although no sophisticated sensible heat flux measurements were taken on the island, the bulk aerodynamic method of calculating the sensible heat flux only requires wind speed and a temperature profile. This method is commonly used over the ocean (Kondo, 1975), where

surfaces are fairly uniform and fetches are large. The sensible heat flux from this method is given by:

$$S = c_p \rho_a C_s (T_s - T_a) u \tag{4}$$

where c_p is the specific heat of air at constant pressure, ρ_a is the air density, C_s is the sensible heat transfer coefficient, and u is the near surface wind speed.

Latent heat flux becomes a significant term during the summer melt season when the liquid water is plentiful at the surface. Energy is absorbed by the water at the surface when there is a phase change into vapor. This energy is then carried off by the vapor as it is transported into the atmosphere. The term can be measured by observing the humidity gradient above the surface and can be represented by the bulk aerodynamic method as:

$$L = \gamma_v \rho_a C_l (q_s - q) u \tag{5}$$

where γ_v is the latent heat of vaporization, C_l is the latent heat transfer coefficient, q_s is the surface vapor density, and q is the near-surface vapor density. Since humidity was not directly measured on the island we will use the assumptions commonly used in the bulk aerodynamic method over the ocean (Large and Pond, 1982) namely that the air is saturated with respect to water both at the surface and slightly above the surface. In this case the saturation vapor density is given by:

$$q = \frac{a}{R_v (T_a - 273)} \exp\left(\frac{b T_a}{T_a + c}\right) \tag{6}$$

where R_v is the gas constant for water vapor, and a, b, and c are constants given by Buck (1981) as 611.21, 17.502, and 240.97 respectively.

Latent heat can also be transferred to the island by water vapor condensing on the ice surface, rain falling and refreezing, or snow falling. Because of the low precipitation rates in the arctic this will not be considered as an important term.

The energy not reflected at the surface of the island is either conducted down into the ice, absorbed by melting the ice, or absorbed by evaporating liquid water. From the thermistor data the island was observed to be isothermal on 10 June and assumed to be isothermal on 7 June as well. This is to say that the average temperature was 0° C although some lower temperatures might be observed at night at the very surface. Because the whole island is at the freezing temperature, there can be no heat conducted and so the term G in (1) becomes zero.

In addition to modeling the ablation of the unprotected spray ice, the model was modified to simulate the melt behavior of a protected surface. When the ice surface is covered by any material, all the terms in (1) are changed to some degree. The energy transfer occurs between the atmosphere and the protection material providing heat which is conducted through the protection material to the ice below. Equation (1) is then modified for the protection material by eliminating the ice melt term on the right side and including the conduction term.

The heat absorbed by the protection material at $z = 0$ can be represented by the sine series:

$$G(0) = \sum_{n=0}^{P} A_n \sin \omega_n t \tag{7}$$

where A_n are the Fourier coefficients, P is the time period over which the time series is measured, and ω_n are the harmonic frequencies. At some depth, z, the heat flux through that layer can be expressed as:

$$G(z) = \sum_{n=0}^{P} A_n e^{-k_n z} \sin(\omega_n t - k_n z) \tag{8}$$

where

$$k_n = \sqrt{\frac{\omega_n}{2\kappa}} \tag{9}$$

and κ is the diffusivity of the protection material. If z is the depth of the protection material and the heat flux is positive, then the heat flux given by (8) the amount of heat available for melting the ice.

Erosion

There are two terms which describe the erosional forces acting on the perimeter of the island. Forced convection is a result of a current forcing water passed the island melting the submarine portion of the island. The rate at which the melting takes place is a function of both water temperature and velocity. The second term stems from the turbulence created by waves which aid to the melting process but is confined to the wave zone around the perimeter of the island. This process is responsible for undercutting the subaerial part of the island which calves off at the same rate as it is undercut. White et al. (1980) use a Reynolds analogy to compute heat transfer to an iceberg as a function of wave friction:

$$F_w = 0.000219\left(\frac{R}{H}\right)^{0.2}\left(\frac{H}{P}\right)\rho\chi(T_w - 273) \tag{10}$$

where F_w is the heat flux due to wave action, R is the roughness length of the ice, H is the average wave height, P is the average wave period, and T_w is the water surface temperature.

Forced convection, as applied to icebergs by El-Tahan et al. (1984), has been expressed as:

$$F_c = Nu \cdot K_w \cdot {}^{T_w}/_{L} \tag{11}$$

where Nu is the Nusselt number, K_w is the thermal conductivity of water, and L is the maximum water line length. The Nusselt number is usually given as:

$$Nu = 0.055\, Re^{0.8} Pr^{0.4} \tag{12}$$

Re is the Reynold's number, and *Pr* is the Prandtl number.

Because turbulent energy transfer is so much more efficient than laminar energy transfer, the wave erosion term dominates the erosion above water island perimeter. The below water portion of the island perimeter erodes more slowly but, because the ice is buoyant, does not add to the weight on bottom and therefore contributes little to the resistance of the island to lateral forces.

FIELD EXPERIMENT

Air temperature and solar radiation data were collected on the island hourly from 7 June to 5 July, 1989. Wind data were collected at Tuk every 6 hours.

Incoming solar radiation was measured with a LI-COR LI-200SZ pyranometer. This pyranometer is calibrated against a more sophisticated Eppley Precision Spectral Pyranometer to give an accuracy of ±5%.

The solar energy absorbed at the island surface is the net solar radiation which is the difference between the incoming and outgoing radiation. In order to calculate the outgoing radiation, the albedo of spray ice must be know. In this case we take the albedo to be that of wet, clean snow which is approximately 0.8. The net radiation is then the incoming radiation multiplied by 0.2. This is plotted in Figure 1.

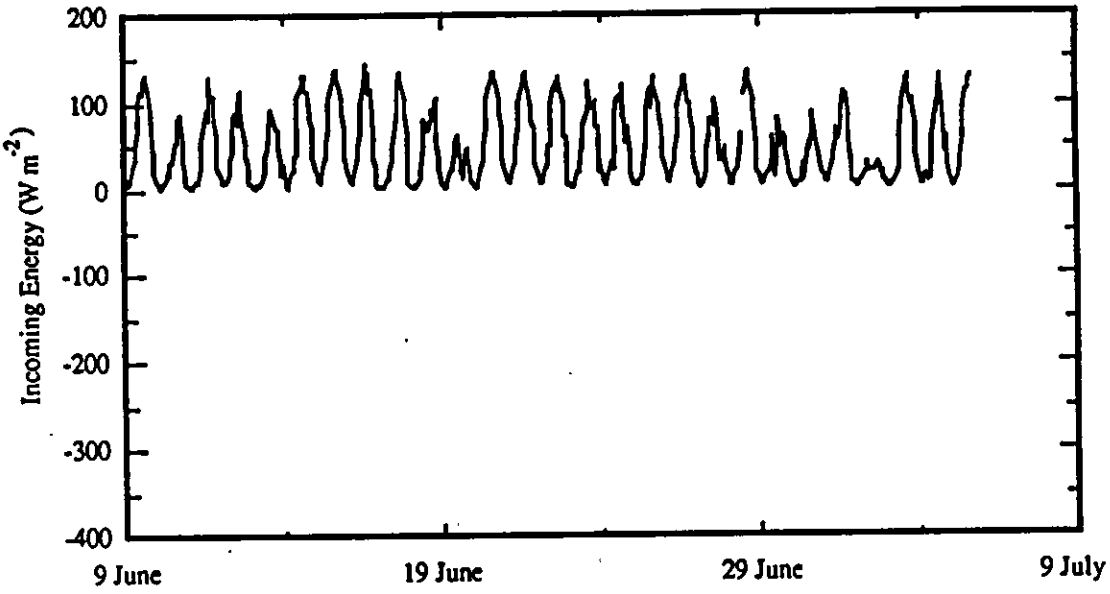

Figure 1. Net solar radiation during the field experiment.

When ablation protection materials such as gravel or sawdust are used this invariably lowers the albedo resulting in greater solar radiation absorption. This could actually result in higher ablation rates if the albedo is raised without a corresponding rise in insulation.

Air temperature data were gathered from thermistors positioned slightly above a gravel pad and the internal temperature of a datalogger. None of the air temperatures gathered were true near-surface (10m) temperature, however, the relationship between the thermistors is assumed to give an indication of what the temperature gradient above the island may be. In Figure 2, two temperature time series are plotted. One is the 30cm temperature and one is the datalogger temperature.

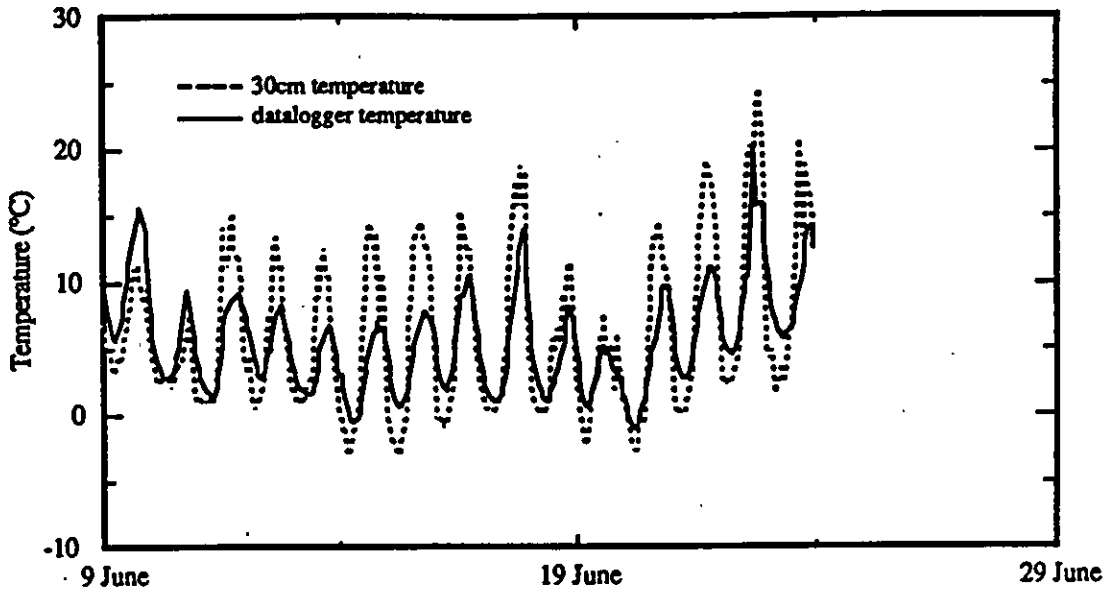

Figure 2. Comparison of two temperature time series gathered on Nipterk.

The two time series track fairly well, although there is more damping on the datalogger time series because it was located inside a tent and was insulated by its own hardware. The 30cm probe was actually located above a small gravel plot which will give a higher reading than if the temperature were taken over the ice. The temperature amplitude fluctuations are higher at the surface since surface temperatures are more susceptible to solar radiation. The air is heated by the surface and, to a much lesser extent, direct solar radiation. In this way air temperatures farther away from the surface have smaller amplitude fluctuations and their fluctuations lag behind the surface fluctuations. This is what is observed in the datalogger temperature time series. Although the datalogger temperature might not duplicate the 10m air temperature, T_a in (2), it is taken to be an adequate approximation.

For the surface temperature calculation, the temperature of the melting ice, 0°C, was taken. This will be used as the temperature, T_s, given in (3). When (2) and (3) are calculated in this way, and (3) is subtracted from (2) the result is the net long wave radiation and is shown in Figure 3.

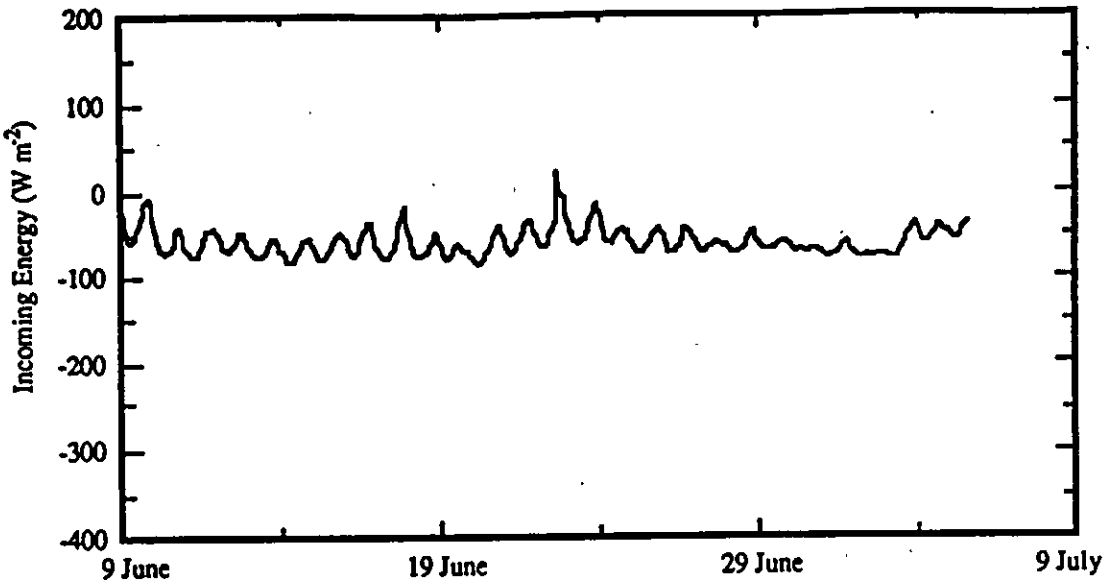

Figure 3. Net long wave radiation.

Of course, when the surface of the island is covered with ablation protection material, the surface temperature is not limited to 0°C and will be more likely to be closer to those temperatures collected by the thermistor mounted at 30 cm. For the ablation protection model, this temperature will be used. Because the surface is allowed to rise to a higher temperature, the outgoing long wave radiation will be higher as well.

The temperature gradient used to calculate both the sensible and latent heat fluxes given in (4) and (5) is given by subtracting the surface temperature from the datalogger temperature. For the sensible heat flux over the ice this yields an almost constantly outgoing heat flux. In the Beaufort Sea near land, this situation will occur since warmer air will be moving off the land onto the ice creating an almost constant inversion.

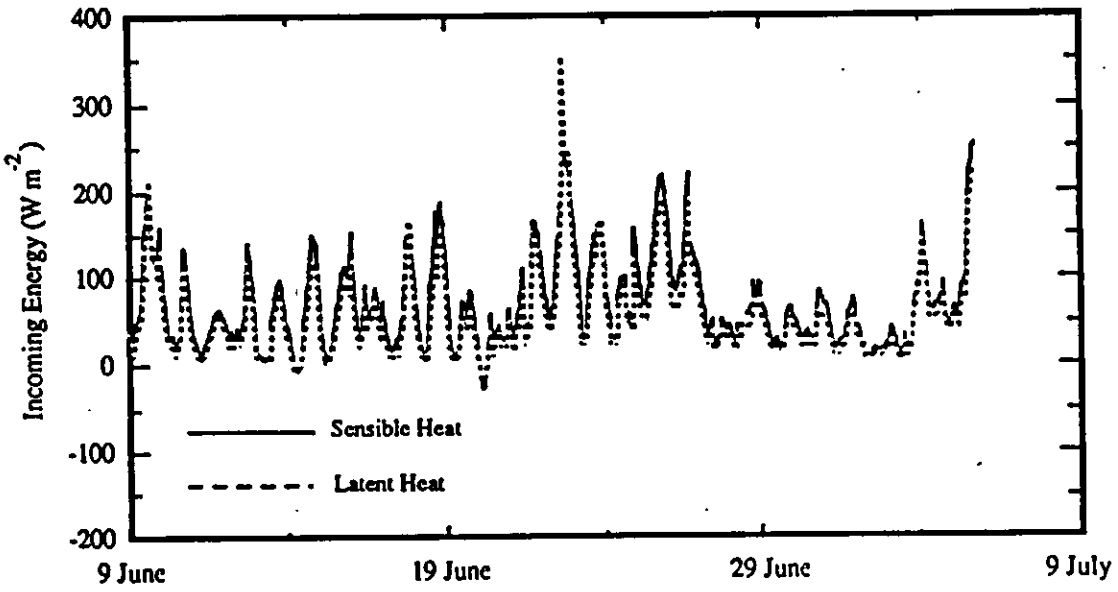

Figure 4. Sensible and latent heat flux off the spray ice.

Figure 4 shows both sensible and latent heat fluxes plotted together. Note that since latent heat flux was calculated from the air temperature using (6), the two fluxes follow each other closely.

When an ablation material is used, quite a different situation occurs. Since the ablation material can rise to higher temperatures than the ice can, the temperature of the surface can become much warmer than the air resulting in a reversal of the heat flux. Despite the higher surface temperatures of the protection material, it can dissipate more heat thus preventing heat from flowing to the ice.

Because of the lack of oceanographic data, some assumptions were made in order to calculate the erosion of the island perimeter. The average wave height was assumed to be 0.5m and the period to be 4 sec. Since the wave heights are constantly changing, making an assumption like this may lead to major errors. For this reason the wave height and period were varied in the model to determine the sensitivity to this term. The first day of open water, when the island perimeter began eroding, was set to 23 June.

Surface water temperature was measured once during the field experiment. The temperature taken was 12°C. This was shortly before the island broke up and the region in which the island was located was under the influence of the MacKensie River outflow. Because this temperature is relatively high for the Beaufort Sea it was not considered to be a constant temperature. Therefore the temperature was assumed to increase linearly from 0°C on 23 June to 12°C on 8 July.

RESULTS

Ablation

In order to use the most consistent set of data, the model was run with data from 7 June to 5 July only. Although some ablation occurred before this date, it would be very difficult to measure the ablation processes with the same kind of accuracy as could be achieved from 7 June onwards. Our reference level then became the level of the ice on 10 June, the first level measurement since radiation and temperature data gathering began at the island.

Because the differences between the sensible and latent heat flux coefficients are within measurement error, they were taken to be equal for this study. A number of different coefficients were tried in the model to determine the model sensitivity. Figure 5 shows some of these results compared with the data measured on the island. From this figure it appears that 0.0012 provides the best fit to the measured data. This compares favorably with a survey Macklin (1983) has done on drag coefficients of sea ice. For smooth, flat ice the drag coefficients ranged from 0.001 to 0.0024. In a paper investigating the relationship between the drag coefficient and the heat transfer coefficient over open ocean, Kondo (1975) estimates $C_s = 0.9C_d$ where C_d is the drag coefficient.

The flat parts in the ablation curves correspond to the night time periods when net heat flux is away from the island. Since there is no heat entering the island surface, no ice is melted. Instead, some of the liquid water present in the surface can then be refrozen which requires subsequent energy absorption to melt again. This accounts for the hard crust on the island surface in the mornings.

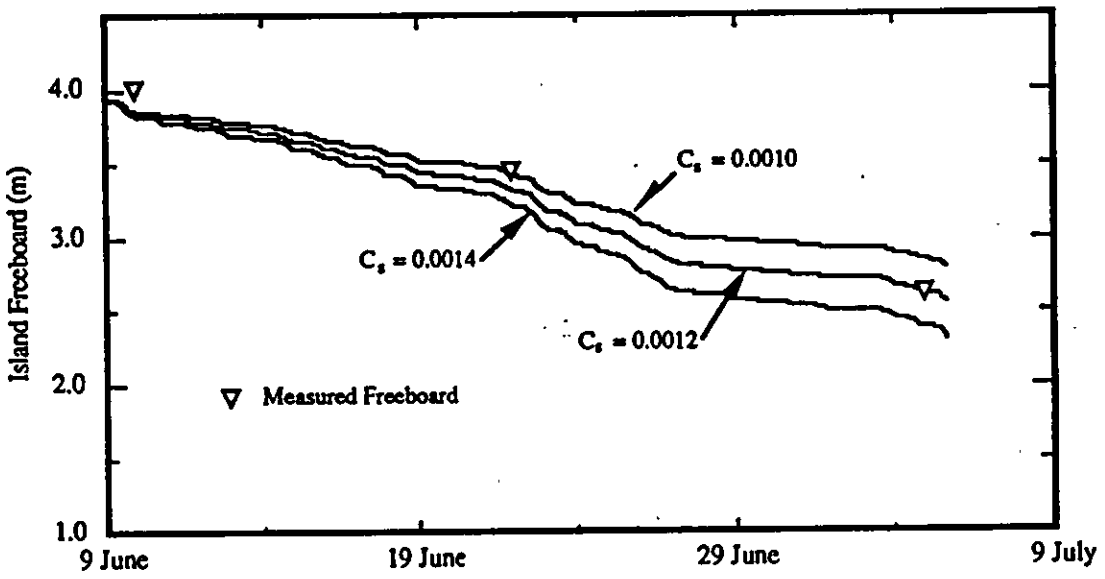

Figure 5. Ablation of the top surface of the ice island compared with measured data.

The model was changed in order to simulate the presence of various ablation protection materials. The materials modeled were gravel pads and sawdust layers of various thickness. A protective material spread over the ice serves to insulate the ice from solar and long wave radiation, and sensible and latent heat flux. The approach taken here was to calculate the energy transfer between the material and the atmosphere and then to calculate the heat conducted through the material to the ice. The resultant heat transferred through the protection material was used to melt the ice.

The results from the sawdust model are shown in Figure 6. Although the results compare favorably, some discrepancies arise due to the fact that the sawdust was modeled as a material of homogeneous thermal conductivity. This may not be the case due to an inhomogeneous distribution of ice or water in the gravel, which would lead to changes in the thermal conductivity of the material. These thermal conductivity inhomogeneities could also change with time since water is added with rainfall, percolates out the bottom, refreezes or thaws.

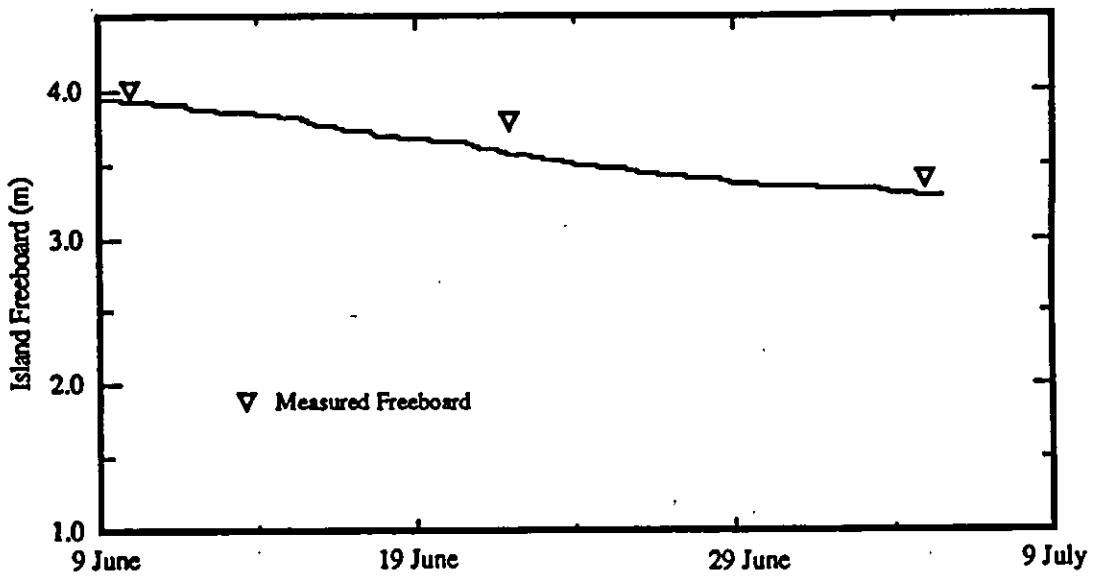

Figure 6. Comparison between measured and modeled ice meltback under 1 cm of sawdust.

The albedo of the sawdust was taken to be 0.35. This figure will change depending on whether the sawdust is wet or dry. However, this was seen to represent and average albedo. The diffusivity which fit the data best was found to be 1.4×10^{-7} m^2 sec^{-1}.

In contrast to the model over estimating the ice meltback in sawdust, the model under estimated the ice meltback under gravel as shown in Figure 7. One possible explanation for this is localized subsidence caused by the weight of the gravel. The albedo used for the gravel was taken as 0.4 again an average between wet and dry . The diffusivity was 2.8×10^{-7} m^2 sec^{-1}.

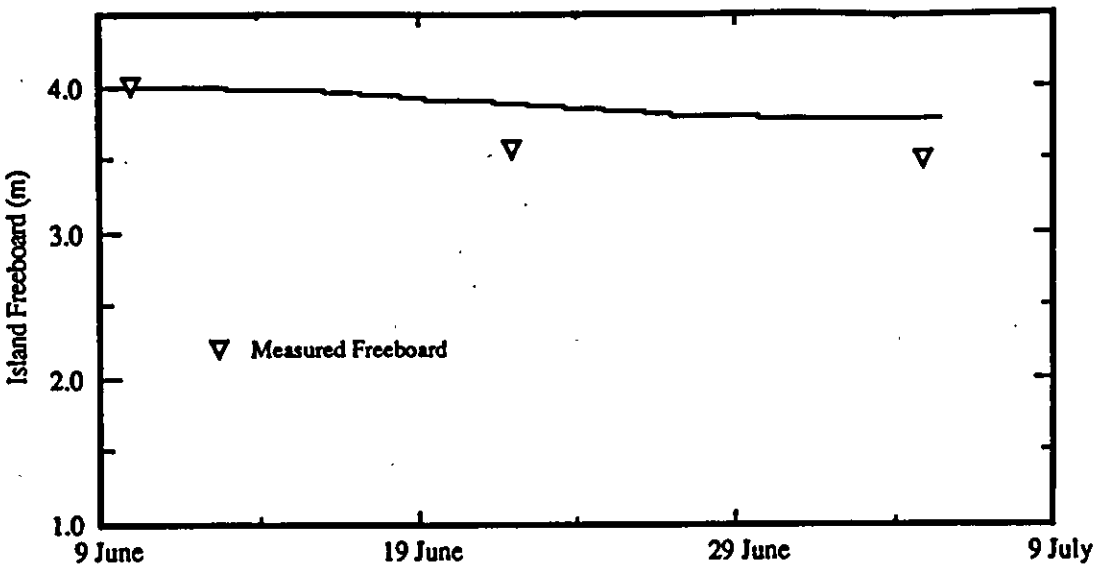

Figure 7. Comparison between measured and modeled ice meltback under 30 cm of gravel.

The wave erosion has been distributed evenly around the perimeter of the island so that the island retains the shape of disc. In reality the erosional forces are directional and the island quickly becomes asymmetrical depending on the predominant directions of the forces. However, one of the most important factors in island survivability is sliding friction between the ice and the seabed. Since the sliding friction is a function of area of contact, the shape of the island is not as critical of a term.

Wave height, period, and water temperature are important factors in the erosion model. Since data were sparse concerning these terms, a variety of different wave heights and periods were input into the model to determine the sensitivity of the model. The results are shown in Figure 3. Waves of 0.25m, 0.5m, and 1.0m were input along with periods of 3 and 4 seconds. The model was run from the first day of open water, 23 June, until 5 July.

As can be expected, the higher wave heights and shorter periods cause the greatest amount of erosion. The closest fit to the data is achieved with an average wave height of 0.5m and a period of 4 seconds.

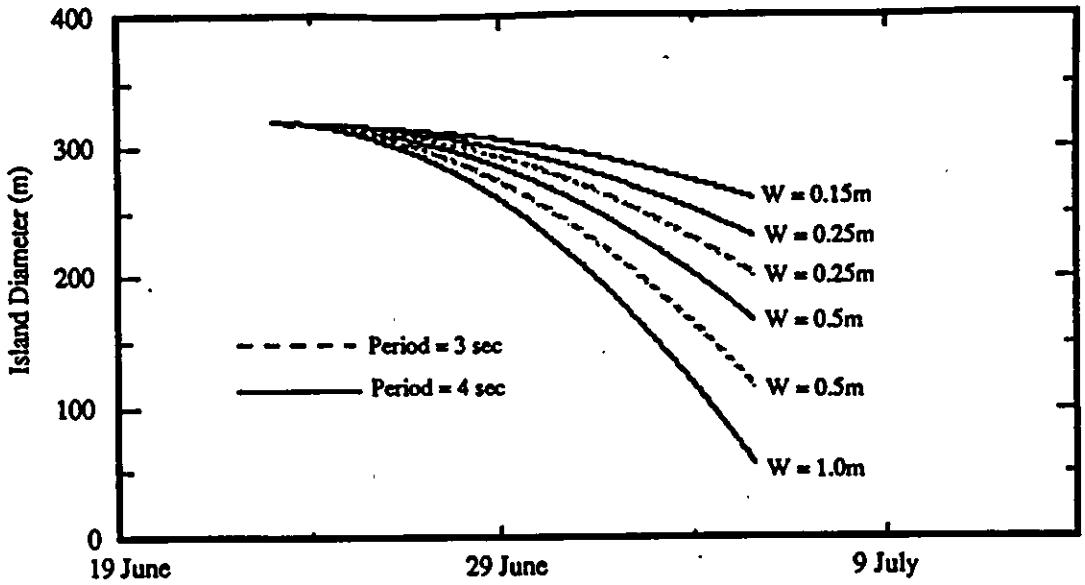

Figure 8. Results of the use of different wave parameters in the perimeter erosion model.

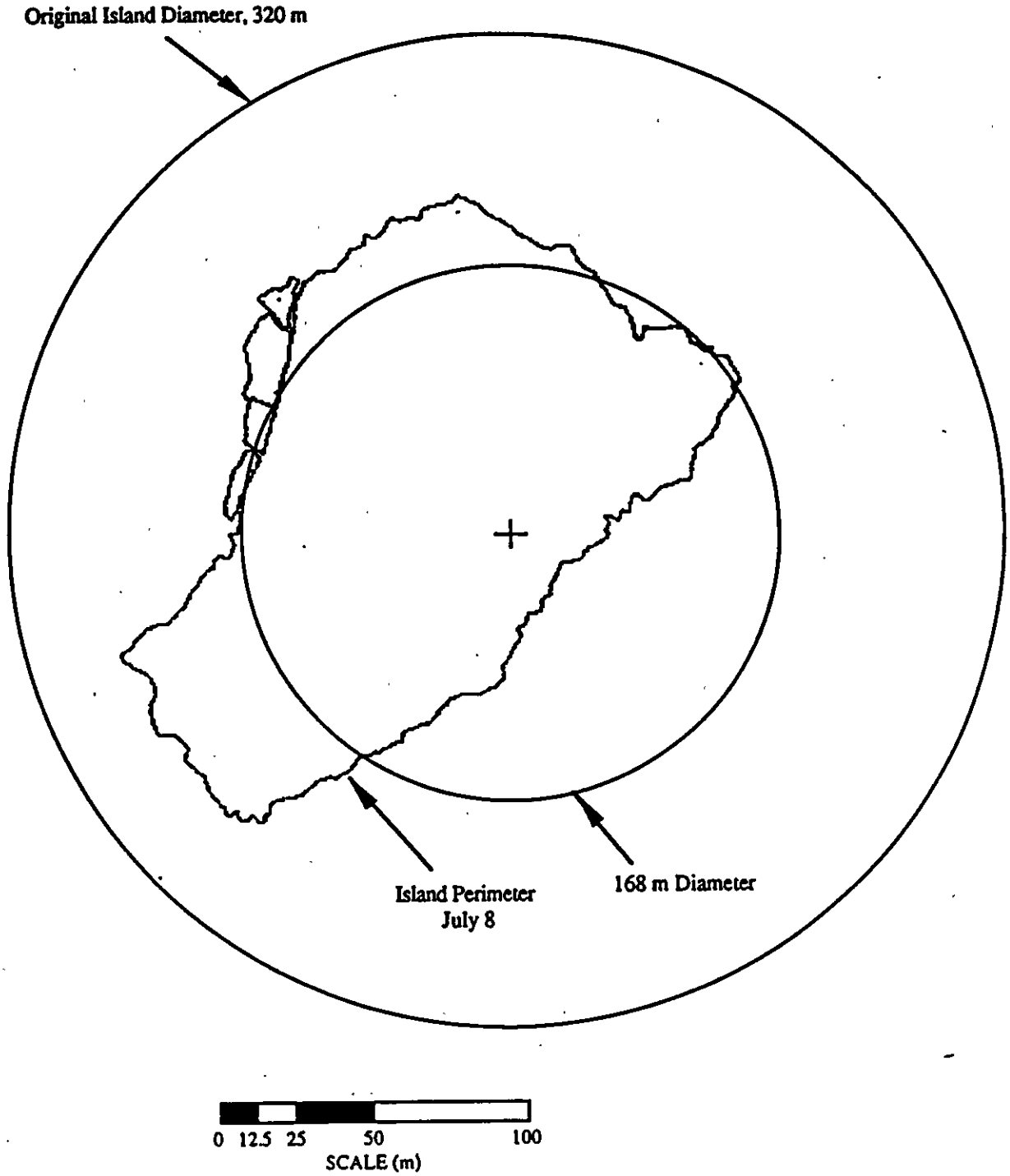

Figure 9. Aerial view of island showing measured perimeter and model results of 8 July.

CONCLUSION

Several changes were made to the original spray ice island model in adapting it for use in this study. Because data were gathered on the island itself, and suplimented with data gathered in the same region, much greater accuracy could be obtained than before. The time scales were reduced from one day to one hour so that greater detail could be observed. Instead of a broad estimate of the sensible and latent heat fluxes, they could be better approximated with air temperature and wind speed. As a result, the output of the model matched the measured data and retained physically meaningful parameters. By retaining a physical basis for the model, the probability for predicting the behavior of hypothetical ice islands improves.

In addition to modeling the deterioration of an unprotected ice island, one major aspect of the study was to observe the effects of various ablation and erosion protection methods. The ablation protection materials change the boundary conditions between the ice and the atmosphere. The albedo decreases, outgoing long wave radiation increases, sensible heat flux both to and from the surface increases, latent heat flux decreases, and the heat capacity of the surface increases. Naturally, these properties vary from material to material, and with the thickness of the material itself. Because of the environmental forces on the ice, the problem of simulating the effects of ablation protection is more than one of simple insulation.

In addition to the materials tested, other materials such as drilling mud, sea floor sediment, or mylar sheets may be investigated to determine if they may offer improved performance or more economical solutions. As we observed on the island, the plastic sheets offers the best ablation protection per unit thickness but may not be either practical nor economical in covering an entire island. Sawdust outperformed gravel for the same thickness and does not increase the subsidence. All these materials have relatively high albedos which could be improved by using lighter varieties or spraying with a light colored coating.

The effects of the perimeter erosion protection was pronounced. It could not be determined which material offered the best protection, but obviously any material was better than nothing. Since wave action was seen to be the dominating term in the perimeter erosion, the reduction of the wave energy would be the best way to mitigate the effects of the erosion. This was the outcome of using the erosion protection, the net effect being a 40% reduction in average wave height.

We have observed the results of applying various protection materials to the island and have investigated the reasons for these results so that possibility of predicting the behavior of an ice island at a particular location can be reasonably performed. The feasibility of building ice islands in deeper water depths or extending their operating season depends on construction techniques, island design, and environmental conditions. What still determines the longeviety of a spray ice island is the weight on bottom and lateral forces. Even if the island could be well preserved through the summer season, if an insufficient amount of ice was used for construction a storm in late summer could result in island break up.

REFERENCES

Macklin, S.A., Wind drag coefficient over first-year sea ice in the Bering Sea, *J.Geophys. Res.*, 88(C5), 2845-2852,1983.

Connolly, S.T., Artificial ice islands for deep water and production structures, *In Proc. Fourth Intl. Conf. Cold Regions Eng.*, Anchorage, ASCE, 58-68, 1986.

Kondo, J., Air-sea bulk transfer coefficients in diabatic conditions, *Boundary-Layer Meteorol.*, 9, 91-112, 1975.

Jahns, H.O., D.H. Petrie, and A.V. Lockett, CIDS Spray Ice Barrier, *In Proc.of 18th Ann. Offshore Tech. Conf.*, Houston, 575-584, 1986.

White, F.M., M.L. Spalding, and L. Gominho, Theoretical estimates of the various mechanisms involved in iceberg deterioration in the open ocean environment, U.S. Coast Guard Report No. CG-D-62-80, 1980.

Idso, S.B., and R.D. Jackson, Thermal radiation from the atmosphere, *J. Geophys. Res.*, 74, 1969.

Buck, A.L., New equations for computing vapor pressure and enhancement factor, *J. Appl. Meteorol.*, 20, 1527-1532, 1981.

Large, W.G. and S. Pond, Sensible and latent heat flux measurements over the ocean, *J. Phys. Oceano.*, 12, 464-482, 1982.

El-Tahan, M., S. Venkatech, and H. El-Tahan, Validation and quantitative assessment of the deterioration mechanisms of arctic icebergs, *In Proc. ASME Offshore Mech./Arctic Engin. Symp.* New Orleans, ASME, 1984.

APPENDIX F

SETTLEMENT MEASUREMENTS

Measurements of surface settlement were performed at as many as five locations during the experiment. Sensing rings were originally mounted to the outside of the Sondex casing at approximately 0.5 m intervals. Settlement surveys were conducted at varying frequencies and locations during the experiment. Settlement data are available throughout the experiment period for locations near the edge of the island working surface.

In addition to the raw settlement data, settlement profiles are also provided. The seabed is at a depth of about 10.5 to 11 m whereas the submerged spray ice is represented by the level 4.5 m below the surface to the seabed. Due to spray ice ablation, the uppermost 2 m of Sondex casing was removed on June 22 due to the height of stick up. Consequently, settlement data for the upper 3-4 m of the island were not collected after the June 22 survey.

An extrapolation of settlement data was performed for June 1 for each of the three drilling pad settlement monitoring stations. The extrapolation may be a bit conservative in that it does not take into account the below freezing air temperatures prevalent throughout most of May.

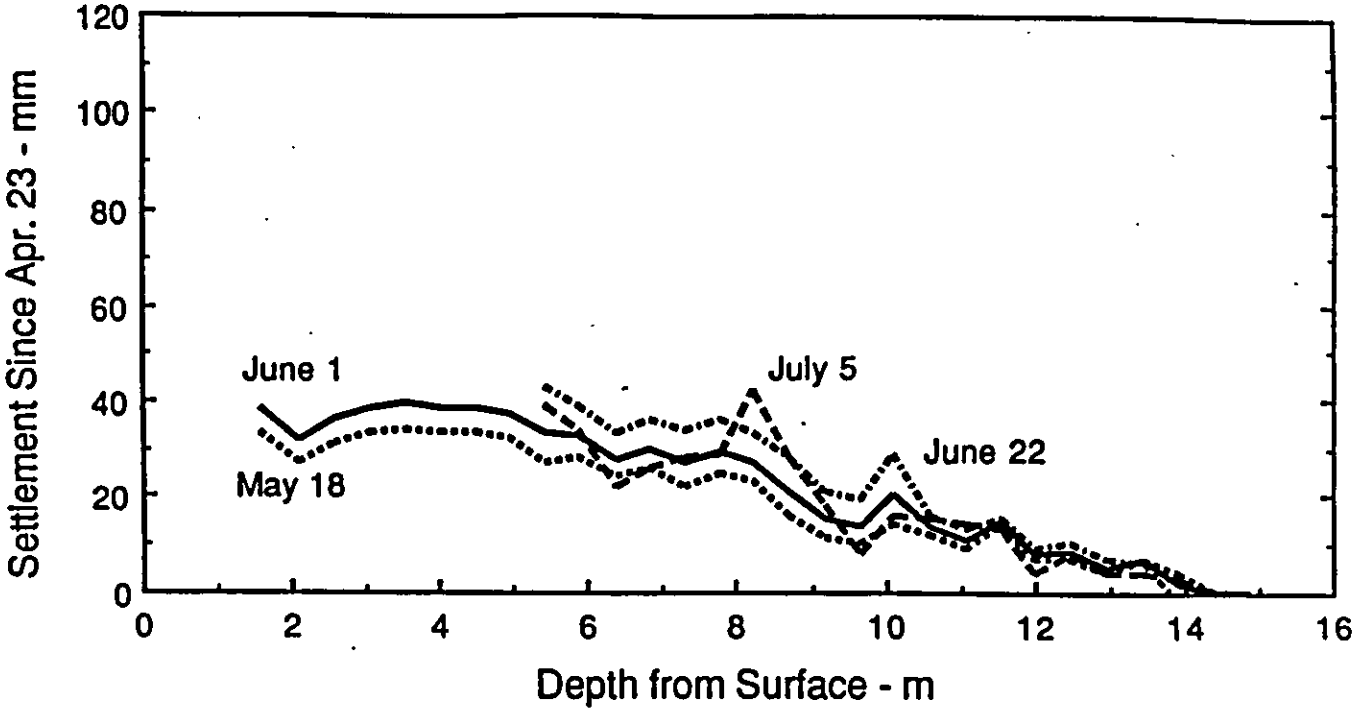

Spray Ice Settlement at North Survey Station

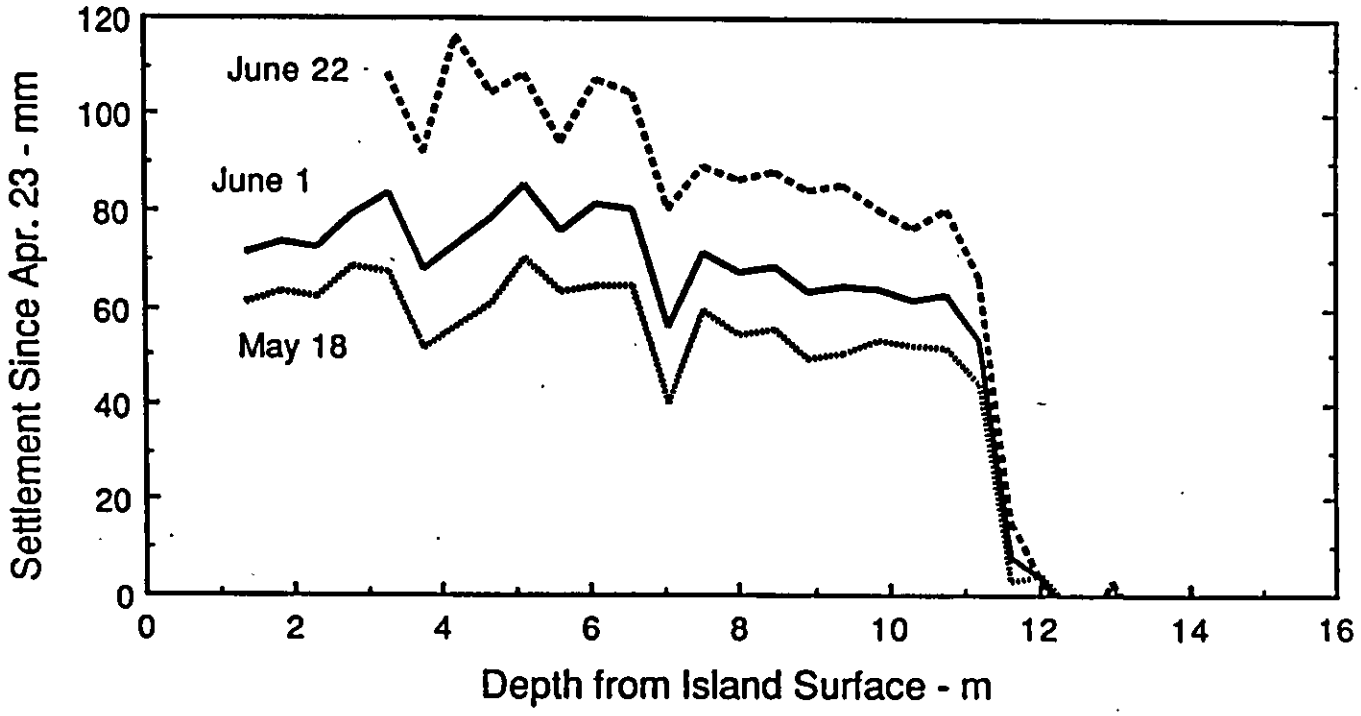

Spray Ice Settlement at North Northeast Survey Station

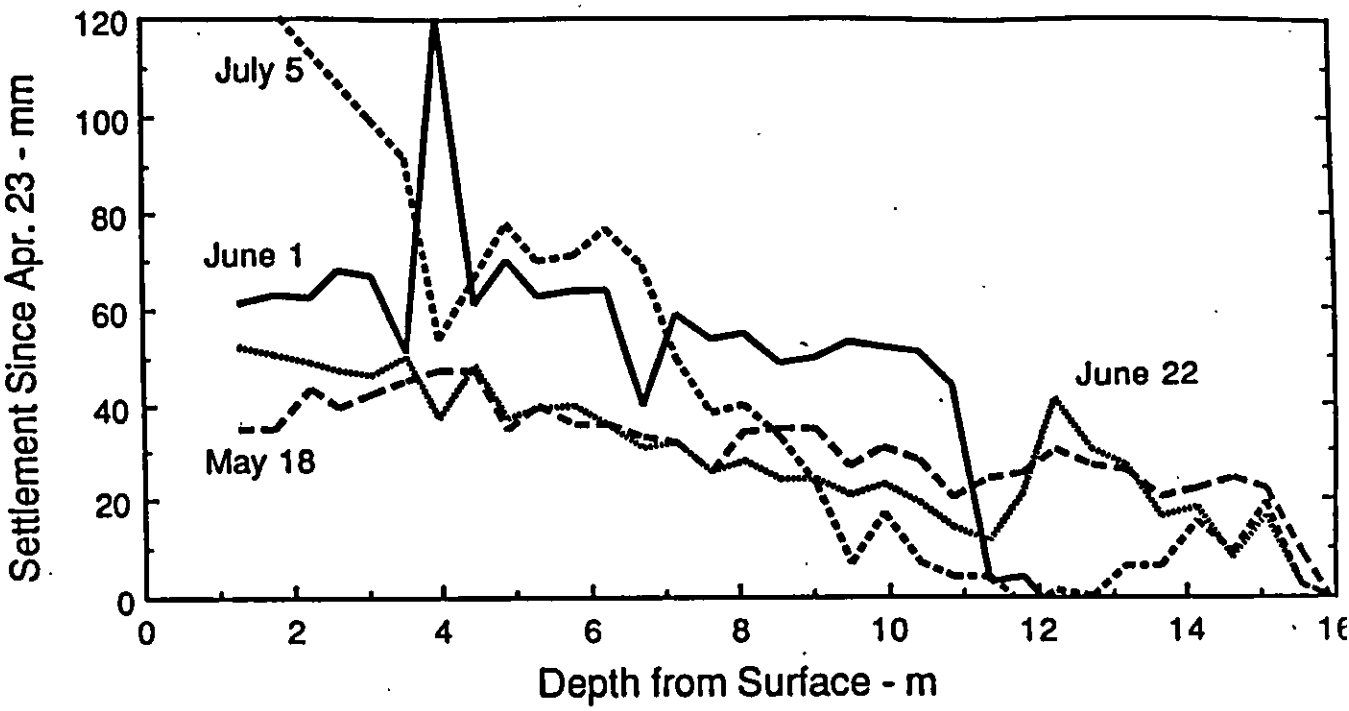

Spray Ice Settlement at Southeast Survey Station

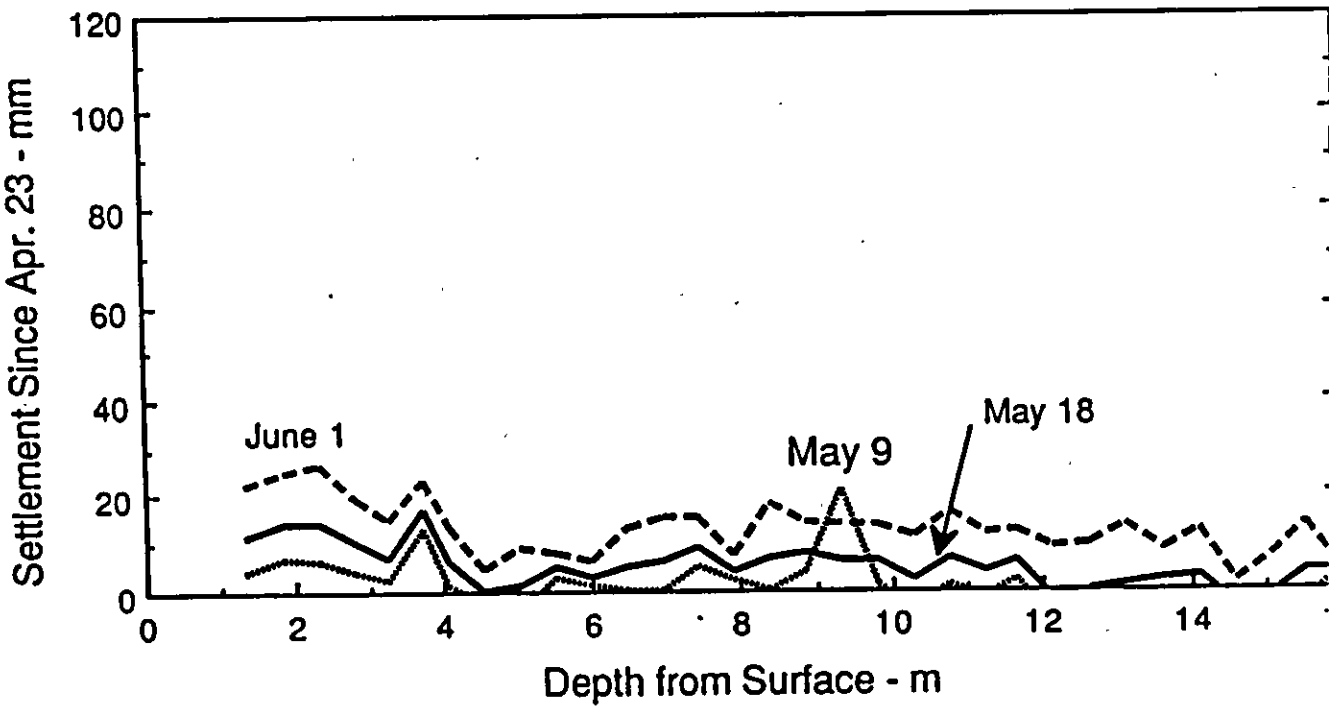

Spray Ice Settlement at South Southwest Survey Station

		Settlement Data from Sondex Survey Stations						
	North Station				Southwest Station			
Depth on April 23 (m)	18-May (mm)	22-Jun (mm)	5-Jul (mm)	Depth on April 23 (m)	9-May (mm)	18-May (mm)	22-Jun (mm)	5-Jul (mm)
1.604	33			1.418	15	26		
2.110	27			2.164	18	24		
2.586	31			2.650	14	20		
3.069	33			3.126	14	20	44	
3.550	34			3.585	13	22	36	
4.022	33			4.054	13	22	50	58
4.506	33			4.511	11	20	31	38
4.965	32			4.960	15	22	39	54
5.419	27	43	39	5.423	12	20	24	36
5.893	28	39	34	5.925	10	13	33	34
6.378	24	33	22	6.415	10	15	29	36
6.845	26	36	26	6.898	8	16	25	23
7.324	22	34	28	7.709	8	14	30	29
7.788	25	36	29	8.314	6	12	26	29
8.251	23	33	42	8.630	9	14	25	27
8.725	16	28	28	9.112	6	12	19	17
9.194	11	21	18	9.579	9	9	21	17
9.667	10	19	8	10.040	-1	6	20	32
10.126	14	29	16	10.705	5	4	10	7
10.610	12	16	15	11.180	-2	0	3	-2
11.087	9	13	14	11.664		5	-3	0
11.554	14	15	13	12.138		3		
12.020	7	9	4	12.643		-2		
12.486	7	10	8	13.140				
12.973	4	7	4	13.650				
13.461	7	6	4	14.161				
13.944	4	-2	3	14.590				
14.415	0	0	0	14.925				
14.901	0	0	0					

	Settlement Data from Sondex Survey Stations					
	Southeast Station				North Northeast Station	
Depth on April 23 (m)	18-May (mm)	22-Jun (mm)	5-Jul (mm)	Depth on April 23 (m)	18-May (mm)	22-Jun (mm)
1.296	35			1.361	61	
1.783	35			1.845	63	
2.267	43			2.328	62	
2.632	39			2.803	68	
3.090	42	46		3.295	67	108
3.554	45	50		3.752	51	92
4.016	47	37	80	4.208		116
4.472	47	48	92	4.679	61	104
4.909	35	37	104	5.142	70	108
5.337	40	39	96	5.629	63	94
5.802	36	40	97	6.105	64	107
6.263	36	36	103	6.563	64	104
6.733	33	31	95	7.066	40	80
7.193	32	32	76	7.551	59	89
7.666	26	26	64	8.020	54	86
8.124	34	28	66	8.489	55	88
8.592	35	24	59	8.958	49	84
9.058	35	24	49	9.423	50	85
9.517	27	21	33	9.886	53	80
9.973	31	23	43	10.337	52	76
10.447	28	19	33	10.798	51	80
10.903	20	14	30	11.223	44	66
11.362	24	11	4	11.627	3	15
11.819	25	21	-2	12.060	4	3
12.271	30	41	1	12.521	-4	-11
12.727	27	30	0	12.983	-2	3
13.190	26	27	6	13.444	0	-8
13.673	20	16	6	13.914	-9	-11
14.142	22	18	15	14.388	0	0
14.615	24	8	9			
15.080	22	16	19			

Settlement Data from Sondex Survey Stations				
	South Southwest Station			
	Depth on			
	April 23	9-May	18-May	
	(m)	(mm)	(mm)	
	1.346	4	11	
	1.834	7	14	
	2.312	6	14	
	2.792	4	10	
	3.252	2	7	
	3.729	13	17	
	4.070	1	6	
	4.551	-3	0	
	5.021	-4	1	
	5.494	3	5	
	5.981	1	3	
	6.459	0	5	
	6.941	0	6	
	7.428	5	9	
	7.905	2	4	
	8.378	0	7	
	8.855	4	8	
	9.337	21	6	
	9.817	1	6	
	10.293	-4	2	
	10.773		7	
	11.262		4	
	11.660		6	
	12.153		-2	
	12.637		0	
	13.128			
	13.619			
	14.107			
	14.595			
	15.077			
	15.560			

APPENDIX G

ISLAND HORIZONTAL MOVEMENT MEASUREMENTS

Five manually read inclinometers (slope indicators) were installed in January as part of the winter island stability monitoring program. Three of the five were at the periphery of the drilling pad wheres the other two were near the edge of the island. Inclinometer casings were installed inside Sondex casings which in turn were anchored at different depths below the seabed. These stations were left intact at the conclusion of the drilling program so that measurements could be continued.

Inclinometer data were collected using the SINCO Recorder Printer Processor (RPP) System. The RPP collected, stored, processed and displayed the digitilt data in terms of deflection versus depth profiles.

Slope indicator surveys were undertaken during each complete site survey except at the south-southwest survey station where the casing deformed to the point that surveys could not be performed after May 18. An initial (reference) slope indicator survey was carried out on April 22 and data from subsequent surveys were compared relatively.

Slope indicator readings were taken at 0.5 m intervals. The readings were taken each time in four geographic directions and are shown as positive values in the north and east directions and negative values in the south and west directions. The island deformations computed from the inclinometer readings are plotted in the Figures.

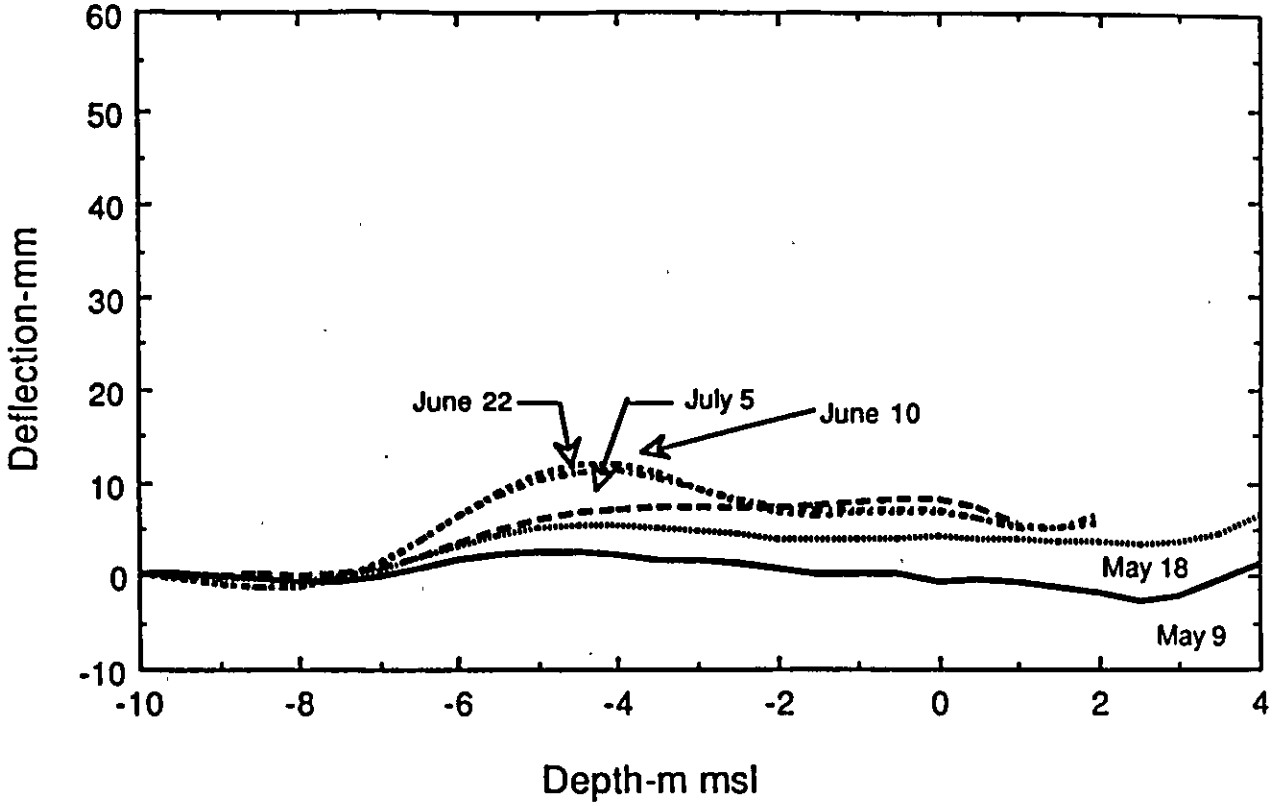

North Slope Indicator Station Deformation Profiles
(North-South Direction)

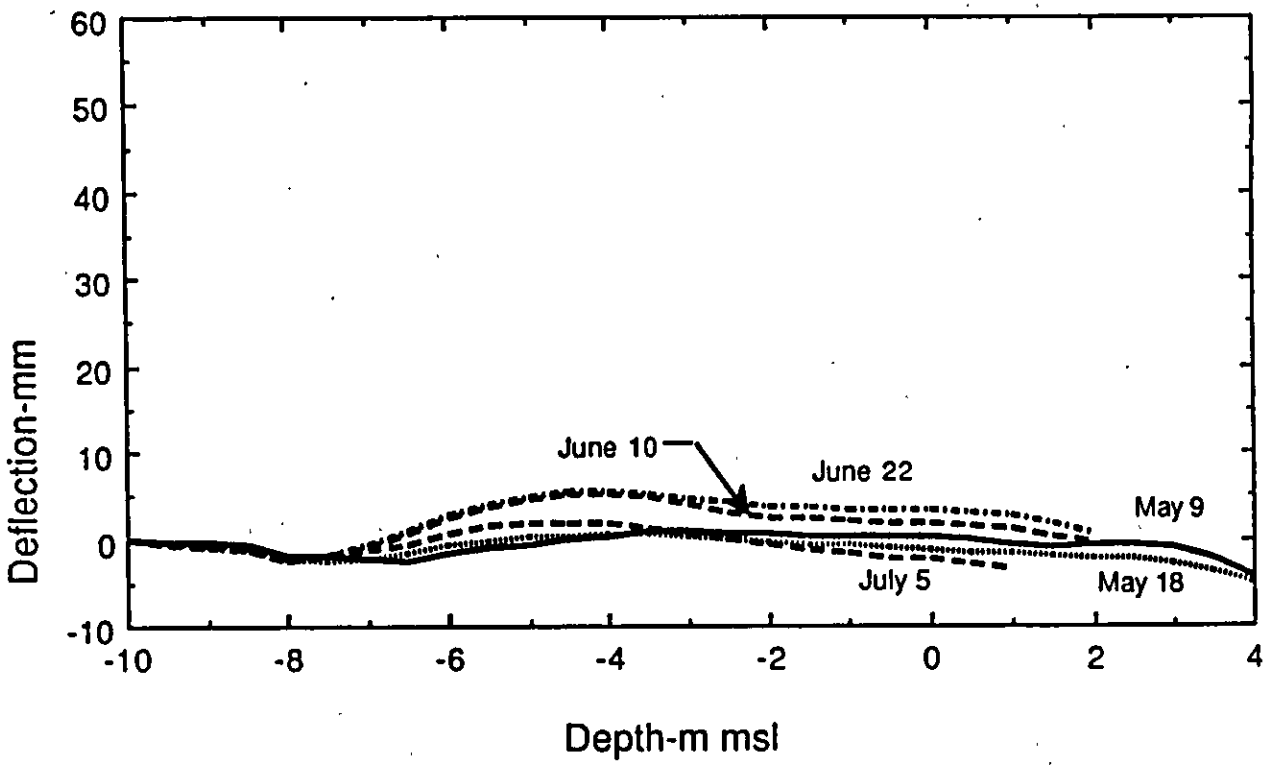

North Slope Indicator Station Deformation Profiles
(East-West Direction)

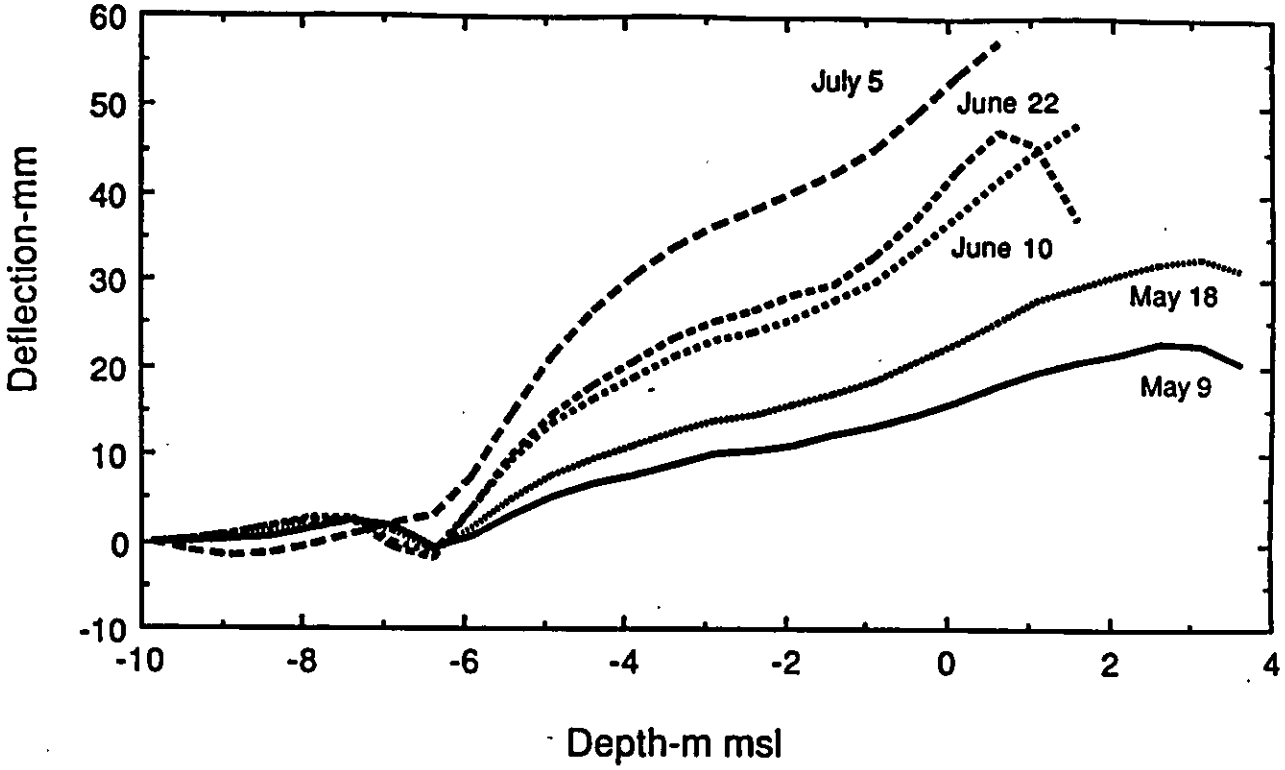

North-Northeast Slope Indicator Station Deformation Profiles
(North-South Direction)

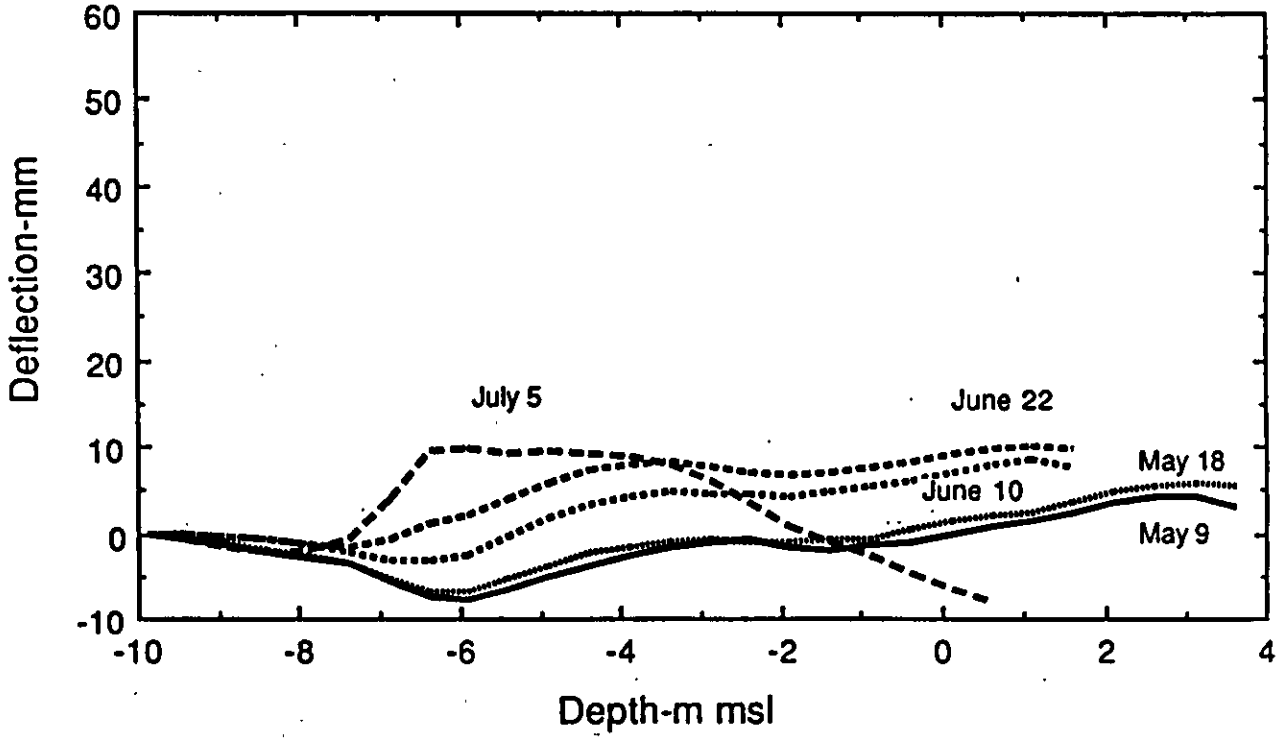

North-Northeast Slope Indicator Station Deformation Profiles
(East-West Direction)

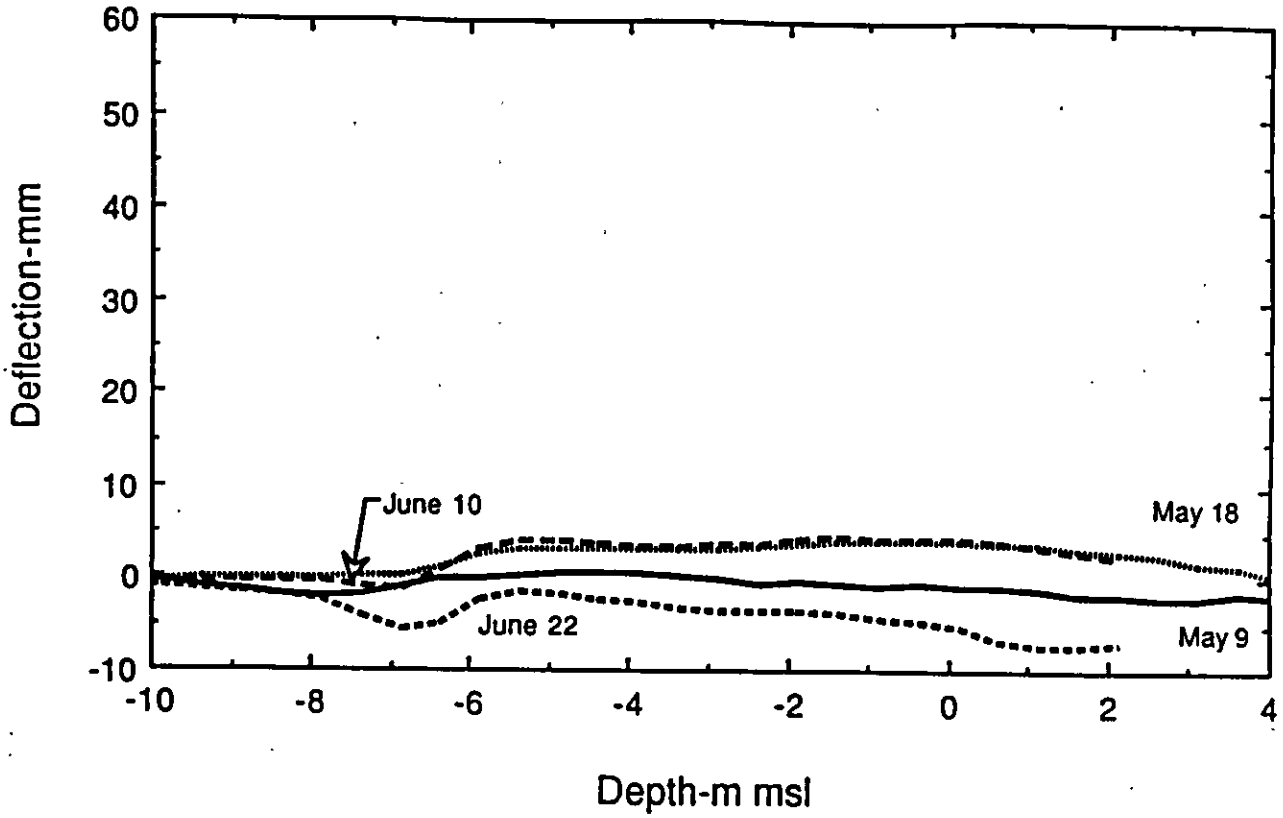

Southeast Slope Indicator Station Deformation Profiles
(North-South Direction)

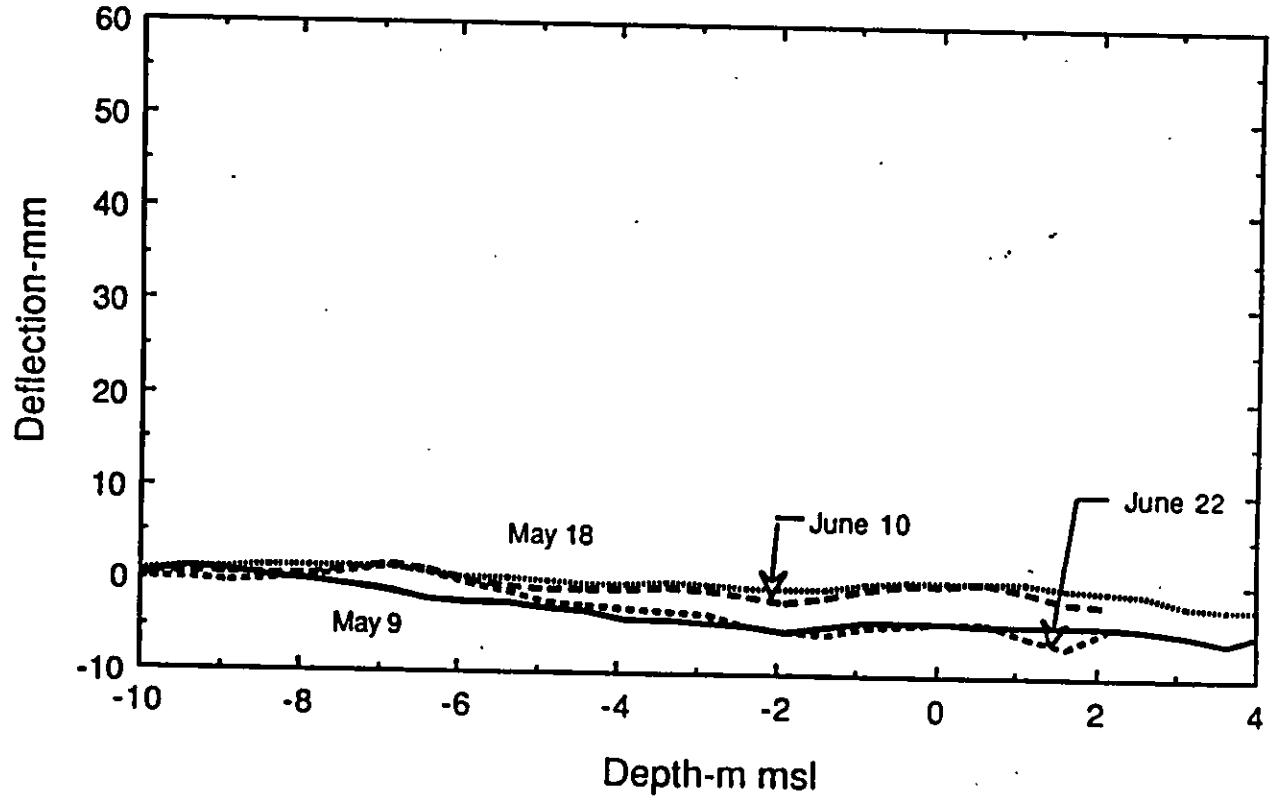

Southeast Slope Indicator Station Deformation Profiles
(East-West Direction)

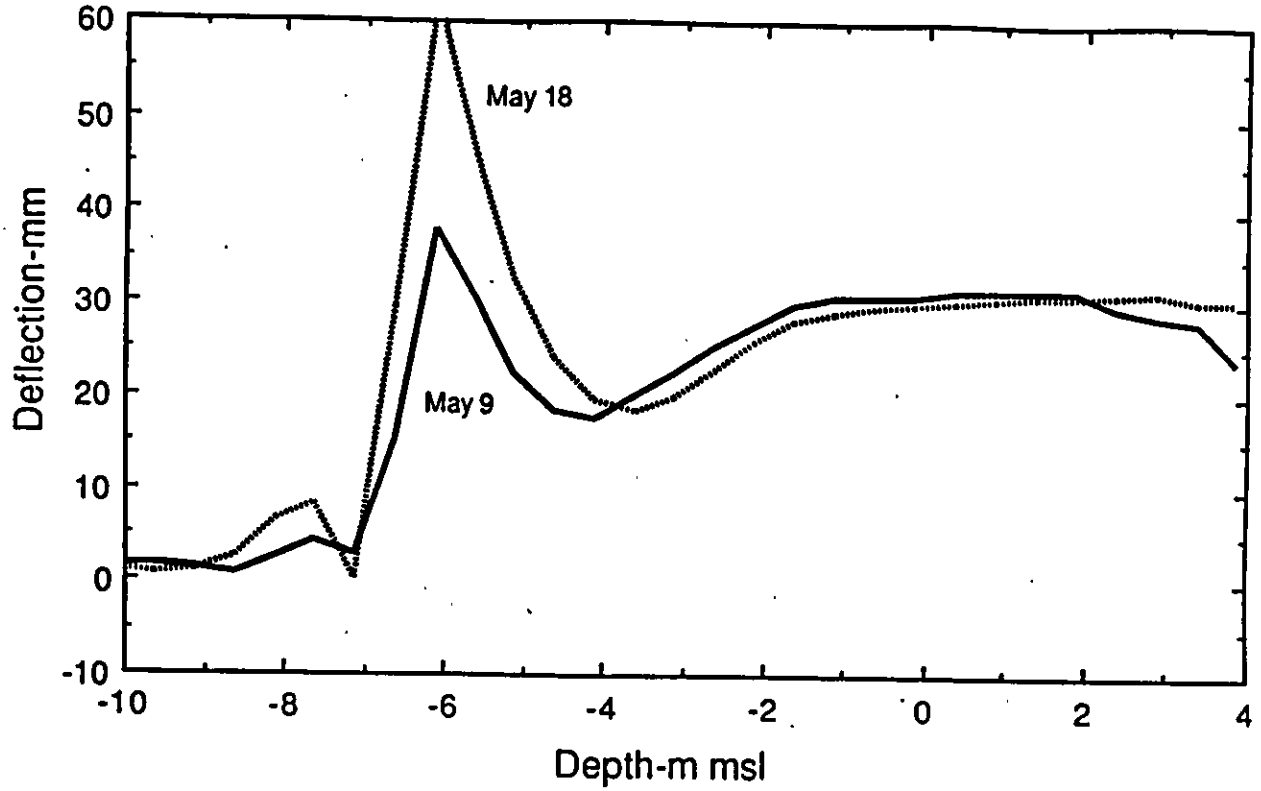

South-Southwest Slope Indicator Station Deformation Profiles
(North-South Direction)

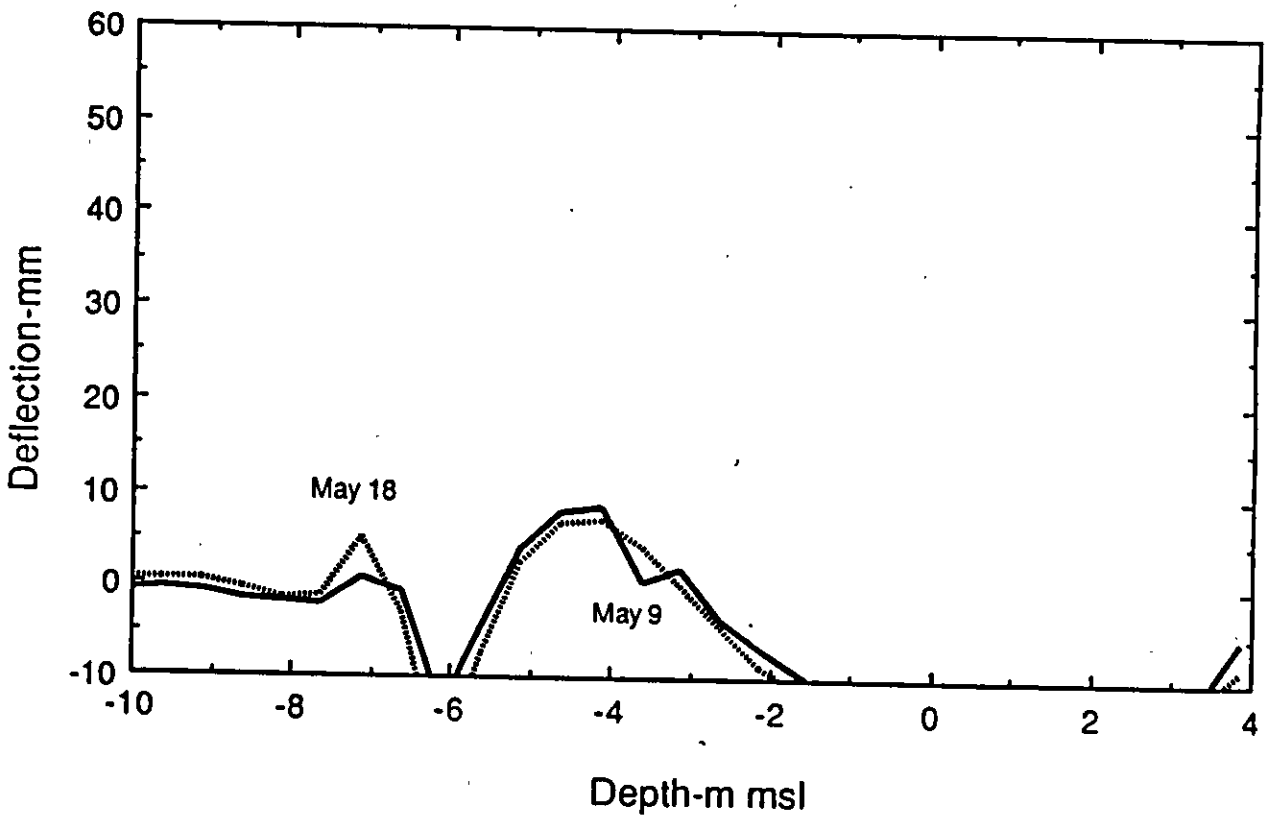

South-Southwest Slope Indicator Station Deformation Profiles
(East-West Direction)

North Slope Indicator Readings

N SI3					N SI3					N SI3				
April 22.					May 18.					June 10.				
	Deformation					Deformation					Deformation			
Depth	North	East	South	West	Depth	North	East	South	West	Depth	North	East	South	West
0.5	-388	300	329	-375	0.5	-266	274	224	-329	0.5	419	115	-93	-311
1	-278	267	240	-345	1	-224	248	176	-308	1	119	97	-96	-272
1.5	-162	227	125	-308	1.5	-139	214	111	-280	1.5	61	184	-100	-270
2	-35	208	-9	-270	2	-46	199	0	-257	2	13	194	-62	-268
2.5	-233	-201	193	97	2.5	-237	-221	202	111	2.5	-207	-226	156	123
3	-304	-252	254	176	3	-299	-267	261	190	3	-297	-281	259	214
3.5	-332	-310	290	241	3.5	-337	-316	296	246	3.5	-369	-337	327	272
4	-282	-356	243	276	4	-279	-365	245	298	4	-304	-365	266	304
4.5	-242	-398	201	319	4.5	-234	-398	200	330	4.5	-246	-394	204	333
5	-233	-390	195	314	5	-226	-405	189	342	5	-226	-398	184	338
5.5	-321	-335	284	257	5.5	-315	-342	281	260	5.5	-313	-348	272	270
6	-260	-316	218	238	6	-262	-329	225	254	6	-276	-320	233	257
6.5	-197	-301	153	231	6.5	-205	-319	166	247	6.5	-235	-333	193	275
7	-125	-286	80	211	7	-132	-297	100	237	7	-194	-342	149	273
7.5	-43	-248	2	174	7.5	-55	-248	27	205	7.5	-114	-305	72	236
8	33	-227	-77	150	8	19	-223	-61	167	8	-10	-255	-33	190
8.5	117	-242	-156	164	8.5	122	-235	-157	161	8.5	119	-248	-161	163
9	149	-223	-187	152	9	167	-207	-205	137	9	198	-185	-239	115
9.5	167	-198	-207	125	9.5	201	-160	-239	94	9.5	255	-129	-294	51
10	168	-154	-205	87	10	215	-116	-251	44	10	276	-58	-314	-12
10.5	149	-107	-193	43	10.5	208	-56	-245	-11	10.5	261	13	-303	-74
11	151	-97	-192	27	11	204	-55	-238	-24	11	248	4	-286	-84
11.5	146	-156	-186	73	11.5	182	-133	-223	52	11.5	212	-86	-255	0
12	152	-203	-192	135	12	171	-223	-208	135	12	185	-183	-227	105
12.5	150	-210	-178	180	12.5	146	-294	-184	209	12.5	154	-278	-196	203
13	127	-340	-171	266	13	132	-357	-169	280	13	121	-367	-166	297
13.5	111	-402	-158	307	13.5	108	-420	-149	336	13.5	93	-418	-135	354
14	113	-440	-157	346	14	113	-462	-154	373	14	94	-460	-133	381

North Slope Indicator Readings

N SI3					N SI3				
June 22.					July 5.				
	Deformation					Deformation			
Depth	North	East	South	West	Depth	North	East	South	West
0.5	35	104	-250	923	3.5	-406	-368	361	291
1	831	247	-462	-721	4	-322	-377	282	320
1.5	-6291	-1746	24	-772	4.5	-239	-387	196	343
2	-1507	1188	-96	-1990	5	-214	-405	174	345
2.5	-144	-221	120	147	5.5	-300	-352	262	273
3	-275	-299	239	227	6	-246	-328	213	277
3.5	-377	-336	344	281	6.5	-185	-317	145	270
4	-318	-365	287	306	7	-113	-304	74	260
4.5	-250	-382	215	334	7.5	-23	-263	-7	210
5	-222	-394	193	330	8	52	-240	-90	175
5.5	-307	-344	280	264	8.5	141	-247	-177	176
6	-272	-318	240	254	9	185	-209	-228	142
6.5	-229	-329	195	265	9.5	216	-164	-258	97
7	-173	-326	138	251	10	227	-88	-264	33
7.5	-87	-286	56	221	10.5	208	-28	-247	-20
8	8	-237	-41	177	11	192	-30	-230	-30
8.5	122	-239	-158	160	11.5	171	-111	-205	57
9	192	-182	-227	121	12	165	-205	-207	132
9.5	241	-130	-276	63	12.5	153	-278	-187	192
10	266	-63	-300	-1	13	137	-344	-175	280
10.5	257	15	-297	-74	13.5	117	-398	-157	334
11	250	16	-283	-89	14	115	-461	-162	397
11.5	212	-83	-250	-2					
12	183	-183	-225	114					
12.5	154	-277	-193	202					
13	124	-358	-163	293					
13.5	96	-411	-137	352					
14	95	-465	-132	383					

North Northeast Slope Indicator

NNE SI4					NNE SI4					NNE SI4				
April 22.					May 18.					June 10.				
	Deformation					Deformation					Deformation			
Depth	North	East	South	West	Depth	North	East	South	West	Depth	North	East	South	West
0.5	709	228	-756	-416	0.5	620	280	-697	-333	0.5	1218	-376	-980	542
1	744	211	-786	-304	1	775	210	-817	-310	1	1350	-211	-1369	403
1.5	790	158	-839	-253	1.5	868	193	-893	-290	1.5	1042	-70	-1191	192
2	843	158	-888	-242	2	910	227	-953	-317	2	1023	26	-1108	-51
2.5	782	173	-823	-247	2.5	870	226	-900	-318	2.5	950	159	-979	-177
3	612	208	-658	-290	3	730	236	-768	-308	3	795	243	-824	-311
3.5	408	285	-458	-354	3.5	542	311	-573	-413	3.5	607	343	-641	-423
4	180	351	-224	-430	4	305	408	-333	-472	4	381	420	-418	-482
4.5	-17	331	-20	-411	4.5	87	390	-118	-465	4.5	161	401	-208	-436
5	-147	310	103	-378	5	-68	324	38	-403	5	-32	348	-4	-405
5.5	-115	286	71	-364	5.5	-44	308	5	-379	5.5	-13	327	-20	-391
6	-104	241	60	-331	6	-50	243	13	-313	6	-18	249	-14	-314
6.5	-23	230	-20	-322	6.5	15	234	-53	-320	6.5	31	224	-70	-302
7	68	340	-113	-433	7	127	339	-169	-442	7	158	336	-198	-422
7.5	43	500	-92	-599	7.5	126	531	-167	-634	7.5	176	536	-214	-629
8	47	709	-93	-788	8	120	742	-157	-847	8	166	757	-204	-849
8.5	157	925	-206	-1017	8.5	251	992	-294	-1087	8.5	302	1013	-341	-1104
9	194	1051	-247	-1132	9	337	1137	-377	-1228	9	416	1175	-455	-1250
9.5	89	1149	-136	-1241	9.5	261	1250	-296	-1318	9.5	366	1287	-398	-1346
10	-191	1250	141	-1310	10	-65	1243	29	-1330	10	57	1294	-82	-1355
10.5	-621	1232	585	-1317	10.5	-714	1148	680	-1245	10.5	-675	1230	654	-1304
11	-791	1131	752	-1219	11	-852	1018	822	-1132	11	-923	1085	891	-1175
11.5	-632	866	592	-969	11.5	-594	824	565	-913	11.5	-620	827	588	-912
12	-433	715	395	-803	12	-388	683	367	-772	12	-381	697	351	-762
12.5	-252	605	210	-686	12.5	-215	570	183	-652	12.5	-204	602	175	-658
13	-119	524	76	-626	13	-94	497	62	-590	13	-84	535	52	-590
13.5	-20	461	-22	-548	13.5	-8	440	-26	-520	13.5	-5	473	-32	-526

North Northeast Slope Indicator

NNE SI4					NNE SI4				
June 22.					July 5.				
	Deformation					Deformation			
Depth	North	East	South	West	Depth	North	East	South	West
0.5	-6053	-1091	11868	16383	3.5	646	176	-602	-334
1	-3705	-1499	-6987	16383	4	402	292	-433	-317
1.5	-1473	-1741	-680	16383	4.5	183	287	-197	-267
2	-1245	572	1234	1069	5	0	242	-30	-291
2.5	387	107	-386	-248	5.5	6	212	-31	-273
3	556	196	-556	-305	6	42	145	-26	-165
3.5	636	332	-672	-398	6.5	84	119	-103	-205
4	459	420	-494	-487	7	214	251	-227	-336
4.5	196	384	-219	-456	7.5	208	492	-238	-548
5	-12	341	-21	-397	8	238	688	-266	-783
5.5	-8	320	-24	-384	8.5	401	942	-430	-996
6	-7	244	-23	-304	9	487	1075	-522	-1155
6.5	46	217	-80	-294	9.5	397	1165	-438	-1211
7	170	304	-205	-412	10	6	1252	-11	-1345
7.5	194	521	-226	-611	10.5	-596	1547	626	-1573
8	187	745	-221	-841	11	-726	1403	745	-1407
8.5	322	1009	-359	-1094	11.5	-540	979	561	-990
9	440	1162	-475	-1238	12	-353	735	351	-802
9.5	391	1278	-429	-1340	12.5	-196	588	179	-646
10	92	1311	-115	-1365	13	-96	503	67	-570
10.5	-670	1325	642	-1380	13.5	-36	436	-1	-491
11	-952	1176	923	-1271					
11.5	-632	859	596	-943					
12	-383	700	354	-767					
12.5	-205	598	172	-658					
13	-87	531	55	-592					
13.5	-5	469	-28	-525					

Southeast Slope Indicator

SE SI1					SE SI1					SE SI1				
April 22.					June 10.					June 22.				
	Deformation					Deformation					Deformation			
Depth	North	East	South	West	Depth	North	East	South	West	Depth	North	East	South	West
0.5	-1665	-356	1593	248	0.5	-1103	-493	873	620	0.5	2695	-819	736	589
1	-1507	-387	1480	280	1	-883	-672	881	606	1	3015	-775	304	120
1.5	-1280	-419	1233	352	1.5	-1066	-552	933	476	1.5	2346	-925	-981	-548
2	-245	394	192	-466	2	-183	343	208	-509	2	-676	515	1738	69
2.5	-49	790	-6	-881	2.5	-74	777	24	-887	2.5	21	898	-48	-968
3	84	1062	-139	-1151	3	44	1023	-89	-1097	3	69	1003	-96	-1086
3.5	292	1063	-337	-1151	3.5	252	1061	-293	-1126	3.5	243	1014	-274	-1098
4	375	968	-419	-1053	4	360	986	-398	-1052	4	316	997	-351	-1069
4.5	280	986	-330	-1068	4.5	288	991	-333	-1082	4.5	265	1018	-306	-1097
5	195	1102	-246	-1192	5	208	1128	-252	-1208	5	193	1128	-232	-1216
5.5	125	1170	-173	-1253	5.5	140	1222	-183	-1288	5.5	118	1212	-156	-1284
6	42	1146	-86	-1229	6	62	1176	-98	-1236	6	31	1153	-65	-1237
6.5	-85	1097	41	-1174	6.5	-69	1076	29	-1142	6.5	-96	1063	62	-1137
7	-212	1078	160	-1171	7	-205	1057	164	-1119	7	-225	1043	185	-1114
7.5	-320	1092	264	-1180	7.5	-313	1092	269	-1154	7.5	-335	1081	291	-1151
8	-379	1044	337	-1141	8	-380	1068	341	-1135	8	-402	1047	367	-1130
8.5	-390	990	346	-1082	8.5	-392	1018	354	-1087	8.5	-413	992	377	-1085
9	-430	925	385	-1015	9	-436	942	402	-1007	9	-456	915	428	-1006
9.5	-442	841	395	-932	9.5	-447	832	411	-901	9.5	-461	810	427	-888
10	-431	828	377	-911	10	-398	789	357	-848	10	-398	763	362	-833
10.5	-311	824	260	-906	10.5	-207	740	170	-806	10.5	-205	729	174	-799
11	-41	720	-4	-828	11	35	692	-73	-754	11	-13	709	-22	-776
11.5	130	598	-177	-693	11.5	131	631	-167	-696	11.5	65	654	-100	-732
12	113	543	-160	-629	12	109	588	-144	-646	12	58	610	-98	-684
12.5	-2	574	-48	-649	12.5	1	592	-39	-657	12.5	-20	609	-19	-683
13	-128	647	73	-735	13	-117	659	80	-724	13	-130	661	88	-739
13.5	-174	740	121	-830	13.5	-166	739	126	-806	13.5	-179	733	141	-823
14	-156	914	103	-1019	14	-155	939	112	-1016	14	-172	936	127	-1023
14.5	-137	1157	77	-1237	14.5	-137	1167	87	-1259	14.5	-156	1157	105	-1238

Southeast Slope Indicator

SE SI1				
July 5.				
	Deformation			
Depth	North	East	South	West
3.5	471	737	-490	-797
4	380	843	-415	-906
4.5	275	947	-302	-1001
5	175	970	-208	-1048
5.5	80	955	-109	-1022
6	-27	865	2	-910
6.5	-151	838	125	-892
7	-247	855	224	-874
7.5	-320	873	287	-926
8	-342	808	311	-882
8.5	-293	688	264	-776
9	-313	483	300	-600
9.5	-534	785	500	-833
10	-1539	2540	1487	-2579
10.5	-2614	3809	2538	-3868
11	-2562	3981	2387	-4025
11.5	-1459	2899	1299	-2872
12	-392	1498	370	-1545
12.5	3	713	-28	-779
13	-65	583	25	-645
13.5	-135	663	100	-741
14	-141	908	94	-981
14.5	-123	1169	78	-1235
15	-108	1263	69	-1315

Southwest Slope Indicator

SW SI2					SW SI2					SW SI2				
April 22.					May 18.					June 10.				
	Deformation					Deformation					Deformation			
Depth	North	East	South	West	Depth	North	East	South	West	Depth	North	East	South	West
0.5	-142	-836	84	724	0.5	-107	-720	126	718	0.5	286	-1886	-1240	2505
1	-165	-685	82	612	1	-124	-643	98	622	1	540	-1165	-366	1324
1.5	-109	-654	72	571	1.5	-121	-642	80	556	1.5	201	-976	-213	905
2	-124	-628	84	539	2	-98	-619	78	549	2	33	-772	-120	640
2.5	-278	-599	244	491	2.5	-258	-609	240	499	2.5	-205	-628	158	544
3	-247	-538	198	505	3	-229	-594	203	503	3	-235	-553	171	502
3.5	-202	-490	149	483	3.5	-177	-552	159	476	3.5	-209	-572	162	496
4	-200	-528	149	458	4	-186	-540	158	460	4	-206	-552	161	478
4.5	-185	-532	136	456	4.5	-174	-547	149	459	4.5	-189	-540	144	475
5	-136	-520	93	465	5	-112	-559	100	475	5	-138	-573	96	495
5.5	-203	-545	156	463	5.5	-194	-553	159	468	5.5	-199	-575	149	489
6	-218	-554	178	475	6	-196	-526	185	494	6	-218	-579	174	509
6.5	-229	-581	185	498	6.5	-228	-584	197	510	6.5	-242	-582	197	511
7	-193	-625	146	530	7	-191	-633	160	543	7	-209	-614	166	535
7.5	-126	-701	76	599	7.5	-120	-712	86	611	7.5	-138	-692	86	608
8	-17	-796	-33	703	8	-1	-813	-38	730	8	-5	-813	-46	725
8.5	36	-813	-72	715	8.5	72	-836	-95	745	8.5	88	-858	-124	767
9	-1	-773	-34	693	9	28	-775	-47	715	9	47	-819	-83	729
9.5	-43	-745	-4	653	9.5	-45	-742	15	668	9.5	-57	-755	15	676
10	112	-762	-157	690	10	119	-790	-153	711	10	114	-785	-155	717
10.5	308	-832	-351	750	10.5	342	-868	-375	778	10.5	363	-877	-408	807
11	345	-840	-384	752	11	401	-816	-401	758	11	398	-860	-442	782
11.5	267	-746	-304	642	11.5	291	-731	-313	643	11.5	293	-747	-334	661
12	171	-627	-215	540	12	193	-616	-217	534	12	187	-635	-229	551
12.5	109	-527	-151	437	12.5	143	-552	-144	441	12.5	107	-548	-153	445
13	84	-434	-125	350	13	139	-379	-122	359	13	84	-441	-131	366
13.5	93	-384	-133	299	13.5	149	-390	-127	296	13.5	90	-387	-134	308
14	49	-360	-96	276	14	66	-371	-96	276	14	58	-360	-107	286

Southwest Slope Indicator

SW SI2					SW SI2				
June 22.					July 5.				
	Deformation					Deformation			
Depth	North	East	South	West	Depth	North	East	South	West
0.5	-59	14	-10495	16383	3.5	-104	-722	143	602
1	-31	21	1435	707	4	-194	-618	168	546
1.5	56	16	-429	-152	4.5	-211	-574	167	512
2	-299	-98	-170	606	5	-156	-579	117	516
2.5	-361	-669	382	568	5.5	-227	-574	174	501
3	-338	-656	307	566	6	-244	-577	199	521
3.5	-227	-599	190	529	6.5	-264	-595	220	528
4	-194	-565	159	491	7	-226	-652	176	567
4.5	-184	-546	149	474	7.5	-141	-740	91	648
5	-138	-569	100	484	8	-9	-833	-45	762
5.5	-201	-569	157	484	8.5	77	-851	-114	777
6	-222	-574	182	507	9	6	-809	-46	740
6.5	-244	-586	202	514	9.5	-67	-755	24	696
7	-212	-626	165	544	10	135	-768	-177	713
7.5	-132	-713	83	620	10.5	346	-784	-389	720
8	2	-818	-53	740	11	363	-737	-407	676
8.5	89	-859	-127	768	11.5	286	-657	-335	594
9	38	-808	-72	733	12	191	-595	-240	522
9.5	-62	-757	17	679	12.5	121	-519	-164	446
10	118	-797	-164	717	13	86	-445	-133	381
10.5	356	-853	-403	769	13.5	88	-385	-133	321
11	383	-826	-420	744	14	53	-362	-101	283
11.5	283	-717	-314	637					
12	175	-618	-217	529					
12.5	105	-525	-145	440					
13	81	-441	-122	358					
13.5	89	-386	-128	301					
14	55	-358	-97	276					

South Southwest Slope Indicator

SSW SI5				
April 22.				
	Deformation			
Depth	North	East	South	West
0.5	179	-142	-189	29
1	-42	-68	-50	-90
1.5	-205	5	147	-140
2	-252	28	245	-134
2.5	-243	38	231	-151
3	-193	99	137	-182
3.5	-166	129	123	-229
4	-174	152	110	-258
4.5	-276	199	238	-286
5	-257	323	210	-405
5.5	-217	320	175	-445
6	-123	283	79	-368
6.5	-64	348	23	-434
7	131	317	-173	-419
7.5	468	146	-515	-266
8	631	-94	-676	-9
8.5	828	-347	-891	242
9	1061	-713	-1113	593
9.5	1311	-1097	-1357	1002
10	1604	-1563	-1640	1500
10.5	2029	-2288	-2078	2191
11	2025	-2472	-2089	2355
11.5	1124	-1461	-1180	1424
12	410	-609	-459	521
12.5	113	-135	-156	28
13	64	47	-113	-134
13.5	96	138	-143	-233
14	106	107	-151	-189
14.5	65	84	-111	-169
15	42	68	-88	-152
15.5	13	49	-63	-136
16	-3	37	-47	-120
16.5	40	18	-86	-103
17	50	-1	-97	-82
17.5	89	-20	-134	-68
18	107	-41	-151	-45
18.5	161	-69	-206	-21

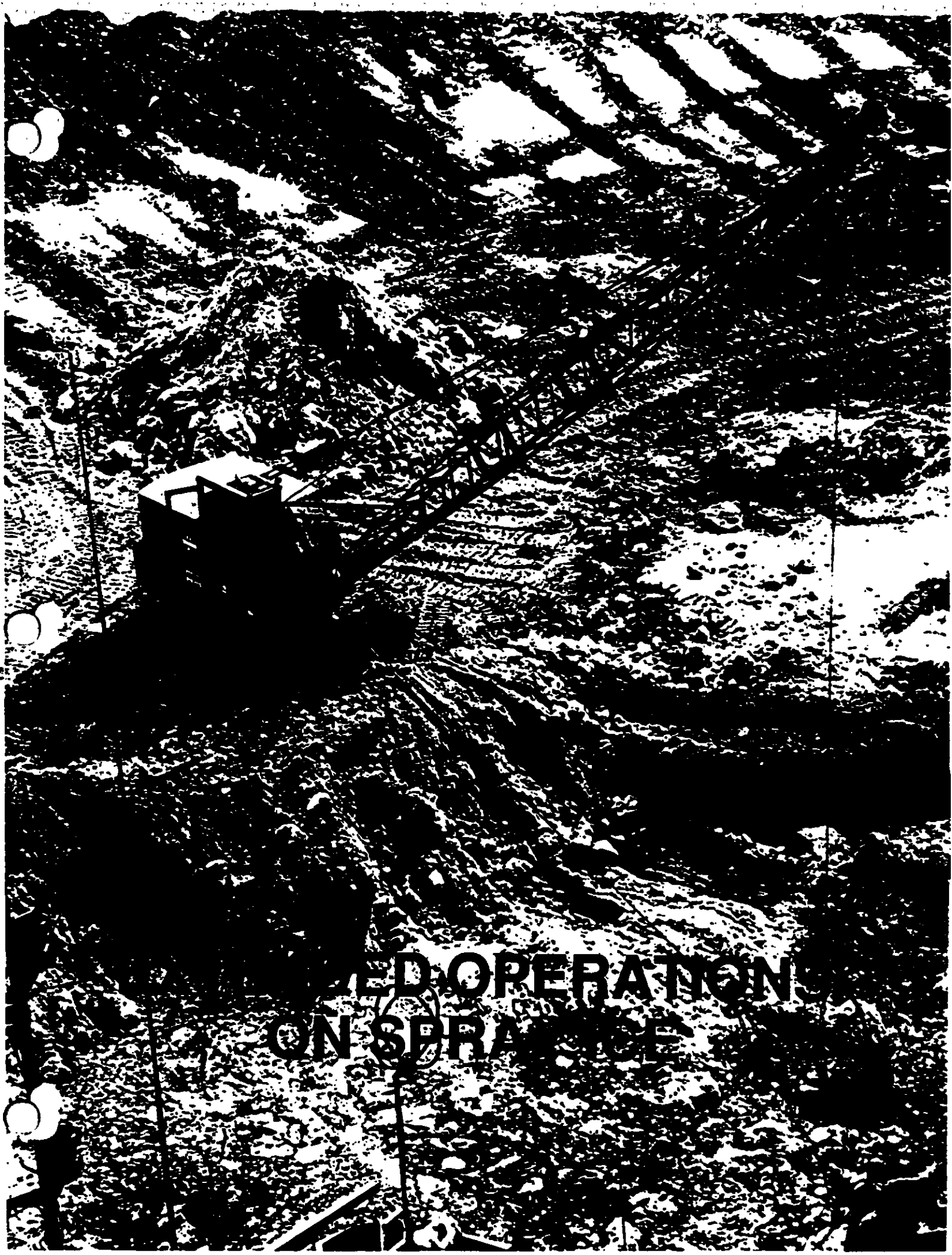
ED OPERATION
ON SPRA

EXTENDED OPERATIONS ON SPRAY ICE

October 25, 1989

Submitted To:

Mr. James P. Poplin
Research Department
ESSO RESOURCES CANADA LIMITED
339- 50th Avenue S.E.
Calgary, Alberta T2G 2B3
Canada

POLAR ALPINE, INC.
1442A Walnut St. #236
Berkeley, CA 94709
(415) 524-1271

TABLE OF CONTENTS

LIST OF PHOTOGRAPHS

LIST OF FIGURES

LIST OF TABLES

INTRODUCTION

This report is the result of experience gained over the past several years operating on spray ice in sub-arctic and marginally arctic conditions. The spray ice structures we have been involved with were constructed at Nome and at the Red Dog Port Site site 6 km south of Kivalina, Alaska. The location of these sites is shown in Figure 1.

The spray ice structures we built differed in several ways from the spray ice structures used as oil drilling platforms. Unlike the fairly massive spray ice islands of the Arctic, the structures built at Nome and at the Red Dog Port Site were relatively small. The quantity of spray ice involved in our structures typically ranged from 150,000 to 300,000 cubic meters. Also the structures tended to be linear as opposed to the quasi-cylindrical nature of spray ice islands. At the Red Dog Port Site a spray ice causeway was constructed which had a length of approximately 250 meters and a working surface width of 15 meters. Over this causeway heavy equipment was moved constantly in temperatures that were often above the freezing point of water.

In the operations at Nome the requirement was to build a protective barrier around the gold dredge Bima and the anchor-handling tug Aquamarine. In addition to providing protection against damage by ice movement, the spray ice barrier at Nome also had to function as work surface over which heavy equipment could be moved. Operations carried out on the spray ice were such that equipment had to be positioned at the edge of over-steepened slopes of the spray ice. In this region work is not usually carried out on spray ice islands.

In both the Nome and Red Dog construction projects it was also necessary that the spray ice structure be removed as soon as possible after the beginning of the open water season. In the Nome operation, any delay in removing the spray ice kept the dredge from operating. In Nome techniques were developed to remove the spray ice by both excavation and agitation of the sea water.

In the case of the Red Dog Seaport project the spray ice causeway disintegrated naturally under the force of wave action on the barrier.

An especially troublesome problem during the course of our work was hardening the surface of the spray ice to enable equipment to operate on it. This was particularly important in the case of the Red Dog project where the spray ice causeway would be utilized as a roadway for dump trucks

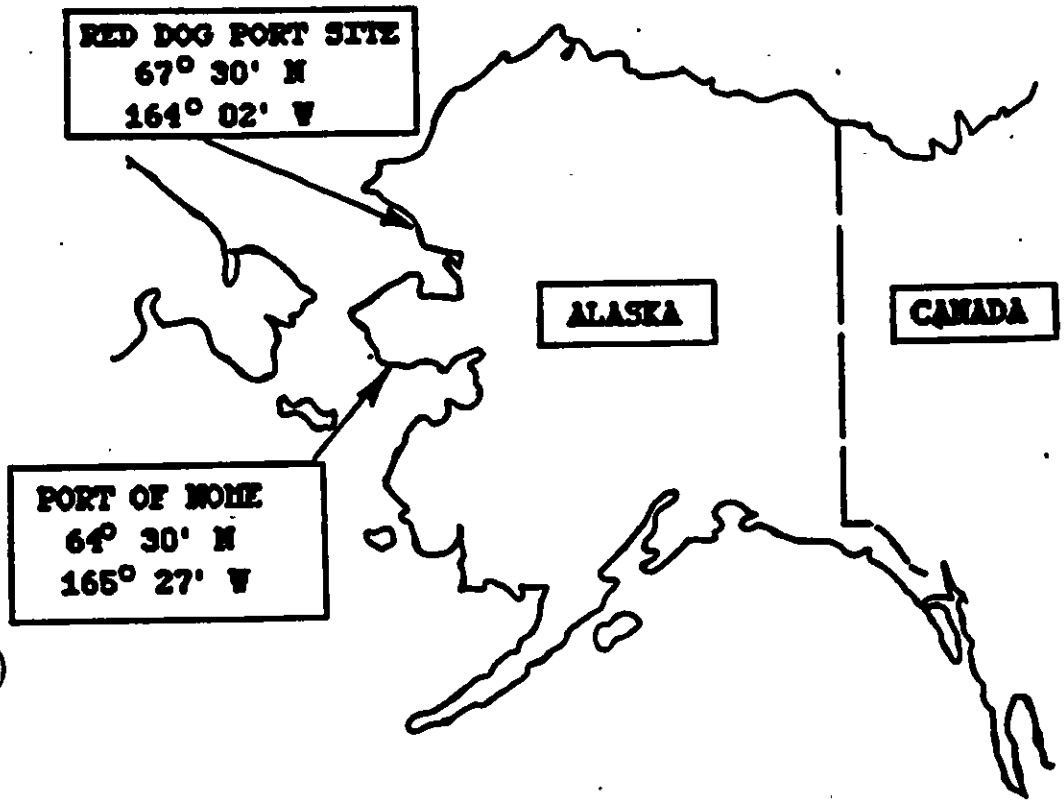

FIGURE 1. Map showing the location of the Red Dog Port Site and the Port of Nome

hauling gravel to construct the permanent port facility. In both the Nome project and the Red Dog project the relatively high ambient air temperatures precluded hardening the surface by spraying water on it and letting it freeze. In the case of the Red Dog site, even if the temperatures were low enough to condition the surface with water, the surface probably would not have survived under the continuous wear and tear imposed by the dump trucks. At the peak of the operation trucks were hauling loads of gravel at three-minute intervals over the spray ice causeway.

In this report we present our experience in working with small spray ice structures in relatively warm environments. The special emphasis in this report is the manner in which we prepared the spray ice surfaces for operation, excavation of spray ice, operating heavy equipment at the edge of spray ice structures and the technique used for removing large quantities of spray ice in a very short time. Preliminary to these discussions, the construction of the spray ice structures that were built is discussed.

SPRAY ICE CONSTRUCTION

Nome

During the winter of 1987-88 and again during the winter of 1988-89 a spray ice barrier was constructed at Nome, Alaska (64° 30'N, 165° 27'W). The purpose this barrier was to protect the gold dredge Bima and the anchor-handling tug Aquamarine from winter and spring ice movements. This was particularly important since neither vessel was ice reinforced.

The spray ice barrier built during the 1987-88 winter was constructed by spraying water into the air in combination with compressed air (described in Polar Alpine Inc. report to ESSO Resources Canada, June, 1988) and also by hauling snow from around Nome. The hauled snow was dumped in place with dump trucks. Photograph 1 is an aerial view of the Bima and Aquamarine inside the protective barrier built during 1987-88.

To establish a scale for Photograph 1, the dredge Bima has a 110 m length and 31 m beam at the waterline and stands 43 m high above the waterline. The tug Aquamarine is 56 m long and has a beam of 15 m. The vessels were moored against the causeway at Nome for the winter in water depths that ranged from 3 m to 4 m. The spray ice barrier was built in a horseshoe around the vessels. The barrier was approximately 300 m along its center line, 30 m across at the waterline and stood 10 m high in places above the waterline. The volume of material used in constructing the 1987-88 barrier was estimated at 175,000 cubic meters.

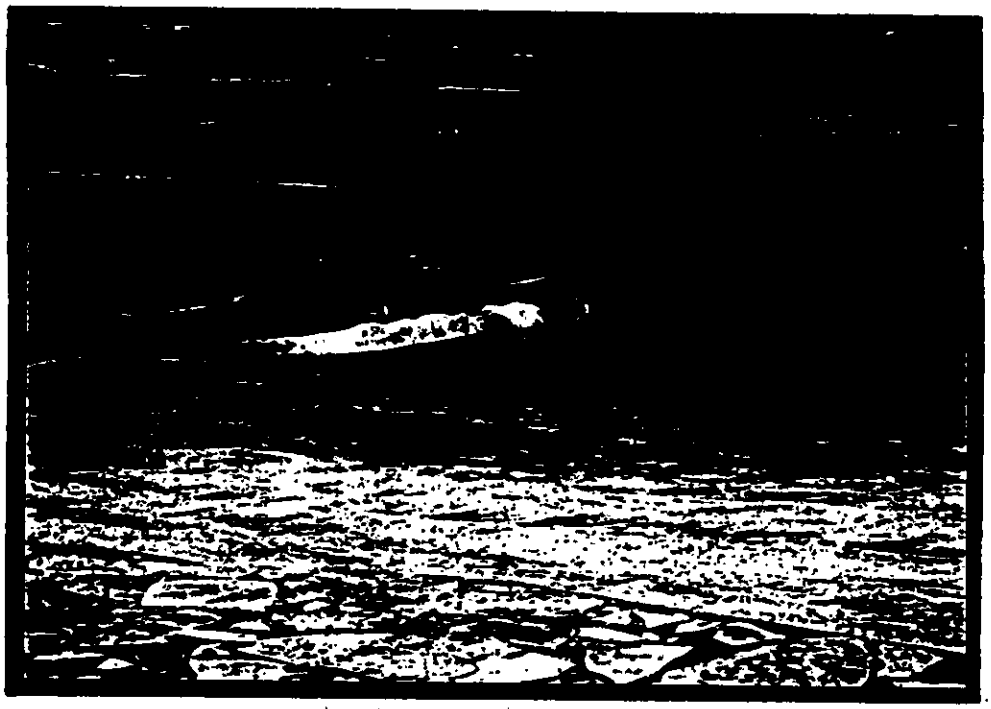

PHOTOGRAPH 1. An aerial view of the dredge Bima and the Aquamarine behind the spray ice barrier constructed at the causeway at Nome.

POLAR ALPINE, INC.

Photograph 1, taken in the spring of 1988, shows the berm in place around the vessels. The white snow of the barrier is where the spray ice was placed primarily by spraying. The dark material at the bow and stern of the Bima is the region where material was placed from snow scavenged from around Nome. When the snow was initially placed the concentration of foreign particles such as dirt and gravel was relatively light and the snow had a tan color. As melting took place the impurities concentrated on the surface to form a solid layer. Initially the rate of melting in the contaminated snow was greater than non-contaminated snow. As melting progressed and the contaminant layer thickened, the rate of surface ablation decreased dramatically.

We observed that the contaminated surface, in addition to slowing the melting rate, was considerably tougher than the the uncontaminated layer. This was particularly evident when heavy equipment was operated over the spray ice.

During the winter and spring of 1988 a number of maintenance operations were carried out on the Bima and Aquamarine. These operations included excavating the spray ice to gain access to the hulls of each vessel and operating cranes and other heavy equipment close to the edge of the excavated ice. Prior to the sea ice around the berm going out, a channel was excavated with a backhoe and a dragline to a point close to the edge of the sea ice-spray ice interface in the vicinity of the Aquamarine. Once the spray ice went out the remainder of the spray ice in the channel was removed and the tug maneuvered outside of the spray ice barrier. The tug (tethered to the Bima) was then used to backwash away the remaining spray ice.

During the winter of 1988-89 the berm around the Bima and Aquamarine was again constructed. Changes made during that season were that the berm was constructed completely with the sprayed water-air system; no material was brought in with trucks. Also, the north end of the berm (the end closest to shore) was left open. Leaving the north end of the berm open was warranted since there could be no significant ice forces generated from this direction due to the proximity of the shoreline. Repair operations were again carried out on the vessels from the spray ice. The spray ice was removed expeditiously in the spring with the Aquamarine.

From our operations at Nome during the 1987-88 season we found that we could build a spray ice structure in the relatively warm climate at Nome; excavate spray ice to contour it to the form we desired; operate heavy equipment close to the edge of the spray ice; harden the surface and slow surface melting with the addition of surface coatings; and remove the spray ice rapidly when required.

Red Dog Port Site

Given the success of the spray ice barrier at Nome during the 1987-88 winter season, we were approached to design and oversee the construction of a spray ice causeway and protective barrier at the Red Dog Port Site (67° 30'N, 164° 02'W) on the Chukchi Sea in Alaska. The purpose of the causeway was to provide a structure over which equipment could be moved to build a sheetpile-encased, gravel-filled "sea cell." The cell to be built was 23 m in diameter and stood 8 m above the sea surface in water 5 m deep. This was the third of three cells to be built and was the farthest of the three from shore. Attempts to construct the cell during the open water season had failed when the cell was destroyed during a storm while under construction.

The primary requirements for this operation were that the causeway be constructed with sufficient strength to support a crane with a mass of 225,000 kg driving and extracting piles. In addition, the surface had to be resilient enough to withstand dump trucks hauling gravel to fill cells No. 2 and 3. (Note: Construction on cell No. 2 had to be terminated before completion due to operating conditions the previous summer.)

In addition to constructing the causeway, a barrier had to be constructed around the area of cell No. 3. The purposse of the barrier was to protect the sheet piling structure before it was filled with gravel and before it had sufficient strength to withstand ice loads.

Photograph 2, taken March 31, 1989 shows cell No. 3 under construction. This photograph also shows the protective spray ice berm around cell No. 3 used for spray ice construction and also a portion of the spray ice causeway leading to the construction area. Cell No. 1 is the cylindrical structure at the left side of the photograph. For scale, the boom on the crane in Photograph 2 is 52 m in length.

At the completion of the causeway construction phase of the program temperatures ranged from -4° to +2° C. The spray ice surface was weak and and there was little hope of operating large trucks and other heavy equipment over the surface. Drawing on our observations at Nome the previous season, we placed a layer of gravel 150 mm to 300 mm thick on the surface of the spray ice. This gravel layer appears as the brown on the surface of the causeway in Photograph 1.

The causeway and protective barrier was constructed using the water-air spray method employed at Nome. When temperatures dropped below -20° * C, spraying was done with water, but no compressed air.

PHOTOGRAPH 2. An aerial view of the spray ice causeway and protective berm constructed at the Red Dog Port Site, Alaska.

To expedite the construction of the barrier in face of temperatures too high for the water-only spraying system or the air-water spray system, snow was scavenged from snowdrifts around the area. The snow was loaded into dump trucks and deposited in the construction area.

Within a 2 km range of the spray ice construction site we estimated that 20,000 cubic meters of snow was deposited in drifts. Interestingly we found that before we could deplete the supply of drifted snow, storms occurred and the source of snow for hauling was renewed due to new drifting in and around structures in the area. Approximately one-third of the spray ice used for construction was from snow hauled to the site from drifts.

As a construction note, the causeway shown in Photograph 2 was built on a second attempt. Initial construction was started December 19, 1988. A storm on January 6, 1989 broke up the sea ice and on January 7 the causeway washed away with a good deal of the construction equipment.

Given this background we can explore in more detail how our experience on these spray ice structures can be transfered to operations in arctic water.

OVER-ICE OPERATIONS

Major concerns while operating on the spray ice surface involved using heavy equipment on the surface and close to the ice edge. Unlike spray ice islands used for exploratory drilling, the Nome and Red Dog structures were relatively narrow.

The spray ice causeway at the Red Dog site had a designed working surface 15m wide. The largest piece of equipment to be moved over the surface was a Manitowoc model 4100 Series-2 crane. With the crawler extended the width of this unit was 6.4 m. The mass of this crane was etimated at 228,000 kg. The ground pressure exerted by this unit was estimated to be 130 kPa. In addition to the dead-load weight, it was determined that maximum loads would be exerted during pile-extraction operations.

While working the crane would be positioned close to a vertical edge of the spray ice. Other equipment was also operated over the causeway. From our experience in Nome the previous season we were fairly confident that we could operate the equipment on the spray ice with a minimum of problems.

Several examples from our Nome experience the previous season illustrate the strength of the barrier. Photograph 3 shows a Caterpillar D-6 operating very close to edge of the spray

ice. In this case an attempt was being made to start a barrier for the Bima and Aquamarine before the sea ice was formed. It was not successful. It is important to note here that in the case illustrated in Photograph 3 the material was loose snow being trucked onto the gravel jetty at Nome and then bulldozed off the jetty to form the beginnings of the ramp shown.

Operating this close to the edge of unsintered spray ice is not recommended. At a latter stage of the operation the toe of the spray ice ramp failed and the cat that was pushing the snow slid down the failed toe and into the water. From Photograph 3 we can see that the material, even though loose and unsintered at the time, had sufficient strength to support an operating D-6.

In contrast to the example of equipment working on loose, unsintered snow, Photograph 4 shows a crane operating on the edge of sintered and seasoned spray ice. As the photo shows, the crane is excavating the spray ice with a dragline. Note that the track of the crawler on the crane is extremely close to the edge of the spray ice. We experienced no spray ice failures operating equipment this close to the edge of seasoned spray ice.

A more conservative approach to operating equipment on spray ice was used on the Red Dog project. Every effort was made to reduce the potential for a material failure while continuing to use the structure. The primary concern was to keep the two Manitowoc cranes from tipping or failing the spray ice.

Table I provides the equipment loads, in terms of ground pressure, that various types of equipment would subject the spray ice to. Cranes were operated off of crane mats (rig mats) to lower the ground pressures. A single section of crane mat consisted of 0.3 m by 0.3 m by 7.3 m timbers fastened together edge to edge. Typically the mats were either 7.3 m by 1.83 m (24'x 6') or 7.3 m by 2.44 m (24'x8'). The mats were used in varied configurations to spread the loads out over the spray ice. The effectiveness of the crane mats in lowering the effective ground pressure is shown in Table I.

As can be noted in Table I, placing the 4100-S2 on a 7.3 m by 7.3 m crane pad reduces the ground pressure by a factor of 3. Considering that a Caterpillar D-8 can be operated on and near the edge of spray ice structures indicates that operating a Manitowoc 4100-S2 crane should present little problem. It should be noted that a D-8 can withstand considerable tipping and operation over rough terrain with little problem. As a last resort a 4100-S2 can be used to extricate a D-8 should it become mired or sunk. However, it would be difficult to remove a 4100-S2 with a D-8 should difficulties arise.

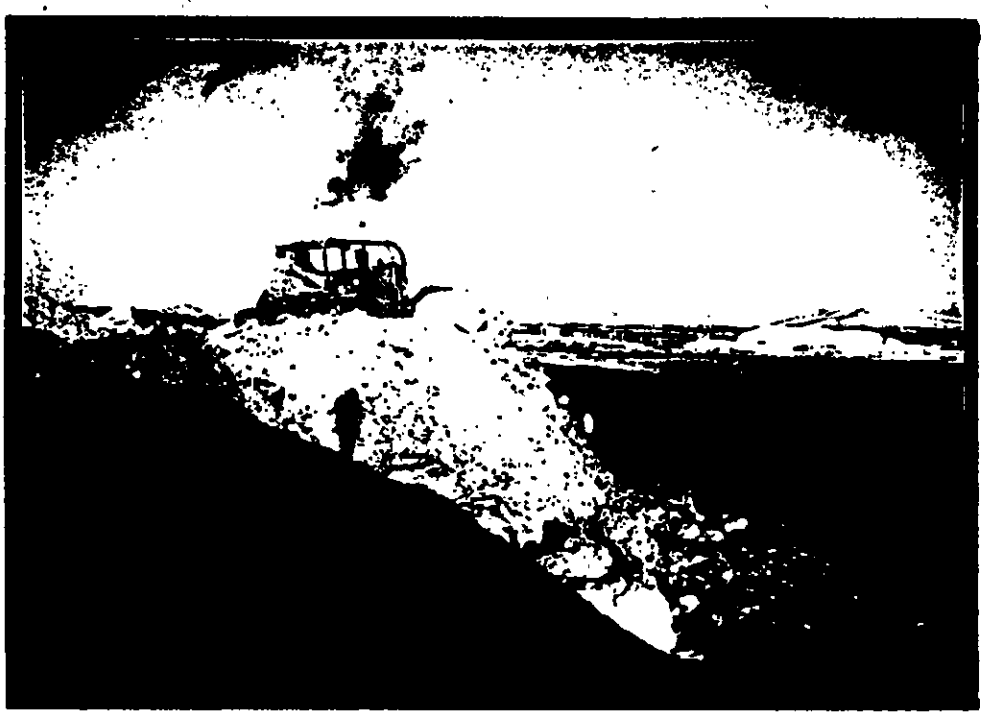

PHOTOGRAPH 3. A D-6 Caterpillar tractor working at the edge of unconsolidated spray ice.

PHOTOGRAPH 4. A crane operating a dragline at the edge of well-sintered spray ice.

TABLE I. Ground pressure of different types of equipment and the effect of using crane mats to lower the bearing pressure.

EQUIPMENT TYPE	WEIGHT (Newtons)	GROUND PRESSURE (kPa)
Manitowoc 4100-S2	2,223,230	130
Caterpillar D-8	409,074*	100
Manitowoc 4100-S2 on a 6m by 7.3m crane pad	2,223,230	50
Caterpillar D-6 Standard Track	168,965*	50
Manitowoc 4100-S2 on a 7.3m by 7.3m crane pad	2,223,230	42
Caterpillar D6H-LGP (wide pad)	191,198	32
Caterpillar D4H-LGP (wide pad)	111,606	28

* estimated weight

As an aside, in remote operations we have always considered what type of equipment would be required to extract another piece of equipment from a difficult situation. If there is a unit that can not be extracted with the equipment at hand, that unit should be operated in a in a conservative manner.

STRESS ANALYSIS

To obtain a quantitative understanding of the stresses involved in operating equipment on small spray ice structures a linear elastic finite element analysis is carried out. The purpose of this analysis is to determine in a general way what loads can be expected to cause failure in the spray ice.

If we make the assumption that spray ice can be represented as a linear viscoelastic material we can invoke the correspondence principal (1). The correspondence principal may be stated that if the loads are applied to a structure at time zero and held constant, the stresses will be the same as in the elastic structure and the displacements depend on time. Considering the creep (settlement) that has been observed in spray ice and our general understanding of the viscoelastic properties of high density snow (2), application of the correspondence principal seems reasonable.

The analysis carred out was not extremely detailed. The failure criterion used in this analysis is developed from recent data published by Chen and Gram (3). Figure 2 is reproduced from the Chen/Gram publication. Chen and Gram conducted a number of triaxial test on both above-water and below-water spray ice samples. When presented in terms of the effective stress state at failure, the data appears to be well behaved for both the above- and below-water samples.

To utilize the failure information from Chen and Gram, the equation for the straight line they drew through their data was used as the failure envelope. From measurements that we made from their data, the line they fit to their data appears to be represented by the equation:

$$(1) \qquad q = (-9{,}800) + (0.791)[s(1)' + s(3)')/2]$$

In Equation 1 q is the maximum shear stress, s(1)' is the maximum principal stress and s(3)' is the minimum principal stress. The (') associated with the values s(1)' and s(2)' indicates the effective stress state, which includes adjustment in the stress value to include a term for the pore pressure. For the above-water spray ice the pore pressure term is negligible.

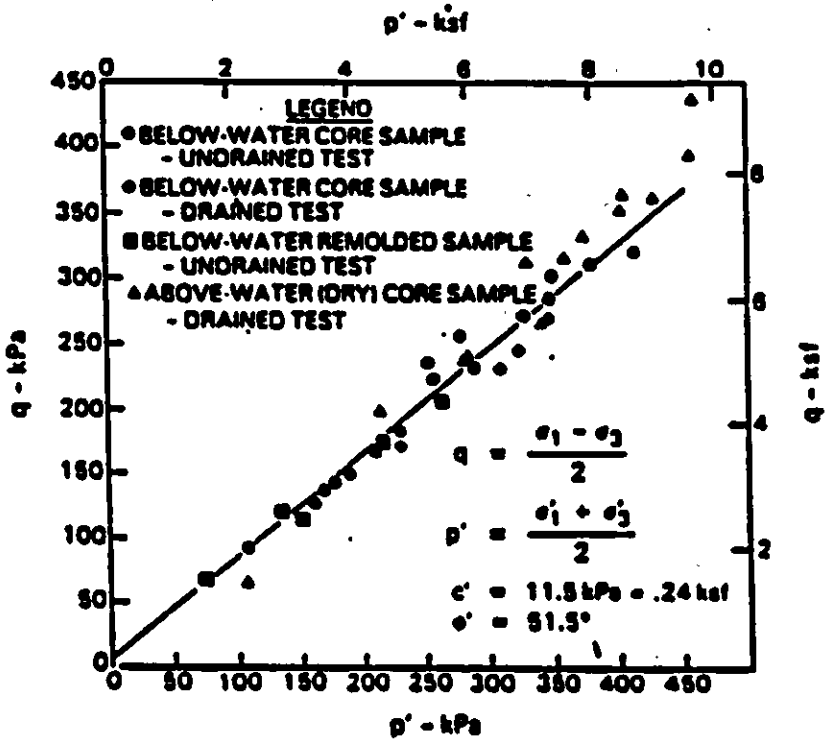

FIGURE 2. Effective stress state at failure. This figure is reproduced from the paper by Chen and Gram, (reference 3)

Equation 1 differs in its representation from that provided by reference (3) in that we admit that spray ice (especially the above-surface spray ice) can support tensional loads. Thus in our application compressional stress is negative and tensional stresses are taken as positive. Mellor (4) suggests that the tensile strength of high-density dry snow is about the same as the shear strength. Also, when operating close to a free surface (such as the equipment shown in Photograph 4) tensional stresses are generated close to the free surface. Typically the tensional stresses are close to an order of magnitude less than the compressional stresses.

As a point of clarification, if the data taken in Figure 2 is interpreted as is presented, it suggests that no matter how low the principle stresses the material will fail. In our analysis we have used a maximum shear stress of 100 kPa (14.5 psi) as the failure stress cut-off value. In the data provided by Chen and Gram our shear stress cut-off excludes all data points except the three lowest. In terms of the above-water spray ice tested, the one low stress failure seemed anomalously low when compared with the other values of above-water strength. We assume the other two data points that fell below this cut off were disturbed samples or represented local weeknesses. Again, our experience with actual loads on spray ice leads to this stress cut-off assumption.

To carry out our analysis we used a four-material model. Figure 3 provides the values used for this model. The values of density for the above-surface and below-surface spray ice were taken from data published by Weaver (4). The moduli values and Poisson's ratio values were taken from data published by Lee et. al. (5) and Mellor (6). The modulus and Poisson's ratio value for sea ice were taken from data published by Croasdale (7). The spray ice was assumed to be resting on a half-meter-thick sheet of sea ice. The sea ice was assumed to be resting on a homogeneous silt layer. The material values used for the silt were taken from Bowles (8). Note that all densities shown in Figure 2 are adjusted for buoyancy.

Only the failure of the spray ice was considered in this analysis. The stress state associated with the silt and sea ice were not considered. In all cases we incorporated the pressures exerted by body forces in the analysis. The finite element analysis conducted was a two-dimensional plane strain analysis.

The initial analysis is carried out on a section of spray ice that is 16 m wide and 6 m thick. The water depth is taken to be 3.5 m. The freeboard of the spray ice is taken to be 3 m. Figure 4a depicts a cross section of the two dimensional plain strain model used.

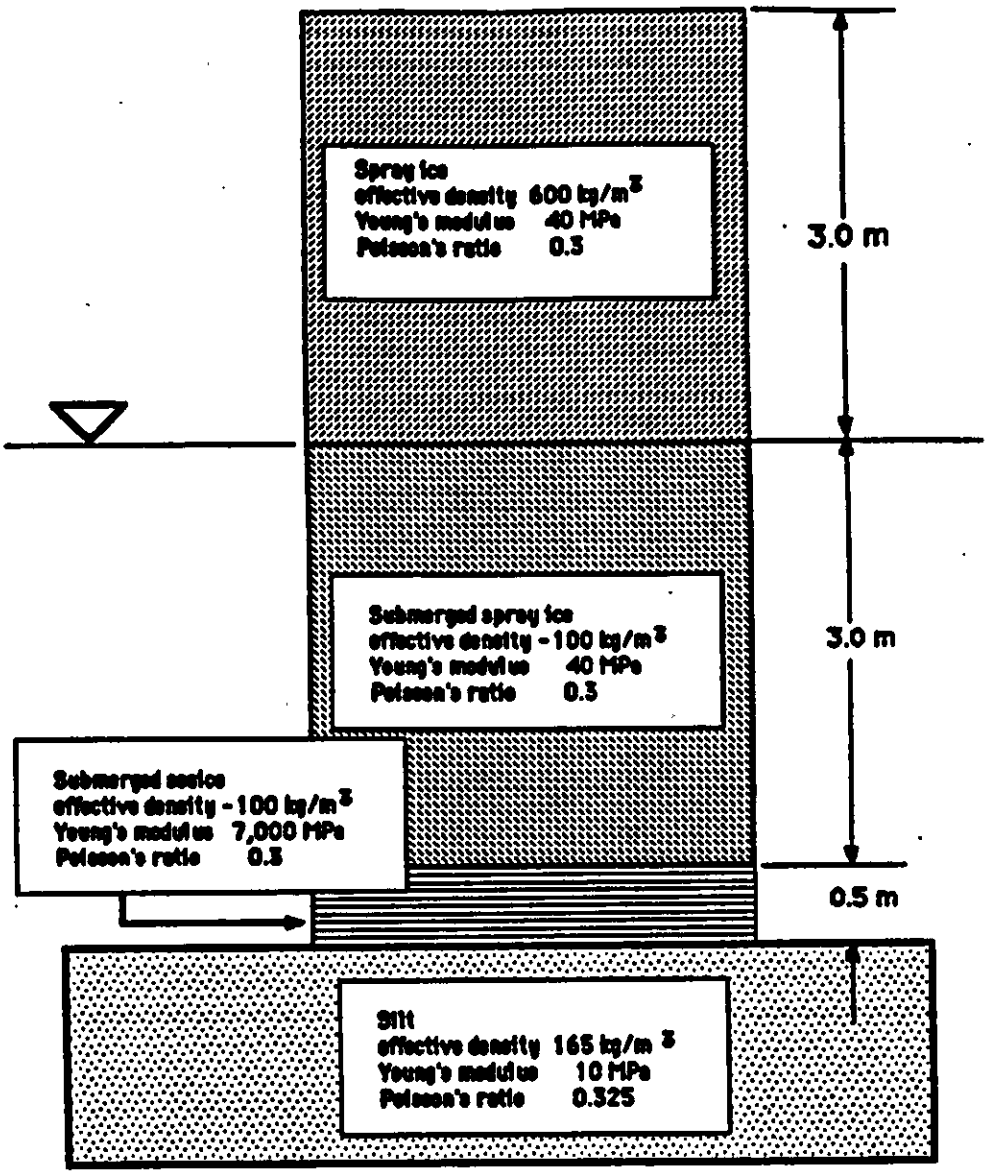

FIGURE 3. Material model used for finite element stress analysis

The first case run (Figure 4a) is for spray ice subjected to overburden pressure only. The purpose of this analysis is to look at the overburden pressure along the section of spray ice and the edge effect present. As predicted from simple analysis of the model used, the maximum overburden pressure should be at the water line. The magnitude of the overburden pressure at the waterline is 17.6 kPa. The overburden pressure at the spray ice/sea ice interface is 14.7 kPa. The effect of the vertical edges on the stress field extends approximately 3 m on each edge. The region of edge effects is shown in Figure 4a It is noted that the magnitude of the stress variation in the edge zone is 2 kPa.

To examine the loads at which failure would take place a load was applied in the center of the spray ice cross section. The load was spread out over a linear distance of 6m in the center of the cross section. This is depicted schematically in Figure 4b. The intensity of the ground pressure was then increased until failure (according to our failure criterion) took place. We found that failure in the spray ice took place at bearing pressures that exceeded 276 kPa (40 psi). Failure was detected in the subsurface layers when ground pressures exceeded 276 kPa. The pattern of failure that occurred when ground pressure increased is depicted in Figure 4c. The total load applied in this analysis is equivalent to 1,700,000 Newtons (186 tons) per unit of thickness.

It should be noted that the maximum shear stress with an applied bearing pressure of 276 kPa remains below the 100 kPa failure cut-off that we used in the failure criteria. However, the maximum principal stress becomes positive beneath the load. In terms of the data presented on spray ice by Chen and Gram, the failure surface is not defined for positive stresses. The maximum principal stress detected for this loading is a tensile stress of 53 kPa. The minimum principal stress associated with this ground load is a compressional stress of 147 kPa. In carrying out this failure analysis we have assumed that the spray ice can carry a tensile load. For unbonded spray ice, obviously no tensional load can be carried. However, for bonded spray ice we know from past experience that tensional loads can be tolerated. Currently little data exist on the failure of spray ice when the maximum principle stress is tensional.

At this point a conservative approach would suggest that ground pressures for large equipment operating away from the edge of narrow spray ice structures be limited to about 140 kPa. To date we have not experienced failures when operating equipment over narrow spray ice structures with this amplitude of ground pressure.

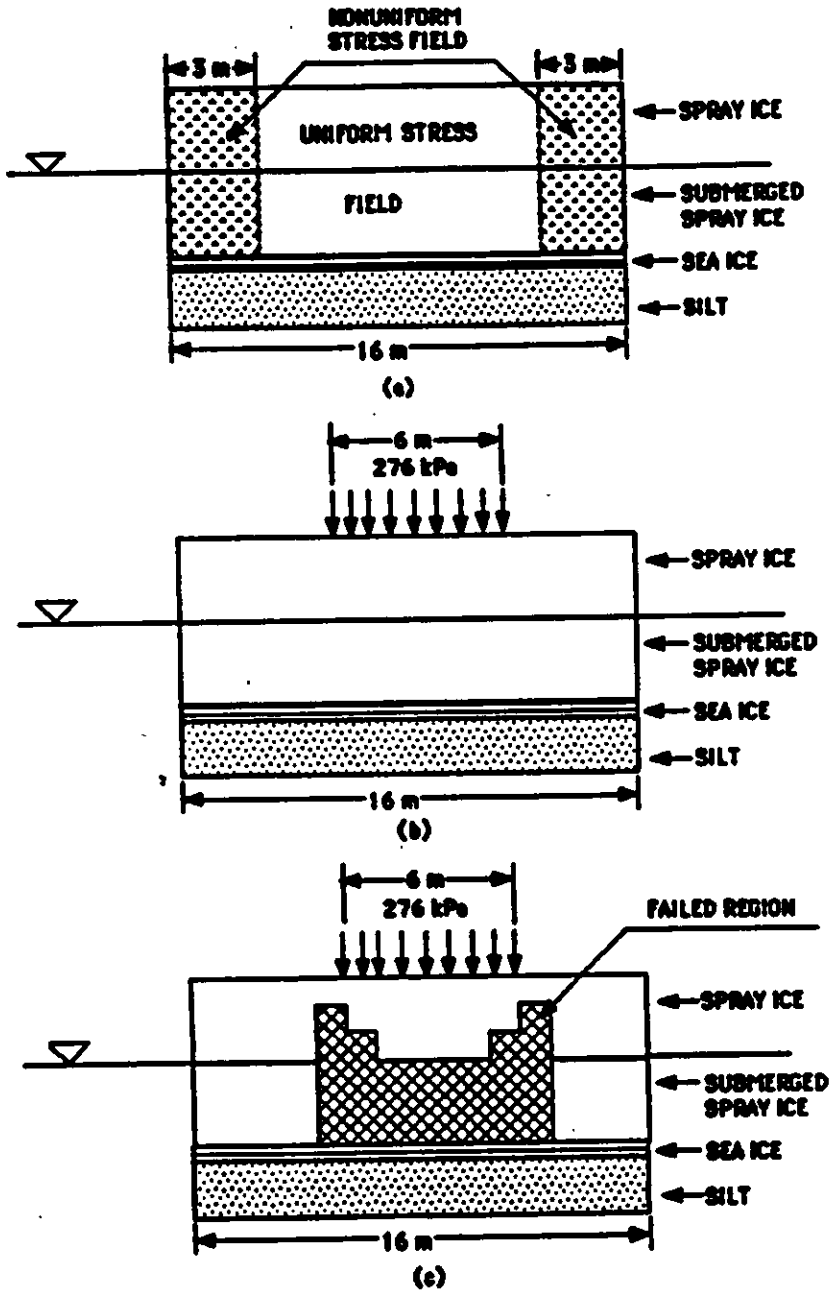

FIGURE 4. Results of stress analysis for different loading configurations, (a) stress field due to body force alone, (b) geometry of a 276 kPa load applied over a 6 m region, (c) region of failed spray ice using Chen/Gram failure envelope.

Having considered operating away from the edge of a narrow spray ice structure, we can look at the magnitude of the loads that can be applied to spray ice when the load is moved to the edge of the structure. To carry out this analysis we used the model in Figure 5. In this case the load was moved to the edge of the spray ice structure. Again the bearing pressure was applied over 6 m. The load was then increased until failure was detected according to the criterion previously established. An edge failure was detected when the bearing pressure reached 145 kPa (21 psi). In this case the failure occurred in the upper edge of the spray ice. When the bearing pressure was lowered to 138 kPa, no failure was indicated. The stress state generated by this loading is close to the stress state generated by the crane operating in Photograph 4.

With all factors considered, we cannot recommend operating equipment with bearing capacities this high close to the edge of a vertical spray ice face. It is feasible, however, to operate heavy equipment at the edge of the spray ice if it is operated off of crane mats or rig mats as described earlier. In the case where a 7.3 m by 7.3 m crane mat is employed with the Manitowoc crane discussed earlier, the bearing pressure drops from 130 kPa to 41 kPa. At this pressure we are operating well away from the failure state for spray ice. It is important to note that when the bearing pressure is dropped to the 41 kPa level the stress field generated in general remains below the failure state defined in (3) without the necessity of imposing a minimum stress cut-off.

The loading configuration shown in Figure 5 should be used only for loading equipment on or off of the spray ice. If the load is moved a short distance from the edge, the edge loading drops significantly. For example, if a 172 kPa load is applied as shown in Figure 5, the maximum shear stress in that vicinity is approximately 122 kpa. If the same load is moved back one meter from the edge, the maximum shear stress drops to 37 kPa at the same point.

Photograph 5 is an example of the application of this principle. In this case a crane pad was built up approximately 1.5 m above the surrounding spray ice. Crane mats were put in place approximately 1 m from the edge and the crane moved onto the mats. The crane worked from this platform for several weeks without the spray ice failing. It should also be noted that the spray ice used was dumped in place. When placed it was a loose material with virtually no cohesion. The strength of this material would fall at the lower end of the failure strengths that Chen and Gram measured.

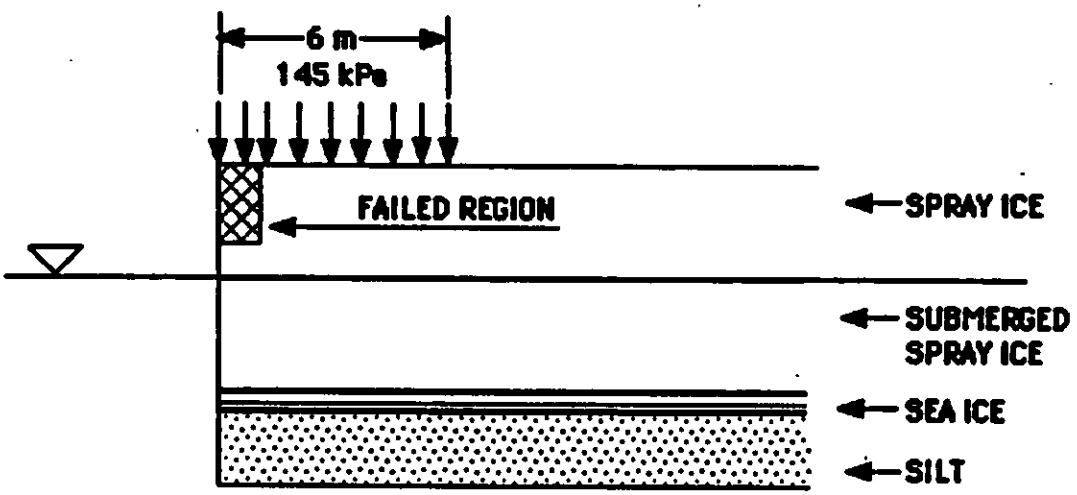

FIGURE 5. Failure threshold when the load is moved to the edge of the spray ice. In this instance failure occured when the ground pressure was raised to 145 kPa.

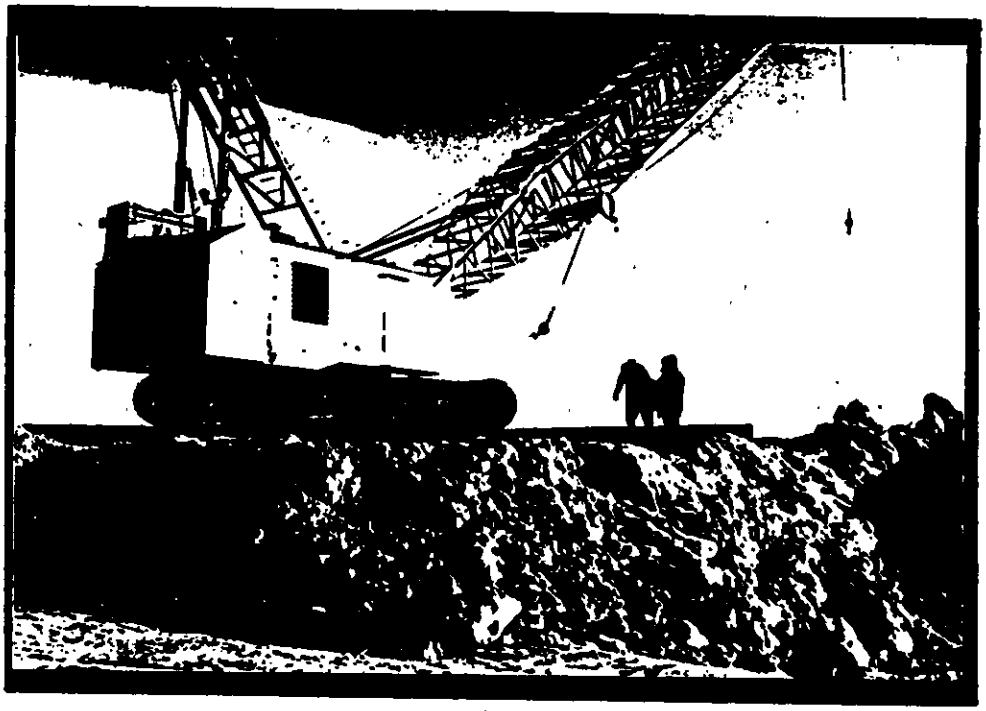

PHOTOGRAPH 5. Manitowoc crane operating on crane mats on a raised spray ice platform.

ABLATION PROTECTION AND SURFACE PREPARATION

In the last section we were able to gain a quantitative insight into the strength of spray ice. When we consider how to prepare the surface of spray ice for over-ice operation and how to retard melting we face a less well-defined topic. In general there is little information in the literature on either strengthening spray ice surfaces or attenuating the ablation of these surfaces.

Some information relevant to the strengthening of snow has been presented by Lee et. al. (5). In their work they attempted to strengthen snow runways in Antarctica. The snow densities they were dealing with were in the vicinity of 532 kg per cubic meter. This density is similar to the density of above-water spray ice. From past experience with both snow and spray ice we again emphasize the materials are identical for all practical purposes.

To strengthen the snow and increase its durability the investigators added polystyrene beads in one instance, and sawdust in another. The results of their investigation showed that adding polystyrene was counter-productive. They obtained limited success with the sawdust.

At concentrations of 10% sawdust by volume the investigators found that at strains greater than 12% a noticeable increase in the stress response and the tangent modulus was recorded. In the field they found that the addition of sawdust or wood chips with the snow significantly increased the density, strength and hardness of the snow surface. They also determined that wood additives worked better at higher ambient temperatures.

On the negative side the investigators found that during periods of warm sunny weather the surfaces became more rutted than snow-only sections of road or runway. They attributed the increased surface roughness to increased melting of the snow surface due to a decrease in the albedo of the snow.

Most literature addresses specifically how to decrease the ablation of snow and ice. Some effort has been made in attempts to increase the rate of snow and ice ablation. Recently Colbeck (9) reviewed the work in this area. In attempts to increase snow melt with surface additives such as carbon black it was found that in some instances the rate of melting was decreased. If the surface coating completely covered the surface it was found that surface ablation was inhibited. One explanation provided is that under this condition, not all of the heat that is applied to the surface of the covering layer is transmitted to the snow layer.

In terms of the thickness of surface coatings, it is reported that a layer of sand, gravel or volcanic ash greater than from 1 to 24 mm inhibits surface melting. It was also found that finer materials tend to insulate better than coarse ones.

The information presented by Colbeck (9) is generally in accord with our own observations. When sand or gravel is mixed with the spray ice, even in relatively small concentrations, the resulting mixture appeared to be stronger than the spray ice alone. As the melt season progressed, spray ice that had dirt particles dispersed in it tended to melt more rapidly than uncontaminated spray ice. However, once the surface melted to the point where the impurities formed a solid layer, the melt rate was retarded. It was also noted at this point when the surface was completely covered a much stronger surface resulted.

When the Red Dog site was nearing completion the temperatures ranged from -4° C to +2° C. Our initial intent was to prepare the surface for operation by spraying water on the surface. Using fresh water at temperatures of -4° C we could not stabilize the surface.

To harden the surface under this condition, a 15- to 30-centimeter layer of gravel was laid down. Using two 12-cubic-yard end dumps (trucks), a surface 200m long and 15m wide was placed in approximately 18 hours. The surface was laid by dumping the gravel and then spreading it with a small bulldozer (D-4). Immediately after the surface layer was placed trucks could operate on it. In fact, to lay the surface the trucks were backed to the edge of the newly spread surface to dump their loads. This causeway was used for a two-month period with virtually no maintenance required to keep the surface intact.

As water and snow mixed with the gravel the surface appeared to harden into a durable operating surface. Over the course of the operation no washboarding of the roadway was experienced. As the work crews became more experienced with operations on the spray ice they also tended to operate the equipment in a more aggressive fashion. At the end of the project in May the cranes were moved onto and off the causeway without the protection of crane mats. Photograph 6 shows a closer view of the spray ice with the gravel surface.

SPRAY ICE REMOVAL AND EXCAVATION

Of some concern in the Nome project and to a lesser extent at the Red Dog Site was how the spray ice could be removed in a timely manner. At the Red Dog Site this did not prove to be

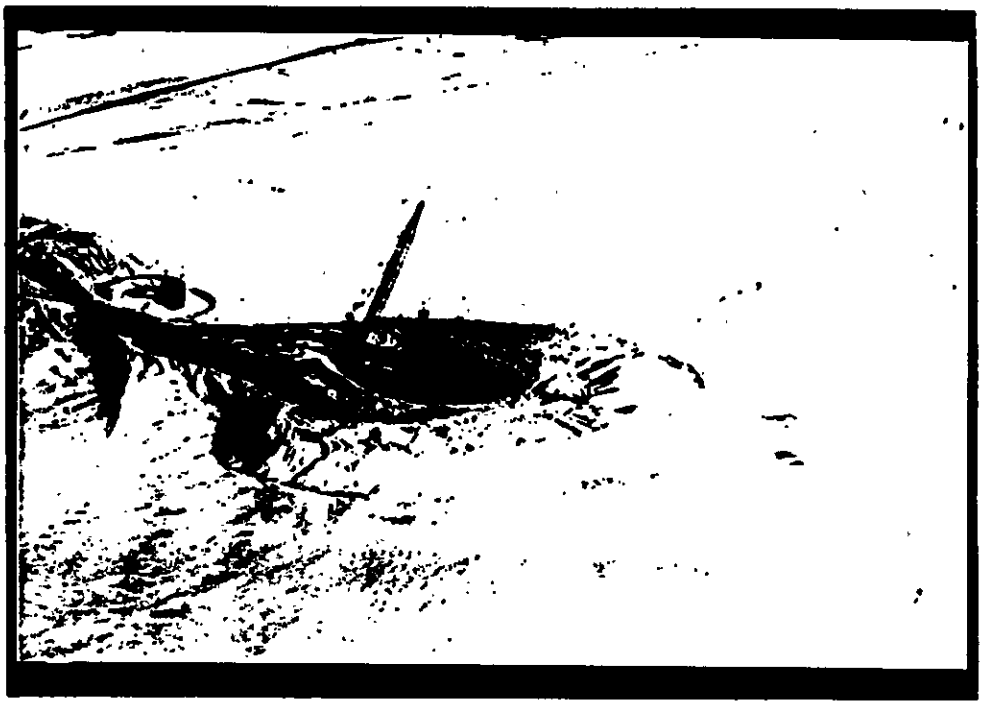

PHOTOGRAPH 6. A closeup view of the spray ice causeway with the gravel surface at the Red Dog Port Site.

a problem. The gravel layer was removed at the end of construction to enhance melting. After the sea ice went out, the wave action against the causeway caused it to break up and wash away. This happened before the first scheduled barges arrived at the seaport.

At Nome the problem was more critical: once the sea ice left the vicinity of Nome, the Bima and Aquamarine would be put in use immediately. Each day the vessels were not working revenue was lost.

At the beginning of this project there was no specific information on how to rapidly to remove spray ice. Around the Bima attempts were made to wash away the spray ice with high-pressure water monitors; to remove it with backhoes and draglines; and wheelwash it away with the propwash from the tug Aquamarine. Of the three methods tried, the use of the tug was by far the most efficient.

Attempts to remove the spray ice by directing high-velocity water at the barrier produced only marginal results. A water stream quickly cut a hole or slot in the spray ice. However the effect was very localized. Several days trial proved this technique unsuccesful in clearing away large quantities of spray ice.

The second method involved removing the spray ice with ordinary excavating equipment. Using backhoes and a dragline attached to a crane, a large quantity of spray ice was removed. Photograph 7 shows a backhoe and a dragline-equipped crane excavating spray ice. Although this method proved successful, it was a slow process. The use of this equipment is helpful for excavating where it is necessary to remove material selectively, i.e., to remove spray ice around structures and to contour the side slopes of spray ice for loading and unloading vessels.

In general spray ice offers little resistance to excavation. This is especially true of the upper layers of the material. What is difficult to remove is the natural sea ice layer that is buried at the bottom of the spray ice structure. This layer appears to bond firmly to the bottom and is difficult to break loose with backhoes and draglines. The most successful method found for removing the very bottom layer of material was to remove the spray ice overburden. With enough overburden removed, the base layer would eventually break loose and float to the surface. However, the extent of the overburden that must be removed and the period of time needed for the bottom layer to break loose has not been quantified. In some cases that we observed nearly 100 square meters of overburden was removed from the bottom layer. It sometimes took several days for the bottom layer to break loose and float to the surface.

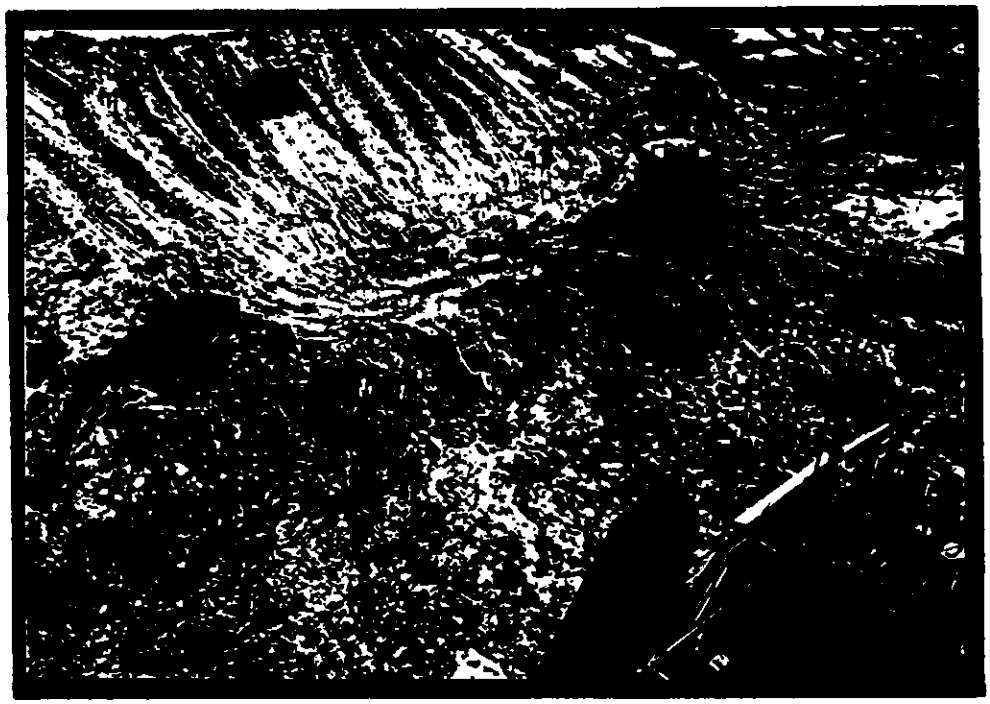

PHOTOGRAPH 7. Backhoe and crane excavating spray ice at the Nome barrier.

For fast and efficient removal of the spray ice wheelwashing the spray ice with the tug was by far the most effective method. The tug Aquamarine is 56 m in length and has a beam of 12 m. It has three propellers and a rated horsepower of 5700. To remove the spray ice the stern of the tug was attached to a hawser that was tied of to a piling. The tug then worked back and forth while its propwash was directed at the spray ice. In a period of eight to 10 hours over 150,000 cubic meters of spray ice were removed. Photograph 8 is a picture of the tug wheel washing the spray ice.

While wheelwashing the spray ice, the propellers operated at relatively low rpm with the boat's engines operating just above idle speed. The exact mechanism by which wheelwashing removes spray ice is not understood. It appears to be a combination of the erosive effects of the water on the spray ice and the thermal degradation of it. Failure of the spray ice takes place when the below water material is sufficiently undercut and the above water portion of the spray ice collapses and was washed away by the propwash. Using this technique there appeared to be no problem removing the bottom layer of natural ice as there was when excavating the material.

SUMMARY

In this report we have outlined our experience operating on spray ice in a somewhat different environment than is usually experienced on spray ice exploration islands in the Arctic. In general, we carried out these operations without prior experience. With minor exception the outcomes were favorable. No equipment was lost and no injuries have occurred. We feel many of the techniques used can be applied to arctic spray ice structures.

Since spray ice structures used for oil exploration are fairly massive, the problems of operating on narrow causeway-type structures are not applicable. However, if plans are made for moving equipment onto or off of spray ice islands onto barges in open water, the experience is directly applicable. Also, to maintain surfaces strong into the melt season surface coatings may be of some use. A landing area for barges loading or off-loading can be prepared with ordinary excavating equipment. If the need should arise to remove a spray ice structure rapidly, a tug boat or icebreaker can be used.

Specifically, to configure the spray ice for a docking operation where equipment can be driven on or off of the structure, ordinary excavating equipment can be used.

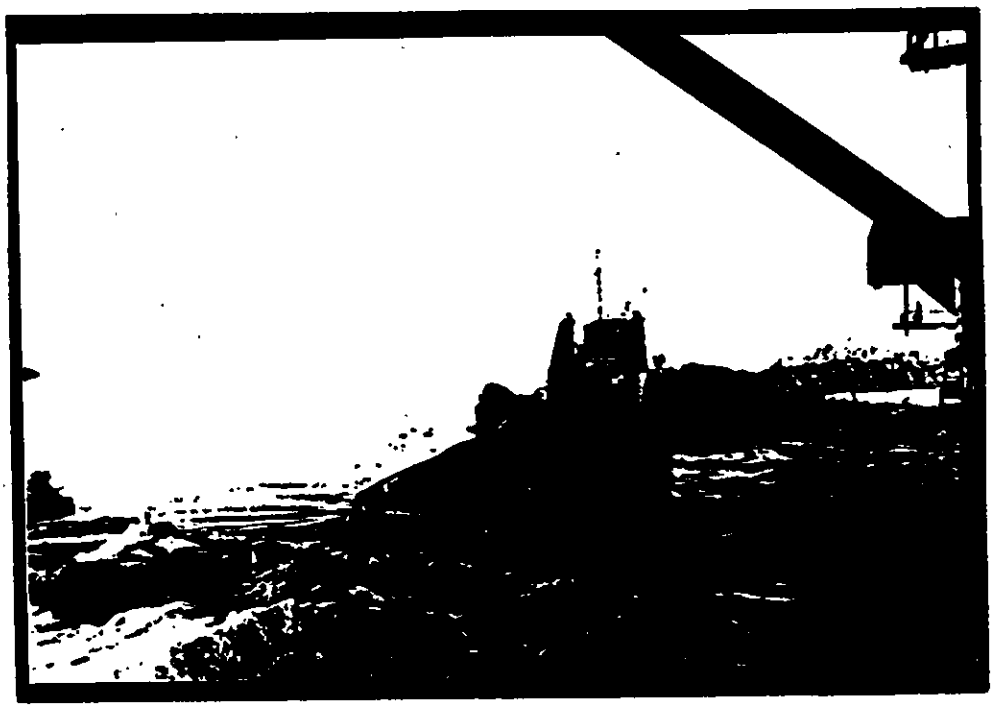

PHOTOGRAPH 8. The tug Aquamarine wheelwashing spray ice.

Considering that spray ice can stand vertically without support, we can excavate a docking area into any surface geometry desired. If a new area needs to be built away from the existing spray ice structure, material can be bulldozed into position. It should be noted that when bulldozing spray ice the edgeslope has a much higher angle than when the material is sprayed in place.

For examples of what type of excavations can be carried out in spray ice and the type of equipment that can be used we suggest Mellor's publication of the exploitation of snowfields (10). As indicated earlier in this report, the structure and properties of above-water spray ice are very similar to the structure and properties of snow on polar snowfields. There is a good body of information on the behavior of polar snow, and a reasonable amount of literature exists on engineering projects that have been carried out on the polar snow caps.

Once a barge has been located alongside a spray ice island it should not be difficult to move equipment directly onto and off of the vessel. Care should be taken to operate high ground pressure vehicles on crane mats or rig mats near the edge of the spray ice.

In terms of strengthening the surface of the spray ice islands, our experience with coating the work surface with gravel should be directly applicable. In operating off spray ice islands where a source of material may be difficult to obtain, silt or gravel dredged from the sea bottom might be used.

Finally, if there is a need to remove the spray ice structure, wheelwashing with a tugboat or ice breaker should be employed. In an open water situation an ordinary tug might be used; in ice-overed waters then an ice breaker might be used. A situation where there is a need to remove spray ice in winter is the case where a protective spray ice barrier is built around an offshore structure such as Global Marine's Concrete Island Drilling Structure, and the need arises to remove the barrier so that the structure can be moved to a new location.

RECOMMENDATIONS

The information in this report is based primarily on actual experience. In most instances the work was carried out with little preparation based on our intuition as to how the spray ice would react. We also gained a great deal of information on the behavior of spray ice as we carried out our operations. Considering that we could not locate the information that was needed beforehand in our programs, it would appear that some work should be carried out to explore in a methodical way the parameters in which we can work with spray ice.

It would be useful to extend failure information for spray ice into the region of tensile stresses. We know that the spray ice will take a considerable tensile load. It would be useful if failure criteria could be extended into the tensile regime.

A large-scale test of failure loads would also be useful. In the simplest form, a large-scale test could be carried out by deliberately overloading a section of a spray ice structure. Our experience indicates that on a large scale spray ice is stronger than indicated by small-scale tests.

The addition of foreign substances to the spray ice such as gravel, sand or silt should also be looked at in terms of how various concentrations of impurities affect the strength of the material. Our experience with impurities in the spray ice has indicated that some strengthening of the spray ice occurs.

The effect of surface coatings on slowing the rate of melting should also be considered. This is an area where little or no data exists. In addition to natural coatings such as gravel polystyrene foams have been used to protect spray ice surfaces. The economics of this on a large scale should be considered.

In our work we used a 5,700 horsepower tugboat to remove the spray ice. This tug was used simply because it was available. Indications are that a boat with much less horsepower could be used. Also, the manner in which propwashing affects the spray ice is not understood.

Finally, investigations should be carried out into how to extend the life of spray ice structures into the open water season. Currently the life of spray ice structures is severely limited by the onset of open water. Greater worth would be gained from the use of spray ice structures if they could be utilized during the open water season.

REFERENCES

(1) Flugge, W. 1967, Viscoelasticity, The Blaisdale Publishing Company, Waltham, MA.

(2) Mellor, M. 1963, Polar Snow - A Summary of Engineering Properties. In Ice and Snow, Proceedings of a conference held at the Massachusetts Institute of Technology, February 12-16, 1962, M.I.T. Press, Cambridge, MA. pp 528-559

(3) Chen, A.C.T. and Gram, K.G. 1989, Strength and Deformation of Spray Ice, The 10th International Conference on Port and Ocean Engineering under Arctic Conditions, June 12-16, 1989, Lulea Sweden, Vol 2. pp 681-693

(4) Weaver, J.S., and Gregor, L.C. 1988, The Design, Construction and Verification of the Angasak Spray Ice Exploration Island. Proceeding of the Seventh International Conference on Offshore Mechanics and Arctic Engineering. Vol 4. Houston, TX pp 177-183

(5) Lee, S.M., Haas, W.M., Brown, R.L., Wuori, A.F. 1989, improving Snow Roads and Airstrips in Antarctica, Cold Regions Research and Engineering Laboratory, Hanover, NH. Special Report 89-22

(6) Mellor, M. 1964, Properties of Snow, Cold Regions Science and Engineering, Part III: Engineering, Sect. A: Snow Engineering, Cold Regions Research & Engineering Laboratory, Hanover, NH. Report III-A1.

(7) Croasdale, K.R. 1980, Ice Forces on Fixed, Rigid Structures, In Working Group on Ice Forces on Structures, A State-of-the-Art Report, T. Carstens, Editor. Cold Regions Research and Engineering Laboratory, Hanover, NH, Special report 80-26, pp 34-103.

(8) Bowles, J.E. 1982, Foundation Analysis and Design, McGraw-Hill Book Company, New York, NY

(9) Colbeck S.C. 1988, Snowmelt Increase Through Albedo Reduction, Cold Regions Research and Engineering Laboratory, Hanover NH, Special Report 88-26

(10) Mellor, M. 1969, Investigation and Exploitation of Snowfield Sites. Cold Regions Research and Engineering Laboratory, Hanover, NH, Monograph III-A2B